Physicochemical studies of clay polymer interactions.

RAWSON, Jolyon O.

l i l t 17

K <so

12*h*

i ° i

Sheffie

REF

Physicochemical Studies of Clay Polymer Interactions

Jolyon Oliver Rawson

A thesis submitted in partial fulfilment of the requirements of Sheffield Hallam University for the degree of Doctor of Philosophy

July 1995

Collaborating Organisation: B.P. Research Centre
Drilling and Completions Branch
Chertsey Road
Sunbury on Thames
Middlesex
TW16 7LN

Acknowledgements

I would like to take this opportunity to express my gratitude to several people:

My supervisors Chris Breen and Brian Mann who both provided advice and encouragement throughout the duration of my PhD for which I am eternally grateful.

My industrial supervisors Paul Reid and Mark Aston who initiated this research project and provided guidance throughout.

British Petroleum for their generous funding of this research project.

The staff of Sheffield Hallam University who helped me throughout the duration of my stay in Sheffield.

My friends and colleagues for their support and excellent jokes about the interesting nature of clay!

A special thank you to my mother and father whose encouragement and support has been invaluable.

Finally, I would like to say a very special thank you to Andrea for all her support and understanding during the writing of this thesis.

Abstract

This thesis reports investigations into the colloid and solid state properties of clay/polymer complexes. The interactions between water soluble polymers and clay were investigated because of their importance to the oil industry which make use of clay/polymer interactions to control certain properties of drilling muds.

^{133}Cs and to a lesser extent ^{23}Na NMR have been evaluated as novel *in situ* probes to study the adsorption of polycations, and other cationic species, onto 25 gL^{-1} suspensions of Westone-L. Westone-L is a low iron containing montmorillonite which was completely exchanged with either Cs^+ or Na^+ cations. The polycations FL15, FL16 and FL17, of general formula $[(Me_2NCH_2CHOHCH_2)_n]^{n+}$, and Magnafloc 1697, $[(CH_2\overline{CHCH_2N(Me)_2CH_2CHCH_2})_n]^{n+}$ have been shown to displace the exchangeable cation from the clay surface more effectively than other cationic species investigated such as Na^+, K^+, MeN_4^+ and paraquat^{2+}. This was shown through a decrease in linewidth and an increase in the ^{133}Cs or ^{23}Na NMR peak integral as cationic species were added to the clay. This information has been correlated with that obtained from particle size and zeta potential measurements in aqueous solution which suggest that the highly charged polycations investigated adsorb onto the surface of the clay via an 'electrostatic patch' mechanism. To complement these aqueous *in situ* techniques, several dry powder studies have been completed, including adsorption isotherms through Kjeldahl N analysis, variable temperature x-ray diffraction and thermogravimetric studies. These dry powder studies show conclusively that the exchangeable cation associated with the clay surface has a large bearing upon the amount and location of polymer adsorbed.

The neutral polyglycol DCP101 is presently finding widespread use as a shale inhibitor in drilling muds. The mechanism by which this polymer interacts with clay has been investigated by recording the ^{133}Cs and ^{1}H NMR spectra of 25 gL^{-1} suspensions of Cs^+ and Mn^{2+} exchanged Westone-L treated with DCP101. These novel *in situ* investigations have shown that DCP101 does not displace the exchangeable cation associated with the clay. They have also shown that the water molecules in the hydration sphere of the Mn^{2+} cation associated with the clay surface are predominantly undisturbed by added DCP101. To complement these aqueous *in situ* investigations, several dry powder studies were carried out including adsorption isotherms through CHN analysis, variable temperature x-ray diffraction and thermogravimetric studies. These dry powder studies show that the exchangeable cation has a large bearing upon the quantity of polymer adsorbed.

One further *in situ* NMR method has been evaluated with a view to investigating clay/polymer interactions. This method involved the addition of 10% D_2O to a 40 gL^{-1} suspension of clay which had been exchanged to the cation of interest. The resulting ^{2}H NMR spectrum showed a residual quadrupolar splitting, the magnitude of which depended upon several factors including clay concentration, state of aggregation of the clay platelets and the exchangeable cation associated with the clay. It was hoped that by monitoring the clay/D_2O interactions via the ^{2}H residual quadrupolar splitting that information about clay/polymer systems in aqueous suspension would be forthcoming. The observed ^{2}H residual quadrupolar splitting was however found to be too sensitive to addition of polymer or ions to the clay suspension, resulting in its collapse to a singlet.

Table of Contents

CHAPTER 1

CHAPTER 2

CHAPTER 3

CHAPTER 4

CHAPTER 5

CHAPTER 8

CHAPTER 9

Abbreviations.

WBM	water based muds
OBM	oil based muds
3xZ-mont	Westone-L montmorillonite exchanged three times with the cation of interest symbolised by Z
Z-montmorillonite	Westone-L montmorillonite exchanged with a cation of interest symbolised by Z
3xZ-bent	Mineral Colloid bentonite exchanged three times with the cation of interest symbolised by Z
meq	milli-equivalents
AEC	anion exchange capacity
CEC	cation exchange capacity
EE	edge to edge flocculation
EF	edge to face flocculation
FF	face to face flocculation
Mwt	molecular weight
PVA	polyvinylalcohol
PA	polyacrylamide
PSS	polysaccharide
PEG	polyethyleneglycol
HPAN	hydrolysed polyacrylonitrile
AM	acrylamide
CMA	N,N,N,-trimethylaminoethyl chloride
PCMA	copolymer of acrylamide and N,N,N,-trimethylaminoethyl chloride
PHPA	partially hydrolysed polyacrylamide
HEG	hexaethylene glycol
DCP101	polyalkylene glycol synthesised by polymerising ethylene and propylene oxide
FL15, 16 and 17	polycations synthesised by copolymerising dimethylamine and epichlorohydrin, general formula $[(Me_2NCH_2CHOHCH_2)_n]^{n+}$

Magnafloc 1697	polycation based upon diallyldimethylammonium chloride, general formula $[(CH_2\overline{CHCH_2N(Me)_2CH_2CHCH_2})_n]^{n+}$
TMA^+	tetramethylammonium ion
Q	amount of polymer adsorbed
Q_{max}	maximum amount of polymer adsorbed
p	fraction of polymer adsorbed in train segments
τ	cationicity of polymer
CHN	carbon, hydrogen and nitrogen analysis
XRF	x-ray fluorescence spectrometry
XRD	x-ray diffraction
TGA	thermogravimetric analysis
NMR	nuclear magnetic resonance
MAS NMR	magic angle spinning nuclear magnetic resonance
T_1	spin-lattice (longitudinal) relaxation time
T_2	spin-spin (transverse) relaxation time
A	anisotropy
B_0	static magnetic field of an NMR spectrometer
ω_o	Larmor frequency
D^c	receptivity of nucleus with respect to ^{13}C
Q	electric quadrupole moment
τ_c	correlation time for molecular tumbling
L	linewidth factor for quadrupolar nuclei
I	spin quantum number
χ	quadrupolar coupling constant ($= e^2qQ/h$)
Θ_{LD}	the angle made between the static magnetic field, B_0, and the local order director of the orientated clay platelets, perpendicular to their surface
Δ	residual quadrupolar splitting

CHAPTER 1

The Role of Drilling Muds in the North Sea.

1. The Role of Drilling Muds in the North Sea.

Whilst drilling for oil in the North Sea, many different rock types may be penetrated. Shales however make up more than 75% of drilled formations and cause more than 90% of wellbore-instability problems.[1] The instability of shale as a drilling medium is caused primarily by the transport of water through it.[2]

Shales are essentially rocks that have been formed by the compaction of marine sediments. Water is squeezed out of the rock as the sediment is buried deeper and deeper by the deposition of further sediment layers. The degree of compaction of marine sediments increases as the depth of burial increases as long as excess water is able to escape from the shale. As a consequence, older shales are more compact, retain less water and as a result are hard and less easily dispersed into water whereas, younger shales are softer and disperse easily when mixed with water. The appearance and behaviour of shales encountered in an oil well vary dramatically yet all shales have one feature in common in that they all contain a large proportion of clay.[3]

The amount and type of clay, the depth of burial and the quantity of water associated with the shale all have a large bearing on the stability of a shale when being drilled. The amount of clay found in shale is dependent on the composition of the shale sediments as they are deposited on the sea bed. The type of clay found in shale not only depends on the composition of marine sediments at the time of deposition but also the conditions to which the sediment is subjected once buried. The types of clay found in shale may be classified as either expandable or non expandable. Expandable clays are able to intercalate large quantities of water which make the clay swell. Swelling clays are known as smectites of which montmorillonite is the most common example. Conversely,

non expandable clays swell to a much lesser degree on wetting with water than expandable clays. The types of clay belonging to this category which are most commonly found in shale are illite, chlorite and kaolinite.

The swelling clay montmorillonite is the type of clay predominantly found in younger, less compacted sediments. As sediments increase with age and therefore the depth to which they are buried, the percentage of illite (non swelling clay) in the shale increases which is attributable to the conversion of montmorillonite to illite. The alteration of smectites to illite is called "diagenesis" and is thought to proceed as a direct result of the temperature attained as sediments were buried deeper rather than the pressure they experienced.[4] Diagenesis also involves the replacement of exchangeable Ca^{2+} and Na^{+} ions usually found in montmorillonite by K^{+} ions.

There are many different forces acting on shales which cause their instability while being drilled. One of the major destructive forces however can be attributed to the adsorption of water which in turn leads to degradation of the drill hole wall (drill hole enlargement) and also disintegration and dispersion of drilled solids during removal from the drill hole (drill hole closure).[5] The mechanism by which shale adsorbs water can be wholly attributed to the clay present in the shale. Expandable clays such as montmorillonite which have the ability to intercalate large quantities of water are therefore the most troublesome type of clay encountered in shale. The force by which clay draws water into the shale can be very large and therefore a mechanism to restrict the ingress of water into shale is required for drill hole stability. Drill hole stability is achieved by formulating a drilling fluid, sometimes called a "mud" which performs many functions to maintain the integrity of the drill hole including minimisation of water ingress

into clay. The three main properties of a drilling fluid that are controlled to maintain drill hole stability are:[6]

Density.

Control of the density of a drilling fluid is required to prevent blowouts from the drill hole which may occur if gasses and oil escape from the porous rocks being drilled.

Rheology.

Rheology control is required for the efficient removal of drilled solids (cuttings) from the drill bit to the drill platform.

Filtration.

Filtration control is effected by the use of solids in the drilling fluid which form a thin layer of low permeability (filter cake) on the inside wall of the drill hole. This reduces the amount of fluid permeating into the pore spaces and therefore prevents excessive wall cake accumulation and fluid loss.

1.1 Drilling Fluid Composition.

Drilling fluids are classified according to the constitution of their continuous phase, two main types predominate.

1.1.1 Water Based Fluids/Muds (WBM).

WBM have a continuous phase of water and are classified as fresh water fluids or salt water fluids according to the salinity of the medium.

The discontinuous phase in WBM maybe a liquid, solid or a gas. The solids found in WBM are often barite used as a weighting agent to prevent blowouts, clay minerals to control rheological and filtration properties and the drilled cuttings. Other

additives include polymers and surfactants which help to maintain drill hole stability. The use of polymers in WBM is mainly to prevent disintegration of cuttings by preventing the interaction of shale with water. The mechanism by which polymers effect this will be discussed later. Soluble salts such as KCl are also added to WBM to reduce the dispersion of clays and promote shale inhibition by shielding the negative charges on the clay.

1.1.2 Oil Based Fluids/Muds (OBM).

When the continuous phase of a mud is oil, it is classified as an oil based mud. OBM usually contain water as the discontinuous phase which may be present in proportions up to 50%. Solids in the drilling fluid consist of barite used as a weighting agent and drilled solids such as clay. Clay minerals are also added to muds to control filtration and rheological properties, however because clay is hydrophilic, surfactants are also required to produce a stable emulsion.

1.2 Environmental Considerations When Choosing A Drilling Fluid.

OBM were first used in the North Sea in the late 1970's and quickly became the most widely used drilling fluid with 265 of the 345 UK wells in 1988 being drilled with OBM.[7] The drilling industry prefers the use of OBM because they provide the most effective stabilisation of reactive shales during drilling.[8] The advantages of using OBM over WBM arises due to the lack of water in their continuous phase which prevents them from (i) hydrating and dispersing water sensitive clays, which leads to loss of bore hole integrity in shales, (ii) dissolving salts, leading to borehole enlargement, and (iii) corroding the ferrous metal of the drill equipment, giving loss of mechanical strength. OBM also provide better lubrication and higher thermal stability than WBM. As OBM

promote good shale inhibition, this in turn means the efficient removal of cuttings from the drill hole to the drill platform. On the drill platform, the cuttings are separated from the mud via a shaker screen. The mud is then recycled back down the drill hole while the oil covered cuttings are discarded into the sea. It is now generally accepted that the oil on the discarded cuttings does have a long term and cumulative effect on seabed-dwelling life. Consequently in the North Sea and offshore US, two of the most active drilling areas world-wide, discharge of any waste from OBM has been banned or severely restricted with the emphasis on zero discharge.[9] Compounding the environmental issues is the fact that industry is placing greater demands on drilling fluids via the drilling of extended reach, horizontal and high pressure/temperature wells. These new requirements of a drilling fluid, in addition to existing ones such as inhibiting shale disintegration, controlling fluid loss and minimising well formation damage have lead to a persistence in the use of OBM when dealing with water sensitive shale. This persistence in using OBM has resulted in expensive and sometimes impractical methods of dealing with oil contaminated cuttings. New ways of dealing with oily cuttings which comply with recent environmental legislation include:

1. **Cleaning the oil from cuttings with solvents before discarding them**[10]

2. **Transporting the cuttings to a land fill site which in effect transfers the problem.**

3. **Re-Injection of cuttings. Here the contaminated cuttings are, slurried in water, ground to a fine size and injected into relatively deep formations behind the well casing.**[11]

To overcome the problems of drilling through shale and recent environmental legislation, water based drilling fluids are being developed which have little environmental impact but offer performances closer to OBM than existing WBM.

If WBM are to be used successfully for drilling wells where shale is present then certain criteria must be fulfilled.[12] They must provide (i) good shale inhibition which is an essential requirement for a drilling fluid in the North Sea, (ii) be highly lubricating to cope with extended reach and horizontal well drilling. OBM must also show good fluid loss control, not increase the risk of differential sticking, cause little formation damage and have acceptable thermal stability.

From a health, safety and environmental standpoint, these muds must be safe to handle, have low human and eco-toxicity and be readily biodegradable. The problem with established WBM such as potassium chloride/polyacrylamide (KCl/PHPA), is that these muds are not nearly as good at promoting shale inhibition as OBM and as a result their use can increase drilling costs substantially. Improved inhibition in WBM has been achieved recently and two categories of improved mud exist.

1. **Drilling fluids containing cationic polymers.**

2. **Drilling fluids containing glycol additives.**

1.2.1 WBM Containing Cationic Polymers.

Cationic polymer additives have been found to be useful as shale inhibitors in WBM with performances approaching those of OBM. Problems have arisen however because some cationic polymer additives have been found to be incompatible with other mud additives.[13] Concerns have also arisen over the environmental impact of some of these cationic species on marine organisms. The major problem with these muds is however their high depletion rates which drastically escalates drilling costs.[12,14]

1.2.2 WBM Containing Glycol Additives.

Polyglycols have recently been added to KCl/PHPA WBM with much success. It has been found with the addition of 3% loadings of polyglycol to the mud that dispersion, swelling and softening of shales are all greatly reduced compared with the base mud. PHPA may also be omitted from the formulation without appreciable loss of inhibition. Polyglycols also show low human and eco-toxicity, are compatible with all common mud additives and due to their low molecular weight do not contribute significantly to mud rheology. Consequently polyglycol mud additives are the preferred additive in WBM to maximise shale inhibition. Present day emphasis has therefore been centred on formulating new mud additives in an attempt to produce a WBM whose inhibition properties are equal to, if not superior to those of an OBM yet do not have their associated toxicity. Improvements in mud additives with shale inhibitive properties can only be realised by a firm understanding of the mechanisms by which currently available polycation and polyglycol mud additives effect shale inhibition in WBM.

One new area of research which has not been mentioned as yet is the investigation into pseudo-oil based mud (POBM). A POBM may be defined as a drilling fluid, the continuous liquid phase of which consists of a low toxicity, biodegradable "oil" which is not of petroleum origin.[15] To date the best POBM, which were first introduced in 1989, have used ester based fluids which have shale inhibition properties comparable to regular OBM. POBM are not however widely used because the ester fluids suffer from the limitation that at well temperatures in excess of 150°C, the ester hydrolyses to the component alcohol and fatty acid, leading to unstable fluid properties. Research is however underway into the use of other biodegradable, non petroleum oils which do not have the aforementioned temperature limitations.

CHAPTER 2

An Introduction to Clay Minerals.

2. An Introduction to Clay Minerals

Clays are composed of silica, alumina, water and usually a quantity of iron, alkalis and alkaline earths. The term clay may be considered from two different perspectives :

From a mineralogical standpoint, clay may be described as a group of minerals which are the product of weathering, have been formed by hydrothermal action, or have been deposited as a sediment. Grim[16] defines clay as a natural, earthy, fine-grained material which develops plasticity when mixed with a limited amount of water. Plasticity is the ability of the clay to be deformed under pressure, the deformed shape being retained with the removal of the pressure.

From a particle size standpoint, the clay fraction of an earthy material is the fraction containing the smallest particles. The upper limit of the clay fraction size is defined differently in different disciplines, for example in geology the Wentworth[17] scale defines the clay fraction as having a particle size less than 4 microns. It is generally accepted however that clay minerals have a particle size of less than 2 microns when slaked in water. Slaking clay is a technique used to separate the clay minerals from non-clay mineral components of soils or other naturally occurring earthy materials. The heavier particles sink to the bottom while fine grained clay mineral particles remain in suspension and the larger clay particles break down to a size of less than 2 microns. This method of clay mineral separation/purification is performed on all the clay used for this study and will be discussed in greater detail later.

Clay minerals have been important to man for thousands of years with the production of earthen-ware vessels and ceramics. Investigation into these materials therefore dates back far into antiquity. The first serious scientific investigations into a

clay were carried out in 1847 by Damour and Salvett.[18] They investigated a clay from the Montmorillion region in France which they later termed montmorillonite. The properties of clay minerals were also being investigated around this time for example in 1852 Way studied the ability of clay soils to adsorb manures.[19]

When a method by which clay minerals could be analysed was finally devised, it was found that clay minerals differed widely in the quantities of alumina, silica, alkalis and alkali earths that they contained. It was also found that clays with the same ultimate chemical composition invariably had different physical properties while clays with similar physical properties often had different chemical compositions. It was not until the middle of this century with the advent of electron microscopy, infra-red spectrometry, X-ray diffraction and thermal analysis techniques that the relationship between the chemical composition, the structure and the physical properties exhibited by a clay began to be understood. The fact that clays have a great diversity of physical properties may then be explained by considering differences in the structural arrangement of the clay's chemical components. In fact clays are comprised of sheets which in turn are composed of one or two basic unit cells which are polymerised into the two dimensional sheet. Different arrangements of these sheets and the presence of different cations greatly determines the physical properties of a clay, (clay composition and physical properties are discussed in greater detail in section 2.1).

Today clays are described as hydrous aluminium or magnesium silicates which contain varying proportions of iron, alkalis and alkaline earths.

2.1 The Structure of Clay Minerals, Their Cation Exchange Capacity and Swelling Properties.

2.1.1 The Fundamental Building Units of Sheet Silicates.

There are two simple sheet forming units from which all clay minerals are constructed;

1. **Silicon tetrahedral units which combine to form the tetrahedral sheet.**
2. **Aluminium or magnesium octahedral units which combine to form the octahedral sheet.**

These two sheets in turn combine to form two dimensional sheet structures, which are stacked one on top of the other to form the clay layers in a clay particle.

2.1.1.1 The Tetrahedral Sheet.

In each silicon tetrahedral unit (Figure 1a), a silicon atom is located at the centre of a tetrahedron, equidistant from four oxygen atoms or hydroxyls. The silica tetrahedra are polymerised into a hexagonal network, by linkage of three oxygen atoms at the base of each tetrahedron, with three adjacent tetrahedra forming a flat tetrahedral sheet. All tetrahedra bases lie in the same plane, consequently all apices point in the same direction, (Figure 1b). The chemical composition of a single silicon tetrahedron is SiO_4^{4-}, after polymerisation into an infinite two dimensional sheet structure, the chemical composition is $Si_4O_6(OH)_4$, (Figure 2).

Key: ○ and ◌ = Oxygen ● = Silicon

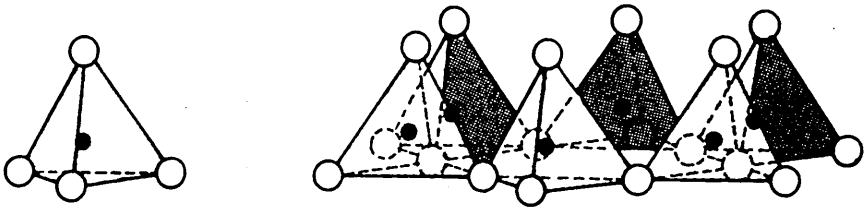

(a) (b)

Figure 1. Diagrammatic sketch of (a) a single silica tetrahedron and (b) the sheet structure of silica tetrahedrons arranged in a hexagonal network.

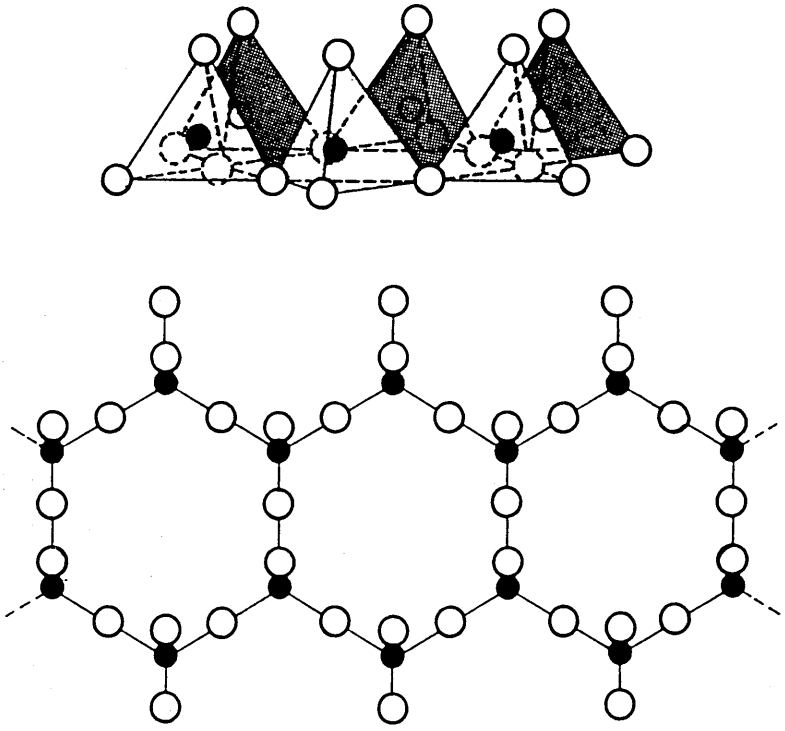

Figure 2. The silica tetrahedral sheet projected on the plane of the base of the tetrahedrons, showing the hexagonal network.

2.1.1.2 The Octahedral Sheet.

The octahedral units (Figure 3a) are polymerised into a two dimensional array or sheet, known as the octahedral sheet. The octahedral sheet consists of two parallel planes of closely packed oxygens or hydroxyls in which Al, Fe or Mg ions are embedded in octahedral co-ordination, (Figure 3b). When aluminium is present, only two thirds of the possible positions in the lattice are filled whereas when magnesium is present, all the positions are filled to balance the structure. The hydroxyl species is formed in the sheet when the oxygen atoms gain a negative charge, due to bonding between the octahedrons in the sheet , and bind a proton to satisfy their valency requirements.

2.1.1.3 The Layer Silicates.

The differences between the various types of clays is the way in which the tetrahedral and octahedral sheets combine to form the clay layer. In fact the ratio of tetrahedral to octahedral sheets and the type of cation in the sheets, is the basis for a classification system used to assign clays to various groups.

The symmetry and almost identical dimensions of the tetrahedral and octahedral sheets, allows for sharing of the oxygen atoms between the two sheets, (Figure 4). When one tetrahedral and one octahedral sheet combine to form a layer, this is said to be a 1:1 (T:O) type clay such as kaolinite. If two tetrahedral sheets sandwich one octahedral sheet between them, this is known as a 2:1 (T:O:T) type clay such as the smectite, montmorillonite. This combining of the tetrahedral and octahedral sheets occurs when

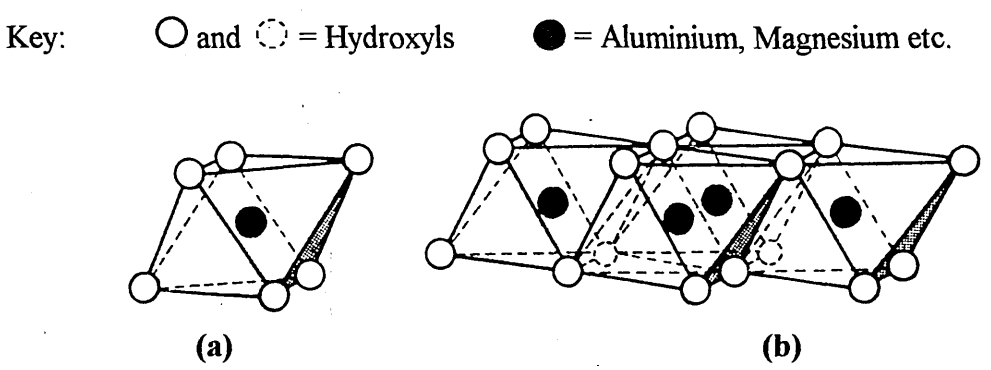

Figure 3. Diagrammatic sketch of (a) a single octahedral unit and (b) the sheet structure of the octahedral units.

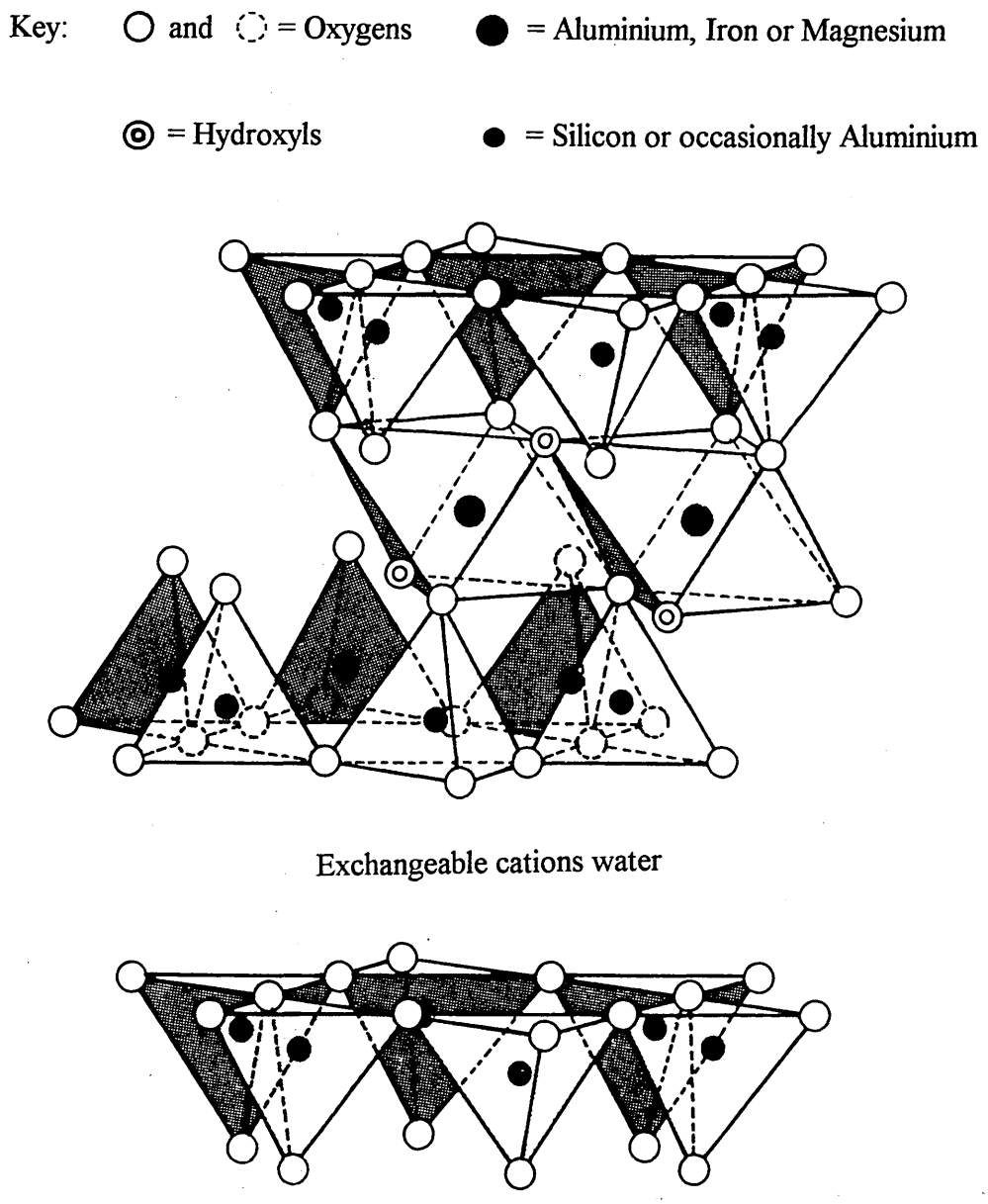

Figure 4. Diagrammatic sketch of the combined tetrahedral and octahedral sheets in a smectite clay.

the oxygen atoms at the apices of the tetrahedral sheets are shared with the plane of oxygen atoms in the octahedral sheet, (Figure 4).

2.1.2 The Structural Classification of Clays.

Most clays fall into the 1:1 or 2:1 type clay groups, and clays that are not members of these groups are usually structurally modified 1:1 or 2:1 clay types. Table 1 lists the major groups of clays and arranges them according to their structural classification.

Property	Kaolin	Mica	Mont*	Chlorite
Layer Type	1:1	2:1	2:1	2:1:1
Crystal Structure	sheet	sheet	sheet	sheet
Particle Shape	hexagonal plate	extensive plates	flake	plate
Particle Size Microns	5 to 0.5	large sheets to 0.5	2 to 0.1	5 to 0.1
Surface Area				
BET-N_2 m^2g^{-1}	15 to 25	50 to 110	30 to 80	140
BET-H_2O m^2g^{-1}	-	-	200 to 800	-
Cation Exchange Capacity meq/100g	3 to 15	10 to 40	60 to 130	10 to 40
Viscosity in water	low	low	high	low
Effect of salts	flocculates	flocculates	flocculates	flocculates

Table 1. A summary of the structure and properties of the most common clay minerals.

Mont* = Montmorillonite.

The differences between clays are often expressed as a combination of the following four parameters:

1. **The layer charge.**
2. **Isomorphous substitution.**
3. **Interlayer cations.**
4. **Ability to intercalate water, organic molecules or cations.**

This list of parameters can be used to describe some of the main differences between the most common clay types as shown below.

(a) The Kaolinite-Serpentine Group.

Examples: Kaolinite $[Al_4Si_4O_{10}(OH)_8]$

Chrysolite $[Mg_6Si_4O_{10}(OH)_8]$

1. Overall the layers are amphoteric, carrying a negative charge on one side of the layer and a positive charge on the opposite side.
2. Interlayer cations do not occur as hydrogen bonding and strong electrostatic forces hold the layers tightly together.
3. Intercalation is limited, but is possible with polar molecules.

(b) The Pyrophyllite-Talc Group.

Examples: Pyrophyllite $[Al_4Si_8O_{20}(OH)_4]$

Talc $[Mg_6Si_8O_{20}(OH)_4]$

1. Carry no layer charge.
2. Isomorphous substitution does not occur.

3. Intercalation is rare, although there have been some reports that water molecules and organic molecules have been detected between the layers.

(c) The Smectite Group.

Examples: Montmorillonite $[(Na_{0.6})(Al_{3.4}Mg_{0.6})Si_8O_{20}(OH)_4]$

Saponite $[(Na_{0.6})(Mg_6)(Si_{7.4}Al_{0.6})O_{20}(OH)_4]$

1. Carries a layer charge of 0.5-1.0 units per unit cell.
2. Isomorphous substitution readily occurs, with the cations absorbed to balance the layer charge.
3. Readily undergoes cation exchange.
4. Intercalation of water and organic molecules also occurs.

(d) The Vermiculite Group.

Example: Vermiculite $[(Mg_{0.6})(Al_4)(Si_{6.8}Al_{1.2})O_{20}(OH)_4]$

1. Carries a high layer charge of 1-2 units per unit cell.
2. Isomorphous substitution occurs only in the tetrahedral sheet.
3. Undergoes cation exchange with some difficulty.
4. Intercalation of water and organic molecules also occurs.

(e) The Illite Group.

Example: Illite $[(K_{1.6})(Mg_6)(Si_{6.4}Al_{1.6})O_{20}(OH)_4]$

1. Carries a layer charge of 1.6 units per unit cell.
2. Isomorphous substitution occurs in the tetrahedral sheet.
3. Exchange of the interlayer cations is difficult.

4. Strong interlayer bonding makes intercalation very rare.

(f) The True Mica Group.

Example: Muscovite $[(K_2)(Al_4)(Si_6Al_2)O_{20}(OH)_4]$

1. Carries a layer charge of 2 units per unit cell, causing strong interlayer bonding.
2. Isomorphous substitution occurs in the tetrahedral sheet.
3. Interlayer substitution of cations is rare.
4. Intercalation is also very rare.

(g) The Chlorite Group.

Examples: Donbassite $[Al_8Si_5O_{22}(H_2O)_7]$

Clinochlore $[Mg_{12}Si_8O_{20}(OH)_6]$

1. No layer charge occurs in this group.
2. Interlayer cations are not replaceable.
3. Intercalation of water occurs only when the hydrogen bonding between the layers is disrupted.

The structure and properties of the 2:1 smectite, montmorillonite, the type of clay examined in this study, will now be considered in greater detail.

2.2 The Structure and Properties of Montmorillonite.

Montmorillonite is a dioctahedral smectite with a typical formula of:

$$Na_{0.33}Al_{1.6}Mg_{0.33}Si_4O_{10}(OH)_2.$$

The three dimensional structure of montmorillonite can be represented two dimensionally, (Figure 4). This model for montmorillonite was proposed by Hofmann-Endel-Wilm,[20] in 1933 and has been modified over the years by Marshall,[21] Madgefrau and Hofmann,[22] and Hendricks,[23] into the structure for montmorillonite which is the most widely accepted today.

A much less widely accepted model for the structure of montmorillonite also exists as proposed by Edelmann and Favajee in the 1940's.[24] With this model, some hydroxyl groups are attached to silicon and the structure is balanced by inverting a number of tetrahedra in the tetrahedral sheet. Alternate silicon tetrahedra are inverted therefore all the apical oxygen atoms in the tetrahedral sheet do not lie in the same plane. This model was later modified to 20% of the tetrahedra being inverted. This was to account for the observed cation exchange capacities of montmorillonite which could not be explained by the model where alternate silicon tetrahedra were inverted. The 'gaps' or 'holes' left in the tetrahedral layer by inversion are filled by hydroxyl groups. No isomorphous substitution occurs in either the octahedral or tetrahedral layer with this model, the cation exchange capacity is supposedly due to the dissociation of hydroxyl groups in the tetrahedral sheet. This model for the structure of montmorillonite is less widely accepted, mainly due to two reasons:

- Si-OH bonds in silicate minerals are rare.

- If dissociation of the hydroxyl groups on the surface of the tetrahedral layer accounts for the cation exchange capacity of montmorillonite, the exchange capacity would vary with changing pH, there is no evidence of this happening. This thesis therefore only considers the modified Hofmann *et al.* model.

Montmorillonite can be distinguished from other smectite clay layers by virtue of the fact that montmorillonite is an aluminous smectite. This is to say that Al^{3+} cations are predominant in the octahedral layer. The Al^{3+} cations may be isomorphously substituted by Mg^{2+} or Fe^{2+} which results in the accumulation of a net negative charge on the layer. Isomorphous substitution of Si^{4+} by Al^{3+} in the tetrahedral layer also occurs but to a much lesser extent. This net negative charge on the layers is balanced by the uptake of cations into the interlayer and accounts for the large CEC of montmorillonite. Because the majority of the isomorphous substitutions are in the octahedral layer, the charge on the clay is sited mainly in the centre of the clay particles. This means that compensating cations are unable to approach the negative charge sites closely enough to completely loose the ionic character of the cation or the mineral surface. This residual ionic character maintains the clay in a stable structure and accounts for many of the properties of a montmorillonite such as intercalation of organic molecules and water.

2.2.1.1 The Cation Exchange Capacity (CEC) of montmorillonite.

Montmorillonite usually occurs naturally in the Ca^{2+} exchanged form, however Wyoming bentonite occurs predominantly in the Na^{+} form and as a result is relatively unique. If natural clay is placed in a solution of a different cation, ion exchange occurs between cations associated with the clay surface and cations in solution (Equation 1).[25]

$$X\text{-}Clay + Y^{+} \Leftrightarrow Y\text{-}Clay + X^{+}$$

Equation 1. The equilibrium set up between cations associated with the clay, X, and cations in solution, Y.

The reaction moves to equilibrium but the extent to which the reaction moves from left to right is dependant on:

1. **The nature of the cations X^{+} and Y^{+}.**
2. **The relative concentrations of X and Y.**
3. **The nature of the clay.**

The CEC of a clay is usually expressed in milliequivalents of each cation per 100 grams of clay (meq/100g). Montmorillonite has the largest CEC of any clay mineral, in the order of 60-130 meq/100g.

The CEC of a clay is dependant on many factors. The structure of the clay determines which of the factors below is most important in determining the magnitude of the clay's CEC.

2.2.1.2 Isomorphous Substitution.

Isomorphous substitution in montmorillonite clays, is usually the substitution of Al^{3+} in the octahedral layer by Mg^{2+} or Fe^{2+}, or less commonly Si^{4+} by Al^{3+} in the tetrahedral layer. The isomorphous substitution gives rise to a net negative charge on the layers which is balanced by the uptake of cations into the interlayer or interlamellar space. With montmorillonite, this process accounts for 80% of the total CEC of the clay. Isomorphous substitution varies in different minerals in the following ways.

- Tetrahedral substitution may be dominant or no substitution may occur at all as in pyrophyllite.
- The extent of isomorphous substitution and therefore the CEC of clays varies enormously.

2.2.1.3 Broken Bonds at The Edges of Silicate Layers.

At the edges of silicate layers, there are aluminium, silicon, oxygen and hydroxyl ions which have unsatisfied valencies or 'broken bonds' as they are often called. These unsatisfied valencies must be accommodated by external ions which become associated with the edge sites in order to ensure electrical neutrality. These counter-ions may be exchanged for other ions and are therefore a source of cation exchange in a clay mineral. In halloysite, a 1:1 type clay, these broken bonds are the major contributing factor to the CEC as no isomorphous substitution takes place. In the case of montmorillonite, broken bonds account for only 15-20% of the total CEC of the clay.

2.2.1.4 Ionisation of Basal Hydroxyl Groups.

Ionisation of basal hydroxyl groups produces a negative charge on the oxygen and a hydrogen ion which may then be exchanged for other cations. This process is thought to account for the remaining CEC on montmorillonite which has not already been accounted for by the two previous processes. The 1:1 clay types such as kaolinite have exposed planes of hydroxyl groups on one side of the silicate layer. The consequence of this should be that hydrogen atoms of these groups could be replaced and therefore should contribute significantly to the CEC of kaolinite clays. This is not thought to be the case as the protons of the hydroxyl group are tightly bound to oxygen making them difficult to remove by a sterically larger cation. The strength of the O-H

bond is one of the main arguments against the Edelmann-Favejee model for the structure of montmorillonite in that inversion of 20% of the silicon tetrahedrons in the tetrahedral sheet would expose a hydroxyl surface to the interlayer space. Exchange of protons from the exposed hydroxyl groups then has to account for approximately 80% of the CEC of montmorillonite clay which is thought unlikely. Again if this model were correct, it would be expected that the CEC would be dependant on pH which is not the case.

2.2.1.5 Exchangeable Cations.

The position of exchangeable cations in the clay structure depends on the cation and the type of clay in question. As stated previously, with montmorillonite, approximately 20% of the exchangeable cations are associated with broken bonds at the edges of the silicate sheet while the other 80% of the CEC is situated on or between the basal surfaces of the silicate layers. The sites that cations occupy within the interlayer of clay, to a large extent depend on the hydration state of the clay. If the clay is anhydrous, small exchangeable cations may occupy the hexagonal cavity in the tetrahedral sheet. As two or more water layers are adsorbed by the clay, the cation is displaced from the hexagonal cavity and lies between the water layers which are now in contact with the basal surface of the clay (Figure 5).

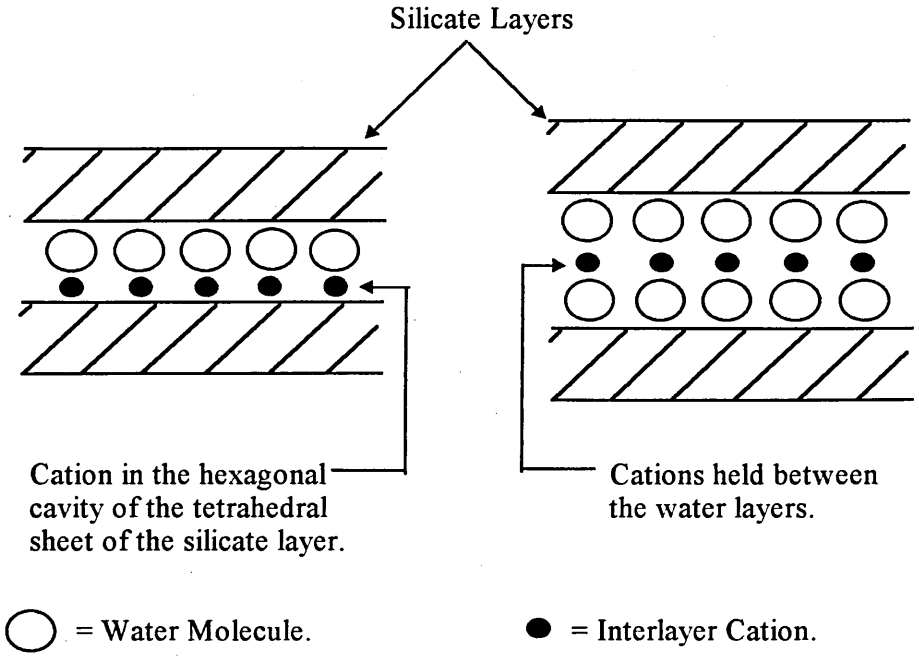

Figure 5. The location of the cation in hydrated montmorillonite which depends upon the hydration state of the clay.

The position of the cation in the interlayer space not only depends on the hydration state of the clay, but also on several other factors including the charge, size and hydration radius of the cation. The replaceability of cations associated with the clay by cations of a chosen type depends on a number of factors:

1. **The concentration of electrolyte solution brought in contact with the clay.**
2. **The population of exchange sites on the clay.**
3. **The nature of the cation i.e. valency, hydration energy, size.**
4. **The nature of the clay mineral.**

The replaceability of one exchangeable cation with another can be difficult to predict as different ions have different attractive forces for the exchange sites on a clay. It is generally accepted that the replacing power of cations follows the series $Li^{+}<Na^{+}<K^{+}<Mg^{2+}<Ca^{2}<H^{+}$. As a rule ions of higher valency replace those of lower valency and are bound more tightly to the interlayer exchange sites. If the cations are of

the same valency, larger ions are generally better at replacing smaller ions until the exchanging ion's size and co-ordination properties do not allow it to fit the hexagonal cavity of the tetrahedral sheet optimally. Hydrogen is an exception to the rule as it behaves like a slightly hydrated di- or trivalent ion. From the replaceability series outlined above, it can be seen that at equal concentrations, Ca^{2+} will displace more Na^{+} than Na^{+} will displace Ca^{2+}. As stated earlier, if the concentration of the replacing cation is increased the exchange reaction may become favourable i.e. at high concentrations of Na^{+}, Ca^{2+} will be replaced.

2.2.1.6 Adsorption of Water By Layer Silicates.

Montmorillonite is able to adsorb polar molecules such as water by virtue of the fact that clay platelets have a residual ionic character. This as mentioned previously is because compensating cations are unable to approach the negative charge sites (mainly situated in the octahedral sheet) closely enough to completely loose the ionic character of the cation or the clay surface. Montmorillonite is able to adsorb water to a greater extent than many other clays because water is not only adsorbed on the external surfaces but also in the interlamellar space (Figure 6)

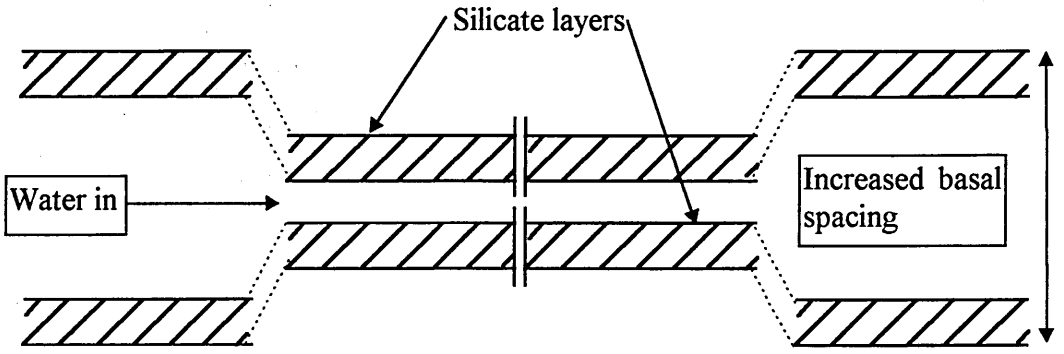

Figure 6. The expansion of the clay layers from the edges inwards upon intercalation of water.

Many of the unique properties of montmorillonite are due to the large surface area which becomes available when water enters the interlamellar space and the clay fully hydrates to produce single layers. In contrast to montmorillonite, kaolinite can only adsorb water on its surface as no interlayer space is available.

Properties of the clay mineral i.e. the charge density on the clay surface and its origin, whether tetrahedral, octahedral or both has a limited affect on the quantity of water adsorbed. Montmorillonite with a low layer charge (see section 2.1.2), intercalates a large quantity of water. Clay minerals with a high layer charge have a lower tendency to intercalate water and organic molecules as the increased electrostatic interaction between the layers and cations make it more difficult for the intercalating molecule to prise the layers apart. Particle size is also important as it determines the proportion of free surface to interlamellar surface.

The main factor governing the quantity of water adsorbed by montmorillonite is the nature of the interlayer cation. The main properties of the interlayer cation which affect water adsorption are:

1. **Size.**
2. **Valency.**
3. **Electronegativity.**
4. **Hydration energy.**

Norrish,[26] showed with Na-montmorillonite that the layers could be expanded stepwise with the addition of water layers to anhydrous Na-montmorillonite at 9.6 Å to give a basal spacing of 40 Å, above which the layers are taken to be completely dissociated. Conversely it was found that Ca-montmorillonite did not expand beyond

19.0 Å. The differences observed for the intercalation of water into Na^+ and Ca^{2+} exchanged montmorillonite can be explained in the following way:

A monovalent cation, such as Na^+, can associate with a charge deficient area on the clay surface such that on hydration, single clay sheets predominate (Figure 7).

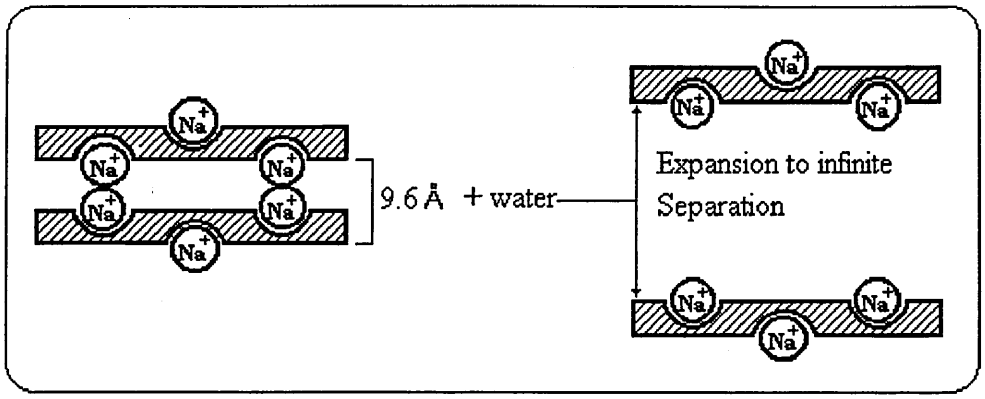

Figure 7. The expansion to infinite separation of Na-montmorillonite on hydration.

A divalent cation, such as Ca^{2+}, cannot associate with two charge deficient areas on one clay surface effectively and as a result must bind two clay sheets together. This results in a reduced surface area and reduced basal spacing of the clay sheets compared with Na-montmorillonite (Figure 8).

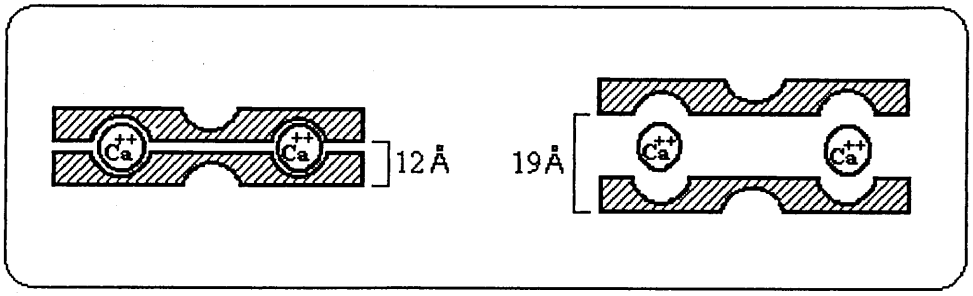

Figure 8. Divalent cations associate with two different clay platelets and consequently their basal spacing upon hydration is small.

CHAPTER 3

Clay Polymer Interactions.

3. Clay Polymer Interactions

The systematic study of clay-polymer interactions is a relatively young scientific discipline. Only since the early 1940's have major advances been made in determining the interactions of organic compounds with clays. Pre 1940's, people knew that clay-organic interactions existed because clays were used in many processes including the decolourising of edible oils and clarifying alcoholic beverages. Clay-organic interactions can even be traced back as far as biblical times when aqueous slurries of crude clay were used for the removal of grease from raw wool, known as the Fulling Process.

One of the main reasons for the rapid advances made in the 1940's occurred because it was realised that the inclusion of polymers into soil gave improved soil structure.[27,28,29] Since the 1940's, the interactions of polymers with clays have found widespread industrial use, not only as soil conditioners but also as fillers and extenders in natural and synthetic rubbers. Clays are also useful fillers in thermoplastic polymers.

Clay/polymer interactions have also been used for many years to control the stability of solid/liquid dispersions. Adsorbed polymers can be used to either keep particles apart (deflocculate) or bind them together (flocculate). Whether flocculation or deflocculation occurs is wholly dependent on the conditions existing in the clay-polymer medium, such as ionic strength and the type of polymer used whether neutral, cationic or anionic. Many industrial processes have grown up around the ability of adsorbed polymers to flocculate or deflocculate clays. The paper making industry for instance makes use of the interactions occurring between kaolinite and polymeric adhesives and dispersants which are mixed prior to contact with dilute suspensions of cellulose fibres.[30] The kaolinite in the paper acts as a filler and also as a coating agent. Flocculation of

suspended particles by polyelectrolytes is also the mechanism by which solid-liquid separation is achieved in mineral processing and also water and sewage treatment. Dispersion mechanisms on the other hand are made use of in paint production. The oil exploration industry has also made use of clay-polymer interactions since 1937 when corn starch was added to a bentonite drilling mud to control the filtration characteristics.[31] Rapid advances in drilling mud technology lead to the introduction of other polymeric compounds such as carboxymethylcellulose, tannins and lignosulphonates which were all common additives by 1945. These polymeric additives were initially used to extend the properties of a simple clay based mud and to protect the clay from salt flocculation. In present day drilling muds, the polymeric additives are often specifically designed for drilling particular formations.

The interactions of polymeric compounds with clay, can to a certain extent be related to the interactions between clay and smaller organic species which have been fairly well characterised with respect to their mode of bonding and orientation on the clay surface. This information gained for short chain organic species plays a large role when trying to interpret the interactions of polymers with the clay surface. Polymers differ from small organic compounds in their adsorption onto clay surfaces in the following ways.[32]

1. **The number of conformations which a molecule can adopt at an interface will increase rapidly with increasing molecular size.**
2. **The large number of possible surface contacts for a polymer molecule give rise to a large net energy of adsorption.**
3. **Polymer systems usually require longer times to reach equilibrium because the sizes of the molecules permit slower diffusion to the interfaces.**

4. **There is a significant probability that the polymer will not adopt a configuration consistent with the minimum free energy of the system but that it will adsorb instead in a metastable conformation.**

Thus, interactions of polymers with clay surfaces is a very complex science, in which even the way that the components of the system are brought together and mixed can have a large bearing on the complex formed. It is because of these numerous clay-polymer interactions that this chemistry is still largely descriptive, however interest in this area is huge because of the industrial applications and therefore a wealth of literature is available. It is for this reason that the present study will concentrate on literature that has a direct bearing on the work carried out in this study.

The effect of the nature and magnitude of the charge on the polymer with respect to adsorption onto clay will now be discussed. Q will be used to designate the amount of polymer adsorbed onto the clay where Q_{max} represents the maximum adsorption value or plateau. Other factors which effect the adsorption of neutral, anionic and cationic polymers will also be considered and are outlined below.

1. **Exchange cation on the clay surface.**

2. **Polymer molecular weight and structure.**

3. **Ionic strength of exchange medium.**

3.1.1 Neutral Polymers.

The adsorption of an uncharged, flexible, linear polymer from aqueous medium onto a clay surface generally leads to the desorption of numerous water molecules.[33,34] The desorption of this number of water molecules from the silicate surface leads to a net gain in entropy. Hydrogen bonding between hydroxyls or other polar groups on the polymer with oxygens of the silicate layer usually results in a very small or even positive enthalpy change.[35] Thus the adsorption of neutral polymers, especially those of higher molecular weight, is largely an entropy driven process.

In solution the polymer tends to exists as a random coil.[35] With adsorption onto the clay surface, the polymer unfurls and spreads out at the solid/solution interface. This unfurling leads to a number of contiguous sequences of polymer segments in close contact with the clay surface which are known as "trains". Trains are interspersed by "loops" which extend away from the clay surface as do the "tails" which are found at either end of the polymer chain, (Figure 9). The fraction of train segments, p, which in uncharged polymers is about 0.4 (i.e. an average of 40% of the total polymer segments may be in contact with the clay surface) is therefore an important parameter when considering the total energy of adsorption. Considering that the net segment-surface interaction energy, ε, is of the order of 1 kT unit, the total energy of adsorption may be largely due to the multiple segment surface interactions.

Adsorption of polymer onto the surface of clay is usually irreversible because it is highly improbable that all the train segments will become unattached simultaneously and remain so long enough for the polymer and clay to separate.[36]

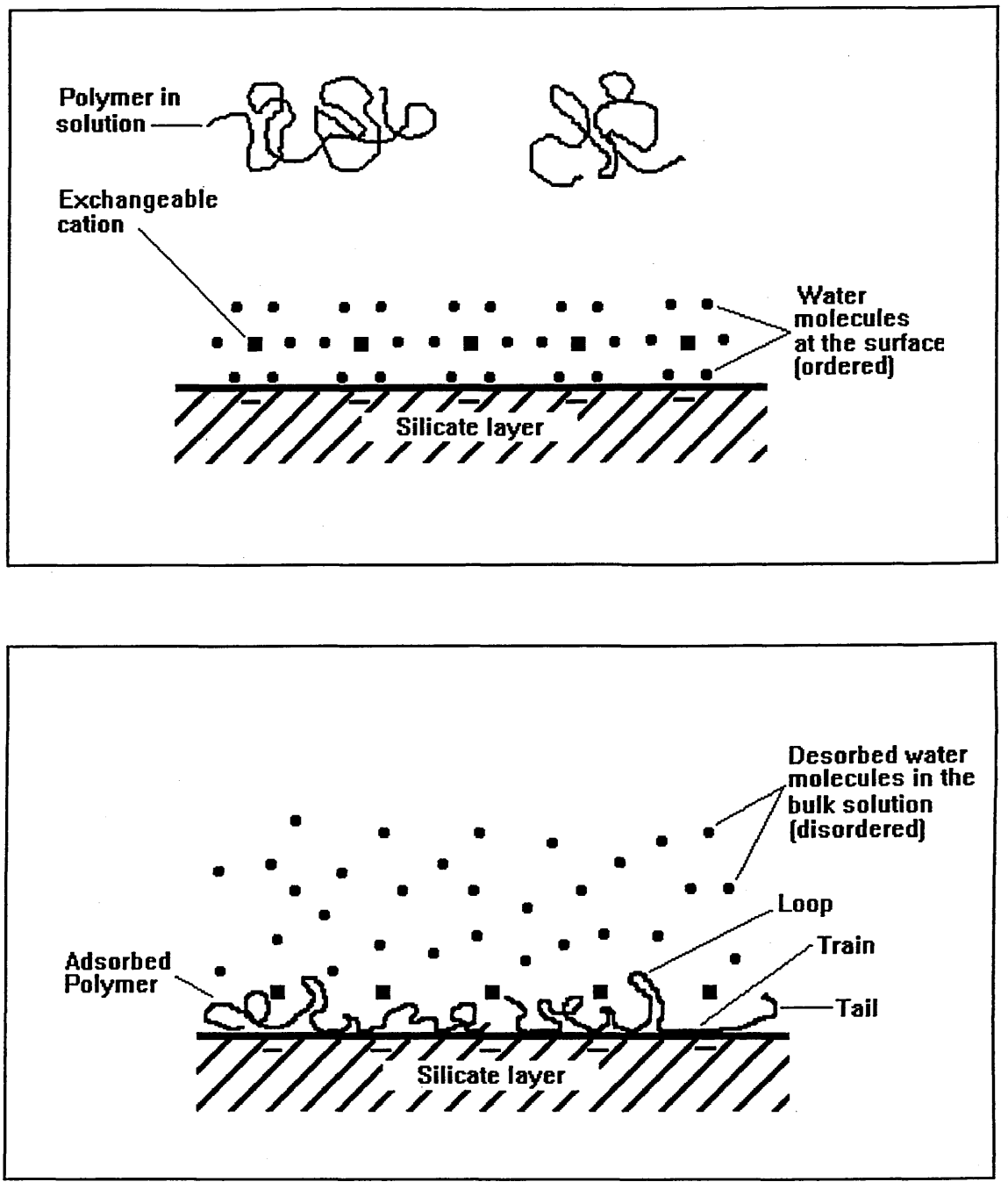

Figure 9. Diagram illustrating the desorption of numerous water molecules from a clay surface during the adsorption of an uncharged linear polymer, leading to a net gain in entropy by the system. The change in polymer conformation from a random coil in solution to a more or less extended chain at the clay/solution interface is also indicated (after Theng,[35] 1982).

Parfitt and Greenland,[33] however found that more than 80% of the polyethylene glycol (PEG) with a molecular weight of 300 could be removed from Ca-montmorillonite by repeated washing with distilled water. Conversely they also found that PEG with a molecular weight of 2000 could not be desorbed from the clay surface by washing with distilled water.

Neutral polymers generally interact strongly with clay minerals, most recorded isotherms are therefore of the "high affinity" H-type. The most informative region of the isotherm is the initial rapid rise from which information concerning the size of loops extending away from the clay surface may be gained. Unfortunately in H-type isotherms, this region is notoriously difficult to map out and even when great care is taken in determining the initial steep rise of the slope, the results may not be particularly enlightening. Burchill *et al.*[34] however determined from the isotherm's initial rapid rise that polyethylene oxide (PEO) adopts a fully extended conformation covering 26, 51 and 61% of the surface of a Na-montmorillonite as the molecular weight of the polymer increased from 800 through 1500 to 4000 respectively.

3.1.2 Examples of Neutral Polymer/Clay Interactions.

3.1.2.1 Influence of Exchangeable Cations.

The exchangeable cation associated with the clay surface can have a large bearing on Q, the quantity of polymer adsorbed by the clay. In a study carried out by Greenland,[37] it was found that the amount of polyvinyl alcohol (PVA) adsorbed by Na-montmorillonite was far greater than that adsorbed by Ca^{2+} or Cs^{+} exchanged montmorillonite. Q_{max} for the addition of PVA (Mwt 25000) to Na-montmorillonite was 800 mg g^{-1} clay whilst the observed Q_{max} on Ca^{2+} and Cs^{+} exchanged montmorillonite

was only 300 and 130 mg g^{-1} clay respectively. Greenland suggested that unlike Ca^{2+} and Cs^{+} exchanged montmorillonite, the surface area of Na-montmorillonite was completely accessible to the PVA. Differences arise in the accessibility of the clay's surface area due to flocculation and aggregation of the clay platelets into tactoids, the extent to which this occurs depends predominantly on the exchangeable cation associated with the clay, (Figure 10). It is also known that when the exchange cation on montmorillonite is exchanged from Na^{+} to Ca^{2+}, there is an increase in tactoid size in the c direction.[38,39] The number of sheets/tactoid increases from 1-2 in Na-montmorillonite to 8-10 in Ca-montmorillonite which leads to a decrease in the surface area available for interaction with polymer. In addition, the basal separation of Na-montmorillonite in water may be larger than 40 Å whereas Ca^{2+} and Cs^{+} exchanged montmorillonites do not expand beyond a d(001) spacing of ~ 19 and 15 Å respectively.[40,41] Differences in basal spacings may therefore have a profound effect on the adsorption of polymers into the interlamellar space. For example some higher molecular weight polymers may have dimensions in solution exceeding those of the basal spacing of the clay and therefore these polymers cannot gain entry to the interlamellar space.

In agreement with Greenland,[37] Hetzel *et al.*[42] also showed that Q_{max} for the addition of PVA (Mwt 11-31000) to Na^{+} exchanged SWy-1 montmorillonite was equal to 800 mg g^{-1} clay. This observed Q_{max} value is also in agreement with that observed by Burchill *et al.*[43] for the addition of PVA to Na-montmorillonite. Furthermore, Hetzel *et al.*[42] also showed that exchanging the largely deflocculated Na-montmorillonite with other cations including Ca^{2+}, Mg^{2+} and K^{+} resulted in a decrease in Q_{max}.

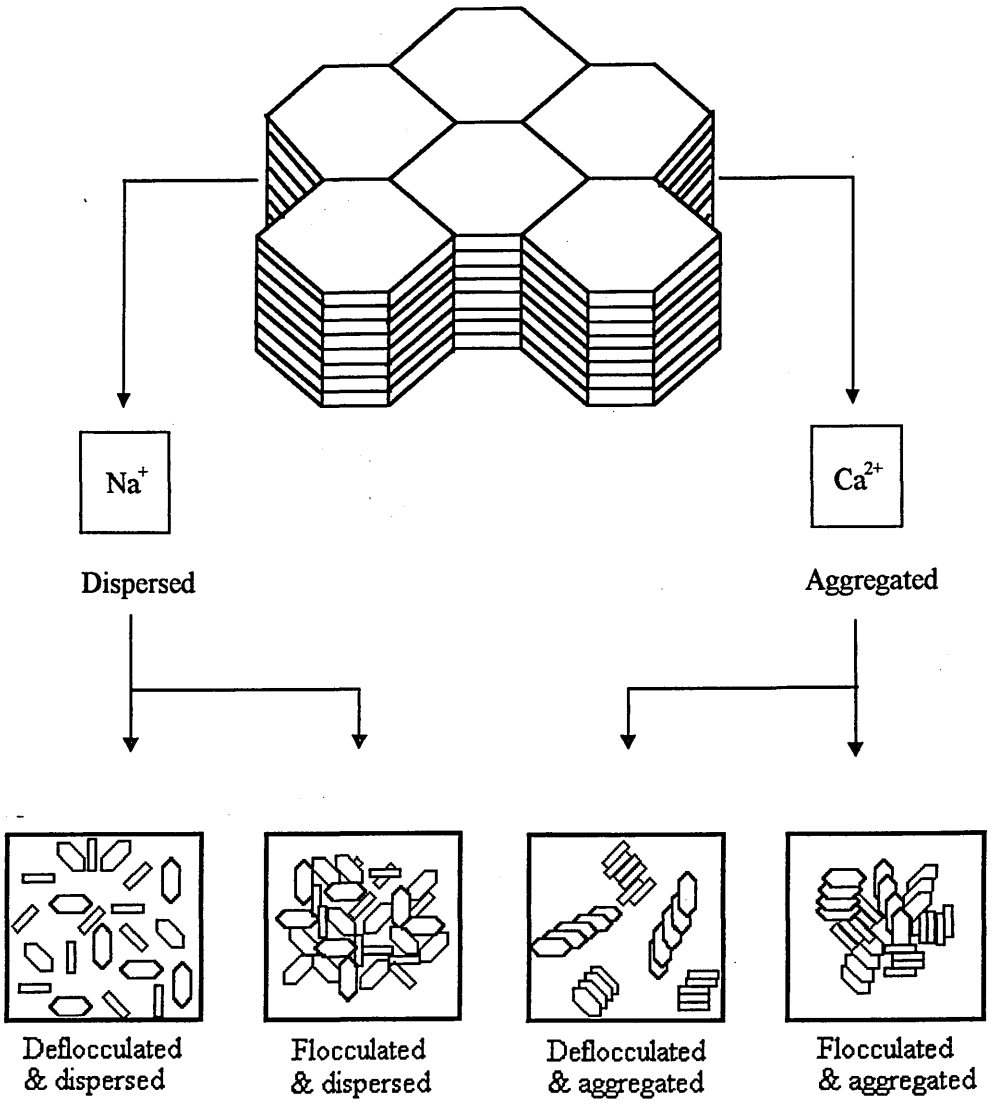

Figure 10. Diagram illustrating the effect of the exchangeable cation on flocculation and deflocculation of the clay platelets.

The addition of PVA (Mwt 11-31000) to these three cation exchanged forms of SWy-1, showed that adsorption increased in the order $Ca^{2+}<Mg^{2+}<K^{+}$ and exhibited Q_{max} values equal to 225, 250 and 400 mg g^{-1} clay respectively. The decrease in Q_{max} observed on exchanging from a predominantly Na^{+} exchanged clay to another form has been attributed to a decreased interlayer distance when the clay is exchanged with K^{+}, Ca^{2+} and Mg^{2+}.[42] Interlayer distances for Ca^{2+} or Mg^{2+} exchanged montmorillonite are similar when in aqueous solution.[44] Consequently the accessibility of interlayer surfaces for PVA uptake should be equal for the two forms of cation exchanged clay resulting in similar Q_{max} values which is in fact the case, as shown above.

In a recent study by Gu and Doner,[45] concerning the interactions between polysaccharides (PSS) with Silver Hill illite, it was observed that only slightly differing amounts of neutral PSS were adsorbed by three different cation exchanged illite clays. The three types of cation exchanged clays under examination were Na^{+}, Ca^{2+} and Al-p illite (Al-p are hydroxy-Al polycations; $10^4 < Mwt < 5x10^4$) all exhibited Q_{max} values of between 37 and 41 mg g^{-1} clay. An earlier study showed that the Q_{max} values observed for the addition of PSS (Mwt 2 million) to three types of cation exchanged montmorillonite increased in the order $Ca^{2+}<Al^{3+}<Na^{+}$ and reached values of 105, 110, and 250 mg g^{-1} clay respectively.[46] In this study, as in others,[47] the cation exchange form of the clay did have a large bearing on the quantity of PSS adsorbed.

3.1.2.2 Influence of Polymer Molecular Weight.

In deflocculated montmorillonite, such as dilute suspensions of Na-montmorillonite, increasing the molecular weight of the polymer increases the amount adsorbed because surface accessibility is not restricted. Bottero *et al.*[48] studied the

adsorption of non ionic polyacrylamide (PA) on Na-montmorillonite and indeed found that as the molecular weight of the polymer was increased from $4.4x10^4$ to $3x10^6$, Q_{max} increased from 190 to 680 mg g^{-1} respectively. The use of ^{13}C NMR spectroscopy in this study has also shown that up to an adsorption value of Q = 200 mg g^{-1}, the polymer is adsorbed largely as trains for all the molecular weights studied. When Q exceeds 200 mg g^{-1} however, the polymer makes larger and larger loops and tails towards the bulk solution. In accordance with Bottero *et al.*, Schamp and Huylebroeck found that Q_{max} for the addition of PA to deflocculated Na-montmorillonite increased with increasing molecular weight.[49] They observed that increasing the molecular weight of the polymer from 300 000 to 400 000 resulted in an increase in Q_{max} from 700 to 850 mg g^{-1}. The Q_{max} values recorded by Schamp and Huylebroeck also reached greater values than those observed by Bottero *et al.*, even for the addition of lower molecular weight PA to the Na-montmorillonite. Greenland,[37] also found that Na-montmorillonite adsorbed larger quantities of PVA as the molecular weight of the polymer was increased from 25-100 000. Finally Q_{max} values recorded for the addition of a range of polyethylene glycol (PEG) molecules with increasing molecular weight to Na-montmorillonite was investigated by Zhao *et al.*[50] They observed that increasing the molecular weight of the PEG molecule contacted with Na-montmorillonite lead to increasing Q_{max} values up to a molecular weight of 2000 at which point Q_{max} was approximately equal to 100 mg g^{-1} clay. Zhao *et al.*[50] state that addition of PEG with a molecular weight > 2000 to Na-montmorillonite lead to no significant increase in the value of Q_{max}. Conversely Burchill *et al.*[48] observed no finite Q_{max} value for addition of PEG with molecular weights > 2000 to Na-montmorillonite. In fact for the addition of PEG with molecular weights equal to 800, 1500 and 4000 to Na-montmorillonite, Burchill *et al.*[48] observed an increase in Q_{max} corresponding to the adsorption of 78, 154, and 202 mg g^{-1} clay respectively.

With clay systems where the exchangeable cation is other than Na^+, increasing the molecular weight of the polymer can lead to a decrease in the quantity of polymer adsorbed due to reduced accessibility of the interlamellar region. Greenland,[37] observed that increasing the molecular weight of PVA contacted with both Ca^{2+} and Cs-montmorillonite resulted in a decrease in Q_{max}. The same phenomenon was seen by Schamp and Huylebroeck who state that Q_{max} decreased for the addition of increasing molecular weights of PA to H-montmorillonite.[49]

Schamp and Huylebroeck also manage to distinguish between "surface adsorption" and "pore" or interlamellar adsorption, postulating that:

- External surface adsorption is fast, has a normal temperature dependence for an exothermic reaction (i.e. increasing temperature decreases the adsorption), adsorption increases with increasing molecular weight and this is the major type of adsorption for deflocculated clays such as Na- montmorillonite.

- Pore or interlamellar adsorption is slow, polymer molecules enter with difficulty and maximum adsorption decreases rapidly with increasing molecular weight.

Slow pore adsorption by the H-montmorillonite was shown to almost disappear when the PA was sufficiently large enough to be completely restricted from the pore region of the clay. Thus Schamp and Huylebroeck confirmed that the only type of adsorption taking place on H-montmorillonite with the addition of very high molecular weight PA was the rapid surface type.

As stated above, the addition of increasing molecular weights of neutral polymer to montmorillonite exchanged with cations other than Na^+ can lead to a decrease in the quantity of polymer adsorbed. One notable exception to this statement would however

be the addition of PEG to different cation exchanged clays. Parfitt and Greenland,[33] have shown that increasing the molecular weight of PEG added to Ca-montmorillonite from 200 to 2000 increases Q_{max} from 70 to 300 mg g^{-1} clay respectively. This increase in Q_{max} maybe because only low molecular weight polymers were added to the Ca-montmorillonite and as a result no interlamellar restriction of polymer occurs. Zhao *et al.*[50] also observed an increase in Q_{max} on increasing the molecular weight of PEG added to a Ca-bentonite.

3.1.2.3 Ionic Strength Effects.

The ionic strength of the clay/polymer medium usually has a large bearing on the quantity of non ionic polymer adsorbed. With increasing salt concentration, the amount of aggregation in the system increases,[51] and the spacing between clay platelets decreases.[37] Both of these parameters result in a decrease in the quantity of polymer adsorbed by the clay. The effect of added salt is to suppress the diffuse double layer of the clay platelets which effectively means that they do not repel each other to the same degree and therefore aggregation may occur, (section 3.3.1). Greenland,[37] found that the basal spacing of the Na-montmorillonite and as a result Q_{max} for addition of PVA to Na-montmorillonite decreased rapidly with the addition of increasing aliquots of $NaNO_3$ to the medium. Q_{max} actually decreased from approximately 750 mg g^{-1} clay to about 120 mg g^{-1} clay on changing the concentration of added salt from zero to 1.0 mol L^{-1}, respectively. Greenland,[37] states that any influence that added electrolyte has on the adsorption of polymer is dominated by the effect that the added salt has on the interlamellar separation of the clay platelets. In agreement with Greenland, Bailey *et al.*[5] also report decreasing adsorption of neutral polymer on montmorillonite when increasing the salinity of the medium. In this study however, K-montmorillonite was contacted with

PA in the presence of increasing quantities of added KCl. The observed Q_{max} for a system with no added salt was 700 mg g^{-1} clay, this value decreased rapidly to approximately 300 mg g^{-1} clay in the presence of 0.4 mol L^{-1} KCl. This decrease in Q_{max} at increasing ionic strength of the medium may again be attributed to a decrease in the interlamellar separation of the clay platelets leading to aggregation and therefore decreasing adsorption of polymer. It should also be remembered that K-montmorillonite exhibits a higher degree of platelet aggregation in a salt free aqueous suspension than does Na-montmorillonite and consequently any addition of salt to K-montmorillonite compounds this problem.

3.1.3 Cationic Polymers.

The adsorption of cationic polymers at the surface of clays is a result of coulombic interactions taking place between the cationic groups on the polymer and the negative sites on the clay.[52,53] These coulombic interactions can actually cause a reversal of the clay's surface charge from negative to positive beyond a given level of polycation uptake.[54] It is also widely accepted that cationic polymers are irreversibly adsorbed onto the surface of clays and consequently no rearrangement in polymer configuration can take place after adsorption. Ueda *et al.*[55] noted that after contacting Na-montmorillonite with polysulfone (Mwt 16.7 x 10^4), no desorption of the polymer occurred even after treatment with 3.0 mol L^{-1} NaCl or $CaCl_2$. Recently, several investigations into the interactions taking place between Na-montmorillonite and copolymers of acrylamide and N,N,N-trimethylaminoethylchloride acrylate (PCMA) have been carried out by a French group. Much of their work will be discussed in the following pages along with observations made by other authors. Denoyel *et al.*[56] investigated the interactions taking

place between Na-montmorillonite and PCMA by microcalorimetry. The structure of PCMA is shown below (Figure 11).

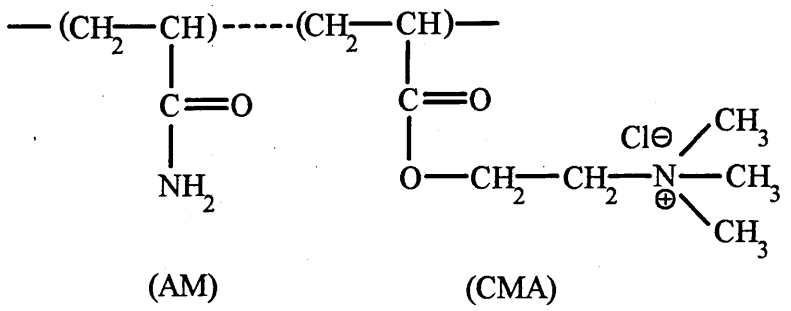

Figure 11. The structure of PCMA prepared by polymerisation of acrylamide (AM) and N,N,N-trimethylaminoethyl chloride acrylate (CMA). Samples of various cationicity were prepared by altering the molar percentage of CMA.

Denoyel *et al.*[56] observed that for cationic polymers, the net segment surface interaction energy, ε, greatly exceeds that observed for neutral polymers and assumes values up to 4 kT for addition of PCMA to clay. They also observed that the enthalpy of exchange for a CMA unit in PCMA is practically independent of the surface coverage ratio, θ, ($\theta = Q/Q_{max}$) whereas the enthalpy has generally been found to decrease with θ for nonionic polymers.[57] They state that the process of PCMA adsorption does not allow complete coverage of the surface. For example the addition of PCMA of molecular weight 2.0×10^4 or 2.1×10^6 to Na-montmorillonite results in θ values of 0.95 and 0.65 respectively. Up to these surface coverage values, ΔH was constant. After which, adsorption occurred with a reduced exothermic effect suggesting that the latterly adsorbed macromolecules are only slightly fixed upon the surface of the clay. They also observed that for PCMA of low cationicity, 1-5%, practically all the CMA groups of the copolymer are adsorbed on the clay surface. This was assumed to be true since the observed value of ΔH/CMA unit was similar to that obtained for the CMA monomer and had a value of approximately 10 kJ mol^{-1}. It was also noted that the value of ΔH/CMA

unit decreased with increasing cationicity of the polymer. For example increasing the cationicity of the PCMA from 1 to 100% caused the value of ΔH/CMA to decrease from 10 to 2.4 kJ mol^{-1}.

Adsorption of cationic polymers generally proceeds via the instantaneous collapse of the polycation chain onto the surface of the clay resulting in a large number of train segments, p, and relatively few short loops.[35] The value of p for the addition of cationic polymers to clay is usually > 0.7 indicating that > 70% of the total polymer segments are in contact with the clay surface at any one time. Ueda *et al.*[55] determined the value of p for the addition of polysulfone at a fixed Mwt of 16.7 x 10^4 to Na-montmorillonite. This was achieved by calculating the anion exchange capacity (AEC) of the clay which in this case is entirely due to the cationic groups contained in the loops and tails of the adsorbed polymer. The difference between the total amount adsorbed and the AEC therefore represents the amount of segments in trains. Interestingly, they found that for up to 50% coverage, p was equal to 1. Even for 100% coverage, only about 25% of the segments are contained in loops and tails.

3.1.4 Examples of Cationic Polymer/Clay Interactions.

3.1.4.1 Influence of Exchangeable Cation.

The exchangeable cation associated with clay normally has a large bearing upon the amount, Q, of cationic polymer adsorbed. In a recent study Gu *et al.*[45] noted that Na-illite exhibited a higher adsorption capacity for cationic PSS than did Ca-illite. The adsorption isotherm obtained for the addition of PSS to Na-illite was of the high affinity type, indicating the strong affinity of PSS for the clay surface. The adsorption isotherm also suggests the possibility of multilayer adsorption indicated by a second steep rise in

the curve after an initial plateau had been reached. The adsorption isotherm obtained for the addition of PSS to Ca-illite indicates that only one layer of PSS is present under the experimental conditions employed. Further, the affinity of PSS for Ca-illite is reduced with respect to that for Na-illite, shown by differences in the initial steep rise of the respective adsorption isotherms.[58] The differences in the adsorption behaviour of PSS on Na^+ and Ca^{2+} exchanged illite were explained by Gu *et al.*,[45] who indicate that Ca^{2+} is more effective than Na^+ at screening the negative surface charge from the cationic polymer which results in decreased adsorption. They also state that Na^+ cations reside in the clay's diffuse double layer and are thus more easily replaced by the polycation than are Ca^{2+} cations.

Parfitt,[59] also noted that the exchangeable cation associated with the clay had a large bearing on Q_{max}. He observed that Na-montmorillonite exhibited a higher adsorption capacity for cationic glucosamine hydrochloride than did Ca-montmorillonite. Na-montmorillonite actually adsorbed 4 times the quantity of glucosamine hydrochloride than was adsorbed by Ca-montmorillonite for addition of the same equilibrium concentration of polymer. Q_{max} values observed for addition of this polycation to Na-montmorillonite equated to approximately 80% of the total exchangeable Na^+ being replaced by the polymer at the surface of the clay.

A related study was carried out by Patzko *et al.*[60] who investigated the interactions taking place between the cationic surfactant hexadecylpyridinium and different cation exchanged montmorillonites. They observed that Q_{max} increased in the order $Ca^{2+}<K^+<Mg^{2+}<Na^+$ for addition of hexadecylpyridinium to the different cation exchanged clays. This order of increasing Q_{max} values is in agreement with the results outlined above for the addition of cationic polymer to clay.

3.1.4.2 Influence of Polymer Molecular Weight and Cationicity.

The value of Q_{max} for the addition of cationic polymers to clay may be highly dependent on the molecular weight of the added polymer. For example Durand-Piana *et al.*[61] investigated the interactions taking place between Na-montmorillonite and PCMA with different molecular weights and cationicities. They observed that when the cationicity, τ, of PCMA was 1%, Q_{max} depended upon the molecular weight of the polymer and increased from 1750 to 2650 mg g^{-1} clay when the molecular weight of the polymer was increased from 8×10^4 to 2×10^6. Conversely when the cationicity of both these different molecular weight PCMA macromolecules was increased to 100%, the value of Q was no longer molecular weight dependant and Q_{max} reached a constant value of approximately 250 mg g^{-1} clay for addition of either molecular weight polymer to the clay. Interestingly they observed little deviation in Q with increasing PCMA molecular weight when τ was in excess of 25%. Durand-Piana therefore suggested that when $\tau <$ 15%, the dominant mechanism of polymer adsorption was through bridging of the clay particles. Bridging was made possible at low τ due to adsorption of a large excess of the nonionic amide groups thus allowing the presence of unadsorbed ammonium groups in long loops and tails which extended into the bulk solution from the surface of the clay. The value of Q_{max} at low cationicity therefore depended upon chain length and ultimately the molecular weight of the polymer. Conversely, when τ was high, > 25%, then charge neutralisation became the dominant mechanism and the PCMA adopted an essentially flat conformation at the clay surface. This type of adsorption exhibited little or no molecular weight dependence because of electrostatic repulsions and chain stiffness which prevented high packing at the clay surface. Further evidence that the adsorption of highly charged PCMA was governed by electrostatic effects was observed by Denoyel *et*

al.[56] who calculated that the total number of charge units/nm^2 was roughly constant for cationicities between 15-100%. Obviously the cationicity of the PCMA is an important parameter in determining whether the polymer adsorbs onto the clay in trains or whether it bridges particles. For the addition of PCMA to Na-montmorillonite therefore, the cationicity of the polymer ultimately determines whether Q is molecular weight dependent or not.

Denoyel *et al.*[56] also noted that as the molecular weight of PCMA added to Na-montmorillonite was increased, the number of polymer segments adsorbed in trains decreased. For example, p, decreased from 0.54 to 0.13 on increasing the molecular weight of the PCMA from 2 x 10^4 to 2 x 10^6, respectively. Denoyel *et al.*[56] state that the decrease in p with molecular weight is due to the fact that crossing of two parts of a chain on the clay surface is not allowed due to steric hindrance and electrostatic repulsion. Consequently one chain has a loop conformation which decreases the value of p. The greater the molecular weight of the polymer, the larger the number of loops and therefore the smaller the value of p.

When the molecular weight of the PCMA was fixed at 5 x 10^5, Denoyel *et al.*[56] observed that an increase in cationicity from 1% to 30% resulted in a decrease in Q_{max} from 2400 mg g^{-1} to 440 mg g^{-1} clay. This decrease in Q_{max} may be attributed to the progressive growth of electrostatic repulsions between the increasingly charged and rigid chains at increasing cationicity.

Several investigations by the same French group have also been carried out concerning the interactions taking place between PCMA and suspensions of silica.[62,63,64] Silica particles usually have a net negative surface charge and therefore cationic polymers

interact with the silica through coulombic interactions as is the case with clay. Consequently the same experimental observations were made for the addition of PCMA to silica as those recorded for its addition to clay. For example, as the cationicity of PCMA at fixed molecular weight was decreased, Q_{max} increased. Also, at τ = 1%, increasing the molecular weight of the PCMA lead to increasing Q_{max} values. At high τ however, increasing the molecular weight did not lead to significant increases in Q_{max} values. These differences in PCMA adsorption may again be related to the degree of cationicity of the polymer which in turn results in the existence of two different adsorption mechanisms. At high τ > 15%, PCMA predominantly adsorbs onto silica via a charge neutralisation mechanism whereas at low τ < 5%, the major adsorption mechanism is via interparticle bridges. Wang *et al.*[62] state that for the intermediate ranges of cationicity, the two effects can operate simultaneously.

3.1.4.3 Ionic Strength and pH Effects.

The ionic strength of the dispersion medium can have a large bearing upon the quantity of cationic polymer adsorbed by clay. Bailey *et al.*[5] carried out Anion Exclusion experiments to determine the total surface area of Na^+ and K^+ exchanged montmorillonite at differing ionic strengths by adding the chloride salt of the appropriate cation to a 5% dispersion medium in the range 1.0×10^{-3} to 0.5 mol L^{-1}. They found that at low ionic strengths, Na-montmorillonite is completely dissociated into single platelets with fully developed double layers on all surfaces. This gave a total surface area of 760 m^2 g^{-1}. Conversely 5% suspensions of the K-montmorillonite are aggregated into tactoids over the entire electrolyte range studied, the maximum observed surface area here was 320 m^2 g^{-1}. This degree of aggregation relates to tactoids consisting of 2-3 platelets.

Bailey *et al.* note that at low ionic strengths (1.0×10^{-3} mol L^{-1} KCl), the energy of adsorption of cationic polyacrylamide on K-montmorillonite is much greater than the attractive forces between the clay sheets, thus the polymer is able to overcome the forces holding the tactoids together. Consequently, the surface area available for interaction increases to that of the individual clay plates, about 760 m^2 g^{-1} and Q_{max} is large, approximately 1300 mg g^{-1} clay. As the ionic strength of the dispersion medium was increased, it was noted that Q fell sharply to a plateau value of 300 mg g^{-1} clay where it remains constant for subsequent additions of KCl. This decrease in Q is due to a change in the association energy of the clay tactoids which increases with increasing ionic strength of the dispersion medium. The available surface area for interaction at high ionic strength therefore falls to that of the external faces of the tactoids, 320 m^2 g^{-1}. Furthermore at high ionic strength, there is also a contribution to decreasing adsorption from the screening of the attractive electrostatic interactions between the positively charged polymer and the negatively charged clay. Finally competition between inorganic cations and cationic polymers for adsorption sites on the negatively charged clay surface increases with increasing ionic strength which also results in decreasing Q_{max} values.[65]

Conversely, Ueda *et al.*[55] noted that addition of NaCl to the dispersion medium resulted in an increase in the amount of polysulfone (Mwt 16.7×10^4) adsorbed onto Na-montmorillonite. This increase in Q was also accompanied by an increase in the AEC of the complex. Consequently, it was proposed that the polysulfone in a dispersion medium containing NaCl exists in a coiled configuration and is therefore adsorbed onto the surface of the clay with retention of this configuration. Ueda *et al.*[55] state that the configuration of the polymer at the clay surface accounts for both the increased polymer adsorption and also the increase in AEC.

Gu *et al.*[45] observed no dependence of Q upon the ionic strength of the medium for the addition of cationic PSS to Na-illite. They explain this by stating that the surface charge on illite does not change with the ionic strength of the dispersion medium. Therefore, because adsorption of PSS on Na-illite is driven primarily by surface charge neutralisation, no variation in Q_{max} is observed. Gu *et al.*[45] also noted that an increase in the pH of the dispersion medium caused a slight increase in Q_{max}. This occurred because an increase in pH increases the negative edge sites on the illite surfaces which therefore results in increased Q_{max} values.

Wang *et al.*,[66] members of the French group investigating the interaction of PCMA with negatively charge particles, studied the interactions occurring between PCMA (Mwt 7.5 x 10^5, τ = 0.5%) and silica particles in a dispersion medium of increasing ionic strength. Q usually increases with ionic strength for colloids and polymers of opposite charge since an increase in the salt concentration decreases the repulsions between the loops and tails of the polyelectrolyte.[67] Hesselink,[68] however pointed out that when charge interaction was the reason for adsorption, Q would decrease on increasing the ionic strength of the dispersion medium. Wang *et al.*[66] state that this is in fact what happened with their system in that Q decreased rapidly as the ionic strength of the medium was increased from 0 to 0.3 mol L^{-1} NaCl. They indicate that this decreased adsorption was due to competition between the cationic groups of the PCMA and the excess Na^+ in the dispersion medium which they state leads to a partial desorption of the polymer and consequently Q decreases.

3.1.5 Anionic Polymers.

On contacting clay with anionic polymer, a relatively low degree of adsorption takes place compared to the addition of cationic or nonionic polymers to clay.[69] This low value of Q is entirely due to a net negative charge associated with the clay platelets which has the effect of repelling anionic polymers which come into close contact with the clay surface. The small uptake of polyanions by the clay surface may be appreciably increased by altering the conditions employed when mixing the clay with the polymer and/or altering the exchangeable cations associated with the clay. A large increase in Q_{max} is observed for all anionic polymers as the pH of the medium is decreased and/or the salinity increased. This is due to charge neutralisation by protonation or charge screening by the electrolyte. Enhanced polyanion uptake may also be observed as the valency of the exchangeable cation associated with the clay is increased.[70]

The conditions on mixing the polymer with clay and the exchangeable cation associated with the clay therefore determine the mode of interaction of polyanions with the clay surface. Ruehrwain and Ward,[71] proposed that the adsorption of anionic polymers occurred through ion exchange which for sodium polymethacrylate, the polyanion they investigated, involved the replacement of hydroxyls associated with the clay by the carboxylate ions of the polymer. Theng,[35] also suggested that polyanions adsorb onto the edges of the clay platelets at low pH through anion exchange due to protonation of exposed aluminium at these sites. Michaels and Morelos,[72] suggested that polyanion adsorption occurs mainly due to hydrogen bonding between the clay and the non-ionised hydroxylic, amidic and carboxylate functions of the polyacrylamide they investigated. A further mode of polyanion/clay interaction was suggested by

Mortensen,[73] who indicated that cationic bridges between the anionic groups on the polymer and the negative sites on the clay surface were formed.

Even with the appreciable increases in adsorption due to high salt, low pH and the presence of polyvalent cations, the extent of polymer adsorption is far below that observed for the adsorption of neutral or cationic polymers onto clay. It is generally accepted that polyanions are adsorbed by relatively few train segments and do not enter into the interlamellar space of layer silicates in the pH range 5-7 relevant to this study.[71,74] Intercalation of appreciable quantities of polyanion may however occur at low pH when the polyanion can behave and adsorb like an uncharged species.[75] Lee *et al.*[76] concluded that the adsorption of high molecular weight hydrolysed polyacrylamide (PHPA) occurred on the basal and edge sites of kaolinite. However Q_{max} for edge site adsorption was significantly higher than for basal surface adsorption especially at low pH or high salinity even though the edge surface of the clay only contributes about 25% of the total surface area in the kaolinite studied. Edge site adsorption is also considered to be the dominant type of adsorption on montmorillonite clays.[73]

3.1.6 Examples of Anionic Polymer/Clay Interactions.

3.1.6.1 Influence of Exchangeable Cation.

As outlined previously, the exchangeable cation associated with the clay has a significant effect on the adsorption maximum for anionic polymers. Espinasse *et al.*[77] studied the adsorption of anionic polyacrylamide and acetamide onto Na^+, Ca^{2+} and Al^{3+} cation exchanged montmorillonite and found that for acetamide, Na-montmorillonite adsorbed the largest quantity with Q_{max} equal to 3 mg g^{-1} followed by Ca-montmorillonite and finally Al-montmorillonite. Increasing the valency of the cation decreases the

adsorption of simple molecules such as acetamide due to flocculation which decreases the edge surface area available for interaction. Conversely Q_{max} for the adsorption of PHPA on the three types of cation exchanged montmorillonite increased in the order $Na^{+}<Ca^{2+}<Al^{3+}$, resulting in Q_{max} values of 2, 8 and 15 mg g^{-1} clay respectively. The authors suggest that protonation of the amidic functions on the polymer assume higher values in the presence of higher valent cations which display a higher polarising power, this inevitably leads to an increase in Q_{max} when going from $Na^{+}<Ca^{2+}<Al^{3+}$ exchanged montmorillonite. In contrast to acetamide adsorption, the edge surfaces on the clay are not saturated when PHPA is involved due to the existence of bridge linkages between the particles. Thus the decrease in surface area due to flocculation which is consistent with increasing the valency of the exchangeable cation does not have a major bearing on the value of Q_{max}. A similar enhancement of considerably less magnitude was observed by Mortensen,[73] for the adsorption of hydrolysed polyacrylonitrile (HPAN) on kaolinite. Again it was observed that the presence of high valence exchange cations on the clay resulted in increased adsorption of polyanion with respect to univalent cation exchanged clays. Mortensen[73] in fact observed increasing Q_{max} values for the following cation exchanged clays in the order, $Na^{+}<K^{+}<NH_4^{+}<H^{+}<Ba^{2+}<Ca^{2+}<Th^{4+}$. He subsequently postulated that the higher valent exchange cations act as bridges between the anionic groups on the polymer and the negatively charged sites on the clay i.e. Clay-Ca-OOCR. In a similar study by Theng,[78] the adsorption of fulvic acid was found to increase for different cation exchanged montmorillonites in the order $Ba^{2+}<Ca^{2+}<Zn^{2+}<La^{3+}<Al^{3+}<Cu^{2+}<Fe^{3+}$. Theng related the affinity of the fulvic acid for the clay surface to the polarising power of the exchangeable cation. He also inferred that the fulvic acid is linked through its ionic carboxylate group to the exchangeable cation by means of water bridges, (Figure 12).

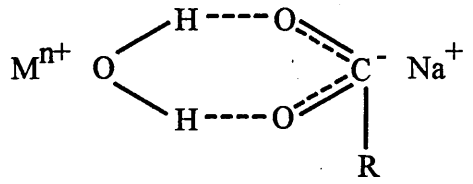

Figure 12. Shows how fulvic acid is linked through its carboxylate group to the exchangeable cation by means of water bridges. M^{n+} and R denote the polyvalent cation associated with the clay and the remainder of the fulvic acid polyanion respectively.[78]

The adsorption of anionic polysaccharide has been examined for Na^+, Ca^{2+} and Al-p-illite by Gu and Doner.[45] The usual increase in adsorption as the valency of the cation increased was seen i.e. Q_{max} increased on going from Na^+ then Ca^{2+} to Al-p-illite. Like Mortensen, Gu and Doner postulated that polyvalent cations acted as bridges between the anionic polysaccharide and the negatively charged clay surfaces leading to increased adsorption of the polymer compared with that of Na-illite.

3.1.6.2 Influence of Polymer Molecular Weight.

The value of Q_{max} for anionic polymers is considerably less dependent on molecular weight than the Q_{max} values observed for addition of uncharged and cationic polymers to clay, consequently few studies have paid attention to its influence. Espinasse *et al.*[77] however observed that as the molecular weight of PHPA was doubled from 6 x 10^6 to 11 x 10^6, the value of Q_{max} only increased from 13 to 15 mg g^{-1} clay on addition to Na-montmorillonite. These results were however obtained in the presence of 100 g L^{-1} NaCl, hence the high Q_{max} values. Stutzmann *et al.*[74] investigated the addition of the same two polymers to Na-montmorillonite in the presence of no added salt. They observed that Q_{max} increased from 2.4 to 2.8 mg g^{-1} on increasing the molecular weight

of the polymer from 6 x 10^6 to 11 x 10^6 which is consistent with the observations made by Espinasse *et al.*[77] It can be seen however that there is a five fold increase in the value of Q_{max} for the addition of PHPA to Na-montmorillonite in the presence of 100 g L^{-1} NaCl. In summary, the influence of molecular weight on polyanion adsorption is minimal even when adsorption occurs from a saline medium.

3.1.6.3 Polymer Hydrolysis and Ionic Strength Effects.

The effects of polymer hydrolysis on the value of Q_{max} have been studied by Stutzmann *et al*[74] They have shown that while Q_{max} assumes a value of 3 mg g^{-1} clay for 15, 20 and 25% PHPA on Na-montmorillonite, there is considerably less affinity between the 15% PHPA and the clay than for the 20 and 25% hydrolysed samples. The differences in adsorption behaviour between differently hydrolysed PHPA are further enhanced at increased ionic strength where Q exhibits a five fold increase to 15 mg g^{-1} for the 20 and 25% PHPA yet barely doubles for the 15% PHPA. Espinasse *et al.*[77] state that the increase in salinity of the clay/polymer medium has the effect of screening the negative charges on the polymer from one another and from those associated with the clay platelets thus allowing the polymer to compact and collapse onto the clay surface, (Figure 13).

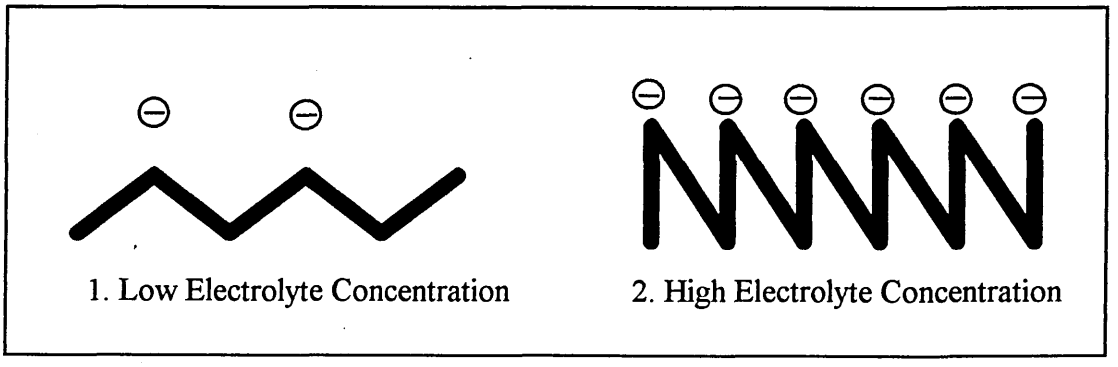

Figure 13. Effect of electrolyte concentration on polyanion configuration.

Mortensen,[79] also observed increased polyanion uptake with increasing salinity of the dispersion medium. He found for the addition of HPAN to Na-kaolinite that Q_{max} increased from approximately 1.0 mg g^{-1} to 4.5 mg g^{-1} clay on increasing the salinity of the dispersion medium from 0 to 0.1 mol L^{-1} NaCl. In agreement with Espinasse *et al.*, Mortensen postulated that increasing the concentration of Na^+ in the dispersion medium caused a reduction in the negative potential on both the clay and the polymer. This leads to a lowering of the electrostatic repulsions between the HPAN and the kaolinite surface which permits an increased possibility of interaction. Again in agreement with Espinasse *et al.*, Mortensen states that an increase in the ionic strength reduced the electrostatic repulsion between the charged sites on the HPAN leading to a reduction in the size and configuration of the polymer to that of a normal random coil.[80] This therefore results in closer packing of the polymer molecules at the clay surface leading to increased Q_{max} values. Page *et al.*[81] also observed increasing PHPA uptake on Na-kaolinite at increased salinity of the dispersion medium.

Mortensen[79] also investigated what effect addition of various metal chloride salts to the dispersion medium had on the quantity of HPAN adsorbed on Na-montmorillonite. As stated previously, the addition of NaCl to the dispersion medium lead to an increase in Q_{max}. It was found however that greater increases in Q_{max} were observed for the addition of other cations such as H^+, NH_4^+ and K^+ all added in the chloride salt form. The effect of these various cations on the value of Q_{max} followed the lyotropic series $H^+ > NH_4^+ > K^+ > Na^+$ where the cations with small effective radii were more effective at shielding the negative charge on both the kaolinite and HPAN leading to an increase in Q_{max}. Addition of 2:1 electrolytes such as $MgCl_2$ or $CaCl_2$ to the dispersion medium was much more effective at increasing Q_{max} than addition of 1:1 electrolytes.

Finally, Bailey *et al.*[5] noted that if PHPA is mixed with clay in the absence of added salt, very little or even no adsorption takes place due to electrostatic repulsions between the polymer and the clay. Consequently, in every study examined which is concerned with the adsorption of anionic polymer on to clay, an increase in the salinity of the dispersion medium dramatically increases Q_{max}.

3.1.6.4 The Effect of pH on Polyanion Adsorption.

Many authors have found that the value of Q_{max} for the addition of anionic polymers to clay is greatly effected by any changes in the pH of the dispersion medium. For example Mortensen,[73] recorded that Q_{max} for the addition of HPAN to kaolinite increased from 1 mg g^{-1} to 8.5 mg g^{-1} clay as the pH of the dispersion medium decreased from pH 9 to pH 3. The increase in adsorption as the acidity of the dispersion medium increased was due to charge screening of the anionic polymer and clay by the proliferation of H^+ in solution at low pH. This charge screening leads to increased interaction between the HPAN and kaolinite and therefore an increase in adsorption. A reduction in the size of the polymer coil may also result at low pH due to screening of the negative charges on the polymer from one another which again leads to increased adsorption. With the addition of PHPA to kaolinite, Lee *et al.*[76] also found that increasing the pH of the dispersion medium resulted in a reduction in Q_{max}. This time however the reduction in Q_{max} is assumed to be due to dissociation of acrylic groups on the PHPA which increases the charge on the polymer. Increasing the pH therefore increases the electrostatic repulsions between the increasingly charged polymer and the clay surface which itself shows an increase in negative charge on its edge surface as pH is increased. Q_{max} was also seen to decrease as the pH was increased for the addition of polyanion to montmorillonite clays.

A completely different type of adsorption for anionic polymers was outlined by Gu and Doner who suggest that at low pH, anionic polysaccharide may become uncharged due to association of hydroxyl groups. This coupled with an increase in positive edge sites at low pH leads to a significant increase in polyanion adsorption.[45] The same phenomenon was also seen by Schnitzer *et al.*[75] who observed appreciable uptake of fulvic acid on Na-montmorillonite which behaved and adsorbed like an uncharged species at low pH.

3.2 Clay Particle Association Systems.

The stability of clay suspensions depends primarily on the nature and concentration of the exchangeable cation associated with the clay. The associations between clay particles is an important phenomenon to the oil industry as it governs many properties of clay suspensions such as viscosity. Clay particle associations may be described in the following terms.

3.2.1 Deflocculated Suspensions.

When clay particles in suspension are well dispersed, which results from an overall repulsive force between the particles, the suspension is described as being peptized or deflocculated. Deflocculation can be achieved by imposing a similar charge on each particle in the clay suspension, (Figure 14).

3.2.2 Flocculated Suspensions.

In flocculated suspensions, there is a net attractive force between the clay platelets, which associate with one another by the formation of edge-to-edge (EE) and edge-to-face (EF) bonds. In dilute suspensions, flocculation is associated with

voluminous aggregates or 'flocs' however in concentrated suspension, it is thought that clay platelets arrange themselves in a rigid "card house structure", (Figure 14).

3.2.3 Aggregated Suspensions.

When clay plates stack one upon the other, face-to-face (FF) associations are dominant, the system is now described as being aggregated. The stacked sheets may be disaggregated by further hydration and/or mechanical sheer. The aggregates may themselves be flocculated or deflocculated, (Figure 14).

3.2.4 Dispersed Suspensions.

Dispersed suspensions arise when any aggregation in a system breaks down. Dispersed and aggregated clay suspensions may themselves also be flocculated or deflocculated, (Figure 14).

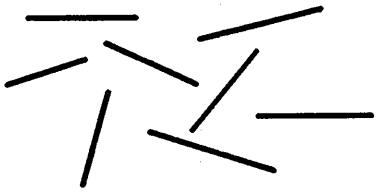

1. Dispersed and deflocculated.

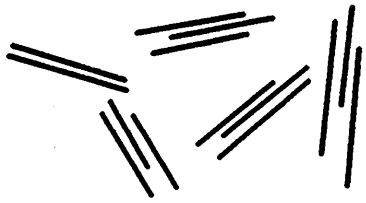

2. Aggregated but deflocculated.

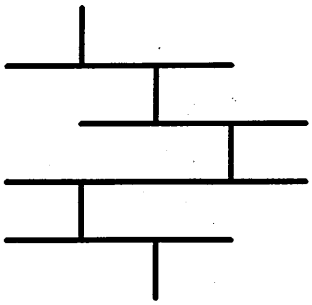

3. Edge to face flocculated but dispersed.

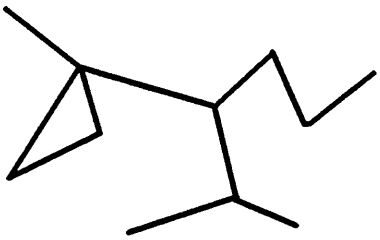

4. Edge to edge flocculated and dispersed.

5. Edge to face flocculated and aggregated.

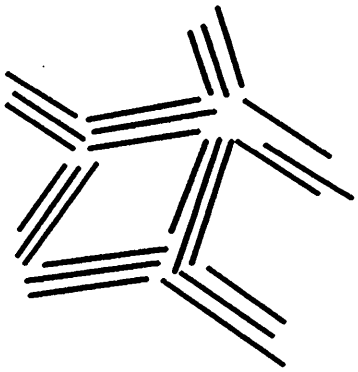

6. Edge to edge flocculated and aggregated.

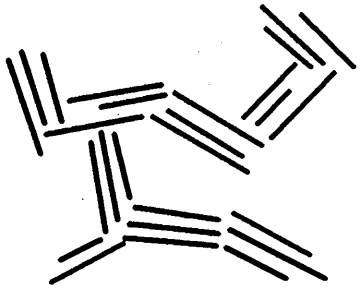

7. Edge to face and edge to edge flocculated and aggregated.

Figure 14. Modes of particle association of clays.

3.3 Forces Acting Between Clay Platelets.

The forces acting between clay platelets may be either repulsive or attractive. In clay suspensions, platelets approach each other as a result of Brownian motion therefore any resulting interactions will be determined by the magnitude of the dominant force between the platelets whether repulsive or attractive.

3.3.1 Electrical Double Layer Repulsion.

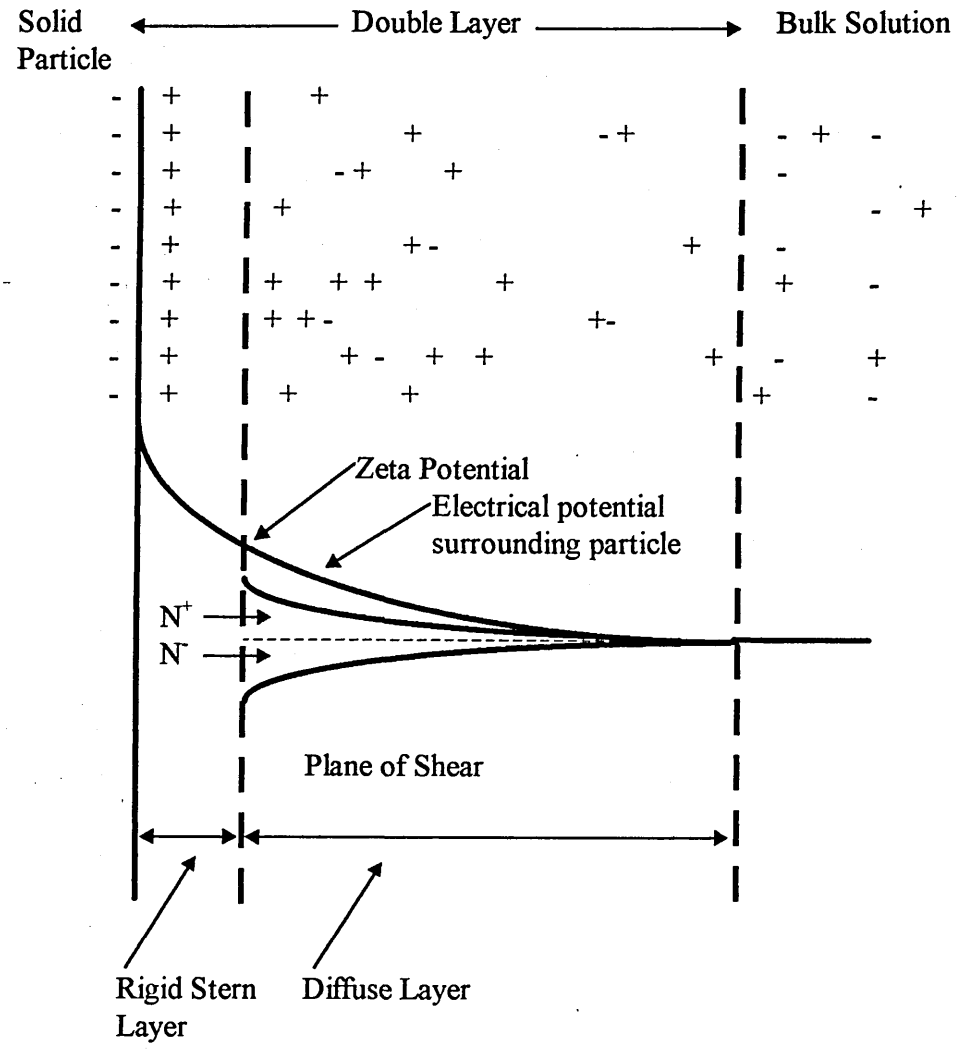

Figure 15. Diagrammatic representation of the electrical double layer.

The Stern model of the electrical double layer of ions may be employed to explain the electrical equilibrium state set up around solid particles in a liquid phase. This model states that the solid has a rigidly fixed electrical charge, for clay particles this charge is negative due to isomorphous substitutions in the lattice. Surrounding the charged clay particles is a layer of practically immobile oppositely charged ions in the liquid phase that are absorbed on the solid. This layer of oppositely charged ions is called the Stern layer (Figure 15).

Further away from the solid, next to the Stern layer is a diffuse layer of mobile ions which consists of both positively and negatively charged ions in the liquid phase. The diffuse layer may have a net charge of the same or opposite sign from that of the Stern layer. The electrical potential that develops across the Stern and diffuse layers is a balance between the electrostatic attraction of the solution counter ions to the solid surface and their tendency to diffuse away from the surface. The potential drop that occurs across the stern layer is called the zeta potential. The size of the diffuse layer can be manipulated by changing salt or electrolyte concentration. If salt or electrolyte is added to a clay suspension, then the diffuse layer will be compressed, the magnitude of which is governed by the valence of the cations in the salt and their concentrations. For example at equal concentrations, $CaCl_2$ will compress the diffuse double layer more effectively than NaCl. Therefore when two clay particles approach each other there is a repulsion between them, the size of the which depends on the diffuse layer, thus repulsion becomes greater the closer the platelets become.

3.3.2 Van der Waals Attractive Forces Between Particles.

Van der Waals forces are responsible for the attraction between clay platelets which approach each other by diffusion. This attraction between atoms of clay platelets may eventually lead to flocculation if repulsive forces do not become dominant. The force between atoms decays rapidly with distance, in fact the force is inversely proportional to the seventh power of the distance. The sum of all atoms in large structures such as a clay platelet may be significant as the attractive forces are additive.

3.3.3 The Net Potential Energy of Particle Interaction.

The flocculation of clay suspensions and the effect of added electrolyte can be explained by considering the net attractive and repulsive potential energy as a function of distance between particles at different electrolyte concentrations. The attractive van der Waals forces are essentially unaffected by electrolyte concentration. Conversely, the electrical double layer repulsion force decreases rapidly with increasing electrolyte concentration. The resultant potential curves show that at high electrolyte concentration, the attractive forces between particles dominate, while at low electrolyte concentrations, repulsive forces dominate.

3.3.4 Flocculation of Clay Suspensions.

In a clay suspension where there is no electrolyte present, EF particle flocculation must occur between the positive edge sites and the negative basal surface of the clay. In dilute suspensions however, montmorillonite has a stable appearance, this is because the flocs formed consist on average of only a few platelets and are thus so light that they are stable and therefore do not settle. With the addition of salt to a suspension, flocculation of clay particles becomes visible and the clay sediments out. Salt addition causes the

diffuse layer of cations around the clay particles to contract, thus the clay platelets move closer to each other allowing the possibility of flocculation. It is thought that the negative basal surfaces of the clay govern salt flocculation and FF aggregation becomes the dominant mechanism, although EE and EF flocculation still occur. FF aggregation causes the formation of dense agglomerates which in turn are much heavier than individual clay platelets and so sediment out of solution easily.

Natural clays where the exchangeable cation is mainly Ca^{2+} are more flocculated than natural clays where the exchange cation is predominantly Na^{+}. This is because salts of polyvalent cations can be associated with more than one exchange site on the surface of more than one clay platelet which in effect flocculates the clay. Therefore to deflocculate a polyvalent cation exchanged clay, polyvalent cations must be replaced by monovalent ones such as Na^{+}.

3.3.5 Deflocculation of Clay Suspensions.

For a clay suspension to be in a deflocculated state, the edge charge or face charge on the clay platelets must be reversed. This charge reversal must then be of a sufficient size so as to prevent flocculation by van der Waals forces. Edge charge reversal is the most common procedure to deflocculate a clay however it is also possible to reverse the charge on the basal surface.

3.3.6 Edge Charge Reversal.

There are two ways to achieve edge charge reversal. The first is to increase the pH of the clay suspension to above 8.0 and therefore increase the number of negative silic acid groups on the platelet edges. The second is to add salts containing large

polyanions such as silicate, polyphosphate and polyacrylate. These anions become chemisorbed at the edges of clay particles by complex anion formation with cations at the edges of broken octahedral sheets. Because the anions are reacting with the positive sites on the edges, which account for a small proportion of the total surface area, the quantity of anion required to deflocculate a clay suspension is often small. Short chain anionic polymers are also useful in deflocculating clay suspensions as they are adsorbed in small quantities onto the positive edge sites of clay particles thus making these edge sites negative overall.

3.3.7 Face Charge Reversal.

The negative charge on the face of a clay platelet can be reversed by the adsorption of certain organic cations such as long chain quaternary salts. Here the cation is first adsorbed by ion exchange, its hydrocarbon chain pointing towards the solution. This condenses the double layer of the platelet and the clay eventually flocculates when sufficient organic cation has been added. Upon addition of further quaternary cations, there is van der Waals attraction between the hydrocarbon chains of the added quaternary cation with those on the surface. The cationic groups of the second layer now point towards the solution and a positive particle is formed. This method of charge reversal is not favoured as large quantities of quaternary salts are required which is not economically viable.

3.4 Clay Particle Flocculation Mechanisms by Adsorbing Polymer

Napper,[82] has indicated several different ways by which added polymer can affect the stability of an idealised colloid suspension, (Figure 16).

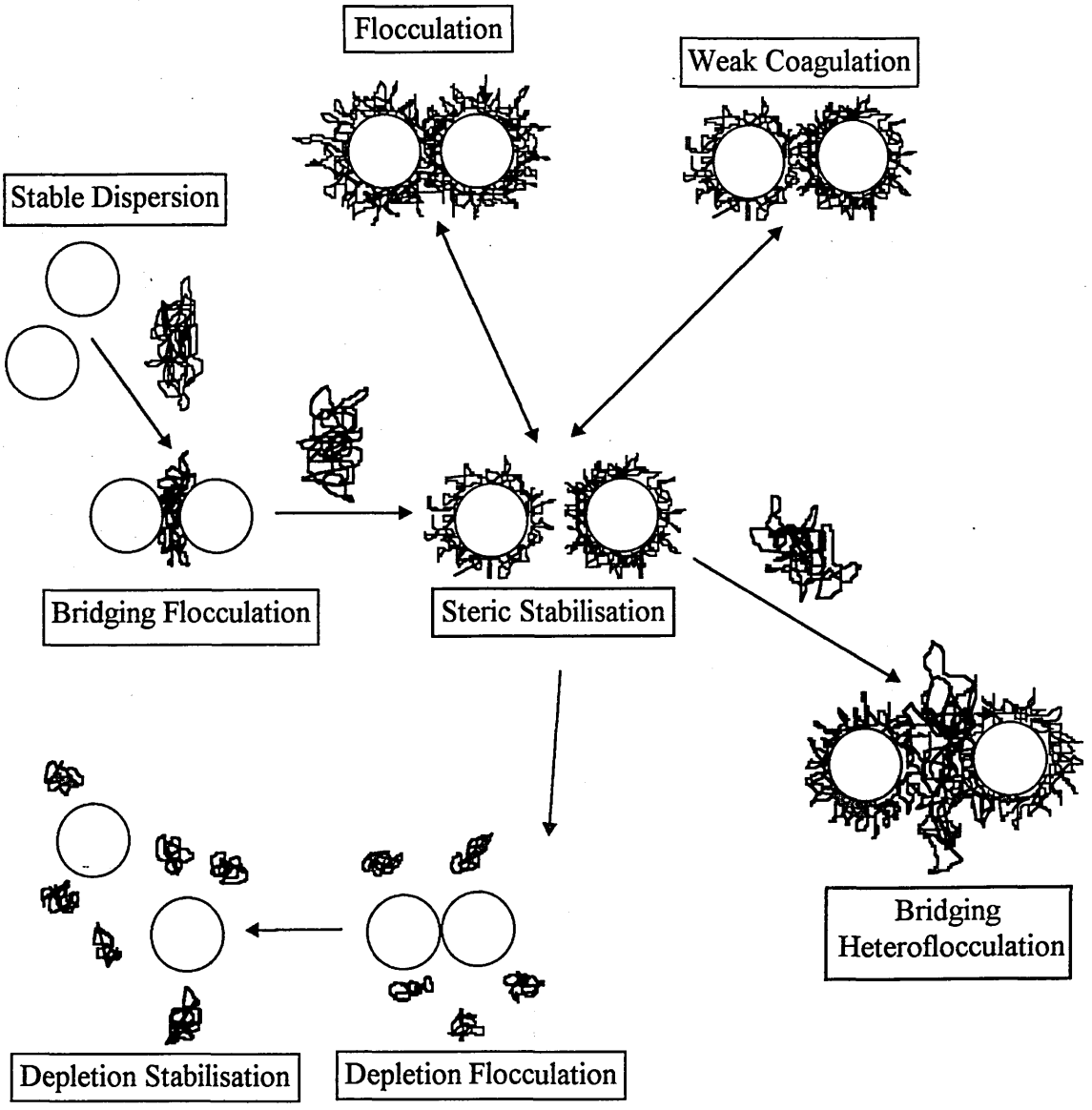

Figure 16. Schematic representation of the ways by which polymers can affect colloid stability (after Napper,[82] 1983).

Napper suggests that when low concentrations of polymer are added to a stable dispersion of colloidal particles, the dominant adsorption mechanism is that of bridging flocculation. At saturation coverage, when the colloidal particles are fully coated with polymer, the particles repel one another due to the adsorbed layer of like charge polymer,

this is known as steric stabilisation. When the sterically stabilising polymer layer is thin, Van der Waals forces may be large enough to cause weak coagulation between the particles. The addition of non-adsorbing polymer to sterically stabilised particles may lead to depletion flocculation or phase separation. Addition of a large concentration of non-adsorbing polymer may eventually lead to what is termed depletion stabilisation. The addition of a low concentration of a second adsorbing polymer to a sterically stabilised dispersion may lead to bridging heteroflocculation. The mechanisms laid out by Napper[82] concerning the ways by which polymers affect the stability of idealised colloidal suspensions can be applied to the interactions of polymers with clay.

Bridging flocculation is not the only mechanism by which colloidal dispersions may be destabilised by addition of adsorbing polymer.[83] The flocculation of charged colloidal particles by polyelectrolytes of opposite net charge may often be better described as a charge neutralisation or charge reversal mechanism.[56,61] This type of adsorption mechanism is particularly favoured when highly charged cationic polymers are mixed with suspensions of negatively charged particles. A further type of flocculation mechanism has been proposed by Gregory.[84] He investigated a system where three highly charged cationic polymers, based upon dimethylaminoethyl methacrylate, were added to suspensions of negatively charged latex particles. The three polymers were of differing molecular weights, equal to 5×10^3, 5×10^4 and 1×10^5. The addition of each of these polymers to a suspension of latex particles caused major flocculation of the system. Gregory states however that the flocculation caused by the added polycation could not be due to particle bridging because of two main reasons.

1. The lowest molecular weight polycation investigated by Gregory (5×10^3) caused substantial flocculation, when considering that the dimensions of the polymer were small in comparison to the size of the particle.

2. The polymers of molecular weight 5×10^4 and 1×10^5, appear to flocculate the latex suspensions at the same rate. If particle bridging were occurring, the higher molecular weight polymer with a longer chain length would be expected to flocculate the latex suspension at a faster rate.

In addition, theoretical analysis predicts that these highly charged polycations adopt an essentially flat configuration at the interface with no significant loops and tails, consequently no particle bridging may occur.[85] Gregory also indicated that a simple charge neutralisation mechanism could not account for the enhanced flocculation rate because he observed a higher flocculation rate for the addition of cationic polymer to latex particles than that observed for the addition of $NaNO_3$.

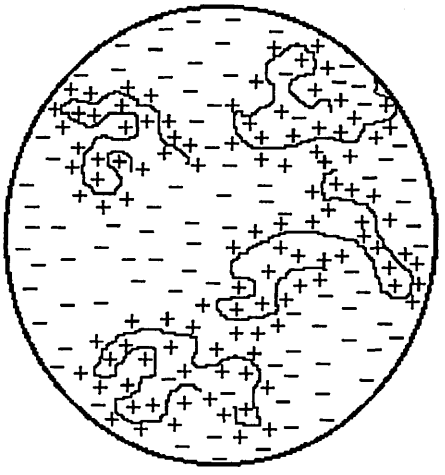

Figure 17. Possible arrangement of adsorbed polycations on a colloidal particle with low negative surface charge density, (after Gregory,[84] 1973).

To explain this enhanced flocculation of latex particles in the absence of a bridging or a simple charge neutralisation mechanism, Gregory proposed the "electrostatic patch" model, (Figure 17). Figure 17 shows areas of high positive charge density surrounded by larger expanses of relatively weak negative charge. Gregory states that differences in the distances between cationic groups on the polymer and negative sites on the particle surface, show that the particle surface charge density is not neutralised uniformly by the adsorbed polymer. This uneven charge distribution then leads to an extra attractive contribution to the interaction energy between two such particles. Consequently if a negatively charged patch encounters a positively charged patch on another particle, flocculation will result, even though the net charge on the particles, if it was uniformly distributed would be large enough to give electrostatic stabilisation.[86] Figure 18 is a highly simplistic representation of how the "electrostatic patch" mechanism of particle flocculation proceeds when negatively charged particles adsorb highly charged polycation. The interactions **a** and **b** are repulsive due to the like charges, whereas interaction **c** is attractive. In another study which investigated the interactions of highly charged polycations with negatively charged silica particles, the "electrostatic patch" model was also considered to be the mechanism by which the particles flocculated.[64] All studies which consider this model agree that at high ionic strength, this mechanism is less likely to operate because of the short range of attraction between patches.

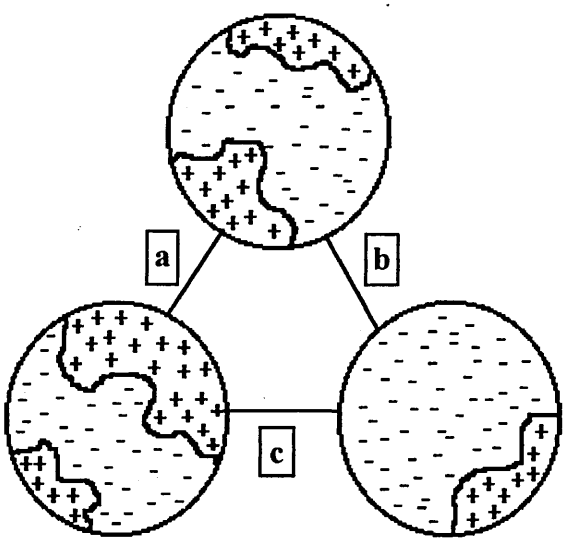

Figure 18. The "electrostatic patch" mechanism of particle flocculation showing how negatively charged particles with surface adsorbed polycation of high charge interact, (after Mabire *et al.*[64] 1983).

CHAPTER 4

The Use of Nuclear Magnetic Resonance (NMR) for the Study of Clay Systems.

4. The Use of Nuclear Magnetic Resonance (NMR) For The Study of Clay Systems.

Multinuclear NMR spectroscopy has found widespread use in the study of clays and clay minerals, its use may be categorised into three distinct areas depending upon the component of the clay under examination.

1) The most common area of research concerns the organisation of Al and Si in the aluminosilicate layer. Recent work in this area has concentrated on high-resolution magic angle spinning (MAS) NMR because this technique offers better resolution of peaks compared with conventional NMR. MAS NMR is particularly useful for examining clay minerals because their structures are not easily determined by other techniques such as x-ray diffraction due to their fine grain size. The ^{29}Si nuclei, with a spin state of 1/2, generally show narrow, well resolved peaks and therefore much structural information concerning clays may be gained from this nucleus, (section 4.1).[87] Spectra of ^{27}Al with a spin state of 5/2 generally have broader peaks, however useful information concerning the structure of clay can still be gained from this nucleus, (section 4.2).[87]

2) NMR spectroscopy has also been used extensively for determining the structure and state of motion of water molecules in the interlayer region of clay-water systems.[88,89,90] These systems have been widely studied not least because of the relative ease with which, in this case, NMR signals may be detected (^{2}H,^{1}H) but also because a better understanding of the nature and properties of water in the vicinity of a surface or interface has implications in environmental and life processes of which water is a major component. NMR is also a particularly good technique for probing the interactions of

water molecules (which may be used as analogues for other molecules) with the clay surface because it provides a method for sampling local molecular arrangements and has a time scale which covers an extremely large range (from 10^{-10} seconds to 1 second).[91] A few authors have carried out extensive research involving ^{2}D NMR of clay suspensions in a solvent of D_2O. This area of research is particularly relevant to the present study because it offers the possibility of an *in situ* technique with which to study the interactions of clay minerals with adsorbate species, (section 4.3).

3) Finally interactions of the exchangeable cations with the clay surface may be used as probes to provide complementary information about interlayer organisation.[92,93] The exchangeable cations have only recently become available as probes because most of the nuclei in question are quadrupolar and therefore require high magnetic fields to enhance resolution which have only recently become available. The use of multinuclear NMR to probe the interactions of exchangeable cations with the clay surface will be discussed in greater detail later with a view to using a chosen exchangeable cation as an *in situ* probe, (section 4.7).

4.1 The Use Of ^{29}Si MAS NMR to Investigate the Structure of Clay Minerals.

Most NMR studies concerning the structural organisation of clay minerals concentrate on the ^{29}Si cation. Diffraction techniques have shown that clay minerals usually contain only one type of tetrahedral site in the average structure whereas ^{29}Si NMR spectra often contain multiple peaks which can be attributed to Si with different numbers of neighbouring Al tetrahedra. If as in pyrophyllite, the Si has no neighbouring Al, then only a single peak is seen.[94] On the other hand for Si in clays with two and three

neighbouring Al, such as beidellite and muscovite, the ^{29}Si spectra show two and three peaks respectively.[94] The standard notation describing the local Si environment is written $Q^m(nAl)$. Here m is equal to the number of bridging oxygens to which a Si is coordinated and n = the number of tetrahedral Al next nearest neighbours to Si. As n increases, not only do ^{29}Si spectra show an increasing number of peaks but also the ^{29}Si chemical shift becomes less negative which allows a distinction to be made between differing ^{29}Si environments.[94]

Variations in the ^{29}Si chemical shift also occur as a function of the tetrahedral and octahedral sheet charge, total layer charge and composition of the octahedral sheet.[94,95] Increasing the tetrahedral and octahedral sheet charge and also the total layer charge all result in less negative ^{29}Si chemical shifts. These chemical shifts are important because they allow an estimate to be made of total layer charge in clays for a given type of Si site *ie* $Q^3(0Al)$. A less negative ^{29}Si chemical shift of approximately 2-3 ppm is also observed for dioctahedral 2:1 minerals when compared to trioctahedral 2:1 minerals of the same net layer charge.[94,95] Similar trends in NMR spectra also occur for ^{27}Al in tetrahedral coordination in clays.[95,96]

The Si/Al(4) ratio ((4) relates to tetrahedral coordination) may also be calculated from ^{29}Si NMR data using the equation shown below, (Equation 2).

$$Si / Al(4) = \frac{3(I_0 + I_1 + I_2 + I_3)}{(I_1 + 2I_2 + 3I_3)}$$

Equation 2. Shows how the Si/Al(4) ratio may be calculated where $I_{0,1,2,3}$ = the intensity of the ^{29}Si NMR peaks with zero, one, two and three neighbouring Al tetrahedra.

This equation only holds true however if Loewenstein's Al avoidance rule is obeyed which states that during the isomorphous substitution of Si by Al, occupancy of adjacent tetrahedral sites by Al is avoided.[97] In fact NMR studies indicate that for all clays analysed, Loewenstein's rule is obeyed.[98,99] In general values for the Si/Al(4) ratios of clay minerals calculated from Equation 2 above have been found to be comparable to values determined from the assumed stoichiometry and chemical analysis.[100] The presence of paramagnetic cations such as Fe^{III} in the clay distort the intensity of the ^{29}Si peaks. The calculated Si/Al(4) ratios for clays containing a sizeable quantity of paramagnetic cations are therefore no longer accurate.

Finally the extent of Si/Al ordering in tetrahedral sites of clay minerals which has always been difficult to elucidate using conventional diffraction methods may be investigated by ^{29}Si NMR. With ^{29}Si NMR, the presence of multiple peaks, and to some extent of increased peak widths, indicate a range of shieldings at the Si nucleus which may be related to a range of chemical and structural environments.[95,101] The use of ordering rules such as Loewenstein's rule and Dempsey's rule which states that Al(4)-O-Si-O-Al(4) linkages are minimised also help to elucidate the Si/Al ordering in tetrahedral sites of clay minerals.

4.2 The Use Of ^{27}Al to Investigate the Structure of Clay Minerals

The main use of ^{27}Al NMR is that it allows a distinction to be made between tetrahedral and octahedral coordinated Al, Al(4) and Al(6), respectively. This is made possible due to a large difference in the chemical shift between the two differently coordinated Al sites. Unlike ^{29}Si, the position of the ^{27}Al peaks also vary with the strength of the applied magnetic field. The ratios of Al(4)/Al(6) may also be determined

by NMR however agreement with chemically analysed samples has in some cases been poor.[98,102,103] Many ^{27}Al studies have however shown good agreement between NMR and chemical data for the Al(4)/Al(6) ratio.[95,104] An extensive study of ^{27}Al in clay by Woessner,[96] showed that if certain spectroscopic procedures were followed, excellent agreement between ^{27}Al NMR and chemical analysis could be obtained for the Al(4)/Al(6) ratio.

4.3 The Use of NMR as an In Situ Technique to Study the Interactions of Clay Minerals with Adsorbate Species.

In general previous NMR studies that have been concerned with the interaction of clay minerals with adsorbate species have been limited to dry powdered clay samples. These samples have usually undergone a variety of preconcentration and drying stages which may contribute to the redistribution of adsorbed species. A dry powdered clay sample open to the atmosphere is considered to contain nominally 10% water. In many industrial applications such as water treatment, paper coating and drilling fluids however, clays are used in an aqueous medium therefore data obtained from powdered clay may not reflect the real situation in suspension prior to drying. A technique is therefore required which permits *in situ* measurement of the dynamics of the interfacial processes while at the same time probing the steady state interactions and distribution of adsorbed molecules at the macroscopic level and with monolayer coverage. One such *in situ* method involves the suspension of clay platelets in D_2O. ^{2}D or ^{17}O spectra may then be recorded which show a residual quadrupolar splitting of the NMR signal. This residual quadrupolar splitting may then be used to provide information concerning the interaction of clays with ions and organic molecules in aqueous suspensions. The origins and practical uses of the method are discussed in greater detail below.

4.4 The Origin and Possible Uses of the ^2H Residual Quadrupolar Splitting of D_2O Molecules.

The ^2H or the ^{17}O NMR spectrum of pure D_2O only shows a single line however the introduction of clay platelets to the D_2O solvent results in a residual quadrupolar splitting in the ^2H or ^{17}O line.[105]

The ^2H nucleus assumes three spin states in a static magnetic field B_0: + 1, 0 and -1. This nucleus therefore has two allowed NMR transitions which are (+1→0) and (0→-1) which for an isolated nucleus are degenerate. Besides possessing a magnetic moment, ^2H also has an electric quadrupole moment which is a non spherical distribution of charge in the nucleus. In fact all nuclei with spin states > 1/2 possess an electric quadrupole moment. This electric quadrupole moment interacts with local quadrupolar electrostatic field gradients and is termed the quadrupolar coupling constant χ.[106] The allowed NMR transitions for a quadrupolar nucleus become non degenerate in the presence of a non vanishing quadrupolar interaction. The use of ^2H NMR spectroscopy to investigate the interface of mineral suspensions in D_2O solvent is one such case where the ^2H NMR transitions become non degenerate and a deuterium residual quadrupolar splitting is observed. Woessner and Snowden,[107,108] in the late 1960's were among the first to realise that the deuterium residual quadrupolar splitting for D_2O molecules in the presence of a clay suspension was due to preferential orientation of water molecules associated with the clay platelets. The clay platelets which are essentially electrically charged sheets are themselves aligned in the applied magnetic field and this clay platelet/magnetic field interaction is very strongly anisotropic.[109,110] From an NMR point of view, it is thought that only the two or three water layers closest to the clay surface behave differently to those in the interlayer and bulk.[111] These water molecules are

consequently responsible for the observed residual quadrupolar splitting and are thought to be associated not only with the charged aluminosilicate sheet but also with the exchangeable metallic cation, (Figure 19).[109]

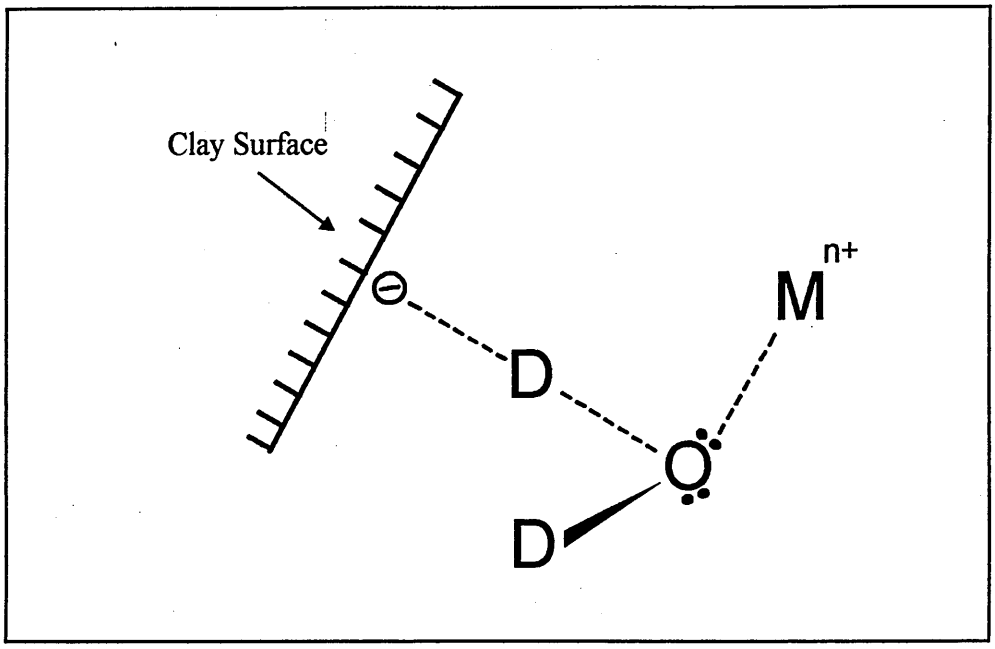

Figure 19. The geometry of D_2O molecules squeezed between the charged aluminosilicate sheet and condensed M^{n+} counter ions.

Hydrogen bonds associate the water with the clay surface while electron lone pairs on the oxygen associate the water with the cation. As a result of these interactions, all the orientations of the water molecule denoted by the angle Θ are no longer equiprobable. These constraints on the reorientations of the water molecule may be translated into a residual quadrupolar splitting if made anisotropic. This is in fact the case as alignment of the clay platelets in the applied magnetic field is highly anisotropic as stated previously, (Equation 3).

$$\Delta = \frac{3\chi}{4I(2I-1)}(3\cos^2\Theta_{LD} - 1)A$$

Equation 3. The parameters which influence the magnitude of the residual quadrupolar splitting Δ.

Where χ is the quadrupolar coupling constant and Θ_{LD} is the angle between the static magnetic field, B_0, and the local order director of the orientated aluminosilicate sheets, perpendicular to their parallel surfaces. The anisotropy, A, which is related to the order parameters, has values between -1 and +1. Its actual value depends upon the orientation of water molecules with respect to the local director (i.e. the surface of the clay). The orientations of the molecular axes of the water molecules (molecular referential) relative to the surface of the clay platelet (director referential), and of the clay platelet relative to the applied magnetic field B_0 (laboratory referential) determines the value of the residual quadrupolar splitting of the D_2O doublet.[112]

Grandjean and Laszlo assume that only a minute fraction of the water molecules, *ca.* 1 in 10000,[109,110] become associated with the clay platelets. However fast exchange occurs between these molecules and the bulk resulting in a measurement of only a time averaged resonance.[113] This therefore means that the residual quadrupolar splitting of the D_2O doublet is only a minute fraction of the quadrupolar coupling constant. Fortunately the quadrupolar coupling constant for deuterons in heavy water is large with a value of about 213 000 Hz.[114,115] In summary, all orientations of free water molecules, denoted by the angle Θ are equiprobable, the sum of $3\text{Cos}^2\Theta - 1 = 0$ and therefore no ^2H residual quadrupolar splitting, calculated by Equation 3 above is observed. Conversely, with bound water molecules, all orientations denoted by the angle θ are no longer equiprobable and the sum of $3\text{Cos}^2\Theta - 1 \neq 0$, therefore a ^2H residual quadrupolar splitting of approximately 213 000 Hz should theoretically be observed. Thus if as stated above, fast exchange occurs between bound and free D_2O molecules, then the observed ^2H residual quadrupolar splitting is therefore a weighted average between D_2O molecules in the free (0 Hz) and the bound (213 000 Hz) sites.

4.5 Experimental Observations and Parameters Effecting the Magnitude and Sign of the ^2H Splitting.

Grandjean and Laszlo,[110] found while conducting experiments on Ecca Gum BP bentonite, an impure form of montmorillonite, that the same maximum deuterium residual quadrupolar splitting for the clay sample was reached irrespective of the field strength of the magnet. Differences were however observed in the time taken (which the authors state is in the order of minutes) to reach this maximum ^2H splitting. They then postulated that increasing the field strength of the magnet increases the speed at which the clay platelets become orientated in the magnetic field which therefore decreases the time taken to observe the maximum deuterium residual quadrupolar splitting. Orientation of single and stacked clay platelets (tactoids) is a co-operative process where at any given time, the fraction of the platelets about to be orientated in the magnetic field is proportional to the total number of already ordered platelets. If the concentration of the clay suspension increases, so does its available surface area and therefore its ability to interact with a greater number of water molecules which therefore results in an increase in the residual quadrupolar splitting. Grandjean and Laszlo,[110] observed that there is a linear dependence of the observed residual quadrupolar splitting, Δ, with the amount of suspended bentonite clay.

The observed ^2H doublet displays differential line broadening which allows a distinction to be made between the two peaks. The splitting is considered positive if the broader component of the doublet is at high frequency. The intensities and also the longitudinal relaxation times, T_1, for both peaks are however equal. The origin of the differential line broadening is thought to be due to coupling between two relaxation mechanisms because taken alone, quadrupolar relaxation cannot explain the inequality of

the observed line widths. Grandjean and Laszlo,[110] suggested three possibilities for the coexistence of another relaxation pathway which after coupling with the quadrupolar relaxation would result in a differential line broadening of the ^2H doublet.

1. For an orientated D_2O molecule, the differential line width of the ^2H doublet may be due to coupling between the quadrupolar relaxation and relaxation due to chemical shift anisotropy.

2. An internal dipole-dipole mechanism may take place where deuterons on the same D_2O molecule relax one another, coupling may then result between the dipole-dipole and quadrupolar relaxation mechanisms.

3. It is also possible that an external dipole-dipole mechanism could be present in the system. Such a mechanism would involve paramagnetic centres in the clay. If coupling then takes place between external dipole-dipole and quadrupolar relaxation mechanisms, differential broadening will result which will rely upon the concentration of paramagnetic impurities.

Grandjean and Laszlo suggest that mechanism 3 above best fits the experimental data thus far obtained,[110] since many clays contain Fe^{III} which is the main paramagnetic impurity. The bentonite used by Grandjean and Laszlo contained about 4% Fe_2O_3 and the broader component of the ^2H doublet was at lower frequency. This order was reversed when gelwhite containing 0.9% Fe_2O_3 was introduced into the magnetic field. Further, with hectorite, another 2:1 smectite which contains very little iron, 0.05%, no difference in the line widths of the two components was observed.[116] Hence the evidence suggests that the origin of the differential line broadening is due to paramagnetic centres in the clay. This may be further emphasised because in the present study, a Texas

bentonite with only 0.7% Fe_2O_3 was used and as with gelwhite, the broader component was at higher frequency, also with this clay differential line broadening was not very pronounced. A subsequent study by Petit *et al.*[116] has shown conclusively that differential line broadening depends linearly on the applied magnetic field and on the concentration of paramagnetic centres in the clay. Petit *et al.*[116] checked these statements experimentally by line shape analysis of the NMR ^2H doublet for clay gels at two Larmor frequencies and by varying the concentration of paramagnetic Gd^{3+} ion added to the clay.

Grandjean and Laszlo,[109,110] found that the observed residual quadrupolar splitting depended strongly on the exchangeable cation associated with the clay. They recorded with Ecca Gum BP bentonite that the residual quadrupolar splitting, Δ, goes from +16.3 Hz to zero as the Mg^{2+}/Na^+ ratio was increased up to 0.27.[109] The most dramatic change in residual quadrupolar splitting occurs when Na^+ is in competition with Ca^{2+}. Here the residual quadrupolar splitting decreases from +16.3 Hz, through zero and assumes a maximum negative value of -23 Hz for Ca^{2+}/Na^+ ratios above 0.2.[109] Grandjean and Laszlo state that the change in sign of the deuterium doublet from positive to negative on changing the Ca^{2+}/Na^+ ratio must be due to a switch in the predominant reorientational mode of water associated with the cation and clay surface. When only univalent Na^+ ions are present, the water molecules are affected by two attractive forces, (i) hydrogen bonds to the aluminosilicate layer and (ii) a bond between the oxygen lone pair and the cation. The introduction of divalent ions such as Mg^{2+} or Ca^{2+} into the system results in the systematic displacement of Na^+ ions from the interface on increasing addition of the divalent ions. Increased attraction between the divalent cation and the clay surface means that the water molecules are squeezed between the two. When only Na^+ ions are present, the water molecules are thought to rotate predominantly around the H-bond (O-

H axis). Conversely when the stronger binding divalent cations are present, the reorientational axis changes to the stronger metal-O bond (Ca^{2+}-O axis). Fast exchange of D_2O molecules between the bulk and the two bound sites, water molecules orientated by (1) the clay surface or (2) the exchangeable cations is therefore responsible for the change in sign of the ^2H doublet from positive to negative. The magnitude of the residual quadrupolar splitting, Δ, was also found to have a temperature dependence which, for high Ca^{2+}/Na^+ ratios increased with increasing temperature. Conversely for low Ca^{2+}/Na^+ ratios the opposite was true.[110]

Grandjean and Laszlo,[105] have also investigated what effect, if any, the location of isomorphous substitution, whether in the octahedral or tetrahedral layer of the clay, has on the ^2H residual quadrupolar splitting in the presence of different cations. Three clays were chosen, two of which were saponite and hectorite which are both trioctahedral, however isomorphous cation substitution occurs in the octahedral layer for hectorite and the tetrahedral layer for saponite. The third clay investigated was a montmorillonite from Gonzales County Texas, where isomorphous substitution occurs in the octahedral layer only. These clays all differed from Ecca Gum BP where substitution occurred in both the tetrahedral and octahedral layers.

No significant variation in the ^2H splitting was observed in the presence of different exchangeable cations for suspensions of saponite and hectorite which are both trioctahedral clays. The observed ^2H splitting for saponite and hectorite was approximately 55 and 26 Hz respectively. The Gonzales County montmorillonite is a dioctahedral clay which also showed no change in splitting even when the clay was exchanged from Na^+ to a predominantly Ca^{2+} exchanged form. The deuterium splitting observed for this clay was constant at approximately 19 Hz. This contrasts with the

observations for Ecca Gum BP which displayed a change in sign upon increasing the Ca^{2+}/Na^{+} ratio. The differences in the ^{2}H splitting upon changing the exchangeable cation associated with the clay may be explained by considering the location of isomorphous substitution in the clay layers. When isomorphous substitution occurs in the octahedral layer as in hectorite and the Gonzales County montmorillonite, water molecules interact less strongly with the clay surface.[117,118] Grandjean and Laszlo state that the reduced interaction confers some hydrophobicity to the clay surface and the water molecules cluster in the interlayer.[105] Even the presence of divalent ions seems to have little effect on these water clusters. When isomorphous substitution is in the tetrahedral layer as with saponite, basal oxygens, near the locus of substitution, interact more strongly with the exchangeable cation and also water.[117,118] These stronger interactions destroy the water molecule clusters and strong bonds may be formed between the hydrated cation and the surface of the clay.

It does not seem to matter whether isomorphous substitution is exclusively octahedral or tetrahedral because no significant changes in the ^{2}H splitting were observed for either case upon changing the exchangeable cation associated with the clay. The Ecca Gum BP represents an intermediate situation with isomorphous substitution occurring in both the octahedral and tetrahedral sheets. As a result stronger interactions occur with the clay surface compared with those in hectorite and Gonzales County montmorillonite. In addition any water clusters formed will be less stable with respect to clusters formed with saponite and their structure will therefore be affected by higher valent cations. Grandjean and Laszlo state that this intermediate situation, where isomorphous substitution occurs in both octahedral and tetrahedral layers, is responsible

for the variations in the ^{2}H and ^{17}O quadrupolar splittings and is due to fast exchange between bulk water and the two types of bound site.[105]

4.6 Practical Uses of the ^{2}H Residual Quadrupolar splitting.

The extensive work carried out by Grandjean and Laszlo has shown that the ^{2}H quadrupolar splitting may be used to gain information about the state of water at the clay interface. They have also shown that the experimental conditions and choice of clay need to be considered carefully in order to maximise the splitting of the ^{2}H doublet. It is proposed that in this study, the splitting of the ^{2}H doublet will be utilised to investigate the interactions of ions and organic molecules with the clay. As previously mentioned, the major advantage of this technique is its *in situ* nature which allows the arrangement of adsorbates to be probed at the clay surface under liquid phase conditions close to those used in working situations by industry. Grandjean and Laszlo,[119] have already made use of the ^{2}H residual quadrupolar splitting (along with other nuclei *i.e.* ^{17}O, ^{14}N and ^{7}Li) to study the interactions of Li-saponite with a binary solvent mixture of acetonitrile and D_2O. In this study they found that, as usual, the water molecules associate with the clay surface *via* H-bonds to form the first solvation shell, coordination also occurs through oxygen to the Li^{+} ion. The constant ^{2}H and ^{17}O residual quadrupolar splittings observed for water molecules at acetonitrile concentrations below 60% vol/vol indicate that the water molecules remain essentially undisturbed by the acetonitrile molecules in this concentration range. Grandjean and Laszlo therefore concluded that water molecules stick to the saponite surface whereas the acetonitrile molecules occupy the second solvation layer, parallel to the first at a distance from the surface governed by the Li^{+} counter ions. They state however that the orientation of the acetonitrile molecules varies greatly in the 0-60% vol/vol range, shown by a significant decrease in

the ^{14}N and ^{2}H splittings observed for this concentration range. Above 60% vol/vol, a steady decrease in the ^{2}H and ^{17}O splittings was observed for the D_2O molecules, indicating that acetonitrile molecules do compete with water for occupation of the first solvation shell at these raised acetonitrile concentrations.

The clay used for most investigations in this thesis was a Texas bentonite, Westone-L, which has a low iron content of nominally 0.7% Fe_2O_3. Only a slight differential line broadening was observed for the ^{2}H doublet of this clay as would be expected for a clay with low iron content, based on Grandjean and Laszlo's work. In this thesis, the maximum splitting observed for Ca^{2+} or Na^{+} exchanged Westone-L was 72 and 36 Hz respectively. There was no observed change in sign of the deuterium doublet from +ve to -ve on changing from a Ca^{2+} to a Na^{+} exchanged clay. As mentioned previously, Grandjean and Laszlo also observed no change in sign of the ^{2}H splitting for saponite, hectorite and Gonzales County montmorillonite. In contrast however, a change in sign of the ^{2}H splitting was observed by Grandjean and Laszlo for Ecca Gum BP. In this thesis, addition of adsorbate species to Westone-L, whether cationic or anionic, led to a narrowing of the observed ^{2}H doublet which eventually resulted in complete collapse of the splitting. After extensive experimentation, it was concluded that the window from which information could be gained was too sensitive to the adsorbate species under examination. This will be discussed in greater detail later, (chapter 8). With this approach closed, interest in the interactions of polymers with clay in aqueous suspension led to the evaluation of the resident exchange cation as an *in situ* probe.

4.7 The use of Nuclear Magnetic Resonance to Study the Exchangeable Cations Associated with Clay.

The use of exchangeable cations as NMR probes to provide information on the surface properties of clays is a relatively new discipline and as a result few studies have been carried out. The lack of data arises from the limitations in the technique itself such as sensitivity and spectral resolution. The questions which need to be addressed are (i) is it possible to collect enough signal in a reasonable amount of time? and (ii) after the data is acquired, are the peaks narrow enough to learn something about the system? With the advent of high magnetic fields however, the resolution and sensitivity of the nuclei under examination have become less of a problem. With the exception of a study in 1976 on ^{7}Li in hectorite,[120] most publications concerning NMR of exchangeable cations associated with clay date back to the late 1980's. Much more attention has however been centred on the NMR spectroscopy of cations associated with zeolites.[121,122] The reason why smectites have received less attention can be attributed to the fact that they are usually aggregated into irregular tactoids and as a result there are many possible states of hydration. Further, most clays contain paramagnetic impurities (a few % Fe_2O_3 for example) in their lattice which leads to broad NMR signals.

Since 1988 several exchangeable cations have been studied by NMR (^{23}Na, ^{39}K, ^{133}Cs, ^{111}Cd and ^{113}Cd) in montmorillonite, hectorite and vermiculite.[92,93,123,124] Most studies have employed the technique of MAS NMR because this technique permits good resolution and hence allows easy measurement of any chemical shift observed in the signal. There are however two studies which have been carried out to analyse the chemical environment of exchangeable cations without the use of MAS NMR.[125,126] Tinet *et al.*[125] have used ^{113}Cd NMR to study cadmium exchanged clays (hectorite and

montmorillonite) in a powder and hydrated gel form. It was noted on hydration of the Cd-exchanged montmorillonite that the ^{113}Cd NMR signal was not a simple one site signal. In fact the ^{113}Cd signal was found to originate from two differing Cd environments in the clay sample, namely the interaction of Cd with water and Cd with clay. A similar phenomenon was encountered by Lambert *et al.*[126] who examined the ^{39}K NMR signal of powdered and hydrated (60 wt. % H_2O and 40 wt. % dry clay) K-montmorillonite. They observed the existence of two well defined signals in the ^{39}K spectra recorded. These spectra consisted of a broad component which they state is similar to the only component observed for air dried K^+ exchanged clays and also a narrow liquid-like component.

XRD studies carried out by Lambert *et al.*[126] show that the dry clay samples are interstratified with layer spacings of 10 Å and 12.4 Å which reflect weakly hydrated exchangeable cations with low mobility. Consequently the broad signal observed in the hydrated sample has been attributed to K^+ in the collapsed layers and to K^+ in interlayers expanded to 12.4 Å.

The narrow liquid like component is due to K^+ in rapid motion which the authors state may have two different origins:

1. K^+ in completely swollen interlayers (>14 Å basal spacing).

2. K^+ on the external surface of the clay.

The authors also state that the presence of paramagnetic centres in the clay may be the cause of some of the broadening seen in the ^{39}K signals.

NMR analysis of the structural environments of Cs^+ in caesium exchanged clays has thus far been limited to MAS NMR.[123,127] In a recent study by Weiss *et al.*[127] high resolution variable temperature (VT) MAS NMR spectroscopy was used to study the nature of the structural sites occupied by ^{133}Cs adsorbed onto clay. ^{133}Cs NMR experiments were carried out on samples of Cs-hectorite at different temperatures, from +80°C to -100°C to show that Cs^+ on hectorite occurs in several different structural environments, depending on the hydration state of the clay. For this study, Weiss *et al.*[127] used three distinct Cs-hectorite samples differing only in the way in which they were prepared. As a result, different Cs^+ environments were seen on the clay depending on the sample in question.

(1) ^{133}Cs VT MAS NMR spectra of < 1μm particle size hectorite in 0.1 and 1.0 mol L^{-1} CsCl slurries were recorded. Weiss *et al.*[127] state that there are two Cs^+ environments on hectorite undergoing rapid exchange which causes motional averaging of the ^{133}Cs NMR signal and results in one peak for samples recorded at temperatures ≥ -40°C. As the temperature is decreased to below -40°C, motional averaging slows which allows resolution of two peaks which represent the two Cs^+ environments.

(2) ^{133}Cs NMR spectra of Cs-hectorite exposed to 100% relative humidity show a single line at temperatures in the range +80°C to -20°C. This single line is considered to be due to a motionally averaged signal from all sites. Below -20°C, two unaveraged signals appear which become better separated at decreasing temperature. Weiss *et al.*[127] attribute these two peaks to Cs^+ in the stern layer, near to basal O and Cs^+ in the Gouy layer surrounded by hydration shell water. A third peak is also seen and can be attributed

to unhydrated Cs^+ which is a result of drying the hectorite in the sample preparation stages.

(3) ^{133}Cs NMR spectra were also recorded of Cs-hectorite heated to 500°C and not allowed to rehydrate. These spectra show two peaks which do not change with temperature. Weiss *et al.*[127] state that these peaks may be due to anhydrous Cs^+ with two different oxygen coordinations which do not undergo exchange or motional averaging because of the absence of water. In this study Weiss *et al.*[127] have shown that Cs^+ may be present in many different structural environments in hectorite, depending on preparation and hydration state of the sample.

It has been shown that NMR spectroscopy may be used as a powerful tool to investigate the environment that exchangeable cations occur in. Careful choice of the exchangeable cation to be studied and the use of a clay with a low Fe content (to avoid interactions between relaxation mechanisms of the cation and paramagnetic centres) should therefore result in a method to probe the interactions of cationic species with clay.

4.8 The Choice of an Exchangeable Cation for Use as an 'In Situ' Probe.

The charge on aluminosilicate sheets due to isomorphous substitution must be balanced and usually occurs through interaction with metallic cations. The alkali metals of group 1A are the major exchangeable cations examined in this study and therefore will be considered in greatest detail. The nuclear properties of the alkali metals are outlined in Table 1 below.

Francium is omitted from the table because it has no known stable isotope, the most stable being ^{223}Fr which has a half life of 22 minutes.[128] The alkali metals under

Isotope	Natural Abundance (%)	I	Gyromagnetic ratio $\gamma(10^7$ rad T^{-1} $s^{-1})$	Quadrupole moment $Q(10^{-28}m^2)$	Receptivity referred to ^{13}C	Resonance frequency ^1H at 400 MHz (MHz)
^6Li	7.42	1	3.9366	$-8x10^{-4}$	3.58	58.862
^7Li	92.58	3/2	10.3964	$-4.5x10^{-2}$	1540	155.454
^{23}Na	100	3/2	7.0761	0.12	525	105.805
^{39}K	93.1	3/2	1.2483	$5.5x10^{-2}$	2.69	18.666
^{41}K	6.88	3/2	0.6851	$6.7x10^{-2}$	0.0328	10.245
^{85}Rb	72.15	5/2	2.5828	0.25	43	38.620
^{87}Rb	27.85	3/2	8.7532	0.12	277	130.885
^{133}Cs	100	7/2	3.5087	$-3x10^{-3}$	269	52.468

Table 1. The common nuclear properties of alkali metals (after Laszlo,[106] 1983).

consideration are therefore ^{6}Li, ^{7}Li, ^{23}Na, ^{39}K, ^{85}Rb, ^{87}Rb and ^{133}Cs. All these nuclei are stable isotopes apart from ^{87}Rb whose half life is $5x10^{11}$ years but is considered stable on an NMR time scale.

The majority of alkali metals have a spin quantum number of 3/2 however ^{6}Li, ^{85}Rb and ^{133}Cs have a spin number of 1, 5/2 and 7/2 respectively. The fact that all the alkali metals have a spin quantum number equal to or greater than 1 means that they all possess a quadrupole moment and therefore their relaxation behaviour is influenced by quadrupolar relaxation mechanisms. The quadrupole moments for ^{23}Na, ^{39}K, ^{41}K, ^{85}Rb and ^{87}Rb, are large and consequently their relaxation mechanism is dominated by quadrupole effects. Conversely ^{6}Li, ^{7}Li and ^{133}Cs have a low quadrupole moment and in theory other relaxation mechanisms can compete with the quadrupole relaxation mechanism. With the ^{133}Cs nuclus however, only the quadrupolar relaxation mechanism has been found to be plausible, irrespective of the low quadrupole moment.[106, 128]

NMR linewidths of quadrupole nuclei are related to Q^2, the electric quadrupolar moment and to the spin of the nucleus I through a line width factor L, (Equation 4).[129]

$$L = Q^2 \frac{(2I+3)}{[I^2(2I-1)]}.10^{56} m^2$$

Equation 4. Showing how the line width factor L is calculated using the electric quadrupole moment Q and spin quantum number I.

Therefore ^{133}Cs with a small electric quadrupole moment ($Q = -3 \times 10^{-3} .10^{-28} m^2$) and a large spin quantum number ($I = 7/2$) has the smallest line width factor of any quadrupole nuclei with $L = 1.2 \times 10^{-6} . 10^{56} m^4$. Consequently ^{133}Cs line widths are narrow compared to those of other alkali cations such as ^{23}Na ($L = 1.3 \times 10^{-2}. 10^{56} m^4$

and ^{39}K ($L = 3.2 \times 10^{-3}.10^{56}$ m^4) which both have line widths in the order of a few Hz. The line widths at half height for concentrated cation solutions of the nuclei ^{85}Rb and ^{87}Rb are broad and are in the order of 150 and 132 Hz respectively.[106] As stated previously, the line widths for both isotopes of Li are very narrow due to their dipolar or spin-rotation relaxation mechanisms.

Of the eight isotopes considered, ^{7}Li, ^{23}Na, ^{39}K and ^{133}Cs nuclei have natural abundances greater than 90%. The receptivities of ^{7}Li, ^{23}Na, ^{85}Rb and ^{133}Cs relative to that of ^{13}C, D^c, are high.

It was decided that the ^{23}Na and ^{133}Cs nuclei were the best *in situ* probes for investigation into the interactions of cationic species with clay minerals. These nuclei were chosen above other alkali metals because, as stated above, both are sensitive nuclei with relative receptivities $D^c = 525$ for ^{23}Na and 269 for ^{133}Cs. Both have a high natural abundance of 100% and both have sharp NMR signals. The chloride salts of Na^+ and Cs^+ are also readily available and the cations easily exchange with exchangeable cations on the clay resulting in a homionic cation exchanged clay.

It was later found that ^{23}Na in the NMR probe used gave a strong background signal which made ^{23}Na NMR difficult but not impossible. Consequently, it was decided to use ^{133}Cs NMR as an *in situ* probe nuclus. An added attraction for using ^{133}Cs NMR spectroscopy is that Cs^+ cations have a strong affinity with the clay surface and therefore any observable interaction will be more pronounced with this cation.

Large quantities of KCl are required (typically 30 pounds per barrel which is equivalent to 1.13 mol dm^{-3}) to promote drill hole stability when drilling an oil well. In a real drilling situation, clay lining the drill hole wall will exchange to a predominantly K^+

form. Therefore, the ideal nucleus for NMR analysis would be ^{39}K. Unfortunately, as discussed earlier, ^{39}K NMR is not sensitive enough for use in this study. One further advantage of using ^{133}Cs NMR is that the Cs^+ cation is a good model for K^+. This is because Cs^+ has a small hydration shell which is comparable in size to that of K^+ and like K^+ interacts strongly with the clay surface and is normally preferentially adsorbed by clay from solutions of other alkali metals.[130]

Certain points, such as the origin of the linewidth, need to be considered before the ^{133}Cs nuclei can be utilised as an *in situ* probe. Work has been undertaken on ^{133}Cs NMR by Boden *et al.*[131] who have studied caesium pentadecafluorooctanoate (CsPFO)/water liquid-crystal systems in a sample cell which allows temperature control at the millikelvin level. They have stated that an ideal ^{133}Cs spectrum consists of seven equally spaced lines of relative intensities, 7:12:15:16:15:12:7 corresponding to transitions between the spin states +7/2→+5/2, +5/2→+3/2, +3/2→+1/2, +1/2→-1/2, -1/2→-3/2, -3/2→-5/2, -5/2→-7/2 respectively, (Figure 20a).

Boden *et al.*[131] have shown that broadening of all transitions apart from the central +1/2→-1/2 occurs when temperature gradients are present in the system, (Figure 20b). Broadening also occurs when the liquid crystal is not permitted to align in the magnetic field.

The use of ^{133}Cs NMR to probe the interaction of cationic species with clay has consequently been utilised in the present study and will be considered in greater detail later, (see section 6.1.5).

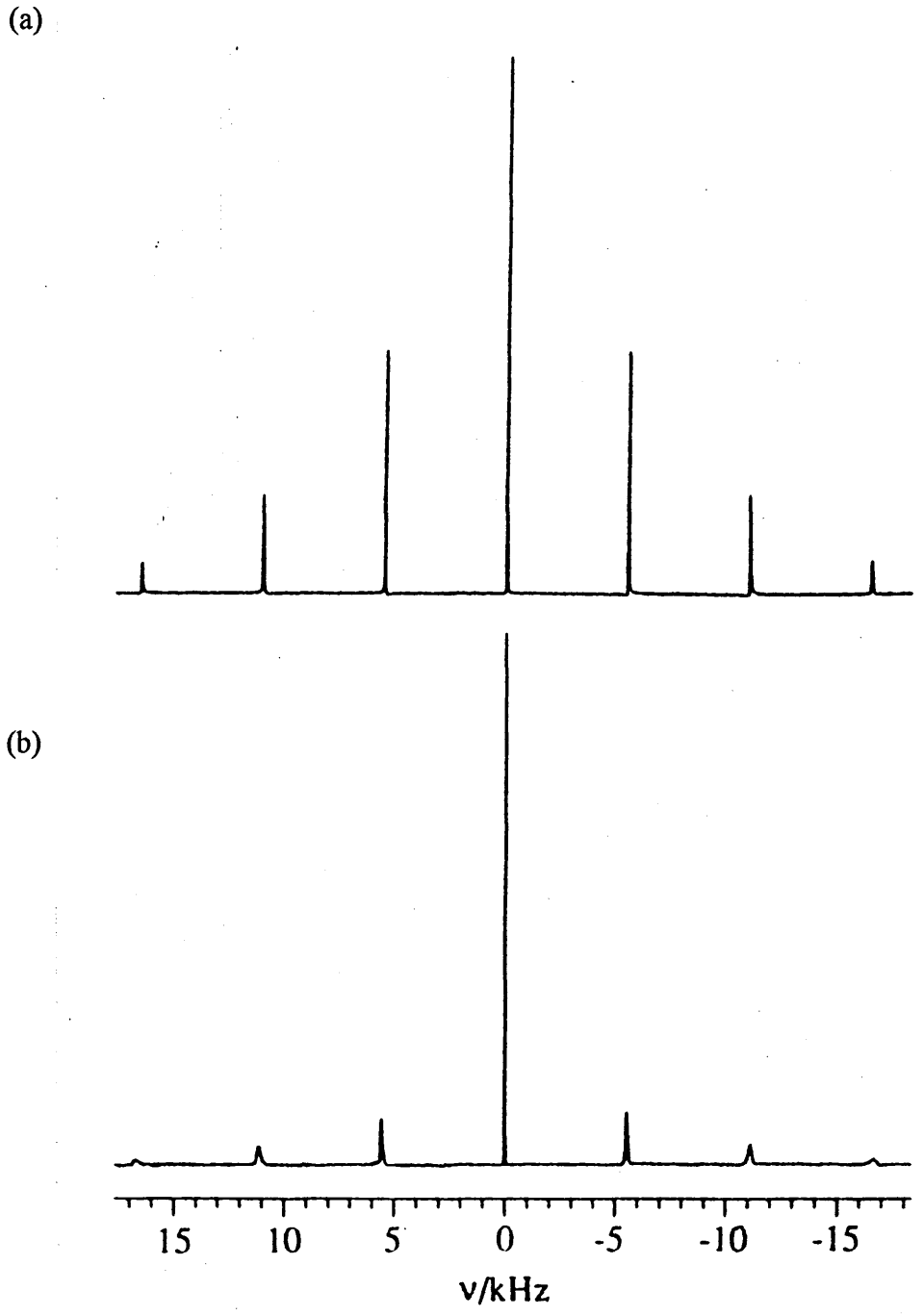

Figure 20. (a) ^{133}Cs NMR spectra of a CsPFO/H_2O sample in a constant temperature water-flow system at 315.5 °K (b) ^{133}Cs NMR spectra of the same sample in a standard air flow constant temperature system. The line broadening in (b) is the result of a temperature gradient of ≈ 30 mK cm^{-1} along the length of the sample, (after Boden *et al.*[131]).

4.9 Nuclear Magnetic Relaxation

The ^{133}Cs nucleus has a spin quantum number I = 7/2 and therefore this nucleus has eight different energy levels associated with it. At thermal equilibrium, in a large applied magnetic field, the spins are distributed among these different energy levels according to a Boltzmann distribution. If this Boltzmann distribution of spins among the different energy levels is then disturbed by an external process, such as moving the sample in and out of the magnetic field, B_0, or irradiating the sample at the Larmor frequency, ω_o, then the nuclear spin system will tend to restore a Boltzmann distribution after a period of time due to relaxation. This relaxation process is characterised by a specific time constant, T_1, and is termed the spin lattice or longitudinal relaxation time. T_1 actually describes the return of the magnetisation, M, to its equilibrium value along B_0. The value of T_1 is therefore a measure of the efficiency of the coupling which restores thermal equilibrium between the nuclear spin system and its surroundings, the lattice. A spin-spin or transverse relaxation process will also be in operation which measures the effect of spin-spin interactions in bringing the spin system into internal equilibrium. The transverse relaxation time, T_2, characterises the return to zero of any finite component of the magnetisation which does not lie in the B_0 direction after perturbation of the system.

In liquid samples, the value of T_1 can typically range from 10^{-3} to 10^2 seconds while for solids, the upper limit can be much larger when the sample is pure. If T_1 is small, relaxation is fast and a large linewidth is usually observed. Figure 21 shows a schematic dependence of relaxation on the correlation time τ_c. τ_c is defined as the time taken on average for a molecule to diffuse a distance equal to its own dimension or rotate through 1 radian.[132] In the short correlation time region, Figure 21 shows that $T_1=T_2$,

this is usually the case for liquids. In this fast motion part of the curve, the correlation time is much shorter than a Larmor period and $\omega_o^2\tau_c^2 << 1$ and is termed the region of extreme narrowing. As the motion slows down, T_1 and T_2 decrease until the value $\omega_o^2\tau_c^2 \approx 1$ is reached where T_1 passes through a minimum, the value of which depends upon ω_o. This minimum corresponds to the region where the considered motion is most efficient in establishing equilibrium with the lattice. When the motion is slow enough, T_1 increases as τ_c increases however in this long correlation region, where $\omega_o^2\tau_c^2 >> 1$, T_2 goes on decreasing. T_2 values in solids are often found in the long correlation region of the curve and may have a value in the order of microseconds which leads to large linewidths.

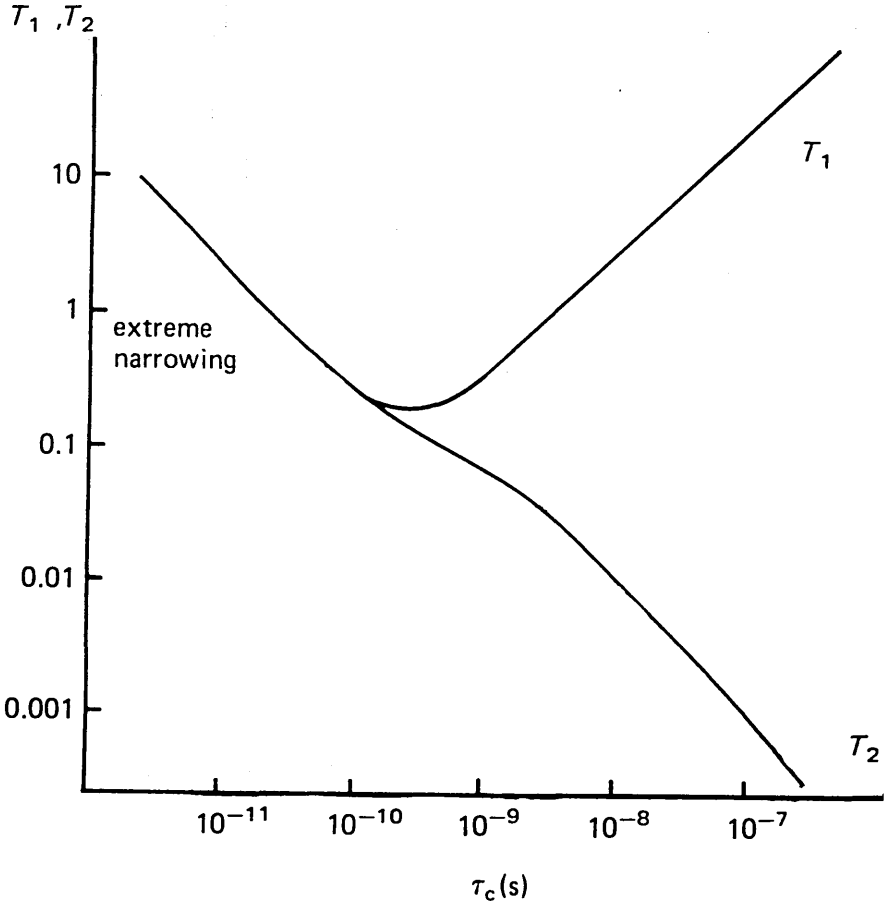

Figure 21. Schematic dependence of T_1 and T_2 on τ_c. Ordinate and abscissa values are approximate.

CHAPTER 5

Experimental

5. Experimental

5.1 Materials

5.1.1 Clay:

The clay used for the majority of experiments in this study was Westone-L montmorillonite. Westone-L has a CEC of 81 milli-equivalents per 100 g (meq/100g) as determined by English China Clays. X-ray Fluorescence (XRF) provided elemental analysis of the clay, the oxides of the major elements found are listed below for Cs^+, Na^+ and unexchanged montmorillonite, (Table 2). XRF analysis showed that this clay had a low Fe_2O_3 content, typically 0.7% by weight, (Table 2). Three other types of clay were also used for analysis of the ^2H NMR splitting and will be discussed later, (section 5.3.7.3).

	Nature of oxide, % of total weight								
Exchange form of clay	CsO	Na_2O	MgO	Al_2O_3	SiO_2	K_2O	CaO	TiO_2	Fe_2O_3
Unexchanged	0.12	0.02	3.41	17.21	69.36	0.07	1.80	0.24	0.75
3xCs-mont	12.20	0.16	2.71	16.47	61.42	0.04	0.05	0.17	0.76
3xNa-mont	0.00	2.50	2.68	16.71	72.15	0.04	0.02	0.24	0.72

Table 2. XRF data showing the elemental composition of Cs^+, Na^+ and unexchanged montmorillonite. Only the major oxides are shown.

5.1.2 Sedimentation/Purification Of Raw Montmorillonite.

Purification of the Westone-L was achieved by sedimentation which removes impurities including quartz, iron oxide, mica and other non clay impurities, leaving an essentially pure clay suspension. Sedimentation required the suspension of 500 g of raw clay in 10 litres of deionised water. The resulting clay suspension was then stirred thoroughly to evenly distribute all the mineral particles. The clay suspension was then covered and left overnight (*ie* > 16 hours), after which the upper 10 cm of the suspension was then siphoned off and collected. The volume of suspension removed from the container was replaced with an equal volume of deionised water, stirred, and the whole process repeated again up to 3 to 4 times storing the siphoned fraction each time. The initial stock suspension was then discarded as it contained mainly impurities from the raw clay. The purified clay fraction, which was nominally < 2 μ particle size, contained mainly Ca^{2+} and Mg^{2+} exchange cations. A < 0.3 μm clay fraction was also prepared from the purified clay fraction. This involved centrifuging a sample of the purified clay in a 30 ml centrifuge tube at 4500 rpm for 3.4 minutes and collecting the top 4 cm of the clay suspension.

5.1.3 Preparation of Cation Exchanged Montmorillonite.

The purified clay fraction, prepared by sedimentation, was altered from a predominantly Ca^{2+} and Mg^{2+} exchanged clay to one with 100% of the CEC satisfied by another cation (Table 2). The five cation exchanged clays used in this study are Cs^{+}, K^{+}, Na^{+}, Ca^{2+} and Mn^{2+} and are all prepared in the same way, using the chloride salt of the cation.

The chloride salt of the appropriate cation was dissolved in aqueous solution and added to the purified clay suspension at concentrations between 0.1 to 1.0 mol L^{-1} depending upon the replaceability of the cations in question (see the replaceability series of exchangeable cations, Chapter 2, section 2.2.1.5). After a suitable period of time (> 2 hours), the clay suspension was centrifuged and the supernatant discarded. A quantity of fresh metal chloride solution equal in volume to the discarded supernatant and equal in concentration to the previously added chloride solution was then added to the clay which was subsequently resuspended by homogenisation and left to equilibrate. This process was repeated three times in all, (subsequent XRF analysis confirmed that the clay was saturated with the cation of interest). Excess ions which may be trapped between the clay platelets were then removed by resuspending the ion exchanged clay centrifugate in deionised water. The clay suspension was then centrifuged and the supernatant again discarded. This was regarded as one wash and was repeated at least six times or until the clay suspension had a conductivity of < 30 μS. The washed clay was then reconstituted to give a suspension at a concentration of 50 gL^{-1} and was subsequently referred to as 3xZ-mont where Z represents the exchangeable cation and 3 represents the number of times the clay came into contact with the exchangeable cation solution.

5.2 Adsorbates

5.2.1 Cationic Adsorbates.

Chloride salts of the cationic species Na^+, K^+ and tetramethylammonium, TMA^+, were prepared at a concentration of 1.0 mol L^{-1}. Aliquots of the prepared solutions were then added to the cation exchanged clay of interest. Paraquat (methyl viologen) was also

investigated by adding aliquots of a 0.1 mol L^{-1} solution to the clay of interest. The structure of paraquat is shown below, (Figure 22).

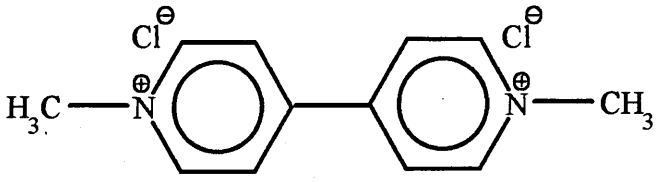

Figure 22. The structure of paraquat.

Three chemically similar cationic polymers FL15 (Mwt 5000), FL16 (Mwt 50 000) and FL17 (Mwt 100 000) were supplied by B.P. for investigation. These polycations are 50% active (*ie* diluted with water by 50%) when supplied and they were diluted a further 10 fold before being added to the clay of interest. These polymers are synthesised by copolymerising dimethylamine and epichlorohydrin, the structure of epichlorohydrin is shown below, (Figure 23).

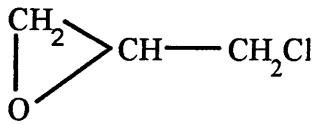

Figure 23. The structure of epichlorohydrin

FL15, 16 and 17 all contain 9% nitrogen by weight, this was confirmed by Kjeldahl analysis. Their general structure is shown below, (Figure 24).

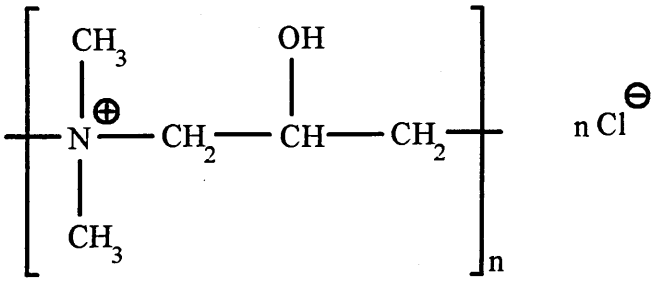

Figure 24. The monomer unit of the polycations FL15, 16, 17.

A polymer based on diallyldimethyl ammonium chloride known as Magnafloc 1697 was also investigated. This polycation is 50% active when supplied and was diluted a further 10 fold before being added to the clay of interest. Kjeldahl analysis confirmed that this polycation contained 8.5% nitrogen by weight. This polycation has a Mwt of 100 000. Its structure is shown below, (Figure 25).

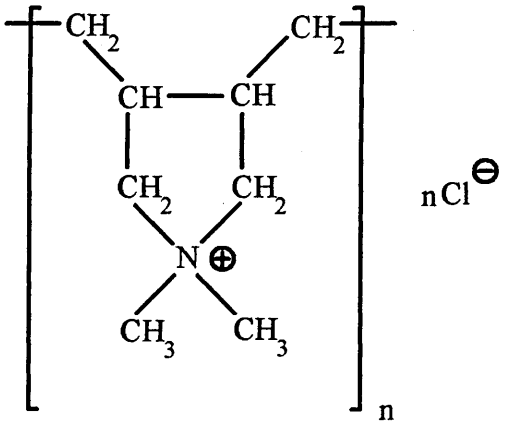

Figure 25. The monomer unit of Magnafloc 1697.

If the cationicity of the polymer is taken as the ratio of the cationic monomer to nonionic monomer in the resulting polymer then FL15, 16 and 17 and Magnafloc 1697 are all 100% cationic. Table 3 shows the approximate dimensions of the cationic polymers investigated in this thesis along with the number of cationic units in each polymer chain.

Type of cationic polymer	Number of cationic units	Distance between cationic centres / Å	Approximate length / Å
FL15 Mwt 5000	36	5.5	150
FL16 Mwt 50 000	360	5.5	1512
FL17 Mwt 100 000	727	5.5	3024
Magnafloc 1697 Mwt 100 000	619	8.5	3813

Table 3. The number of cationic units per polymer chain and approximate dimensions of the polycations investigated in this thesis.

5.2.2 Neutral Adsorbates.

The neutral polymer investigated was supplied by BP Chemicals and was a polyalkylene glycol named DCP101 which was copolymerised from ethylene and propylene oxide and has a molecular weight of ≈ 600. Aliquots of this polymer were added undiluted to the clay suspension of interest. The structure of polyalkylene glycol unfortunately cannot be illustrated due to company legislation.

5.2.3 Synthesis of a Deuterated Compound Chemically Similar to DCP101.

A deuterated compound, chemically similar to DCP101 was synthesised using the method outlined below. This compound was synthesised in the hope that ^2H NMR of clay suspensions containing the synthesised compound could provide some insight into how DCP101 interacts with clay

Dimethylmaleate (5.6 ml, 0.04 mol L^{-1}) was added to toluene (50 ml) in a round bottom flask (100 ml). The reaction was catalysed by addition of $[RuClH(PPh_3)_3]$ to the flask, taking care to purge the system of any air, which destroys the catalyst before starting the reaction. Deuterium gas, synthesised by dropwise addition of a D_2O/THF solution onto Na metal was then passed through the reaction mixture. The reaction

mixture turned from purple to brown on completion of the reaction. The reaction followed the route outlined below, (Figure 26).

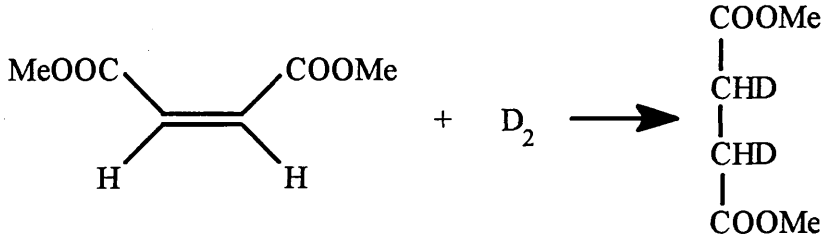

Figure 26. Reaction scheme showing the deuteration of dimethylmaleate.

The product of the reaction outlined above comprised of an 80:20 mixture of dimethylsuccinate and dimethylfumarate respectively as determined by ^{1}H NMR. The presence of dimethylfumarate in the product did not cause a problem and therefore the next stage in the reaction mechanism was carried out after the product mixture had been distilled and then purified using a silica column.

The deuterated dimethylsuccinate (2.7 g, 0.0185 mol L^{-1}) was then dissolved in a small quantity of dry THF (5 ml) and added to hexaethylene glycol (10.44 g, 0.370 mol L^{-1}). HCl gas was then passed through the solution for 5-10 minutes and the reaction mixture subsequently distilled. After the THF and MeOH had distilled off, the liquid product was collected and will subsequently be referred to as the deuterated hexaethylene glycol (HEG) compound. The reaction taking place is outlined below, Figure 27. ^{1}H NMR spectra were again recorded of the product.

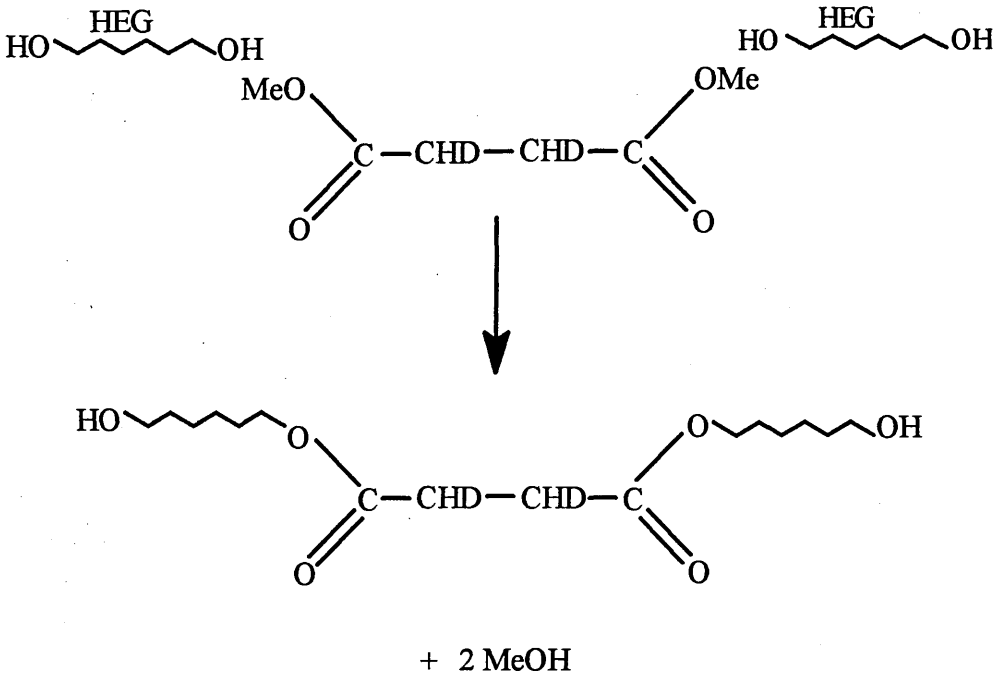

Figure 27. Reaction scheme showing the route taken to synthesise a deuterated compound similar to DCP101. HEG refers to hexaethylene glycol.

5.2.4 Anionic Adsorbates.

The anionic polymer used in this study was supplied by Allied Colloids. The polymer was a partially hydrolysed polyacrylamide (PHPA) which was 40% anionic and was made up into a 1% solution before addition to clay. The structure of PHPA is shown below, (Figure 28).

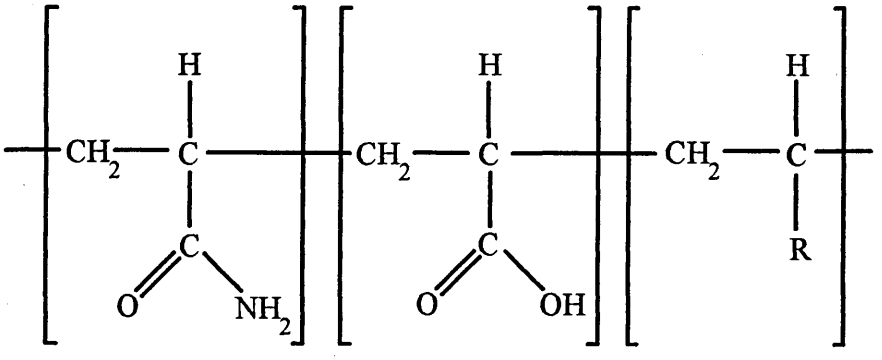

Figure 28. The structure of partially hydrolysed polyacrylamide, PHPA.

5.3 Analysis Techniques Used to Investigate the Interactions Taking Place Between Polymers and Clay.

Several established clay analysis techniques were used along with multinuclear NMR to investigate the interactions taking place between polymers and clay. The analysis techniques used included:

The experimental procedures used for each analysis will now be discussed in greater detail.

5.3.1 Kjeldahl Analysis of Various Exchange Forms of Westone-L Contacted With Different N Containing Cationic Adsorbates.

The Kjeldahl technique for total N analysis was used to gain information about the adsorption characteristics of several N containing cationic species. Samples were prepared by introducing 10 ml of 50 gL^{-1} 3xZ-mont (0.5 g clay) into a low density polyethylene bottle together with a quantity of cationic species and sufficient deionised water to give a total volume of 20 ml. This gave a final clay concentration of 25 gL^{-1}. Each sample was then oscillated at 280 rpm at 28 °C in a New Brunswick gyrotary water bath shaker (model G76D) for two hours. This method of mixing clay with adsorbate was used in all other analyses and will be quoted in the following text. The suspensions

were then centrifuged at 20 000 rpm for 20 minutes and the supernatant decanted off. The clay was then washed once which involved resuspension in 25 ml of deionised water and then centrifuging down once more to remove the supernatant which contained any unadsorbed species. The clay was then dried at 120°C, ground into a powder and stored at 120°C. Weighed quantities of this clay were then taken and added to a digestion tube containing 25 ml of concentrated H_2SO_4 (low nitrogen) and two 5 g catalyst tablets containing 94% K_2SO_4, 5.5% $CuSO_4.5H_2O$ and 0.5% Se. The K_2SO_4 in these tablets accelerates the digestion by raising the boiling point of the H_2SO_4, while the Cu and Se act as catalysts for the reaction. The samples were then digested by heating the digestion mixtures to 380°C for four hours in a Kjeldahl digester unit. During the digestion process, the nitrogen containing compounds react to give ammonium sulphate, water and carbon dioxide.

After digestion the samples were analysed for total nitrogen using a Gerhardt Vapodest Kjeldahl Autoanalyser. This instrument automatically analyses for total nitrogen by first making the digestion solution basic by adding 30 ml of 40% NaOH. This converts all the NH_4^+ in solution to NH_3 which is then steam distilled and adsorbed into a 4% boric acid solution. The ammonia-boric acid complex formed is a strong base which is then titrated with 0.1 mol L^{-1} HCl to determine the percent nitrogen by weight in the sample.

To confirm that the Kjeldahl method for the determination of total nitrogen in clay samples was both accurate and precise, a range of test samples were made up consisting of a known quantity of tetramethylammonium exchanged montmorillonite (TMA-mont) and a quantity of untreated Westone-L to give 1g in total of clay. The

samples were then analysed for total nitrogen using the Kjeldahl technique and the results recorded, (Table 4).

		% N found in duplicate		
Westone-L / g	**TMA-mont / g**	**1**	**2**	**% N average**
1.00	0.00	0.016	0.016	0.016
0.95	0.05	0.122	0.109	0.110
0.90	0.10	0.180	0.180	0.180
0.85	0.15	0.238	0.244	0.241
0.80	0.20	0.307	0.311	0.309
0.60	0.40	0.511	0.551	0.551
0.40	0.60	0.818	0.817	0.818
0.20	0.80	1.057	1.043	1.050
0	1.00	1.308	1.292	1.300

Table 4. The % N detected by Kjeldahl analysis for the addition of increasing quantities of TMA-mont to untreated Westone-L to give 1 g in total of clay.

A graph showing the quantity of TMA-mont in each sample versus the %N detected was then plotted and is shown below (Figure 29).

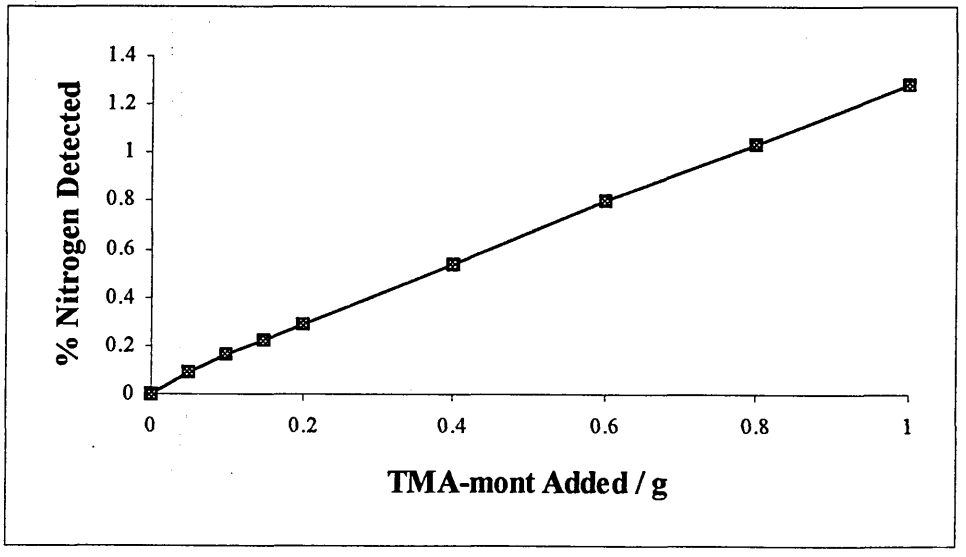

Figure 29. Graph showing the %N detected by Kjeldahl analysis for the addition of increasing quantities of TMA-mont to untreated Westone-L to give 1g in total of clay.

Figure 29 shows a straight line which passes through the origin, confirming that the precision of this technique is good. Untreated Westone-L has a quantity of nitrogen 0.016% associated with it, the quantity of nitrogen seen in 1g of TMA-mont is therefore 1.28%. The calculated value of percent nitrogen in fully exchanged TMA-mont is 1.28% which shows that the experimental value obtained agreed well with the calculated value.

5.3.2 CHN Analysis of Different Cation Exchanged Forms of Westone-L Contacted With DCP101.

CHN analysis was performed on different cation exchange clay samples contacted with varying amounts of DCP101. Results from these analyses were used to construct representative adsorption isotherms which may then provide information about the affinity of DCP101 for the various types of exchanged clay under examination. The Kjeldahl technique could not be utilised for this study because DCP101 does not contain any N. The %C carbon values obtained from CHN analysis were used to calculate the weight of DCP101 adsorbed on the various types of clay. This then allowed the construction of representative adsorption isotherms for each form of cation exchanged clay.

All samples were prepared by introducing 2 ml of 50 gL^{-1} 3xZ-mont (0.1 g clay) into a low density polyethylene bottle along with a quantity of DCP101 and sufficient deionised water to give a total volume of 4 ml. Some 3xCs-mont samples however also contained 0.025 mol L^{-1} KCl along with the added DCP101. KCl was added to these samples because this salt is used as an additive in all drilling muds containing DCP101 and therefore it was important to know what effect it had on the quantity of DCP101 adsorbed onto the selected clay. These samples were formulated by adding the desired

quantity of KCl to the aliquot of deionised water which was added to each sample to give a total volume of 4 ml and a final clay concentration of 25 gL^{-1}. All samples were then mixed in the usual way, centrifuged down and the supernatant discarded. Each sample was then resuspended in 20 ml of deionised water and centrifuged down again before the supernatant was discarded, this constituted 1 wash of the sample. All samples were then dried in an oven at 120°C, then ground to a powder before being replaced in the oven. After a further 4 hours of heating at 120°C, each sample was then removed from the oven, quickly sealed and then sent off for CHN analysis by a Perkin Elmer 2400 CHN Elemental Analyser.

5.3.3 The Use of XRF to Determine the Elemental Composition of Clays.

XRF was used to study the elemental composition of the different cation exchanged clay forms of Westone-L. The X-ray spectrometer system used in all analyses was the Philips PW 2400. The principal behind XRF involves bombarding the sample with primary radiation which causes the ejection of core electrons. The vacancies in the core orbitals are filled by electrons from intermediate levels and in doing so release the excess energy gained in the form of secondary radiation, fluorescence. A characteristic fluorescent radiation is emitted for each energy transition. The wavelength of the emitted radiation is inversely proportional to the difference between the initial and final energy level of the electron. The elements in samples under test therefore produce unique fluorescence comprising of radiation at a number of specific wavelengths. These wavelengths may be diffracted by directing the emitted beam onto a suitable crystal which has lattice planes parallel to its surface. By changing the angle θ, the angle at which the secondary radiation strikes the crystal, individual wavelengths may be detected using a gas filled proportional detector for the longer wavelengths and a scintillation

detector for short wavelengths (below 0.08 nm). The intensity of radiation at any given wavelength is proportional to the concentration of the element in the sample which is responsible for that radiation. The amount of any given element present in a sample can therefore be quantitatively calculated.

The elemental composition of several different cation exchange clay forms was analysed by XRF. Each sample analysed was first ground into a powder and then dried at 120°C. All samples were then sealed in an air tight vial and then dispatched for analysis. XRF analysis required that exactly 1g of the dried powdered clay be taken and mixed with exactly 10 g of powdered lithium-tetraborate. The mixed powders were then placed into a platinum crucible and heated in an oven at a temperature of 1250°C for six minutes, after which time the powders had fused to form a melt which was then swirled to aid mixing and replaced in the oven for a further six minutes. This homogenous melt was poured into a mould and left to solidify, after which time the resulting fused bead was analysed by XRF using software which enabled the oxides of numerous elements to be determined quantitatively. All clay samples were analysed using this oxide program however it was necessary to make up a standard bead for the quantitative analysis of Cs^+ in 3xCs-mont because this element was not dealt with in the oxide program. This bead contained a quantity of dried unexchanged clay and exactly 10% Cs^+ by weight from the addition of Cs_2CO_3 to give a total sample weight of 1g. This sample was then mixed with lithium-tetraborate and again fused into a bead and analysed by XRF. Quantitative analysis of caesium exchanged clay samples could then be carried out by comparison to this standard bead.

5.3.4 XRF Analysis of Polymer Treated 3xCs-mont

XRF analysis was carried out to see whether or not any Cs^+ could be detected in 3xCs-mont contacted with FL17 at loadings exceeding the CEC of the clay. This investigation therefore involved the addition of 4.80×10^{-2} mol L^{-1} of N from FL17 to 25 ml of 3xCs-mont 50 gL^{-1}. The sample was then made up to a total volume of 50 ml with deionised water to give a final clay concentration of 25 gL^{-1}. After mixing in the usual way, the sample was centrifuged down and the supernatant which contained the displaced Cs^+ ions discarded. The polymer contacted clay was then washed five times (or until the conductivity of the suspension was < 50 μS) with deionised water to remove any remaining desorbed Cs^+. Washing the clay sample involved resuspension in deionised water then discarding the supernatant after centrifugation. The washed polymer contacted clay was then dried in an oven at 120°C, ground into a powder and then replaced in the oven until required. Exactly 1 g of the clay was then taken, mixed with powdered lithium-tetraborate and again fused into a bead and then analysed by XRF.

5.3.5 XRD Analysis of Clay/Polycation Complexes.

XRD was used to determine whether or not adsorbed polymer resides between the layers of the clay platelets or is it simply adsorbed onto the surface of the clay. These analyses were carried out by measuring changes in the d-spacing of the first order basal reflections (d 001 spacing) of all clay/polymer complexes. In addition all samples were analysed at increasing temperatures to determine how stable the clay/polymer complexes were at elevated temperatures. A Philips PW1050 X-ray diffraction instrument was used for all analyses. The voltage and current used in all analyses was 40 kV and 20 mA respectively. High voltage is required to accelerate electrons across the gap in the X-ray

tube while the current determines the number of electrons that are available to be pulled across the gap to strike the target. A cobalt tube was chosen for all analyses because it has a wavelength of 1.79 Å which is long compared to the more common copper tubes (1.54 Å). In clay minerals the low angle peaks are usually the most important and consequently an increase in wavelength which shifts low angle peaks to slightly higher values is extremely useful for clay mineral analysis. The cobalt Kα radiation then leaves the X-ray tube through a window of beryllium, passes through the shutter and then through a series of slits which collimate, control and direct the beam towards the sample which they penetrate. If the beam falls on a series of atom bearing planes in the sample, each a distance *d* apart, at an angle θ, then for a sharp diffracted beam to be produced,

$$n \,.\, \lambda = 2d \,.\, \sin\theta$$

where λ is the wavelength of the rays and *n* is an integer. A sharp peak is therefore only produced when the path lengths of diffracted rays differ by an exact multiple of the wavelength. The reflected part of the beam then passes through another series of slits before it reaches the detector. All XRD traces were recorded from 4° to 35° using an angular increment of 0.04° every 2 seconds.

All samples were prepared by introducing 2 ml of 50 gL^{-1} 3xZ-mont (0.1g clay) into a low density polyethylene bottle along with a quantity of the polymeric species under examination and sufficient deionised water to give a total volume of 4 ml. Some of the clay samples contacted with the neutral polymer DCP101 also contained 0.025 mol L^{-1} KCl. These samples were formulated by adding the desired quantity of KCl to the aliquot of deionised water which was added to each sample to give a total sample volume of 4 ml and therefore a final clay concentration of 25 gL^{-1}. All samples were then mixed

in the usual way. After mixing the clay suspensions were then transferred using a plastic dropping pipette onto glass slides where they were spread out evenly and left to air dry. A number of clay samples contacted with DCP101 were also washed once before being transferred onto a glass slide. Washing of a sample involved centrifuging down the clay/polymer complex, discarding the supernatant and then resuspending the sample in 20 ml of deionised water after which each sample was again centrifuged down and the supernatant discarded. Each sample was then resuspended in exactly 4 ml of deionised water and subsequently transferred onto a glass slide for drying. The heating stage used to support the glass slides in all XRD experiments required that each slide be cut to the approximate dimensions of 10 x 30 x 1 mm. XRD traces were then recorded for each sample at six different temperatures, these included ambient, 50, 100, 150, 200 and 250°C. After recording an XRD trace at a particular temperature, the temperature of the heating stage and consequently the orientated clay film was increased to the desired value. A time interval of 25 minutes was then allowed for the sample to gain equilibrium at the raised temperature before the next XRD trace was recorded.

5.3.6 TG Analysis of Clay/Polymer Complexes.

Another technique used for the analysis of clay/polymer complexes was TGA. This technique is useful for determining the quantity of water be it interlayer or lattice OH which is lost from the clay at increasing temperatures. The quantity and thermal stability of polymer adsorbed onto the clay may also be monitored by TGA. The principal behind TG analysis is to monitor weight loss from a sample as the temperature is increased at a linear rate.

All samples were prepared by introducing 2 ml of 50 gL^{-1} 3xZ-mont (0.1g clay) into a low density polyethylene bottle along with a quantity of the polymer under examination and sufficient deionised water to give a total volume of 4 ml. Some of the clay samples contacted with the neutral polymer DCP101 also contained 0.025 mol L^{-1} KCl. Samples containing KCl were formulated by adding the desired quantity of KCl to the aliquot of deionised water which was added to every sample to give a total sample volume of 4 ml and therefore a final clay concentration of 25 gL^{-1}. Each sample was then mixed in the usual way, centrifuged down and then the supernatant discarded. Each clay/polymer complex was then reconstituted in deionised water, centrifuged down and again the supernatant which contained any unadsorbed polymer was discarded. This process constituted 1 wash of the sample. The washed clay samples were then dried at 120°C and subsequently ground into a powder before analysis by TG.

Thermogravimetric traces were obtained using a Mettler TG50 thermobalance equipped with a TC10A processor. TG analysis required that 6-10 mg of each sample be weighed into a ceramic cup, placed into the TG furnace at room temperature and purged with dry N at a flow rate of 20 cm^3 min^{-1} for 20 minutes or until constant sample weight had been attained. The weight of each sample was noted before purging with N as the weight loss from the sample during purging gave some indication of the ability of each clay/polymer complex to adsorb water from the atmosphere. After purging, the samples were analysed which involved ramping the temperature at 20°C min^{-1} between 35°C and 800°C whilst recording the weight change of the sample.

5.3.7 The Use of NMR Spectroscopy to Investigate Clay/Polymer Interactions

NMR spectroscopy was used to investigate the interactions taking place between polymers and clay. Three distinct areas of investigation were carried out which involved the use of NMR, these included:

- **Investigation of the interactions taking place between cationic polymers and clay.**
- **^{2}H NMR spectroscopy of D_2O molecules associated with clay.**
- **Investigation of the interactions taking place between neutral polymers and clay.**

5.3.7.1 NMR Investigation into the Interactions Taking Place Between Cationic Polymers and Clay.

5.3.7.2 ^{133}Cs and ^{23}Na NMR Spectroscopy.

All samples were prepared by introducing 2 ml of 50 gL^{-1} Cs^{+} or Na^{+} exchanged Westone-L (0.1g clay) into a low density polyethylene bottle along with a quantity of the cationic species under examination and sufficient deionised water to give a total volume of 4 ml. This gave a final clay concentration of 25 gL^{-1}. Each clay/polymer suspension was then mixed in the usual way and then allowed to equilibrate overnight. 3 ml of each clay suspension was then transferred into an 8 mm diameter NMR tube which in turn was placed into a 10 mm diameter tube containing a quantity of deuterated acetone to lock onto (Figure 30).

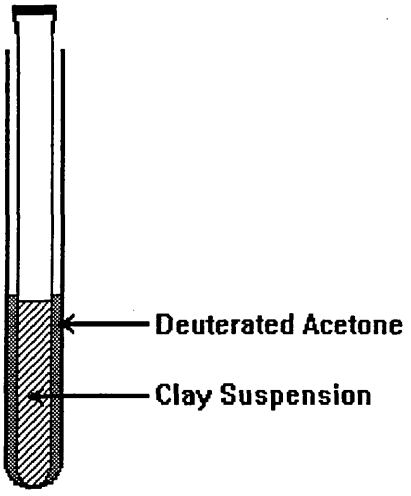

Figure 30. The coaxial tube arrangement used in this study.

All spectra were recorded on a Bruker WH400 NMR spectrometer (B_0 = 9.4T) at a frequency of 52.468 MHz for ^{133}Cs and 105.805 MHz for ^{23}Na. In a typical experiment, 800 transients were acquired in 1 K points, with a typical sweep width of 20 000 Hz, and were transformed with 16 K points. The pulse width used was 10 μs, a line broadening factor of 100 Hz was applied to each peak before the free induction decay (FID) was transformed. Consequently all quoted linewidths have 100 Hz subtracted from their value to account for this line broadening factor. These conditions were optimised by acquiring spectra at different pulse and sweep width until reproducible maximum peak integrations were obtained, this will be discussed in greater detail later, (section 6.1.5.1).

The proportion of Cs^+ associated with the clay, which was detected by NMR, was determined by reference to a 0.01 mol L^{-1} CsCl solution saturated with $CuSO_4.5H_2O$ to broaden the peak and will subsequently be referred to as the broadened CsCl peak. The added Cu^{2+} was used to broaden the linewidth of the CsCl peak by providing a better

relaxation pathway for the ^{133}Cs nucleus which resulted in a decrease in T_1 and hence a broader peak. This facilitated the measurement of peak area.

Experiments were then carried out to determine what effect if any that varying the 3xCs-mont concentration had on the Cs^+ integral. The purpose of this experiment was to show whether or not at higher clay concentrations some Cs^+ becomes trapped in pores formed by flocculated platelets. It was thought that any trapped Cs^+ will no longer be visible to NMR and therefore the Cs^+ integral will decrease. Four different 3xCs-mont clay concentrations were made up and the Cs^+ integral measured for each sample by ^{133}Cs NMR. The same ^{133}Cs NMR method and coaxial tube arrangement outlined above was utilised.

It was also possible to integrate the 3xCs-mont plus cationic species peak with respect to the broadened CsCl peak and thus estimate the quantity of Cs^+ detected by NMR in the clay suspensions. The same method can be applied for Na-exchanged clay however the reference used then is 0.01 mol L^{-1} NaCl again broadened with $CuSO_4.5H_2O$ and referred to as the broadened NaCl peak. The NMR operating conditions used for both broadened peaks, CsCl and NaCl, were identical to those used for clay samples however a relaxation delay equal to 1 second was required to prevent saturation of the signal. The linewidths of the ^{133}Cs or ^{23}Na peaks were also measured as a function of added cationic species. It was also checked whether or not addition of polycation to 0.005 mol L^{-1} CsCl made any contribution to the ^{133}Cs linewidth.

Experiments were then carried out to determine whether or not at polymer loadings equal to 100% of the clay's CEC that all the charged groups on the cationic polymer FL17 were satisfied by negative sites on the clay surface. This experiment

involved taking 6 ml of 50 gL^{-1} 3xCs-mont to which was added 1.152 x 10^{-1} mol L^{-1} of N from FL17 and enough deionised water to give a total suspension volume of 12 ml. The quantity of polymer added to the clay was sufficient to displace all the Cs^+. The clay polymer suspension was then mixed in the usual way, after which 4 ml was removed and stored before analysis by ^{133}Cs NMR. The remaining 8 ml of the suspension was then centrifuged down and the liquid portion discarded. The clay was then resuspended in an equal quantity of deionised water and the conductivity of the clay suspension measured. This process of washing the clay was repeated until the conductivity of the clay suspension was < 30 μS. This low conductivity shows that the vast majority of the extraneous Cs^+ ions have been removed. 4 ml of this washed clay/polymer suspension was then stored for analysis by ^{133}Cs NMR. The remaining 4 ml of washed clay/polymer suspension was then added to 4 ml of 3xCs-mont at a concentration of 25 gL^{-1} and mixed in the usual way. ^{133}Cs NMR experiments were performed on all three samples to determine how much Cs^+ was present in each one. This was carried out by utilising the same method and coaxial tube arrangement outlined above.

5.3.7.3 ^2H NMR Spectroscopy of D_2O Molecules Associated With Clay.

Experiments were carried out to investigate what effect the addition of cationic, anionic and neutral species to different clays had upon the residual quadrupolar splitting associated with D_2O molecules in clay suspension. The different types of natural clay used in this study included Westone-L montmorillonite, Mineral Colloid bentonite, Texas bentonite and Laponite which contained 0.75%, 3.92%, 3.40% and 0% Fe_2O_3 by weight, respectively, (Table 5).

	Nature of oxide, % of total weight							
Type of clay	Na_2O	MgO	Al_2O_3	SiO_2	K_2O	CaO	TiO_2	Fe_2O_3
Westone-L montmorillonite	0.02	3.41	17.21	69.36	0.07	1.80	0.24	0.75
Mineral Colloid bentonite	2.20	2.13	17.74	66.16	0.14	0.82	0.10	3.92
Texas bentonite	2.55	1.66	16.86	66.37	0.50	1.68	0.14	3.40

Table 5. Elemental composition of the three natural clays used in this study.

Westone-L is found naturally in the Ca^{2+} and Mg^{2+} exchanged form while Mineral Colloid and Texas bentonite occur naturally with Na^+, Mg^{2+}, Ca^{2+} and a small proportion of K^+ all present as exchange cations. The Mineral Colloid clay was purified and exchanged with the cations of interest in exactly the same way as Westone-L, outlined previously. Texas bentonite and Laponite (a synthetic clay) were dispersed at the desired concentration in deionised water having undergone no purification or exchange procedures. All natural clay samples were suspended in water at a concentration of 40 gL^{-1}.

NMR analysis required that 0.3 ml of D_2O was added to 3 ml of the clay suspension in a 10 mm diameter NMR tube which was shaken vigorously before analysis. All spectra were recorded on a Bruker WH400 NMR spectrometer (B_0 = 9.4T). In a typical experiment, 8 transients were acquired in 2 K points, with a typical sweep width of 1000 Hz and were transformed with 4 K points. The $\pi/2$ pulse width was 50 μs. Measurement of T_1 by the inversion recovery sequence (180°- t - 90° (FID) - Td)$_n$ was then performed on selected samples.

On introduction into a magnetic field, clay platelets align with or perpendicular to the field. The time taken for alignment may be several minutes, therefore data on the speed at which platelets align was required. Alignment time was deduced by recording spectra of the clay samples at increasing residence times in the magnetic field and noting the magnitude of the ^2H doublet splitting.

5.3.7.3.1 The Effect of Added Salt on the ^2H Splitting.

The effect of the extraneous ions on the magnitude of the ^2H was also investigated. Here aliquots of NaCl (1.0 mol L^{-1}) and $Ca(NO_3)_2$ (0.25 mol L^{-1}) were added to Na^+ and Ca^{2+} exchanged montmorillonite. The samples were mixed in the usual way and stored overnight before analysing by NMR.

5.3.7.3.2 The Effect of Added Polymer on the ^2H Splitting.

The effect of polymer on the magnitude of the ^2H splitting was also studied. The polymer investigated was 40% anionic PHPA. Samples were prepared containing 4 ml Na^+ exchanged montmorillonite (40 gL^{-1}) and an aliquot of polymer. Prior to mixing, PHPA was made up to a 1% w/v solution. The clay polymer suspensions were then mixed in the usual way and stored overnight. ^2H NMR was then carried out using the conditions outlined above.

5.3.7.3.3 The Effect of the Synthesised, Deuterated HEG Compound on the ^2H Splitting.

Different aliquots of the deuterated HEG compound, up to 10% v/v, were added to 4 ml 3xNa-mont (40 gL^{-1}), mixed in the usual way and stored overnight. After introduction of the clay/HEG suspension into a 10 mm NMR tube, the ^2D NMR

spectrum was recorded. In a typical experiment, eight transients were acquired in 2 K points, with a typical sweep width of 1000 Hz and were transformed with 4 K points.

5.3.7.4 The Use of NMR Spectroscopy to Investigate the Interactions Taking Place Between DCP101 and Clay.

5.3.7.5 ^{133}Cs and ^{23}Na NMR

Usually when drilling an oil well, DCP101 is added to a drilling mud along with a number of other additives. Two examples of such additives are KCl or polycations. Three separate series of experiments have been carried out to investigate the interactions of DCP101 with 3xCs-mont in the presence and absence of such additives.

1. Samples were made up using aliquots of undiluted DCP101 which were added to 2 ml of 50 gL^{-1} 3xCs-mont, these solutions were then made up to a total volume of 4 ml with deionised water, mixed in the usual way and stored overnight. ^{133}Cs NMR spectra were then recorded using the same coaxial tube arrangement and NMR operating conditions used previously for the addition of cationic polymer to 3xCs-mont, see section 5.3.7.2. The ^{133}Cs integral intensities from the 3xCs-mont plus DCP101 samples were then compared with the broadened CsCl peak as described previously, any changes in the ^{133}Cs linewidth were also recorded. These initial experiments were then repeated, this time however the clay used was 3xNa-mont. The integral intensity of the ^{23}Na associated with the clay was compared with that for broadened NaCl as described earlier in section 5.3.7.2.

2. Samples were then made up with differing volumes of FL15 added to 2 ml of 50 gL^{-1} 3xCs-mont along with a fixed 3% v/v quantity of DCP101. Each sample was

then made up to a total volume of 4 ml with deionised water, mixed in the usual way and stored overnight. ^{133}Cs NMR spectra were then recorded using the same coaxial tube arrangement and NMR operating conditions used previously for the addition of cationic polymer to 3xCs-mont. The ^{133}Cs integral intensity from each sample was then compared with the broadened CsCl peak as described previously and the quantity of Cs^+ seen by NMR calculated.

3. Further samples were made up containing different aliquots of 1 mol L^{-1} KCl added to 2 ml of 50 gL^{-1} 3xCs-mont. Each sample was then made up to a total volume of 4 ml with deionised water. Two subsequent sets of samples containing the same quantity of KCl and 3xCs-mont as above were made up, this time however 0.1% v/v of DCP101 was added to each sample in one set and 0.01% v/v of DCP101 was added to each sample in the other set. All samples were mixed in the usual way, stored overnight and then analysed by ^{133}Cs NMR. The ^{133}Cs integral intensity from each sample was then compared with the broadened CsCl peak as described previously and the quantity of Cs^+ seen by NMR calculated.

5.3.7.6 ^1H NMR

The ^1H NMR linewidth of the water peak observed for 3xMn-mont clay suspensions was utilised in order to gain information concerning the interactions of DCP101 with clay. Initially a series of samples with different 3xMn-mont clay concentrations spanning a range from 0.6 to 23 gL^{-1} were made up. All the samples were then mixed in the usual way, stored overnight and analysed after introduction into a 5 mm NMR tube. The ^1H signal from the water protons in the sample was then recorded on a Bruker WH400 NMR spectrometer (B_0 = 9.4 T). In a typical experiment 8

transients were acquired in 32 K points, with a typical sweep width of 10000 Hz and were transformed with 32 K points.

Three further series of samples were made up spanning the same 3xMn-mont concentration range. This time however each series contained a different, fixed concentration of added DCP101, the three concentrations were 10, 2 and 0.1% v/v. A typical sample might therefore contain 1 ml of 3xMn-mont at a given concentration plus 2 % v/v DCP101. A fourth series of samples was then made up again spanning the same 3xMn-mont clay concentration range, this time however 0.001% v/v 1,2-diaminoethane was added to each sample. The water peak for all samples was then analysed by ^{1}H NMR and the spectra recorded as above. 3xMn-mont samples containing 1% v/v 1,2-diaminoethane were also made up, at this concentration however severe clay flocculation occurred which prevented analysis by NMR.

5.3.8 The Use of Zeta Potential to Study Clay/Polymer Suspensions.

The zeta potential for several clay polymer suspensions was measured using a Malvern Zetasizer II instrument. Zeta potential studies involve measurement of the potential drop which occurs across the stern layer of ions surrounding each clay particle, see section 3.3.1 for more detail concerning the Stern model. The Malvern Zetasizer makes use of a neon laser beam which is divided into two beams and focused to a crossing point in the sample cell or electrophoresis chamber. This crossover region defines a 'probe volume' from which data will be extracted. The sample cell has a voltage applied across it which causes the charged particles to drift to one or other of the electrodes. As the clay particles pass through the probe volume, they experience a periodic illumination. Scattered light from this probe volume is then imaged by receiving

optics onto the photo-cathode of the photomultiplier. The detected light with a given frequency is then processed as individual photon detection pulses by a signal processor and the zeta potential calculated.

All samples were prepared by introducing 2 ml of 50 gL^{-1} 3xZ-mont (0.1 g clay) into a low density polyethylene bottle along with a quantity of the polymer under examination and sufficient deionised water to give a total volume of 4 ml. The samples were then mixed in the usual way before analysis. Measurement of the zeta potential for each clay/polymer suspension required that each sample be diluted considerably to allow the laser beam to penetrate the sample. Typically 3-4 drops of the clay/polymer suspension (25 gL^{-1}) were mixed into 50 ml of deionised water and then introduced into the sample cell of the instrument. The instrument indicated whether or not the sample had been diluted sufficiently before it allowed measurement of the zeta potential. The zeta potential of several different clay/polymer suspensions were then recorded.

5.3.9 Measurement of Particle Size in Clay/Polymer Suspensions.

All particle size measurements were recorded using a Leeds and Northrup Microtrac Particle Size Analyser. This instrument measures particle size by initially directing a laser beam through a transparent sample cell containing a moving stream of the clay particles under investigation. The clay particles were kept in continual motion through the sample cell by use of a sample recirculator (pump). Each clay/polymer suspension therefore has to be diluted in the recirculating liquid, in this case water, before analysis. Light rays from the laser beam which strike the moving clay particles are forward scattered through angles which are inversely proportional to the size of the particle. A photodetector array then measures the quantity of forward scattered light or

flux at several predetermined angles. Electrical signals proportional to the measured light flux values are then processed by a microcomputer system to form a multichannel histogram of the particle size distribution. Before any clay/polymer suspensions were analysed however, it was necessary to record a background signal for pure water which was automatically subtracted from the sample measurement data. The particle size range which could be measured by this instrument was from 0.12 to 704 microns.

All samples were prepared by introducing 2 ml of 50 gL^{-1} 3xZ-mont (0.1 g clay) into a low density polyethylene bottle along with a quantity of the polymer under examination and sufficient deionised water to give a total volume of 4 ml. The samples were then mixed in the usual way before analysis. Measurement of particle size of the clay/polymer suspensions required that these suspensions were diluted in the recirculating water before analysis. The instrument then indicated whether the correct concentration of clay/polymer suspension had been added to the recirculating volume before particle size analysis could continue.

CHAPTER 6

Investigation into the Interactions Taking Place Between Cationic Species and Westone-L

6. Investigation into the Interactions Taking Place Between Cationic Species and Westone-L.

The observed interactions taking place between several different cationic species and Westone-L montmorillonite will be recorded and discussed in this chapter. Investigation of these clay/cationic species interactions required the use of several different analysis techniques including:

The results obtained by each of these analysis techniques are outlined and discussed below.

6.1 Results Obtained Using Different Analysis Techniques to Investigate the Interactions of Several Cationic Species with Westone-L.

6.1.1 Kjeldahl Analysis of Westone-L Contacted With Various N Containing Cationic Species.

3xCs-mont, 3xNa-mont and 3xK-mont were contacted with several different cationic nitrogen containing species. The observed percent N in each sample, determined by Kjeldahl analysis, was then recorded (Table 6, Table 7).

Figure 31 and Figure 32 show the adsorption isotherms obtained for the addition of FL15, FL17, Magnafloc 1697 and TMA^+ to 3xNa-mont, 3xCs-mont and 3xK-mont.

The ^{133}Cs NMR spectra obtained for the isotherm points designated 1 to 4 in Figure 31 are shown in Figure 44. FL15, FL17 and Magnafloc 1697 all exhibited high affinity adsorption isotherms on all three cation exchanged forms of Westone-L. The FL series of polymers, however, showed the greatest affinity for the clay surface shown by the initial steep rise in the isotherm curves. As the quantity of each polymer contacted with the clay was increased, a plateau was eventually reached where the amount of polymer adsorbed did not increase significantly. With the addition of FL17, FL15 and Magnafloc 1697 to 3xCs-mont, the onset of the plateau region occurred for the addition of between 2.30 and 2.88 x 10^{-2} mol L^{-1} of N from the polymer. This quantity of added N was similar to the CEC of the clay which was satisfied by the addition of 2.4 x 10^{-2} mol L^{-1} of N. Conversely with the addition of FL17 and Magnafloc 1697 to 3xK-mont and 3xNa-mont, the onset of the plateau region occurred at much higher loadings of polymer which greatly exceeded the CEC of the clay. For example, with the addition of FL17 to 3xK-mont and 3xNa-mont, the onset of the plateau region occurred for the addition of 3.84 x 10^{-2} mol L^{-1} of N from the polymer. A less well pronounced plateau region was observed upon addition of Magnafloc 1697 to 3xK-mont and 3xNa-mont which occurred for the addition of 4.50 x 10^{-2} mol L^{-1} of N from the polymer. The plateaux observed for the addition of FL17 and Magnafloc 1697 to each cation exchanged clay form show that the maximum amount of polymer adsorbed, Q_{max}, increased with exchange cation as $Cs^+<K^+<Na^+$. Q_{max} was equal to 113 (Cs^+), 144 (K^+) and 171 (Na^+) mg g^{-1} for the addition of FL17 to the three types of cation exchanged clay while Q_{max} for the addition of Magnafloc 1697 was equal to 74, 112 and 177 mg g^{-1} respectively. With the addition of FL15 to 3xCs-mont, Q_{max} was equal to 109 mg g^{-1}. The TMA^+ ion exhibited a low affinity adsorption isotherm when added to 3xCs-mont. Q_{max} for the addition of this ion to 3xCs-mont was equal to 46 mg g^{-1} in the region studied.

Sample	Mol L^{-1} N added to clay	% N detected by Kjeldahl	Amount adsorbed mg g^{-1}
3xCs-mont + FL15			
	4.80×10^{-3}	0.324	24
	9.60×10^{-3}	0.575	44
	1.44×10^{-2}	0.814	63
	1.92×10^{-2}	0.989	78
	2.40×10^{-2}	1.179	94
	2.88×10^{-2}	1.257	101
	3.84×10^{-2}	1.281	103
	4.80×10^{-2}	1.350	109
3xCs-mont + FL17			
	4.80×10^{-3}	0.455	34
	9.60×10^{-3}	0.671	51
	1.44×10^{-2}	0.926	72
	1.92×10^{-2}	1.160	92
	2.40×10^{-2}	1.276	102
	2.88×10^{-2}	1.326	107
	3.84×10^{-2}	1.370	111
	4.80×10^{-2}	1.398	113
3xNa-mont + FL17			
	4.80×10^{-3}	0.302	22
	9.60×10^{-3}	0.590	45
	1.44×10^{-2}	0.925	72
	1.92×10^{-2}	1.298	104
	2.40×10^{-2}	1.368	111
	2.88×10^{-2}	1.559	128
	3.84×10^{-2}	1.875	158
	4.80×10^{-2}	1.916	162
	5.76×10^{-2}	1.927	163
	6.72×10^{-2}	2.012	171
3xK-mont + FL17			
	4.80×10^{-3}	0.224	17
	9.60×10^{-3}	0.503	38
	1.44×10^{-2}	0.700	54
	1.92×10^{-2}	0.864	67
	2.40×10^{-2}	1.048	83
	2.88×10^{-2}	1.249	100
	3.84×10^{-2}	1.598	132
	4.80×10^{-2}	1.691	141
	5.76×10^{-2}	1.619	134
	6.72×10^{-2}	1.683	140

Table 6. The quantity of N detected by Kjeldahl analysis for the addition of FL15 and FL17 to 3xZ-mont.

Sample	Mol L^{-1} N added to clay	% N detected by Kjeldahl	Amount adsorbed mg g^{-1}
3xCs-mont + 1697	4.53×10^{-3}	0.192	18
	9.06×10^{-3}	0.322	30
	1.36×10^{-2}	0.476	45
	1.81×10^{-2}	0.495	47
	2.27×10^{-2}	0.565	54
	2.72×10^{-2}	0.764	74
	3.63×10^{-2}	0.618	59
	4.53×10^{-2}	0.692	66
	6.35×10^{-2}	0.715	69
	7.30×10^{-2}	0.769	74
3xNa-mont + 1697	4.53×10^{-3}	0.233	21
	9.06×10^{-3}	0.410	38
	1.36×10^{-2}	0.603	57
	2.27×10^{-2}	0.932	92
	2.72×10^{-2}	1.119	112
	3.63×10^{-2}	1.356	139
	4.53×10^{-2}	1.519	158
	5.44×10^{-2}	1.613	170
	6.35×10^{-2}	1.669	177
3xK-mont + 1697	4.53×10^{-3}	0.262	24
	9.06×10^{-3}	0.322	30
	1.36×10^{-2}	0.438	41
	1.81×10^{-2}	0.646	62
	2.27×10^{-2}	0.671	64
	2.72×10^{-2}	0.816	79
	3.63×10^{-2}	0.981	97
	4.53×10^{-2}	1.061	106
	5.44×10^{-2}	1.123	112
	6.35×10^{-2}	1.099	110
3xCs-mont + TMACl	4.80×10^{-3}	0.188	10
	9.60×10^{-3}	0.306	16
	1.92×10^{-2}	0.430	23
	2.40×10^{-2}	0.517	27
	2.88×10^{-2}	0.518	28
	3.36×10^{-2}	0.563	30
	3.84×10^{-2}	0.630	33
	4.80×10^{-2}	0.673	36
	5.76×10^{-2}	0.736	39
	6.72×10^{-2}	0.793	42
	7.68×10^{-2}	0.843	46

Table 7. The quantity of N detected by Kjeldahl analysis for the addition of Magnafloc 1697 and TMA^+ to 3xZ-mont.

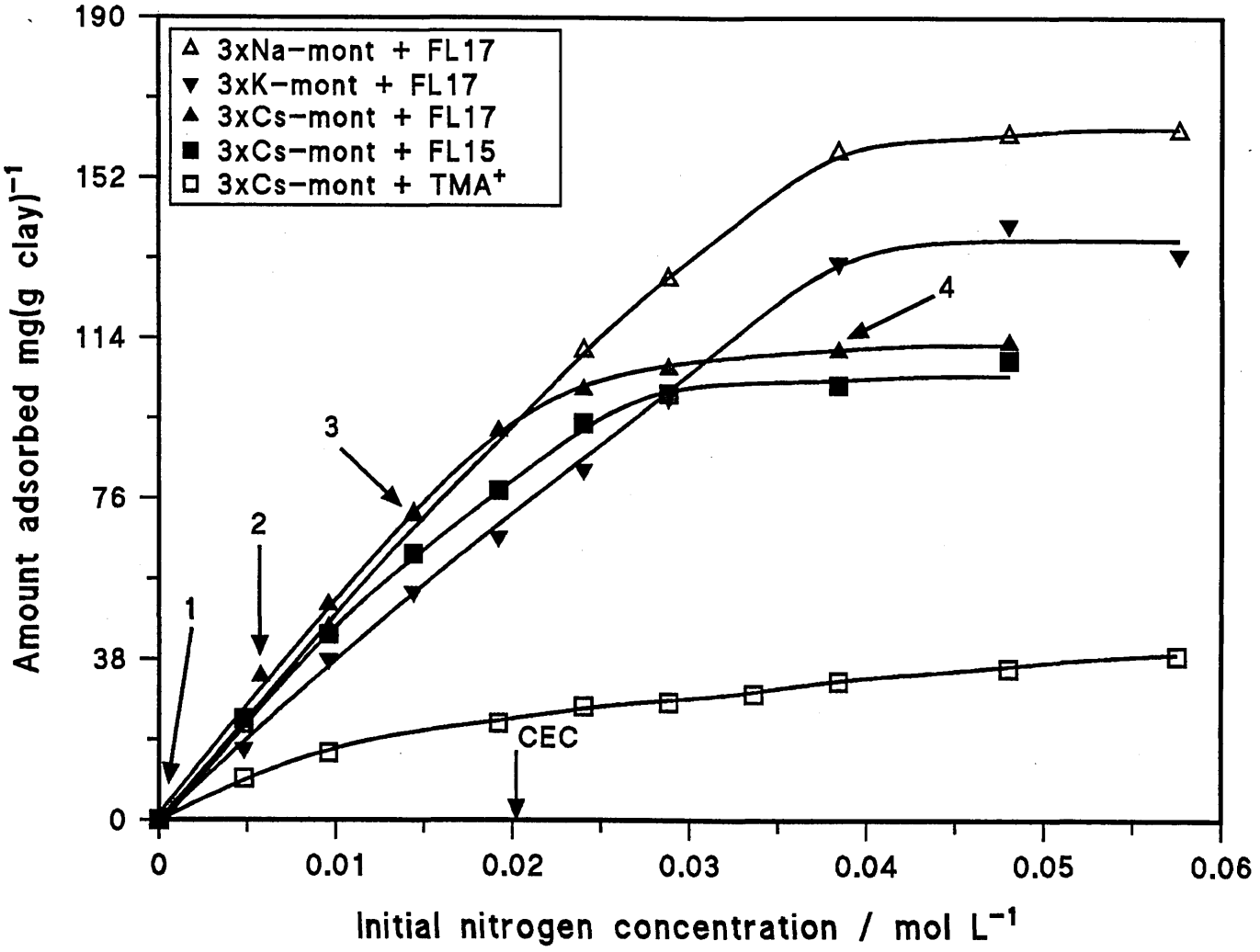

Figure 31. Adsorption isotherms obtained for the addition of several cationic species to 3xZ–mont.

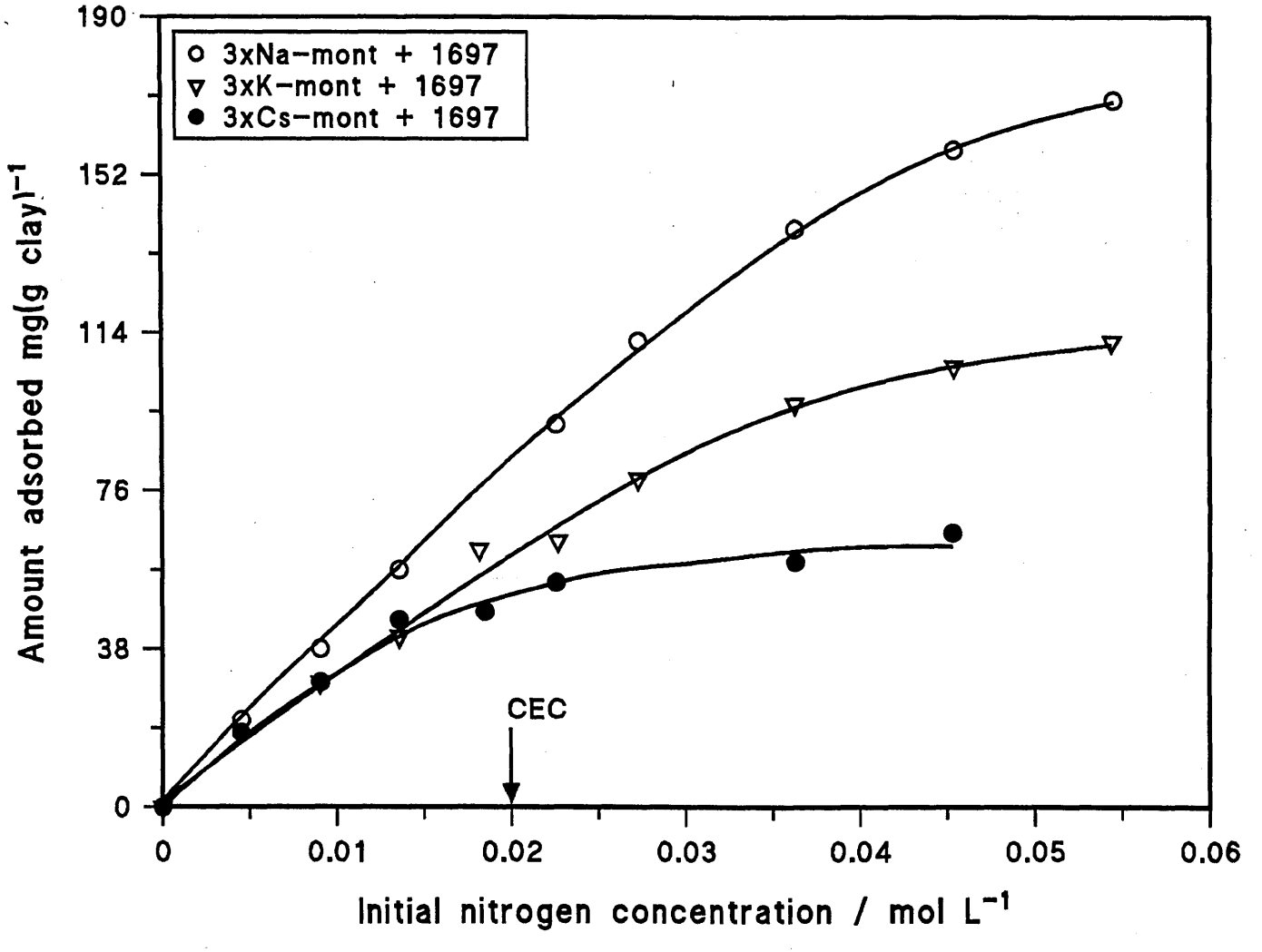

Figure 32. Adsorption isotherms obtained for the addition of Magnafloc 1697 to 3xZ–mont.

6.1.2 XRF Determination of the Elemental composition of Different Cation Exchanged Clay Forms.

The elemental composition of several different cation exchanged clay forms was analysed by XRF and the oxides of the major elements present are listed below, (Table 8). The elemental composition of a polymer treated, washed 3xCs-mont sample is also shown.

	% Oxide found in different cation exchanged clays					
Oxide	**Unexchanged mont**	**3xNa-mont**	**3xK-mont**	**3xMn-mont**	**3xCs-mont**	**3xCs-mont + FL17**
CsO	0.13	0.00	0.00	0.00	13.23	2.31
Na_2O	0.02	2.64	0.05	0.01	0.05	0.02
MgO	3.66	2.83	3.19	3.18	2.85	3.16
Al_2O_3	18.49	17.09	18.53	18.49	16.58	18.50
SiO_2	74.53	76.26	72.87	73.63	66.08	74.83
K_2O	0.07	0.04	4.39	0.04	0.04	0.05
CaO	1.90	0.02	0.01	0.02	0.04	0.03
Mn_3O_4	0.01	0.02	0.02	3.45	0.00	0.00
TiO_2	0.25	0.25	0.26	0.26	0.20	0.24
Fe_2O_3	0.81	0.76	0.81	0.81	0.57	0.71
Oxide Sum	100	100	100	100	100	100

Table 8. The elemental composition of several different cation exchanged clay samples, calculated on a 1000°C basis.

The sedimented, unexchanged Westone-L was predominantly in the Ca^{2+} and Mg^{2+} exchanged form. By contacting this clay with a solution of metal chloride, the exchange cations were replaced by the cation of interest. The efficiency of this replacement process was monitored using XRF. The results shown in Table 8 show that the exchange process was very efficient. From the results obtained by XRF, it was then

possible to calculate what percentage of the clay's CEC was satisfied by the exchange cation of interest (Table 9).

	3xNa-mont	3xK-mont	3xMn-mont	3xCs-mont
% CEC satisfied	99	109	103	102

Table 9. The percent of the CEC satisfied by the various exchange cations.

Table 9 shows that the cation exchange capacity of Westone-L was completely satisfied by each of the exchange cations contacted with the clay.

6.1.3 XRD Analysis of Clay/Polycation Complexes.

XRD was used to analyse several clay samples contacted with different polycations to establish whether or not polycation was adsorbed exclusively on the surface of the clay or whether some resided between the clay platelets in the interlayer. The presence or absence of polymer in the interlayer may be determined by measuring changes in the d-spacing of the first order basal reflections (d 001 spacing) for each sample, (Table 10).

At room temperature, no difference in the basal spacing was observed between different cation exchanged clay with no added polymer and the same cation exchanged clays with low loadings of FL17 and Magnafloc 1697. The basal spacings observed for these low loadings of polymer exhibited values between 12.7 and 13.0 Å, depending on the type of cation exchanged form investigated. These observed basal spacings at room temperature therefore appear to be similar to the d spacings observed for the presence of one water layer between the aluminosilicate layers. With thermal treatment at 50°C for 25 minutes however, two separate d 001 spacings were observed for 3xNa-mont

contacted with 4.80 x 10^{-3} mol L^{-1} N from either of the polymers FL17 or Magnafloc 1697.

	Observed d-spacing for the first order basal reflections, Å.					
	Ambient	**50°C**	**100°C**	**150°C**	**200°C**	**250°C**
3xCs-mont	12.7	11.8	12.0	10.7	10.3	10.1
3xCs-mont + FL17						
4.80 x 10^{-3} mol L^{-1} N	12.7	11.8	11.4	11.3	11.3	11.3
3.84 x 10^{-2} mol L^{-1} N	14.8	14.7	14.6	14.6	14.3	12.7
3xCs-mont + 1697						
4.80 x 10^{-3} mol L^{-1} N	12.6	11.5	11.4	11.5	11.5	11.5
3.84 x 10^{-2} mol L^{-1} N	13.3	12.8	12.7	12.6	12.6	12.3
3xNa-mont	13.0	12.5	10.3	10.3	10.3	10.2
3xNa-mont + FL17						
4.80 x 10^{-3} mol L^{-1} N	13.0	14.6 11.4	14.7 10.6	14.6 10.5	11.5	11.5
9.59 x 10^{-3} mol L^{-1} N	14.8	14.6	14.8	14.6	10.8	10.7
1.92 x 10^{-2} mol L^{-1} N	14.8	14.8	14.7	14.7	14.7	13.3
3.84 x 10^{-2} mol L^{-1} N	16.0	15.8	15.8	15.7	14.6	13.5
3xNa-mont + 1697						
4.80 x 10^{-3} mol L^{-1} N	12.9	15.0 10.6	15.4 10.4	15.3 10.3	15.0 10.3	14.6 10.3
9.59 x 10^{-3} mol L^{-1} N	15.1	12.6	15.1	15.3	15.1	14.8
3.84 x 10^{-2} mol L^{-1} N	DISORDERED					14.8
3xK-mont	12.1	10.7	10.6	10.5	10.5	10.5
3xK-mont + FL17						
4.80 x 10^{-3} mol L^{-1} N	12.8	14.5 10.7	14.5 10.7	14.3 10.6	10.5	10.5
3.84 x 10^{-2} mol L^{-1} N	15.0	14.9	14.8	14.8	14.6	13.0
3xK-mont + 1697						
4.80 x 10^{-3} mol L^{-1} N	12.6	10.7	10.7	10.5	10.5	10.4
3.84 x 10^{-2} mol L^{-1} N	DISORDERED					15.8

Table 10. The observed d-spacing for the first order basal reflections of several clay/polycation complexes.

Figure 33 and Figure 34 illustrate this point showing that the adsorbed polymer was segregated in different interlayers at low loadings which only becomes apparent at temperatures above 50°C.

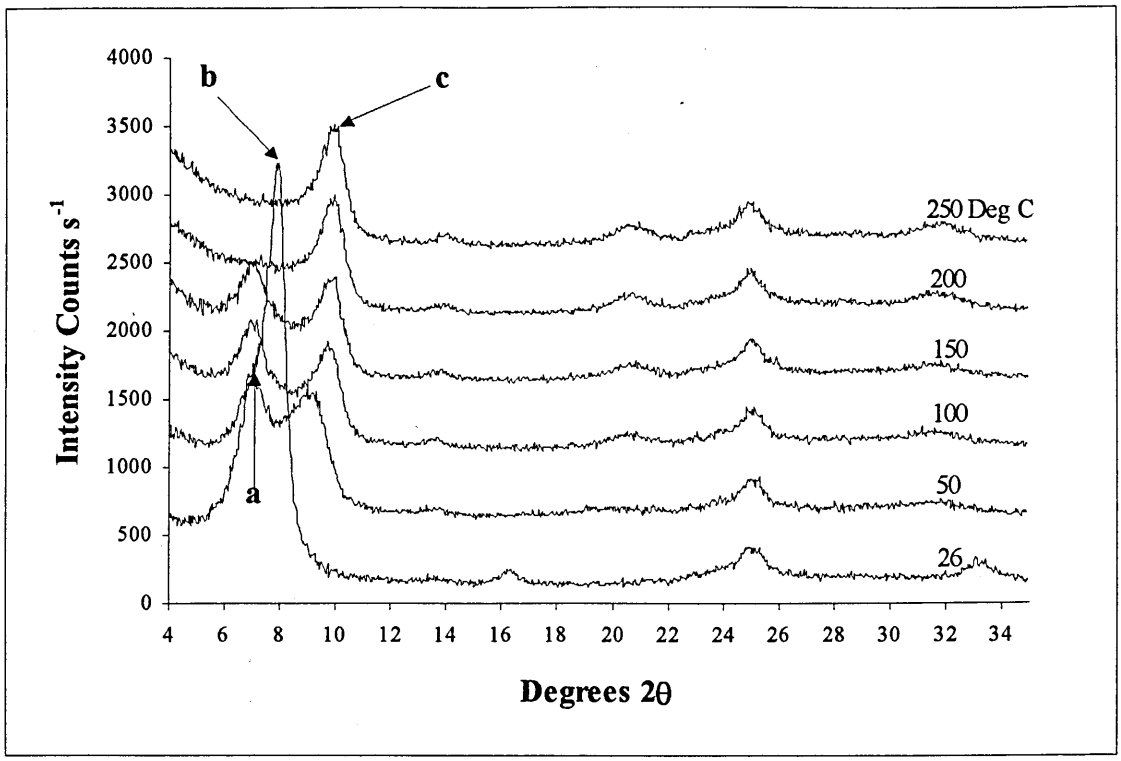

Figure 33. XRD traces showing the change in the d 001 spacing with increasing temperature for 3xNa-mont contacted with 4.80 x 10^{-3} mol L^{-1} N from FL17. The peaks a, b and c had spacings of 14.6, 13.0 and 11.5 Å respectively.

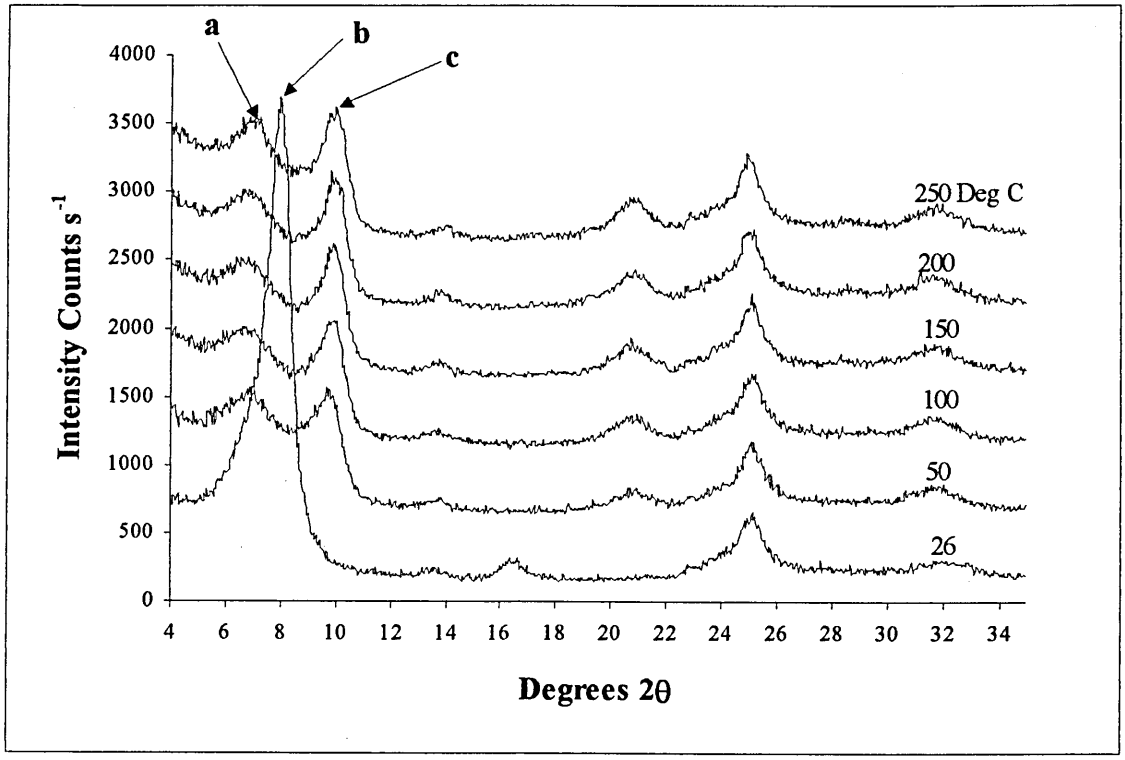

Figure 34. XRD traces showing the change in d 001 spacing with increasing temperature for 3xNa-mont contacted with 4.80 x 10^{-3} mol L^{-1} N from Magnafloc 1697. The peaks a, b and c had spacings of 14.6, 12.9 and 10.3 Å respectively.

The appearance of two different d 001 spacings at elevated temperatures becomes apparent because thermal treatment at 50°C for 25 minutes was sufficient to almost completely dehydrate the water-filled layers resulting in their collapse.[133] Conversely the polymer-filled layers required higher temperatures to denature the polymer and consequently collapse of these layers did not occur at this low temperature. With the addition of 4.80×10^{-3} mol L^{-1} N from FL17 to 3xNa-mont, collapse of the polymer-filled layers did however occur between 150 and 200°C, shown by the disappearance of peak **a**, Figure 33. Conversely, with addition of the same quantity of Magnafloc 1697 to 3xNa-mont, no collapse of the polymer-filled layers and therefore no denaturing of the polymer was observed even up to temperatures of 250°C. This was shown to be true by the existence of peak **a** in Figure 34, suggesting therefore that Magnafloc 1697 is thermally more stable than FL17.

Figure 35 shows that on contacting 3xNa-mont with higher loadings of FL17, increased d 001 spacings were observed. In fact with the addition of 3.84×10^{-2} mol L^{-1} N from FL17, a basal spacing of 16.0 Å was recorded at room temperature which is consistent with the presence of one layer of polymer between the clay layers shown by peak **a**, Figure 35. The polymer again denatured slightly at temperatures above 150°C, however the layers do not collapse completely even at 250°C shown by the basal spacing of 13.5 Å observed for peak **b**, Figure 35. Figure 36 shows the XRD traces observed for the addition of 3.84×10^{-2} mol L^{-1} N from Magnafloc 1697 to 3xNa-mont. All the traces show that this system was less well ordered, indicated by the broad featureless peaks. Figure 36 also shows that the polymer does not seem to denature markedly below 250°C, shown by peak **a** which has a d-spacing of 14.8 Å.

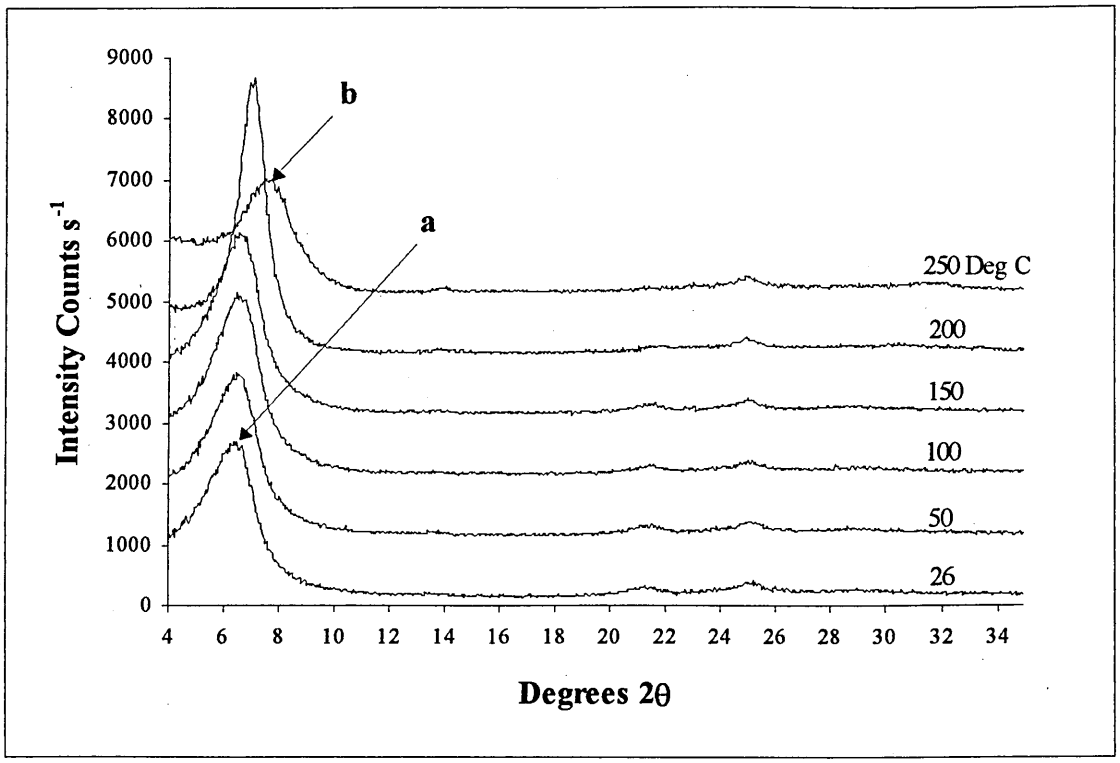

Figure 35. XRD traces showing the change in d 001 spacing with increasing temperature for 3xNa-mont contacted with 3.84 x 10^{-2} mol L^{-1} N from FL17. The peaks a and b had spacings of 16.0 and 13.5 Å respectively.

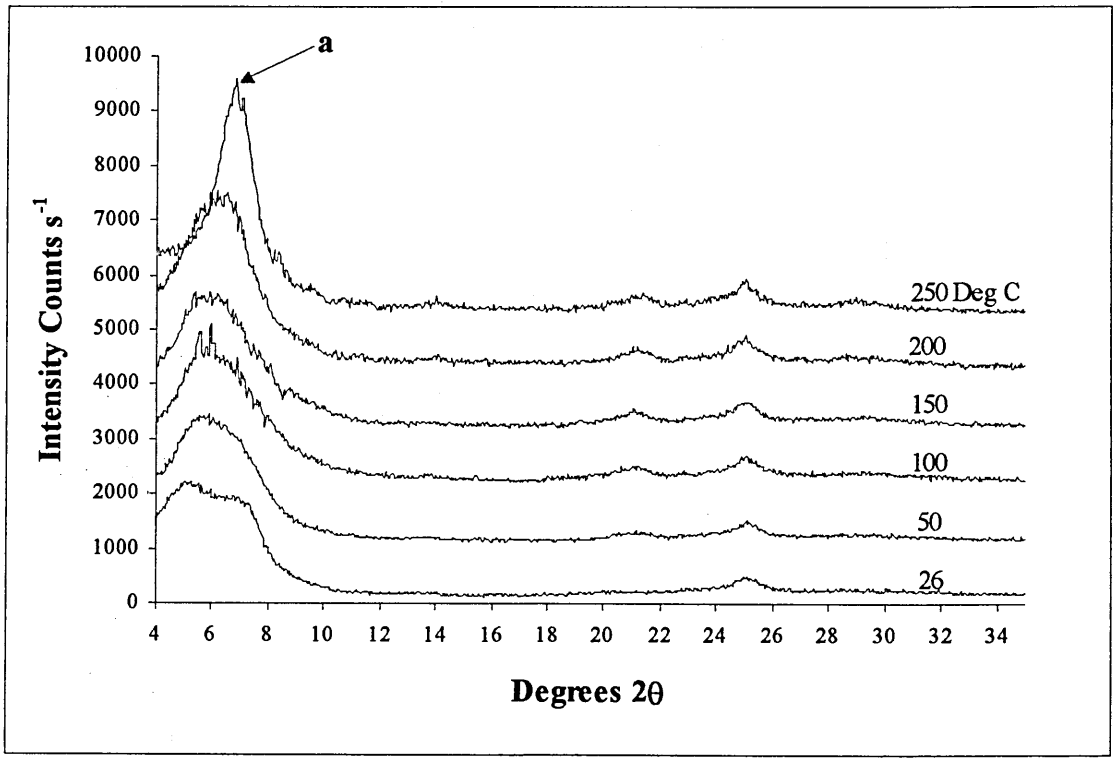

Figure 36. XRD traces showing the change in d 001 spacing with increasing temperature for 3xNa-mont contacted with 3.84 x 10^{-2} mol L^{-1} N from Magnafloc 1697. Peak a had a basal spacing of 14.8 Å.

Figure 37 shows that upon contacting 3xCs-mont with low loadings of FL17, it was not obvious that any polymer resided between the clay layers. This was indicated by peak **a**, Figure 37 which shows a small basal spacing of 12.7 Å recorded for the addition of 4.80 x 10^{-3} mol L^{-1} N from FL17. Further, there was also a partial collapse of the spacing at temperatures above 50°C to 11.5 Å which is also the basal spacing observed for temperatures as high as 250°C. With higher loadings however (3.84 x 10^{-2} mol L^{-1} N), FL17 caused an increase in basal spacing to 14.8 Å shown by peak **a**, Figure 38, indicating that some polymer was indeed present between the clay layers. FL17 again denatured slightly at temperatures above 150°C, however the layers do not collapse completely even at 250°C shown by the basal spacing of 12.7 Å observed for peak **b**, Figure 38. Similar results were obtained for the addition of Magnafloc 1697 to 3xCs-mont. This time however, at higher polymer loadings, the observed basal spacing assumed lower values than those recorded for addition of the same quantity of FL17 to 3xCs-mont, indicating that less polymer was adsorbed in the interlayer. With the addition of low loadings of FL17 to 3xK-mont, similar diffraction traces to those seen for the addition of the same type and quantity of polymer to 3xNa-mont were observed. For example, at these low loadings the polymer was again segregated in different interlayers which resulted in the observation of two different basal spacings at elevated temperatures. One basal spacing relating to the dehydrated collapsed layers which were water-filled at room temperature and the other relating to polymer between the layers which was more stable at elevated temperatures. The observed basal spacing for the addition of low loadings of Magnafloc 1697 to 3xK-mont however indicated that no significant quantity of polymer was adsorbed between the clay layers which, as mentioned previously, was also the case for addition of low loadings of polymer to 3xCs-mont.

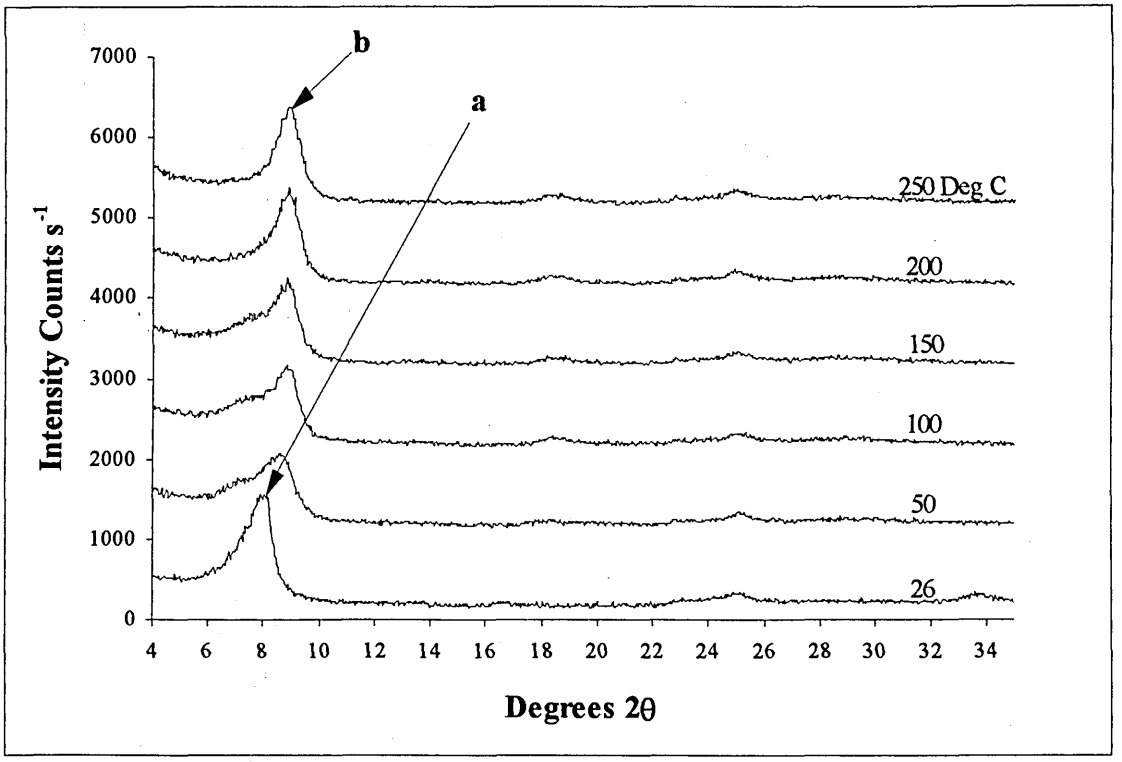

Figure 37. XRD traces showing the change in d 001 spacing with increasing temperature for 3xCs-mont contacted with 4.80 x 10^{-3} mol L^{-1} N from FL17. The peaks a and b have values of 12.7 and 11.3 Å respectively.

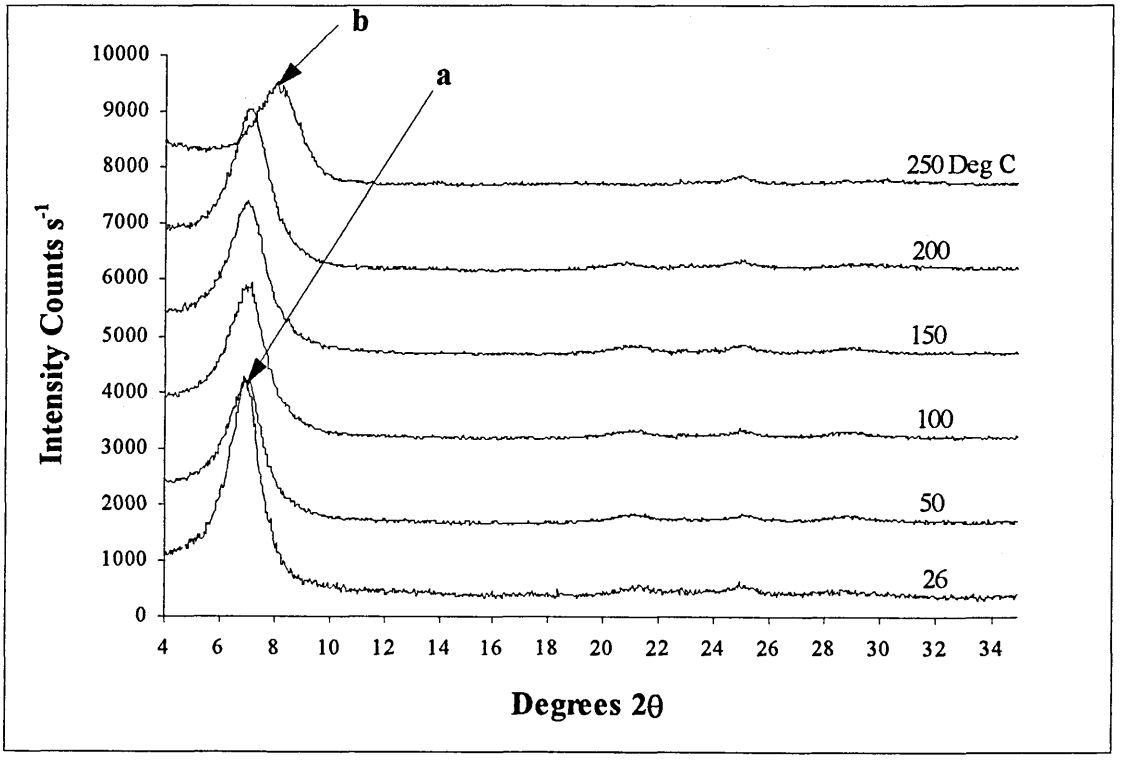

Figure 38. XRD traces showing the change in d 001 spacing with increasing temperature for 3xCs-mont contacted with 3.84 x 10^{-2} mol L^{-1} N from FL17. The peaks a and b correspond to a basal spacing of 14.8 and 12.7 Å respectively.

Again at higher loadings, the basal spacings observed for the addition of FL17 and Magnafloc 1697 to 3xK-mont indicated that both these polymers were adsorbed between the clay layers.

The XRD traces recorded for the addition of FL17 and Magnafloc 1697 to 3xNa-mont indicated that these systems were well ordered. The traces observed for the addition of polymer to 3xCs-mont and 3xK-mont however generally reflected less well ordered systems.

In summary, the XRD traces showed that at low polymer loadings (4.80×10^{-3} mol L^{-1} N), FL17 penetrated the interlayer of 3xNa-mont and 3xK-mont but not 3xCs-mont. Magnafloc 1697 on the other hand could only be detected in 3xNa-mont at such low loadings. In contrast, at high polymer loadings (3.84×10^{-2} mol L^{-1} N), both FL17 and Magnafloc 1697 were found in the interlayers of all the cation exchanged clays studied.

6.1.4 TG Analysis of Clay/Polycation Complexes.

TG analysis was performed on 3xNa-mont and 3xCs-mont contacted with different quantities of FL17 or Magnafloc 1697. These analyses were carried out in order to corroborate results obtained by Kjeldahl analysis and to establish the stability of the clay/polymer complexes formed which has already been briefly addressed by using variable temperature XRD.

Figure 39 illustrates the derivative thermograms observed for the addition of increasing volumes of FL17 to 3xCs-mont. The relatively sharp peak centred at a temperature of 90°C was due to loss of interlayer water associated with the clay. All of the interlayer water was lost from the clay at temperatures approaching 150°C.

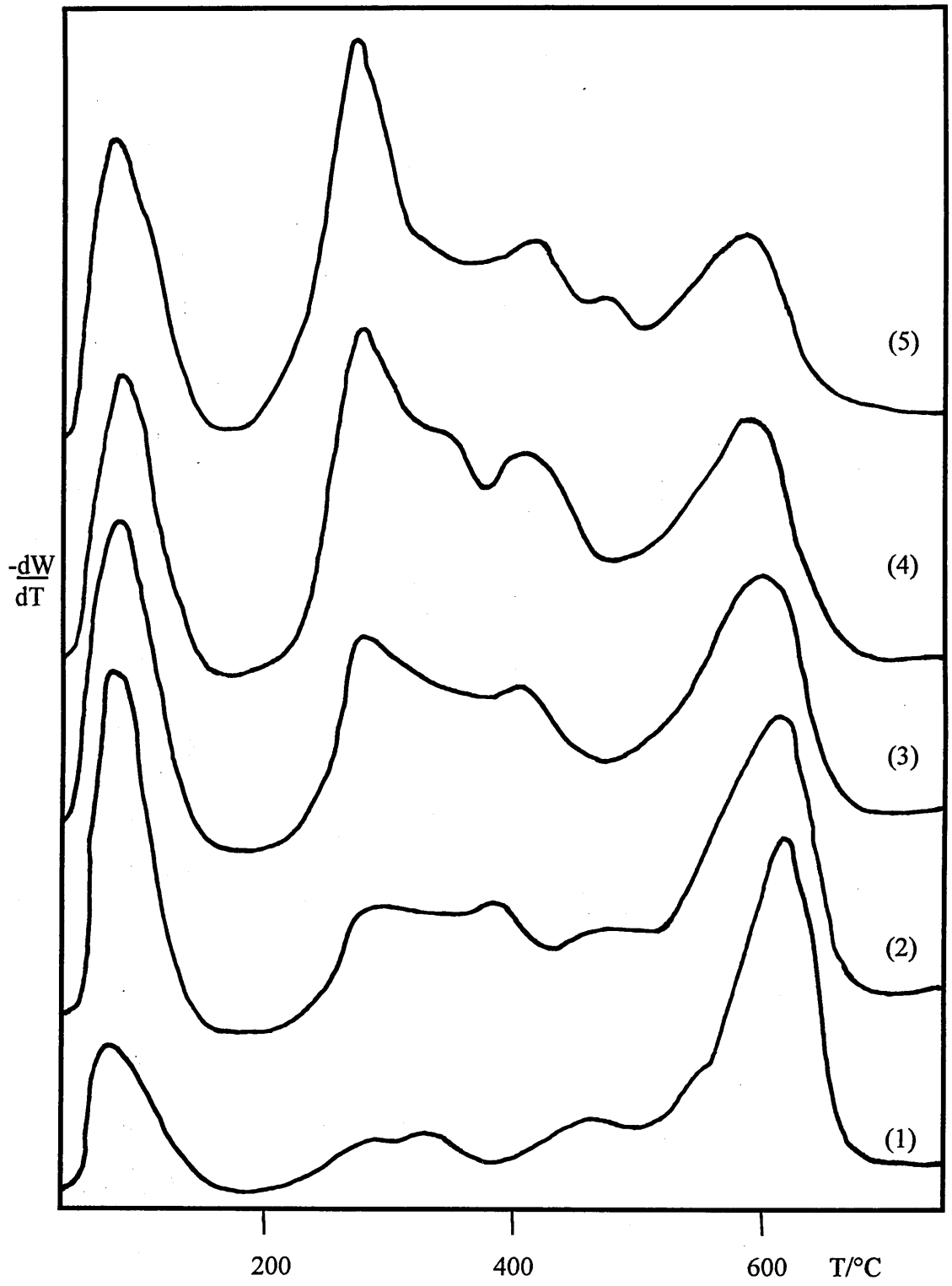

Figure 39. TGA traces recorded for the addition of increasing volumes of FL17 to 3xCs-mont. The numbered traces (1)-(5) relate to the amount of polycation offered to the clay which was equal to 4.80 x 10^{-3}, 9.60 x 10^{-3}, 1.44 x 10^{-2}, 1.92 x 10^{-2} and 3.84 x 10^{-2} mol L^{-1} N respectively.

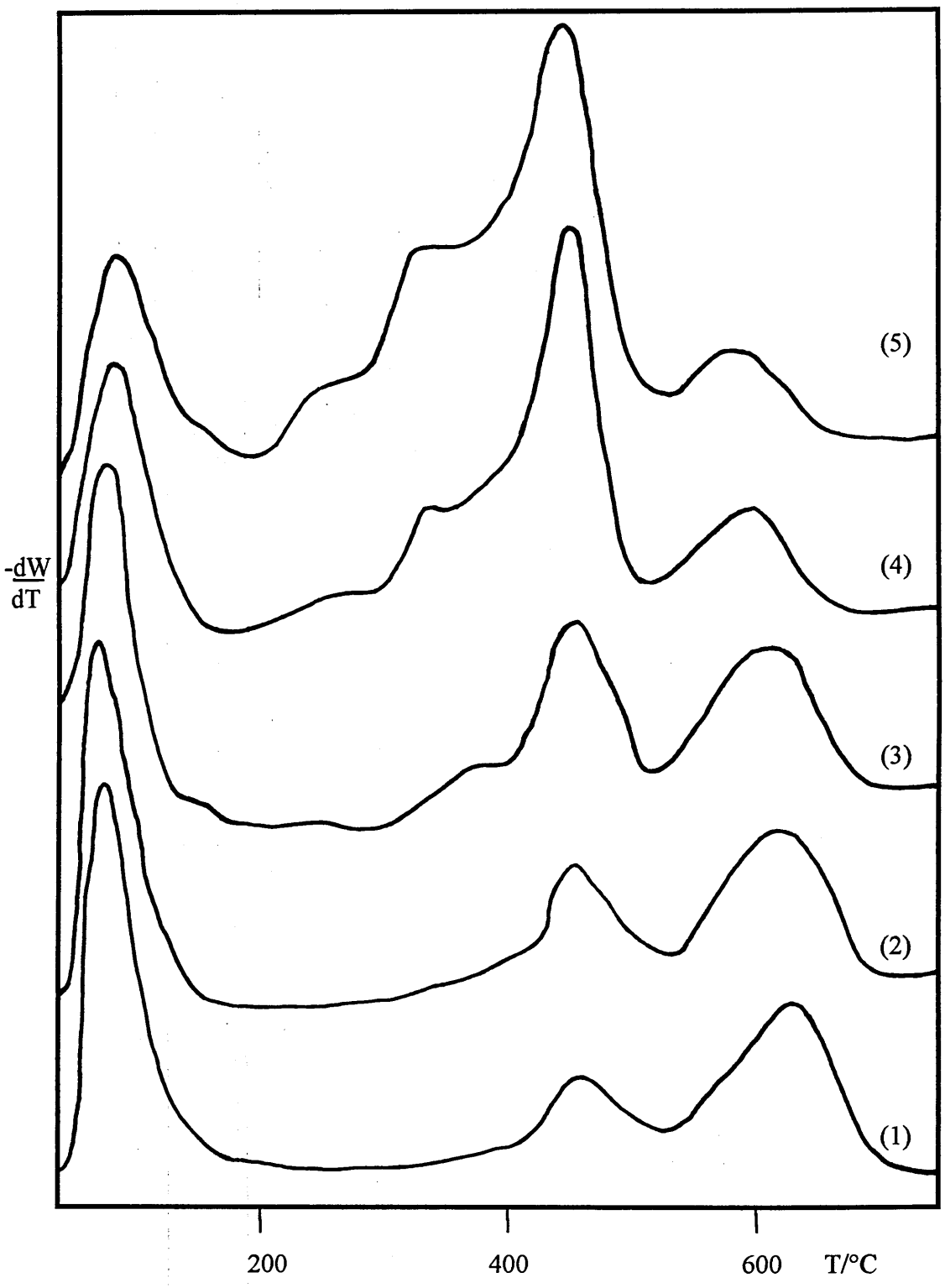

Figure 40. TGA traces recorded for the addition of increasing volumes of Magnafloc 1697 to 3xNa-mont. The numbered traces (1)-(5) relate to the amount of polycation offered to the clay which was equal to 4.80 x 10^{-3}, 9.60 x 10^{-3}, 1.44 x 10^{-2}, 1.92 x 10^{-2} and 3.84 x 10^{-2} mol L^{-1} N respectively.

As the amount of FL17 added to the clay was increased, the intensity of the peaks observed at approximately 275 and 410°C increased. These two peaks were due to the breakdown of polycation at these temperatures. The major loss of polymer however occurred around 275°C shown by the intensity of this peak in comparison to the peak observed at 410°C. This is in agreement with XRD data which also showed loss of polymer from the interlayer of clay at temperatures approaching 250°C. The broad peak observed between 590 and 620°C was due to the loss of structural hydroxyl groups from the clay.

Figure 40 illustrates the TGA traces obtained for the addition of increasing volumes of Magnafloc 1697 to 3xNa-mont. Here again, the peak centred at 90°C was due to loss of interlayer water. An increase in intensity for the peak at 445 to 455°C was observed as the amount of Magnafloc 1697 added to the clay was increased. This peak was therefore due to the breakdown of polycation at this temperature. Finally the broad peak observed between 590 and 630°C was again due to the loss of structural hydroxyl groups from the clay.

Figure 39 and Figure 40 also indicate that Magnafloc 1697 was thermally more stable than FL17, shown by the major desorption peaks at 455 and 275°C respectively. This thermogravimetric data was in agreement with XRD results which also indicate that Magnafloc 1697 is thermally more stable than FL17, shown by the collapse of basal spacings for FL17 treated clay at lower temperatures than for Magnafloc 1697.

Table 11 shows the TGA results obtained for the addition of FL17 and Magnafloc 1697 to 3xNa-mont and 3xCs-mont. The sample weight before and after purging with dry N were recorded in order to gain some idea of the quantity of physisorbed water associated with the clay.

Mol L^{-1} N added	Wt before purging / g	Wt after purging / g	Difference / g	% Wt loss from 160 to 520 °C
3xNa-mont	9.589	9.335	0.254	3.12
3xNa-mont + FL17				
9.60×10^{-4}	9.740	9.427	0.313	3.27
2.88×10^{-3}	9.606	9.269	0.337	3.66
4.79×10^{-3}	8.800	8.215	0.585	3.65
9.60×10^{-3}	8.248	7.970	0.278	4.78
1.44×10^{-2}	8.900	8.603	0.297	5.52
1.92×10^{-2}	10.590	10.322	0.268	6.92
3.84×10^{-2}	8.845	8.6510	0.194	9.62
3xCs-mont	9.280	8.946	0.334	2.13
3xCs-mont + FL17				
9.60×10^{-4}	8.410	8.087	0.323	2.56
2.88×10^{-3}	7.860	7.607	0.253	3.11
4.79×10^{-3}	7.160	6.867	0.293	3.29
9.60×10^{-3}	8.220	7.955	0.265	4.53
1.44×10^{-2}	8.640	8.334	0.306	6.24
1.92×10^{-2}	8.825	8.504	0.321	7.78
3.84×10^{-2}	8.930	8.689	0.241	9.30
3xNa-mont + 1697				
9.05×10^{-4}	7.964	7.818	0.146	2.88
2.72×10^{-3}	7.035	6.924	0.111	3.30
4.53×10^{-3}	9.035	8.793	0.242	3.27
9.06×10^{-3}	8.390	8.132	0.258	3.93
1.36×10^{-2}	8.254	8.046	0.208	4.30
2.27×10^{-2}	7.976	7.733	0.243	6.21
2.72×10^{-2}	10.00	9.705	0.250	10.07
3.63×10^{-2}	9.673	9.460	0.213	11.11
3xCs-mont + 1697				
9.05×10^{-4}	6.507	6.365	0.142	2.63
2.72×10^{-3}	7.232	6.989	0.243	2.96
4.53×10^{-3}	7.107	6.888	0.219	3.03
9.06×10^{-3}	7.910	7.693	0.217	3.51
1.36×10^{-2}	7.900	7.697	0.203	3.98
1.81×10^{-2}	8.210	7.942	0.268	4.76
2.72×10^{-2}	8.205	7.955	0.250	5.98
3.63×10^{-2}	9.815	9.573	0.242	5.89

Table 11. The weight loss from the sample between 160°C and 520°C, this relates to the denaturing of polymer adsorbed onto the clay.

No significant trends in the quantity of physisorbed water were however observed upon addition of either polycation to either cation exchanged clay. The percentage weight losses recorded in Table 11 for the region 160 to 520°C were entirely due to loss of polymer from the clay. Table 11 also shows that as the amount of polycation offered to the clay was increased, the percentage polymer weight loss from the clay also increased as would be expected. TGA results indicate from percentage weight loss data that polycation adsorption on 3xCs-mont had some dependence on the structure of the polymer. This was noted because upon addition of FL17 to 3xCs-mont, the maximum percentage weight loss from the clay in the temperature range 160 to 520°C was 9.30%. Conversely, for the addition of a similar quantity of Magnafloc1697 to 3xCs-mont, only 5.89% weight loss was observed in the same temperature range. This indicated that more FL17 was adsorbed onto 3xCs-mont in the range of added polymer studied which is in agreement with the adsorption isotherm data.

Conversely the percentage weight losses observed for the addition of either polymer to 3xNa-mont were fairly similar, indicating that like quantities of either polymer were adsorbed onto this clay. This is again in agreement with the adsorption isotherm data. Finally the broad peak observed between 590 and 630°C was again due to the loss of structural hydroxyl groups from the clay.

Figure 41 shows the amount of polymer detected by Kjeldahl, mg(g clay)$^{-1}$, versus the % weight loss determined by TGA for the addition of FL17 to both 3xNa-mont and 3xCs-mont. The straight lines observed suggest that thermal treatment of this polymer proceeds via the same breakdown products irrespective of polymer loading. TGA % weight loss results may therefore be used to estimate the quantity of FL17

adsorbed on montmorillonite by extrapolating a line back to the x axis and noting its intersection.

Figure 42 shows the amount of polymer detected by Kjeldahl, mg(g clay)$^{-1}$, versus the % weight loss determined by TGA for the addition of Magnafloc 1697 to both 3xNa-mont and 3xCs-mont. The addition of this polymer to both cation exchanged clays resulted in curves which suggest that the thermal breakdown products of this polymer varied with increasing polymer adsorption. Consequently the TGA % weight loss results may not be used to estimate the quantity of Magnafloc 1697 adsorbed.

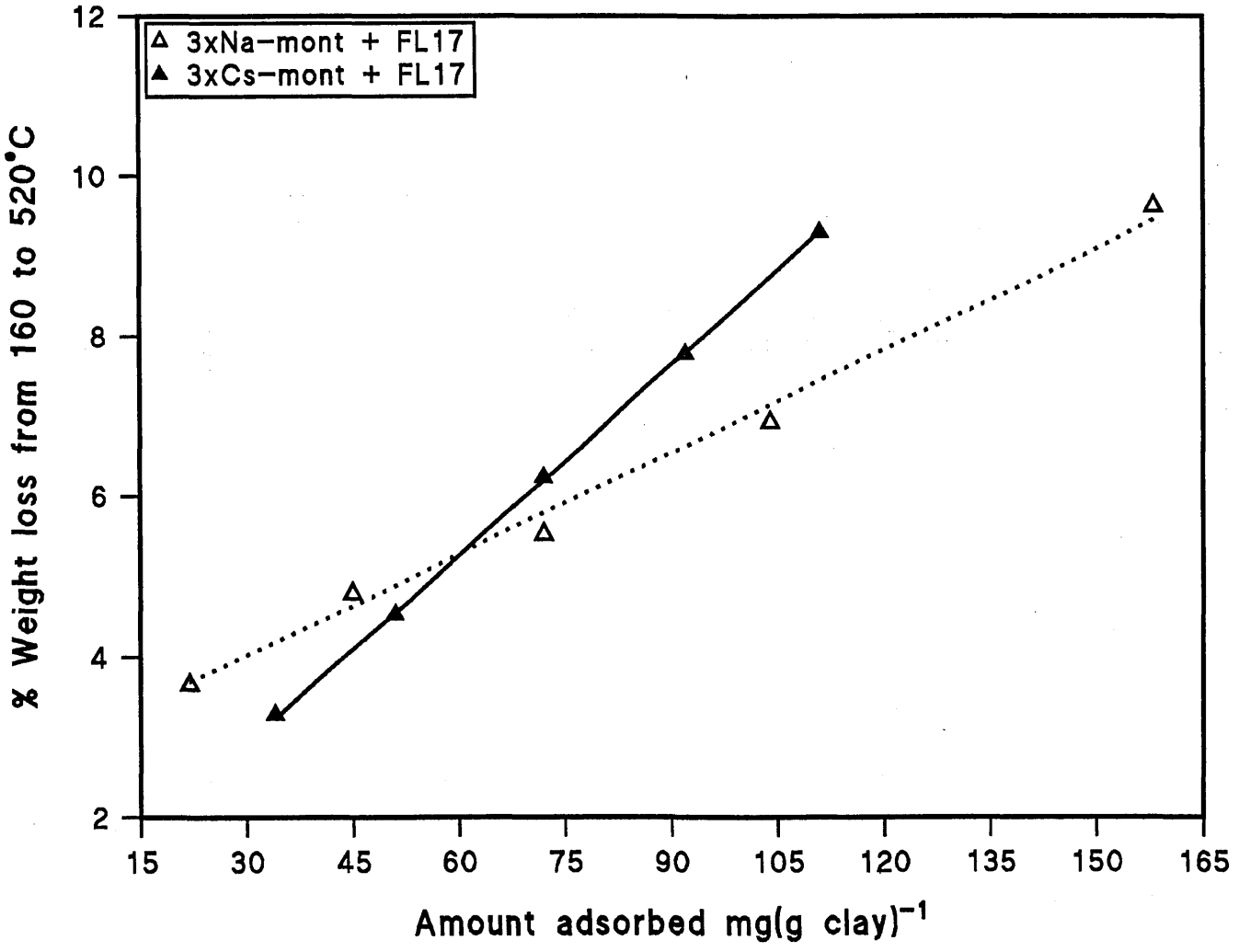

Figure 41. Amount of FL17 adsorbed versus the % weight loss

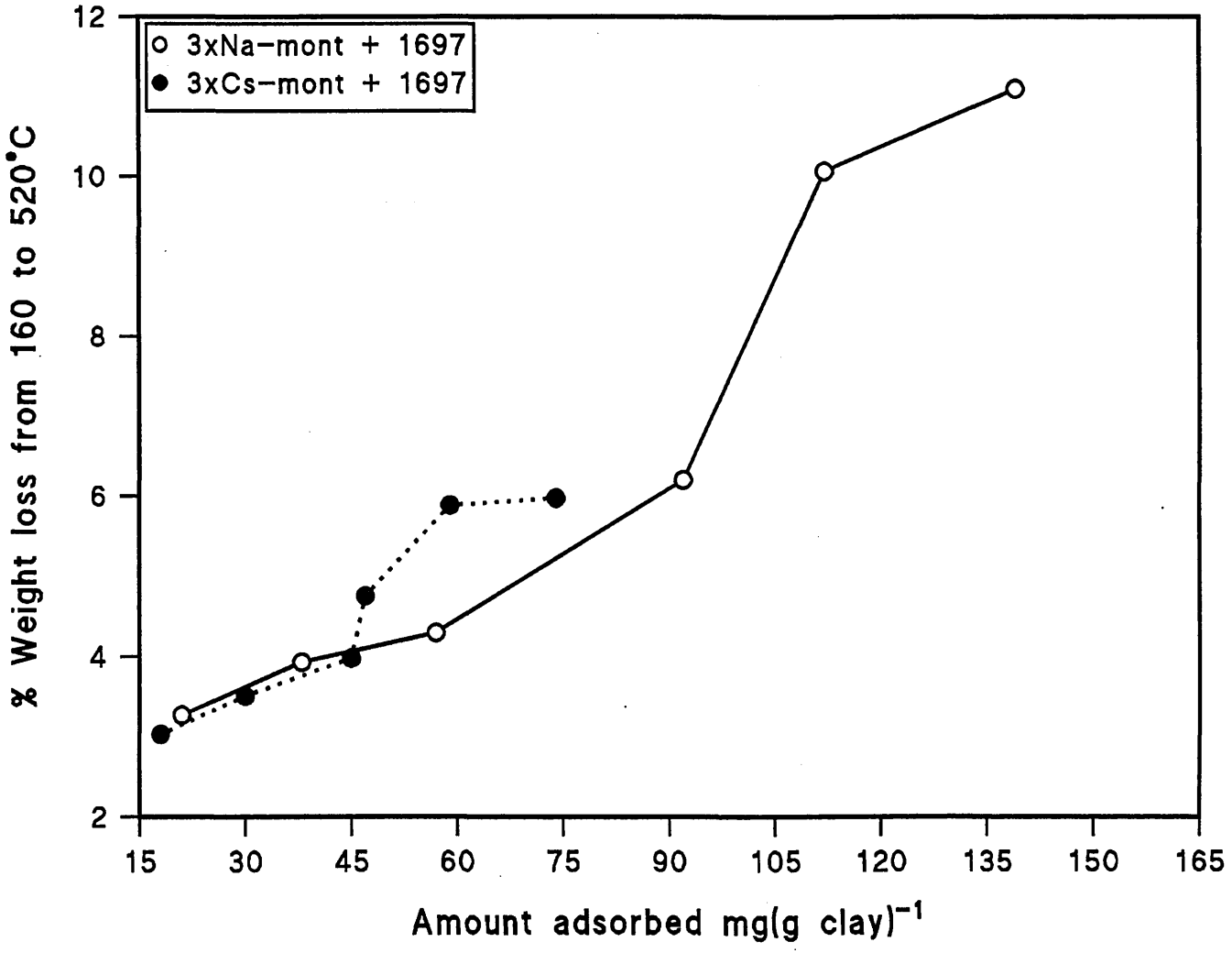

Figure 42. Amount of Magnafloc 1697 adsorbed versus the % weight loss

6.1.5 The Use of NMR Spectroscopy

6.1.5.1 Optimisation of NMR Operating Conditions for ^{133}Cs and ^{23}Na NMR.

Optimising the NMR operating conditions proved to be time consuming because quantitative analysis required that the intensity of the signal from 3xCs-mont was ratioed to that for the broadened CsCl (0.01 mol L^{-1} CsCl solution saturated with $CuSO_4.5H_2O$). Comparison of the integrated peak area for 3xCs-mont with that for the broadened CsCl initially showed a fluctuating ratio which was found to depend strongly on four operating parameters. These parameters were the number of acquisition points, relaxation delay, pulse width and sweep width. Each parameter was investigated systematically by fixing all other parameters to deduce exactly what effect it had on the intensity of the NMR signal.

It was found that the number of acquisition points did not adversely effect the ratio of the integral intensity of the 3xCs-mont with respect to the broadened CsCl provided there were enough acquisition points to encompass all of the FID signal. It was therefore deemed acceptable to alter the number of acquisition points between comparative samples if required.

The signals from the broadened CsCl and NaCl samples both required a relaxation delay = 1s to avoid saturation between pulsing. The cation exchanged clay samples, 3xCs-mont and 3xNa-mont, did not require a relaxation delay and therefore none was applied. When paraquat or the cationic polymers FL15, 16 and 17 were added to the clay samples Cs^+ or Na^+ was displaced from the clay depending upon the particular cation exchanged form used. Consequently as greater quantities of these cationic species were added, more exchangeable cation was displaced from the clay surface into solution

and the signal from the probe cation became more liquid-like. A relaxation delay = 1s was therefore required when large quantities of exchangeable cation were displaced from the clay.

The pulse width used when acquiring a spectrum had a large influence on the intensity of the observed ^{133}Cs signal. It was found in numerous experiments that decreasing the applied pulse width resulted in an increase in signal intensity. In fact when the pulse width was systematically decreased from 40 μs to 5 μs, the integral intensity of the 3xCs-mont peak, with respect to the broadened CsCl peak, increased more than four fold. A further experiment was carried out where the delay time, normally fixed by the sweep width, was varied using a constant maximum sweep width of 150 KHz. This experiment showed conclusively that an increase in delay time at a constant sweep width resulted in a decrease in the integral intensity of the 3xCs-mont with respect to the broadened CsCl signal. From the evidence outlined above, it may be stated that an enhanced signal was seen from the 3xCs-mont when the pulse width and delay time were decreased. The obvious conclusion from this was that the Cs^+ signal from the clay decayed rapidly after pulsing. Therefore the time taken between pulsing the sample and recording the free induction decay (FID) was critical to ensure that no signal was lost. The two parameters delay time and pulse width are responsible for this time delay. Consequently experiments were carried out to estimate the maximum time span allowable between pulsing the sample and recording the FID to minimise signal loss from the sample. These experiments involved the application of different pulse widths to the clay sample for two different sweep widths, 20 KHz and 50 KHz, respectively. From these data it was deduced that if the spectra were recorded no longer than 30 μs after pulsing, then no signal was lost. In the studies reported here, the sweep width was set to 20000

Hz, consequently the delay time was automatically set to 12 μs. The pulse width used in all experiments was equal to 10 μs therefore the delay time plus pulse width had a value which was comfortably less than the experimentally determined 30 μs.

A further source of error in the value of the integral intensities may have arisen from the sample settling out in the NMR tube. By recording NMR spectra of the same sample for increasing residence times in the magnet, it was shown that the integral intensity of the 3xCs-mont peak, with respect to the broadened CsCl peak, remained constant for at least 20 minutes. Therefore on the time scale of the NMR experiments used in this analysis, no loss of signal due to sample flocculation was observed.

6.1.5.2 ^{133}Cs NMR.

Using the optimised NMR operating conditions, comparison of the integrated areas of the peaks for 3xCs-mont at a concentration of 25 gL^{-1} and broadened CsCl indicated that 0.004 mol L^{-1} Cs^+ associated with the clay was seen by NMR. This quantity of caesium was equal to 20% of the total Cs^+ known to be associated with the clay (XRF analysis, section 6.1.2). It was also noted that the same 3xCs-mont sample had a large linewidth equal to approximately 1500 Hz.

T_1 for a 0.01 mol L^{-1} CsCl solution was approximately 11 seconds while T_1 for Cs^+ associated with 3xCs-mont had a value in the order of 0.4 seconds. The equation linking the linewidth and T_2 is shown below, (Equation 5)

$$\text{Linewidth} = 1/\pi T_2$$

Equation 5. The relationship between linewidth and T_2.

Later, in section 6.2, the linewidth of Cs^+ associated with clay has been estimated to be approximately 150 Hz, giving a corresponding T_2 value of approximately 2 milliseconds, showing that T_1 is much greater than T_2. Consequently, when considering the graph relating T_1 and T_2 with τ_c, it is proposed that both T_1 and T_2 lie in the long correlation region of the graph where $\omega_o^2\tau_c^2 >> 1$, (Figure 51, section 4.9).

6.1.5.2.1 Effect of the 3xCs-mont Clay Concentration on the ^{133}Cs Integral.

The effect of increasing the concentration of 3xCs-mont in suspension on the ^{133}Cs integral was analysed and the resulting graph was plotted, (Figure 43). This experiment was crucial because it is not unrealistic to assume that some Cs^+ may become trapped in pores formed by flocculated clay platelets at higher clay concentrations. If there was some trapped Cs^+, it will not be visible to NMR and therefore any results obtained would not be accurate.

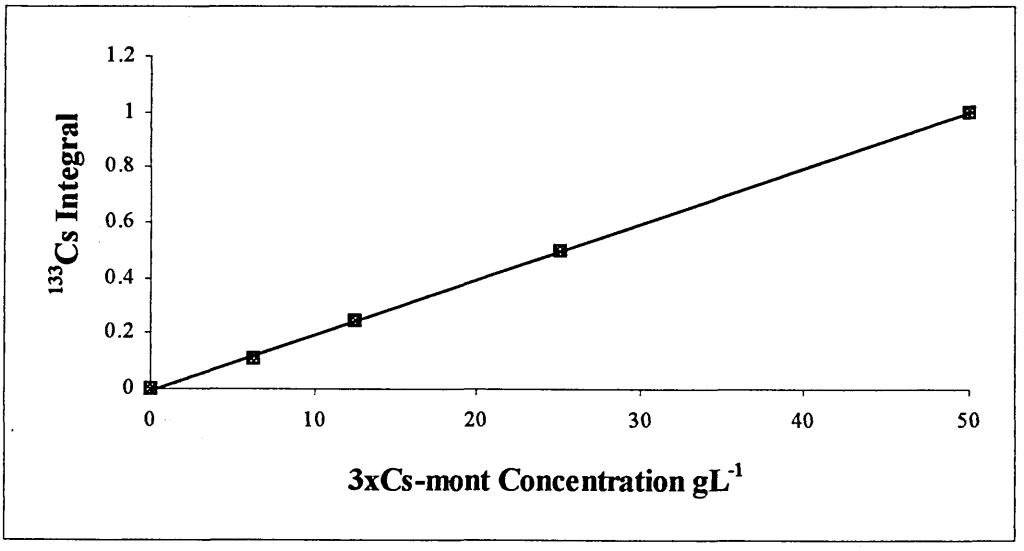

Figure 43. Graph showing the relationship between 3xCs-mont concentration and the resulting ^{133}Cs Integral.

Measurement of the ^{133}Cs integral at decreasing clay concentrations should show a straight line passing through the origin if there is no trapped Cs^+. The graph does in fact show a linear relationship between the ^{133}Cs integral and the 3xCs-mont clay

concentration. Consequently, any aggregation effects that may occur upon increasing the clay concentration do not effect the amount of Cs^+ visible to NMR.

6.1.5.2.2 The Change in ^{133}Cs Linewidth and Concentration of Cs^+ Detected Upon Addition of Increasing Amounts of Cationic Species to 3xCs-mont.

Samples were prepared containing a fixed quantity of 3xCs-mont and the cationic species of interest, added to the clay over a range of concentrations from 0 to 0.05 mol L^{-1}. The concentration range relates to the number of cationic centres, not the species in which they occurred. The cationic species chosen for this work were Na^+, K^+, TMA^+, paraquat and the four cationic polymers FL15, FL16, FL17 and Magnafloc 1697. ^{133}Cs NMR spectra were then recorded for each sample, noting the resulting linewidth and concentration of Cs^+ detected by NMR after addition of cationic species to the clay, (Table 12, Table 13). The quantity of Cs^+ detected by NMR, after addition of cationic species was measured in the same way as described above *ie* by comparison of the peak integrals for the treated 3xCs-mont with the broadened CsCl. Experimental results show that the linewidth of 3xCs-mont with no added cationic species was about 1500 Hz, (spectrum (1), Figure 44). This large linewidth was then used to probe the interactions taking place between cationic species and the clay surface. This was made possible because as cationic species were added to 3xCs-mont, a quantity of the exchangeable Cs^+, which depended upon the added cation, was displaced from the surface of the clay into the bulk solution. This resulted in a decrease in the ^{133}Cs linewidth. Figure 44 shows some typical ^{133}Cs NMR spectra recorded for the addition of increasing amounts of the polycation FL17 to 3xCs-mont. The changes in the ^{133}Cs NMR linewidth and integral with the addition of increasing concentrations of different cationic species to 3xCs-mont are shown graphically in Figure 45 and Figure 46.

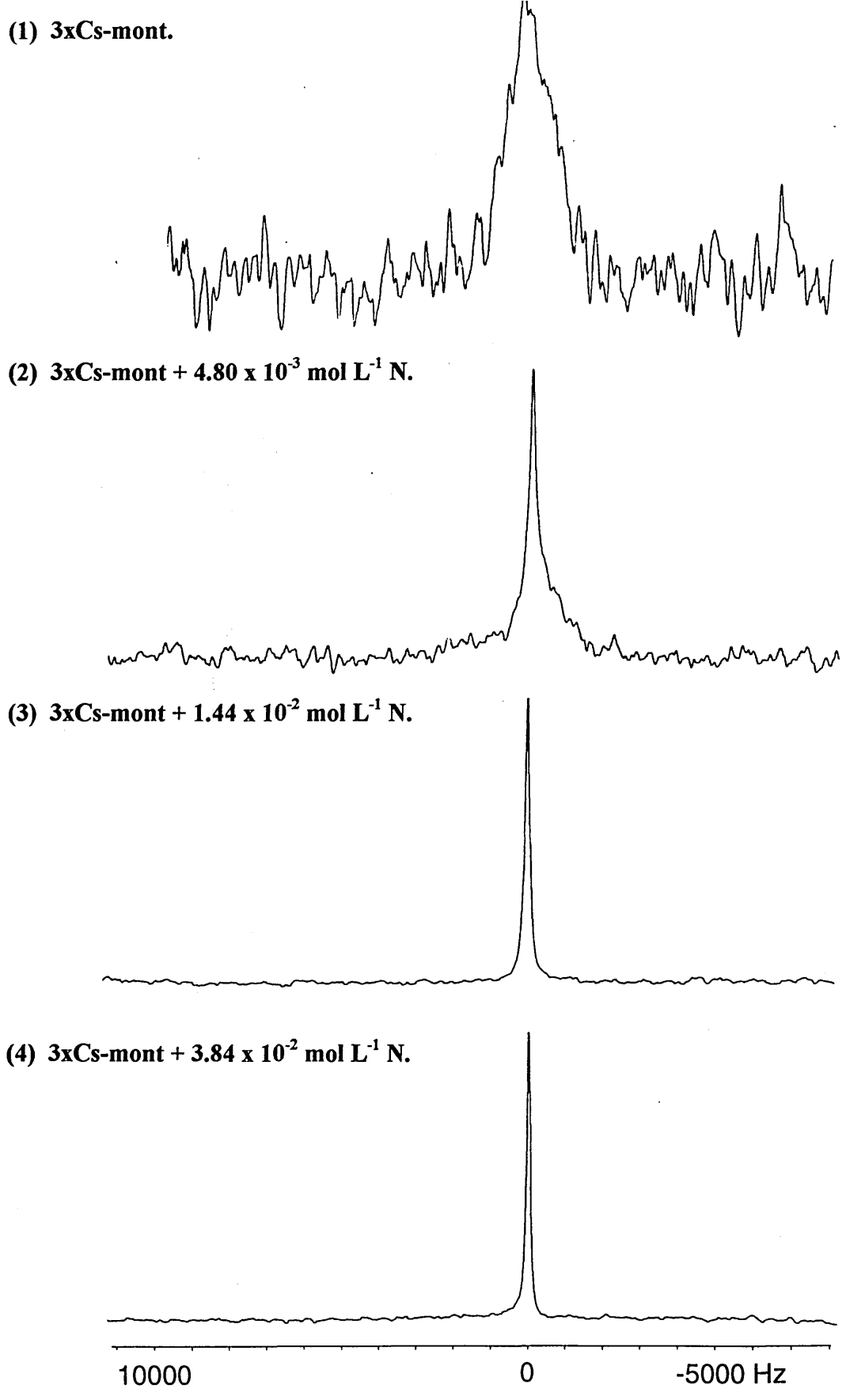

Figure 44. Typical ^{133}Cs NMR spectra obtained for the addition of increasing amounts of FL17 to 3xCs-mont.

	Classification of cationic centre added to 3xCs-mont			
	K^+		Na^+	
Concentration of cationic centres added	Linewidth / Hz	Cs^+ / mol L^{-1}	Linewidth / Hz	Cs^+ / mol L^{-1}
0.00	1500	4.0×10^{-3}	1500	4.0×10^{-3}
9.60×10^{-4}	1140	4.4×10^{-3}		
2.40×10^{-3}	930	4.7×10^{-3}	1356	5.2×10^{-3}
4.80×10^{-3}	846	4.5×10^{-3}	1242	5.4×10^{-3}
9.60×10^{-3}	867	5.7×10^{-3}	993	5.4×10^{-3}
1.44×10^{-2}	757	4.8×10^{-3}		
1.92×10^{-2}	720	6.0×10^{-3}	950	5.6×10^{-3}
2.40×10^{-2}			843	5.2×10^{-3}
2.88×10^{-2}	544	6.7×10^{-3}	866	5.1×10^{-3}
3.84×10^{-2}	447	6.2×10^{-3}	615	5.6×10^{-3}
4.80×10^{-2}	437	7.0×10^{-3}	486	5.8×10^{-3}
	TMA^+		Paraquat	
0.00	1500	4.0×10^{-3}	1500	4.0×10^{-3}
9.60×10^{-4}	1441	4.9×10^{-3}	1271	5.9×10^{-3}
1.92×10^{-3}	1313	4.7×10^{-3}	1014	4.9×10^{-3}
2.88×10^{-3}	1271	5.6×10^{-3}	804	4.9×10^{-3}
4.80×10^{-3}	1057	5.6×10^{-3}	578	6.4×10^{-3}
6.71×10^{-3}	971	6.6×10^{-3}	389	8.3×10^{-3}
9.60×10^{-3}	650	7.4×10^{-3}	202	1.18×10^{-2}
1.20×10^{-2}	436	8.2×10^{-3}	132	1.44×10^{-2}
1.44×10^{-2}			85	1.76×10^{-2}
1.63×10^{-2}	394	9.5×10^{-3}		
1.92×10^{-2}	346	9.5×10^{-3}	59	2.12×10^{-2}
2.88×10^{-2}	260	1.13×10^{-2}	27	2.30×10^{-2}
3.84×10^{-2}	209	1.31×10^{-2}	27	2.29×10^{-2}

Table 12. The effect on the ^{133}Cs linewidth and quantity of Cs^+ displaced from 3xCs-mont upon addition of increasing concentrations of cationic species.

	Classification of cationic centre added to 3xCs-mont			
	FL15		FL16	
Concentration of cationic centres added	Linewidth / Hz	Cs^+ / mol L^{-1}	Linewidth / Hz	Cs^+ / mol L^{-1}
0.00	1500	4.0×10^{-3}	1500	4.0×10^{-3}
4.80×10^{-4}	1392		1450	
9.60×10^{-4}	1232		1118	4.8×10^{-3}
1.44×10^{-3}	994		420	
1.92×10^{-3}	610	6.0×10^{-3}	217	6.0×10^{-3}
2.40×10^{-3}	336	6.0×10^{-3}	217	5.9×10^{-3}
2.68×10^{-3}			138	6.9×10^{-3}
2.88×10^{-3}	238	6.7×10^{-3}	138	7.4×10^{-3}
3.84×10^{-3}	217	7.3×10^{-3}	122	8.1×10^{-3}
5.75×10^{-3}	125	8.7×10^{-3}	91	9.1×10^{-3}
7.67×10^{-3}	112	1.05×10^{-2}	80	9.1×10^{-3}
9.60×10^{-3}	91	1.24×10^{-2}	70	1.02×10^{-2}
1.15×10^{-2}	73	1.37×10^{-2}	49	1.40×10^{-2}
1.44×10^{-2}	67	1.52×10^{-2}	38	1.53×10^{-2}
1.92×10^{-2}	44	1.93×10^{-2}	23	1.96×10^{-2}
2.88×10^{-2}	17	1.96×10^{-2}	12	1.98×10^{-2}
3.84×10^{-2}	15	1.98×10^{-2}	12	2.00×10^{-2}
	FL17		Magnafloc 1697	
0.00	1500	4.0×10^{-3}	1500	4.0×10^{-3}
4.80×10^{-4}	1372	4.8×10^{-3}		
9.60×10^{-4}	980	5.1×10^{-3}	1357	
1.15×10^{-3}	560			
1.34×10^{-3}	269			
1.44×10^{-3}	273			
1.92×10^{-3}	196		475	
2.40×10^{-3}	138	6.1×10^{-3}		
2.68×10^{-3}	138	6.8×10^{-3}		
2.88×10^{-3}	138	7.8×10^{-3}	246	
3.84×10^{-3}	112	8.4×10^{-3}	137	6.8×10^{-3}
5.75×10^{-3}	99	1.05×10^{-2}		
6.72×10^{-3}			146	9.3×10^{-3}
7.67×10^{-3}	91	1.10×10^{-2}		
9.60×10^{-3}	80	1.35×10^{-2}	112	1.00×10^{-2}
1.15×10^{-2}	59	1.52×10^{-2}		
1.44×10^{-2}	44	1.54×10^{-2}	89	1.20×10^{-2}
1.92×10^{-2}	12	1.92×10^{-2}	80	1.55×10^{-2}
2.88×10^{-2}	12	1.96×10^{-2}	74	1.60×10^{-2}
3.84×10^{-2}	12	2.00×10^{-2}	64	1.60×10^{-2}

Table 13. The effect on the ^{133}Cs linewidth and quantity of Cs^+ displaced from 3xCs-mont upon addition of increasing amounts of polycation.

Experiments were also carried out to determine whether or not the addition of polycation to a solution of CsCl had any effect on the linewidth of the ^{133}Cs signal. The linewidth of a 0.005 mol L^{-1} CsCl solution was measured and found to be equal to 5.3 Hz. This concentration of CsCl solution was chosen for investigation as it was approximately equal to the concentration of Cs^+ detected by NMR on 3xCs-mont. On addition of increasing volumes of the polycations FL15, 16 and 17 to the CsCl solution, the linewidth gradually increased until a maximum value of approximately 12 Hz was observed for the addition of 2.40×10^{-2} mol L^{-1} of N^+. It was therefore concluded that addition of polymer to CsCl had a negligible broadening effect when compared to the ^{133}Cs linewidth in the presence of clay (1500 Hz).

Figure 45 shows that the ^{133}Cs linewidth decreased steadily with the addition of increasing amounts of NaCl to 3xCs-mont. From this figure it is also apparent that Na^+ cations are poor at displacing Cs^+ from the clay, shown by the large ^{133}Cs linewidth of 615 Hz even after 3.84×10^{-2} mol L^{-1} of Na^+ had been offered. Conversely, the addition of K^+ to 3xCs-mont caused an initial rapid reduction in linewidth suggesting that some exchange sites on the clay are particularly favoured by K^+. Addition of further volumes of KCl to 3xCs-mont revealed a slope approaching that observed for the addition of Na^+. When 3.84×10^{-2} mol L^{-1} of K^+ were offered to 3xCs-mont, the minimum linewidth observed was 447 Hz. The reduction in linewidth from 1500 Hz to 209 Hz upon offering 3.84×10^{-2} mol L^{-1} of TMA^+ showed that this cation was more effective than Na^+ and K^+ at displacing Cs^+ from 3xCs-mont. Addition of paraquat to 3xCs-mont resulted in a rapid decrease in linewidth of the ^{133}Cs peak from 1500 to 27 Hz upon offering 3.84×10^{-2} mol L^{-1} of N^+. Figure 45 also shows a rapid decrease in the linewidth of the ^{133}Cs peak upon addition of increasing amounts of FL15 or FL17 to 3xCs-mont.

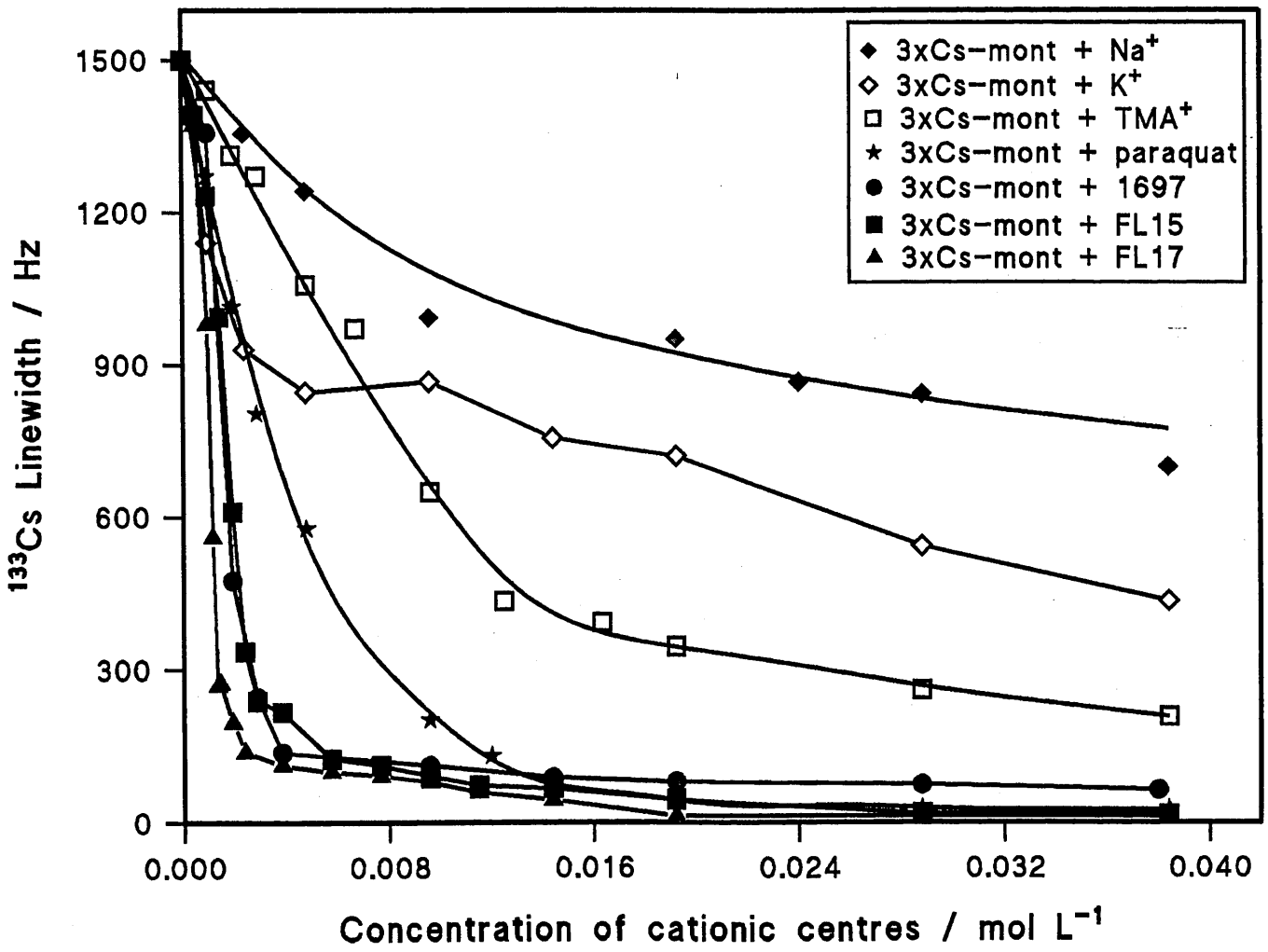

Figure 45. Decrease in the ^{133}Cs linewidth upon addition of cationic species to 3xCs–mont.

With both these polycations, the linewidth decreased from 1500 Hz to approximately 12 Hz upon offering 3.84 x 10^{-2} mol L^{-1} of N^+ to 3xCs-mont, (spectrum 4, Figure 44). Magnafloc 1697 was not as effective as FL15 and FL17 at displacing Cs^+ from the clay and therefore the minimum linewidth observed for the addition of 3.84 x 10^{-2} mol L^{-1} of N^+ was 64 Hz.

Figure 46 shows that a small yet measurable quantity of Cs^+ was displaced from the 3xCs-mont following addition of the cations K^+ and Na^+ whereas a greater proportion of the Cs^+ was displaced from the clay by the addition of TMA^+. The steep rise in the curve for the addition of paraquat to 3xCs-mont showed that this cationic species had a greater affinity for the clay than K^+, Na^+ or TMA^+. As the quantity of paraquat available to the 3xCs-mont was increased, a plateau was reached where the quantity of Cs^+ displaced from the clay remained constant. The onset of the plateau region occurred for the addition of 2.40 x 10^{-2} mol L^{-1} of N^+ to the clay while the quantity of Cs^+ displaced from 3xCs-mont in this plateau region was equal to 2.30 x 10^{-2} mol L^{-1}. Figure 46 shows that the addition of FL15 and FL17 to 3xCs-mont resulted in the efficient displacement of Cs^+ from 3xCs-mont. The initial steep rise in the curves reflects the high affinity of FL15 and 17 for the clay surface. As with paraquat, a plateau was reached for both FL15 and FL17 where no more Cs^+ was displaced from the clay. With both these polymers, the onset of the plateau region occurred for the addition of 1.92 x 10^{-2} mol L^{-1} of N^+ to 3xCs-mont while the quantity of Cs^+ displaced from the clay in this region was equal to 2.00 x 10^{-2} mol L^{-1}. The points 1 - 4 on the curve for the addition of FL17 to 3xCs-mont correspond to the representative ^{133}Cs NMR spectra obtained, (Figure 44). A third cationic polymer of different structure, Magnafloc 1697, was also studied.

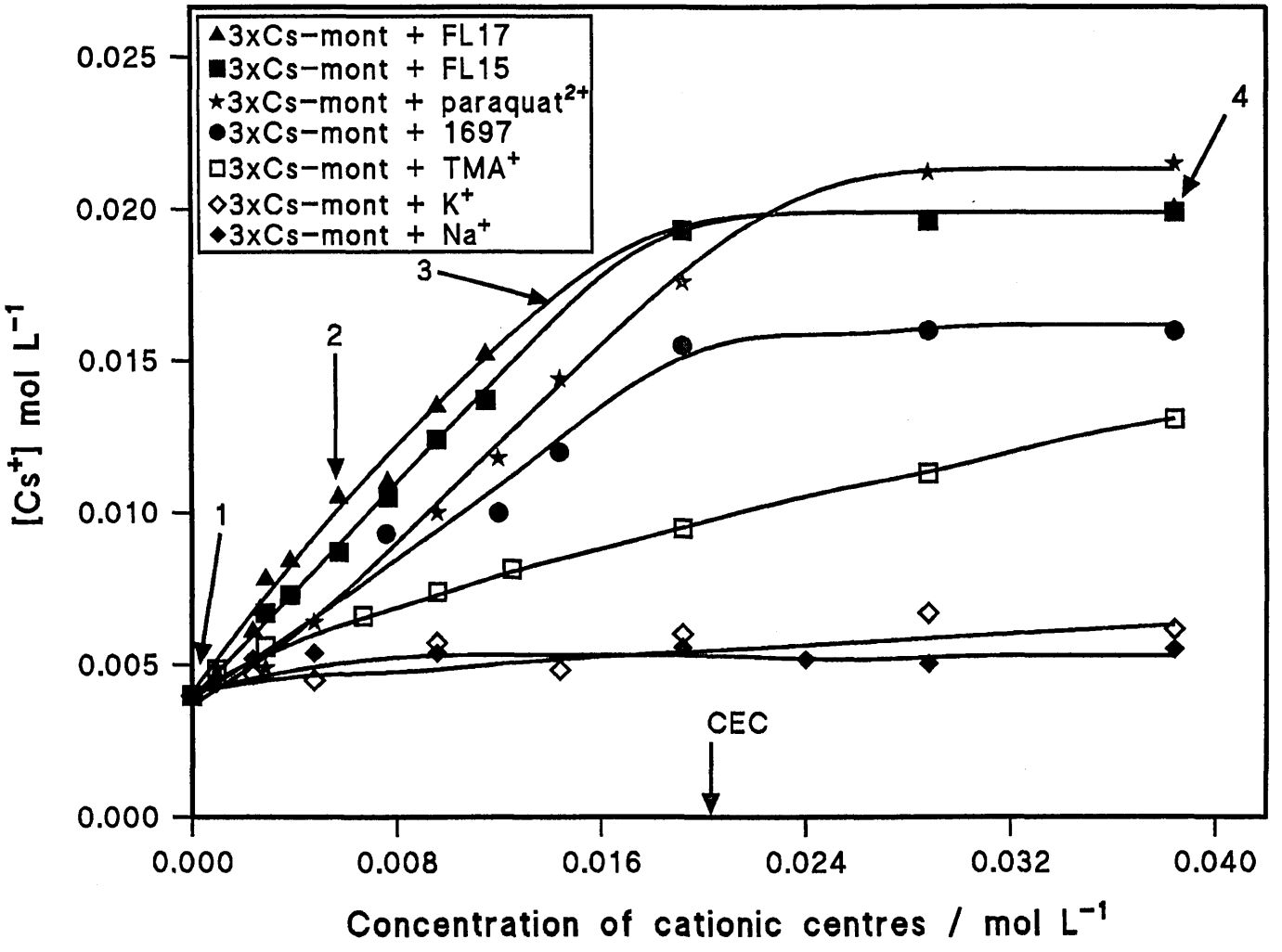

Figure 46. Increase in the observed $[Cs^+]$ upon addition of cationic species to 3xCs-mont.

Figure 46 shows that Magnafloc 1697 displaced less Cs^+ from the clay, suggesting that it had a lower affinity for the clay surface than either FL15 or FL17. A plateau region was again reached for the addition of 1.92×10^{-2} mol L^{-1} of N^+ to 3xCs-mont this time however the quantity of Cs^+ detected by NMR in the plateau region was only equal to 1.60×10^{-2} mol L^{-1}.

6.1.5.2.3 ^{133}Cs NMR Analysis to Determine Whether or Not all the Cationic Groups on FL17 Were Satisfied by Negative Sites at the Clay Surface at loadings equal to 100% of the CEC.

Three different clay/polymer suspensions were made up for analysis, these were;

1. **3xCs-mont to which was added sufficient polymer to displace all the Cs^+ from the clay.**
2. **Identical to sample 1 except that all the displaced Cs^+ ions were washed from the suspension.**
3. **Equal aliquots of suspension 2 and fresh 3xCs-mont to give a final clay concentration of 25 gL^{-1}.**

Comparison of the ^{133}Cs integral for suspension 1 with that for broadened CsCl showed that 2.00×10^{-2} mol L^{-1} of Cs^+ were displaced from the clay by FL17 (*ie* the plateau value seen in Figure 46) . This quantity of Cs^+ equates to approximately 100% of the total Cs^+ associated with the clay and is consistent with previous results. In contrast only a negligible amount of Cs^+ (2.0×10^{-4} mol L^{-1}) was seen in suspension 2 which had been washed to remove all the extraneous Cs^+ ions displaced by FL17. Comparison of the Cs^+ integral obtained for suspension 3 with that for broadened CsCl, suggested that 0.007 mol L^{-1} of Cs^+ were seen by NMR. Given that 0.004 mol L^{-1} of Cs^+ were visible by NMR in untreated 3xCs-mont, this suggests that an extra 0.003 mol L^{-1} of Cs^+ were displaced from the 3xCs-mont by polymer on the washed treated clay. This is clear evidence that at polymer loadings equal to 100% of the CEC that not all the cationic

groups on the polymer were satisfied by negative sites on the clay surface. To account for this extra 0.003 mol L^{-1} of Cs^+, polymer on the washed treated clay sample, sample 2, must have polycation segments which are not satisfied at the surface of the clay.

6.1.5.3 ^{23}Na NMR.

The optimised NMR operating conditions determined for 3xCs-mont were examined for use with 3xNa-mont and were found to be equally acceptable. This was deduced because the integral intensity for the 3xNa-mont peak compared with that for broadened NaCl was optimised under the same operating conditions.

^{23}Na NMR proved more difficult than ^{133}Cs NMR due to interference from a broad signal arising from ^{23}Na in the NMR probe. All ^{23}Na spectra consisted of a relatively sharp signal from the sample, superimposed upon a broad probe signal. After baseline correction using the spline method, it was possible to compare the integral intensities of the 3xNa-mont peaks with that for broadened NaCl and therefore determine the concentration of Na^+ detected by NMR, (Table 14). It was also possible to measure the ^{23}Na linewidth of the sample peaks which are also recorded in Table 14. Figure 47 illustrates the difference between the ^{23}Na spectra obtained for sample and probe together, spectrum 1, and for the sample with the probe signal removed, spectrum 2. Comparison of the integrated areas of the peaks for 3xNa-mont and broadened NaCl indicated that 6.80×10^{-3} mol L^{-1} Na^+ associated with the clay was seen by NMR. This quantity of Na^+ was equal to 35% of the total Na^+ known to be associated with the clay (see XRF analysis, section 6.1.2). FL17 was the only cationic species added to 3xNa-mont which was analysed by NMR. Figure 48 shows that the linewidth of 3xNa-mont was a fraction of that observed for 3xCs-mont and had a value of about 154 Hz.

(1) ^{23}Na Signals from the sample and the probe.

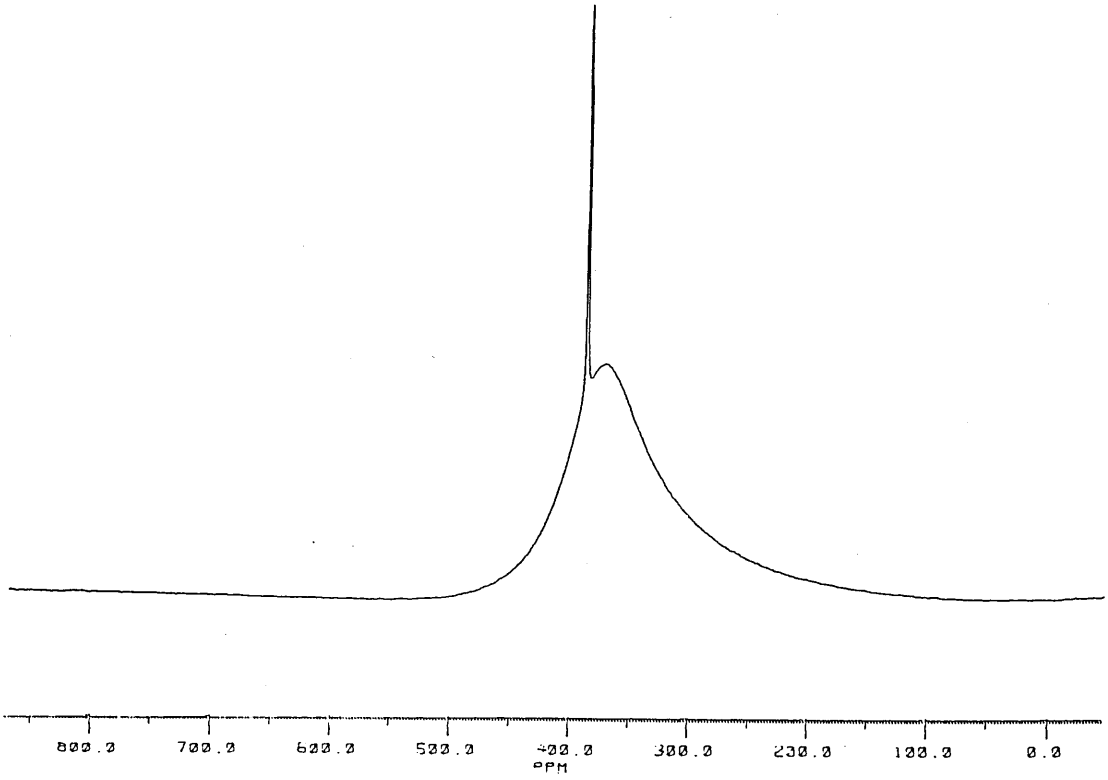

(2) ^{23}Na signal from the sample after subtraction of the ^{23}Na signal from the probe.

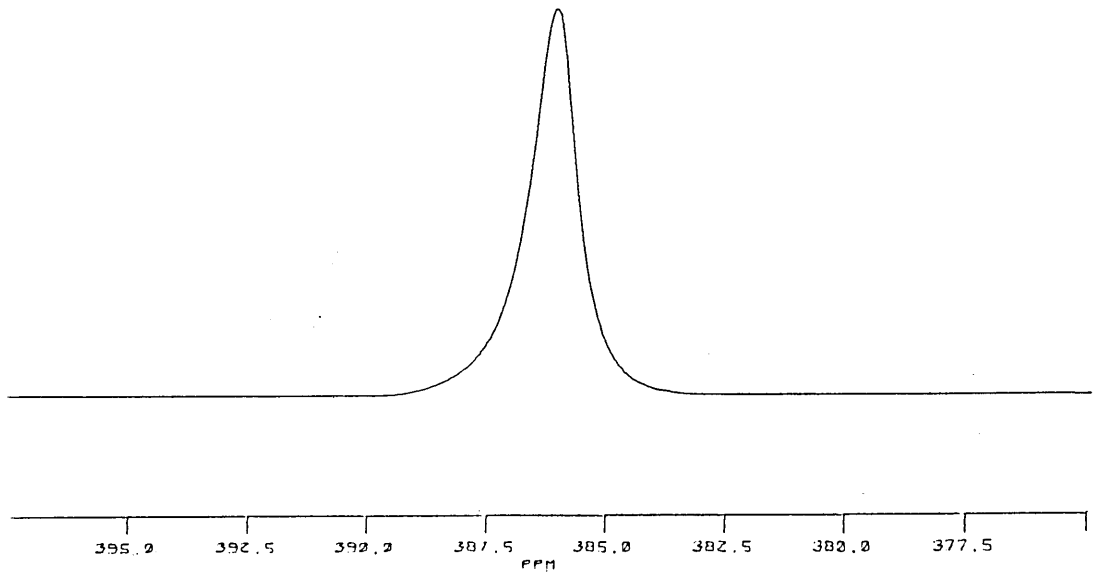

Figure 47. Representative ^{23}Na spectra for the addition of 3.84 x 10^{-2} mol L N^{+} from FL17.

	FL17	
Concentration of cationic centres added	**Linewidth / Hz**	**Na^+ / mol L^{-1}**
0	154	6.80×10^{-3}
1.92×10^{-3}	122	6.70×10^{-3}
4.80×10^{-3}	90	6.90×10^{-3}
6.72×10^{-3}	74	7.60×10^{-3}
9.59×10^{-3}	59	1.08×10^{-2}
1.15×10^{-2}	48	1.31×10^{-2}
1.44×10^{-2}	43	1.36×10^{-2}
1.68×10^{-2}	35	1.68×10^{-2}
1.92×10^{-2}	27	2.10×10^{-2}
2.88×10^{-2}	17	2.10×10^{-2}
3.84×10^{-2}	17	2.10×10^{-2}

Table 14. The effect on the ^{23}Na linewidth and concentration of Na^+ detected by NMR upon addition of FL17 to 3xNa-mont.

The addition of increasing volumes of FL17 to the 3xNa-mont caused a progressive decrease in linewidth from 154 Hz to 17 Hz following the addition of 3.84×10^{-2} mol L^{-1} of N.

Figure 49 shows that the addition of small quantities of FL17 to 3xNa-mont resulted in virtually no increase in the quantity of Na^+ detected by NMR. This is in direct contrast to results obtained for the addition of FL17 to 3xCs-mont which showed an initial steep rise in the curve relating to the displacement of large quantities of Cs^+ even at low loadings of polymer. As the quantity of FL17 available to the 3xNa-mont was increased, the curve rose steeply until a plateau was reached where the quantity of Na^+ displaced remained constant. As with the addition of FL17 to 3xCs-mont, this plateau began after the addition of 1.92×10^{-2} mol L^{-1} of N^+. The maximum quantity of Na^+ displaced from the clay, denoted by the plateau was equal to 2.10×10^{-2} mol L^{-1} and is in agreement with the total quantity of Na^+ associated with the clay.

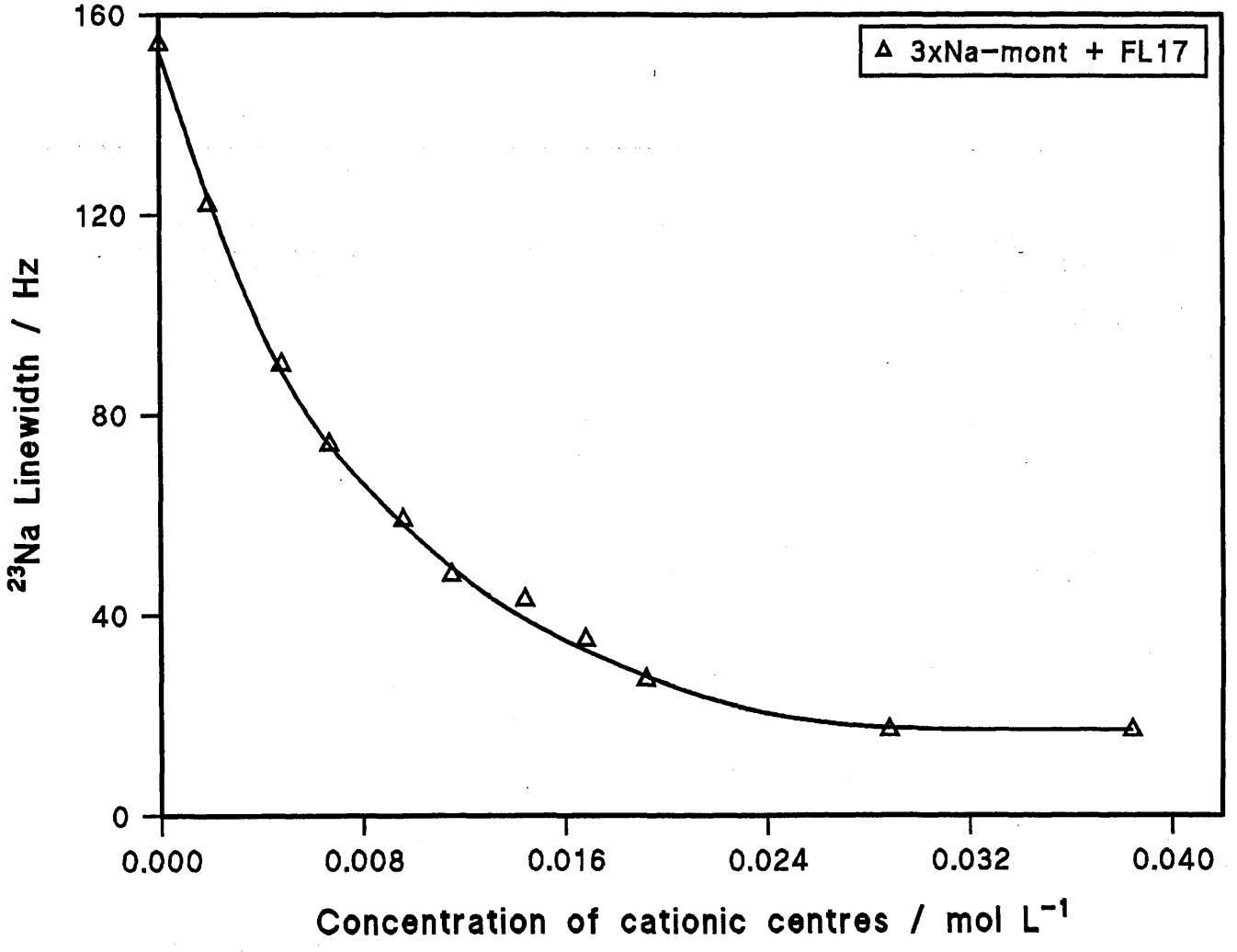

Figure 48. Decrease in the ^{23}Na linewidth upon addition of FL17 to 3xNa–mont

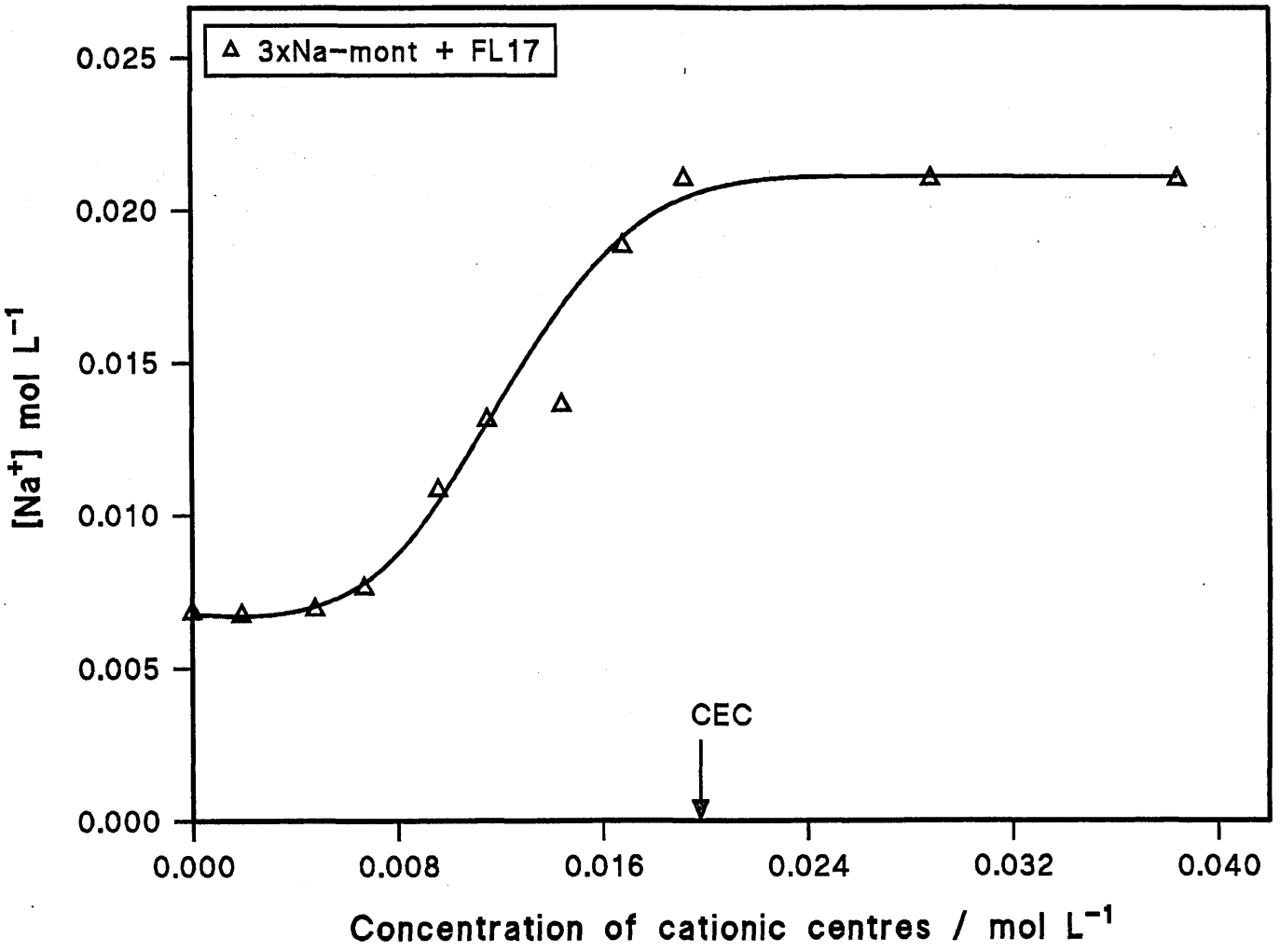

Figure 49. Increase in observed $[Na^+]$ upon addition of FL17 to 3xNa–mont.

6.1.6 The Use of Particle Size Analysis and Zeta Potential to Study Clay Polymer Suspensions.

Particle size and zeta potential measurements of several clay/polymer suspensions were recorded in order to provide complimentary information about the state of flocculation and surface charge of clay particles in suspensions containing polymer. Figure 50 illustrates the raw particle size data recorded using the Microtrac Particle Size Analyser for the addition of increasing amounts of Magnafloc 1697 to 3xCs-mont. From this figure it may be seen that the average particle size of 3xCs-mont was about 1.6 microns. Figure 50 shows that when Magnafloc 1697 was added to 3xCs-mont the peak at 1.6 microns representing polymer free particles decreased gradually in intensity. Simultaneously, a peak depicting particles of larger size increased in intensity. This larger particle size peak was due to flocculation of the clay by the polymer, resulting in flocs with an average size of about 10 microns. The peak at 1.6 microns was present throughout the range of polycation additions and in fact after passing through a minimum for the addition of 4.53×10^{-3} mol L^{-1} N^{+} from Magnafloc 1697, it increased in intensity to values approaching those observed at the outset of the experiment. This suggests that as the experiment proceeded, the Magnafloc 1697 initially caused flocculation. Subsequent build up of positive charge on the clay platelets due to the adsorbed polymer then caused repulsion of the platelets and a decrease in particle size.

Figure 51 and Figure 52 illustrate the particle size data recorded for the addition of FL15 to 3xNa-mont and 3xCs-mont respectively. The average particle size for both cation exchanged clays without added polymer was again 1.6 microns. Figure 51 shows that upon addition of FL15 to 3xNa-mont, the intensity of the peak at 1.6 microns, relating to bare clay particles, decreased markedly. This peak in fact showed zero

intensity upon addition of 1.44 x 10^{-2} mol L^{-1} N^{+} from FL15 and did not reappear throughout the course of the experiment. As this peak decreased, maxima showing increased particle size, relating to flocculated clay platelets increased in intensity. These peaks indicate that the average size of the clay/polymer floccules formed spanned a range from 13 to 40 microns, (Figure 51). Figure 52 shows that when FL15 was added to 3xCs-mont, the peak at 1.6 microns, corresponding to the bare clay platelets, decreased gradually as was observed for the addition of Magnafloc 1697 to the same cation exchanged clay. Further, as with the addition of Magnafloc 1697 to 3xCs-mont, this peak decreased in intensity to a minimum upon addition of 1.05 x 10^{-2} mol L^{-1} N^{+} from FL15 and then increased in intensity. This suggests that the FL15 initially flocculates the 3xCs-mont platelets and then causes them to redisperse due to a build up of positive charge upon the surface of the clay.

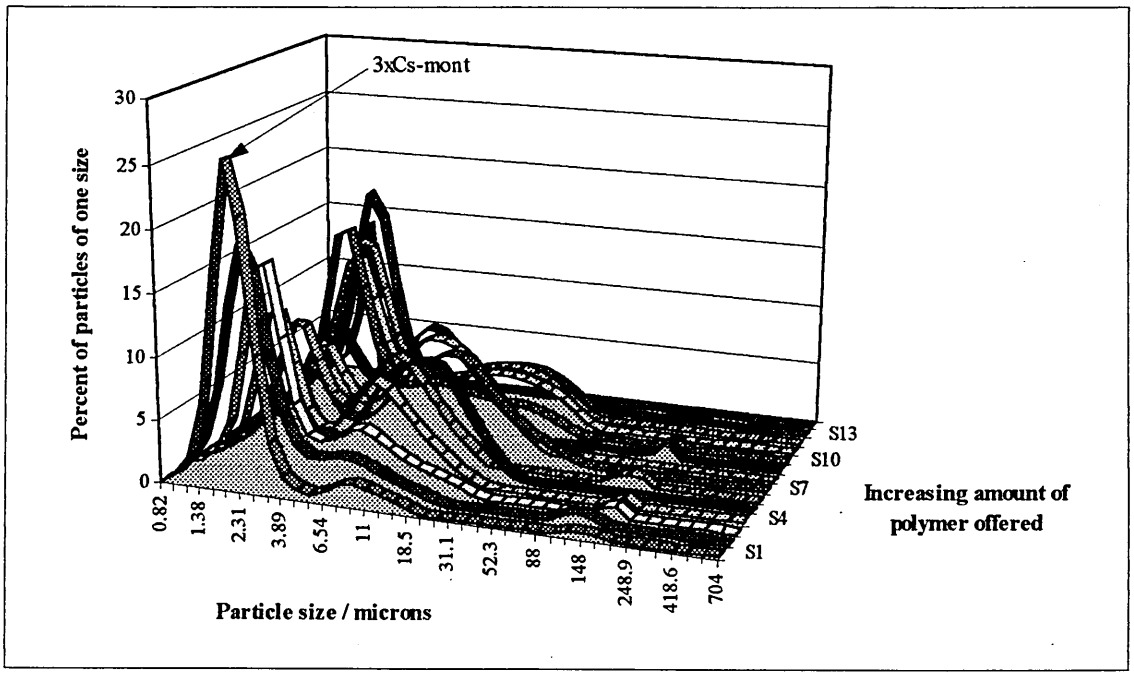

Figure 50. The change in particle size upon addition of increasing amounts of Magnafloc 1697 to 3xCs-mont.

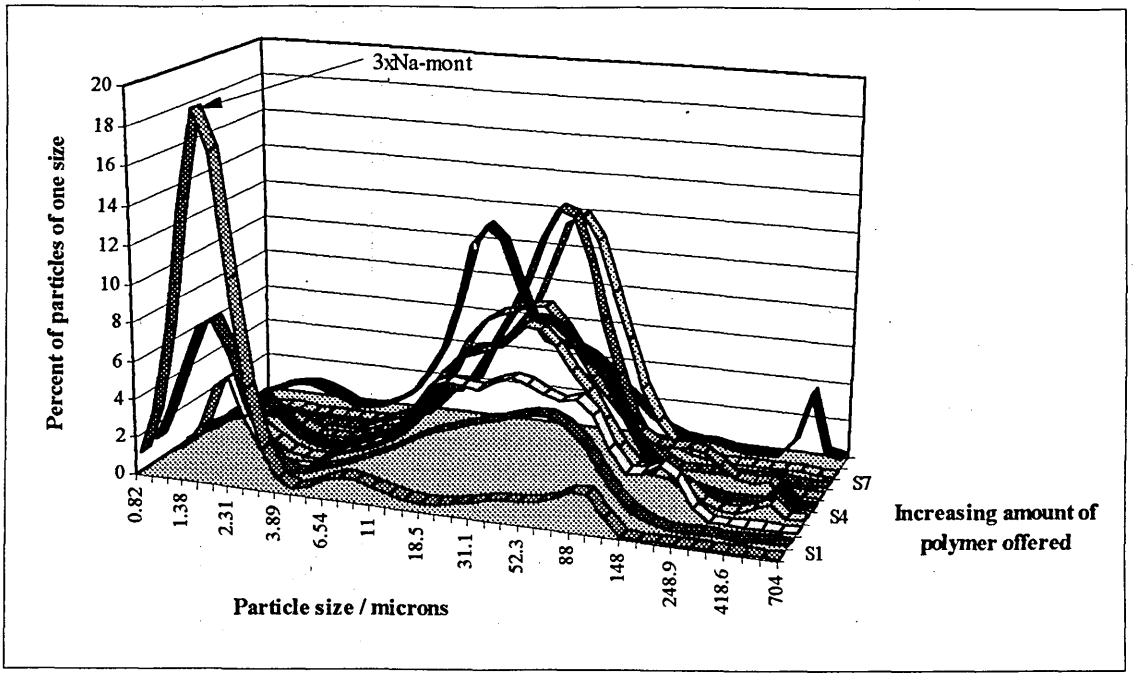

Figure 51. The change in particle size upon addition of increasing amounts of FL15 to 3xNa-mont.

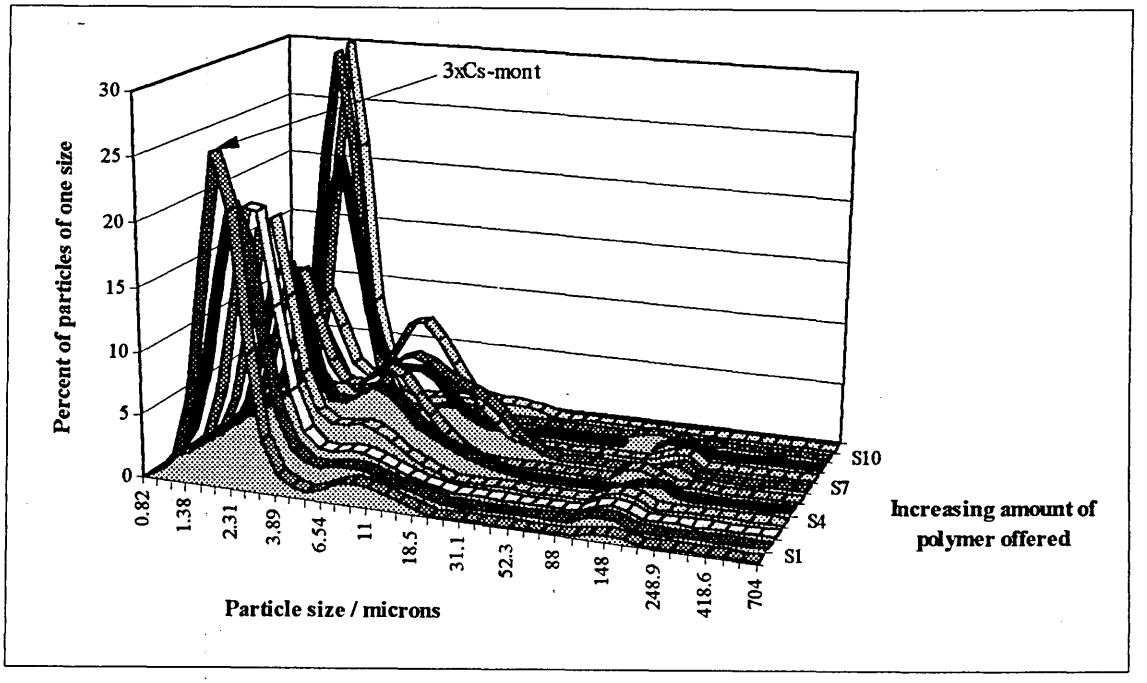

Figure 52. The change in particle size upon addition of increasing amounts of FL15 to 3xCs-mont.

The average particle size of these flocculated clay platelets was approximately 8 microns. Interestingly, it is obvious that similar trends in the particle size data were recorded for the addition of both Magnafloc 1697 and FL15 to 3xCs-mont.

The particle size and zeta potential data for the addition of Magnafloc 1697, FL15 and FL17 to 3xCs-mont, 3xNa-mont and 3xK-mont were recorded in Table 15, Table 16 and Table 17 respectively. Two graphs were then plotted from the data in these tables to illustrate the effect that addition of polycation had on the zeta potential and particle size of 3xCs-mont and 3xNa-mont clay suspensions, (Figure 53 and Figure 54).

N / Mol L^{-1}	Zeta potential / mV		% of total particles below 4 microns size	
Magnafloc 1697	**3xK-mont**	**3xCs-mont**	**3xK-mont**	**3xCs-mont**
0	-45	-50	100	100
4.53×10^{-4}	-45	-47	63	79
9.05×10^{-4}	-46	-45	40	68
1.81×10^{-3}	-43	-45	19	50
2.72×10^{-3}	-41	-42	14	29
3.63×10^{-3}	-44	-40	15	
4.08×10^{-3}		-37	12	
4.53×10^{-3}	-42	-26	8	25
4.99×10^{-3}		+5	7	31
5.43×10^{-3}	-40	+21	8	38
7.24×10^{-3}	-35	+36	2	67
9.06×10^{-3}	-33	+47	0	65
1.09×10^{-3}	-23	+50	0	57
1.36×10^{-2}	+32	+56	0	66
1.81×10^{-2}	+42	+63	5	62
2.72×10^{-2}	+45	+71	7	71
3.63×10^{-2}	+55	+75	16	75

Table 15. The zeta potential and particle size recorded for the addition of increasing volumes of 1697 to Cs^+, Na^+ and K^+ exchanged montmorillonite.

With the addition of increasing quantities of polycation to a clay suspension, the zeta potential of the suspension increases from around -50 mV to zero and beyond.

When the zeta potential of the clay suspension equals zero, the diffuse layer thickness approaches zero and the potential drop between the solid and the bulk solution occurs totally within the Stern layer. Under these conditions, a point of zero charge (PZC) or zero surface charge (ZSC) exists on the solid surface. With the adsorption of polycations onto negatively charged clay particles, a PZC should therefore be reached when the number of cationic centres matches the number of anionic centres. If the PZC is attained before the CEC is satisfied then this indicates that there is a build up of positive charge on the clay/polymer particle.

N/mol L^{-1}	**Zeta potential / mV**			**% of total particles below 4 microns size**		
FL15	3xK-mont	3xCs-mont	3xNa-mont	3xK-mont	3xCs-mont	3xNa-mont
0	-45	-50	-51	100	100	100
4.80×10^{-4}	-47	-55	-50	99	85	38
9.60×10^{-4}	-44	-51	-51	96	84	15
1.92×10^{-3}	-41	-49	-49	63	79	14
2.88×10^{-3}	-40	-47	-48	27	64	7
3.84×10^{-3}	-40	-47	-42	30	60	9
5.75×10^{-3}	-37	-47	-42	13	63	5
7.67×10^{-3}	-36	-44	-40	3	49	4
9.60×10^{-3}	-36	-40	-37	3	43	6
1.05×10^{-2}		-30			26	
1.15×10^{-2}	-36	-17	-35	2	40	2
1.34×10^{-2}		+7			28	
1.44×10^{-2}	-31	+37	-15	1	45	0
1.92×10^{-2}	-12	+44	+25	2	78	0
2.88×10^{-2}	+42	+51	+38	11	96	4
3.84×10^{-2}	+45	+50	+47	67	92	11
4.80×10^{-2}	+51			68	92	
5.75×10^{-2}	+53			60	93	

Table 16. The zeta potential and particle size recorded for the addition of increasing volumes of FL15 to Cs^+, Na^+ and K^+ exchanged montmorillonite.

N/mol L^{-1}	Zeta potential / mV			% of total particles below 4 microns size.		
FL17	3xK-mont	3xCs-mont	3xNa-mont	3xK-mont	3xCs-mont	3xNa-mont
0	-45	-	-51	100	100	100
4.80×10^{-4}	-60	-	-49	96	80	17
9.60×10^{-4}	-53	-	-50	54	55	24
1.92×10^{-3}	-48	-	-48	16	28	10
2.88×10^{-3}	-44	-	-44	6	34	8
3.84×10^{-3}	-44	-	-41	3	23	3
5.75×10^{-3}	-43	-	-41	10	13	5
7.67×10^{-3}	-40	-	-39	3	29	1
9.60×10^{-3}	-40	-	-36	1	20	0
1.05×10^{-2}		-				
1.15×10^{-2}	-37	-	-32	1	40	0
1.34×10^{-2}		-				
1.44×10^{-2}	+14	-	-8	1	38	0
1.92×10^{-2}	+34	-	+20	1	75	0
2.88×10^{-2}	+37	-	+38	18	88	4
3.84×10^{-2}	+45	-	+52	20	90	7
4.80×10^{-2}	+50	-		23	93	
5.75×10^{-2}	+52	-		45	93	

Table 17. The zeta potential and particle size recorded for the addition of FL17 to Cs^+, Na^+ and K^+ exchanged montmorillonite.

The observed zeta potential for a suspension of 3xNa-mont was -51 mV. Figure 53 shows that addition of FL15 to 3xNa-mont caused the zeta potential to become less negative. This change in zeta potential initially occurs very slowly after which time there is a rapid change to positive zeta potential values. This rapid change to positive zeta potential values occurred about the PZC which, for the addition of FL15 to 3xNa-mont, happened when 80% of the CEC was satisfied. Flocculation of the clay platelets increased rapidly upon addition of very low concentrations of FL15, shown by the rapid decrease in the number of small particles. The particle size curve shows that once

flocculated, the platelets remained so throughout the experimental conditions investigated, this can also be seen clearly in Figure 51. Maximum flocculation values also coincided with the PZC as would be expected.

The observed zeta potential for a suspension of 3xCs-mont was equal to -50 mV. Figure 53 shows that with the addition of FL15 to 3xCs-mont, the zeta potential becomes less negative. The zeta potential curve again shows a rapid change from negative to positive values about the PZC. This time however the PZC was reached when only 60% of the CEC was satisfied by added polymer. The curve depicting the flocculation of the clay platelets upon addition of FL15 shows a steady decrease until the PZC is reached at 60% of the CEC. This decrease in the curve relates to increasing flocculation. Addition of larger amounts of polymer to the clay then resulted in a build up of positive charge on the platelets, leading to repulsion and consequently to a decrease in particle size shown by the rise in the curve which coincided with the PZC. Figure 52 shows the raw particle size data which illustrates this point.

The adsorption of Magnafloc 1697 on 3xCs-mont resulted in the PZC and maximum flocculation point being reached when only 24% of the CEC was satisfied by added polymer, (Figure 54). This low value suggests that Magnafloc 1697 adsorbs mainly onto the external faces of the 3xCs-mont clay platelets, causing marked flocculation at very low loadings. This observation agrees with diffraction data where there was little evidence of interlamellar penetration of Magnafloc 1697 on 3xCs-mont at low loadings.

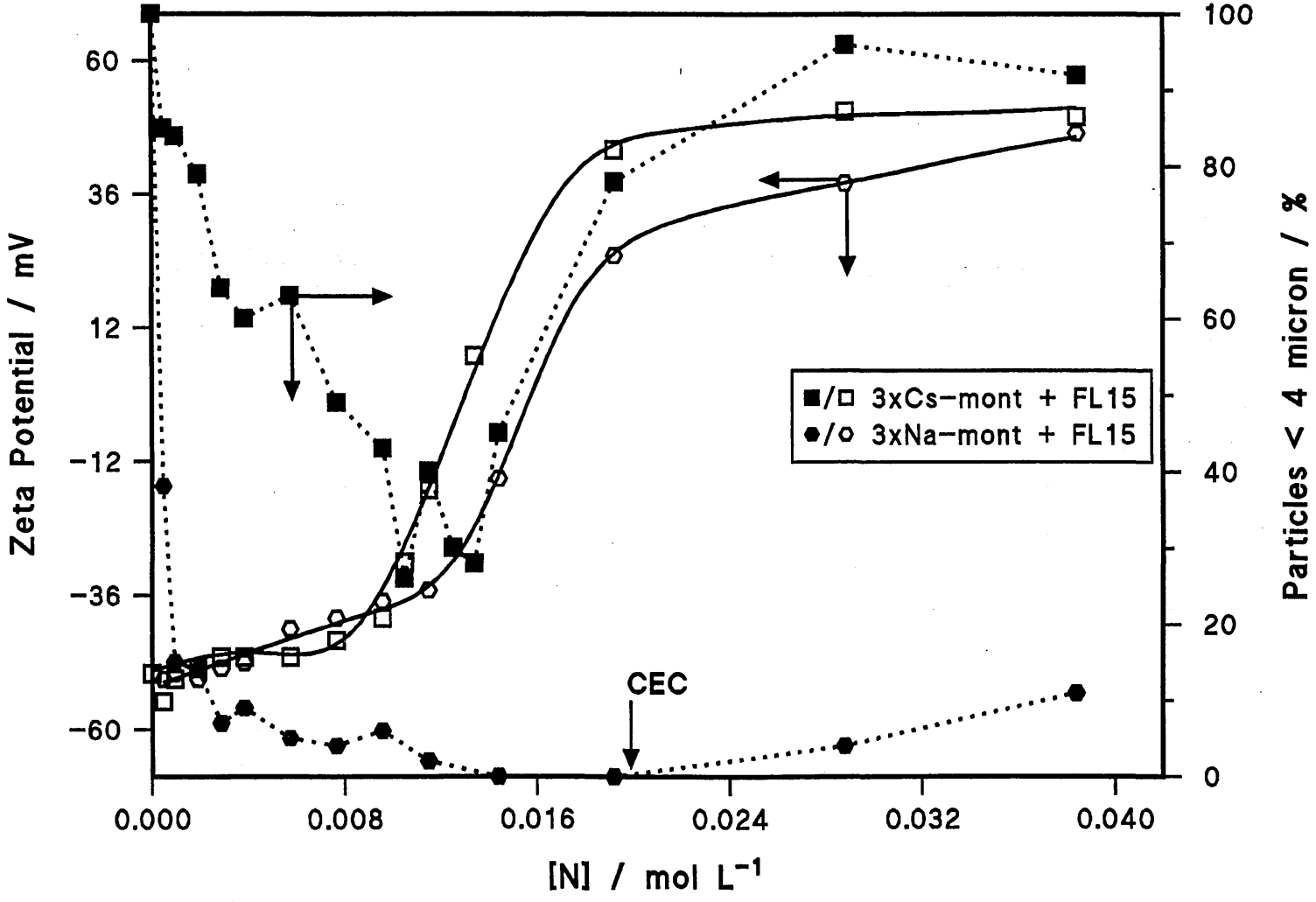

Figure 53. Variations in zeta potential and particle size upon addition of FL15 to 3xZ-mont.

Figure 54 illustrates the particle size and zeta potential data recorded for the addition of FL17 to 3xNa-mont. This figure again shows that the PZC and maximum particle flocculation coincide at 80% of the CEC as was observed for the addition of FL15 to the same cation exchanged clay. Further, the particle size curve shows that once flocculated, the platelets remained so throughout the range of added polycation, which was also observed for the addition of FL15 to 3xNa-mont. Figure 53 and Figure 54 therefore show that similar particle size and zeta potential data was observed for the addition of both FL15 and FL17 to 3xNa-mont, even though FL17 has a chain length 20 times longer than FL15.

Zeta potential and particle size data were also recorded for the addition of FL15, FL17 and Magnafloc 1697 to 3xK-mont. Upon addition of Magnafloc 1697 to 3xK-mont, the PZC and maximum flocculation values again coincided and were attained when only 60% of the CEC was satisfied by cationic groups on the polymer. This value was greater than that obtained for the addition of Magnafloc 1697 to 3xCs-mont which was equal to 24% of the CEC. With the addition of FL15 to 3xK-mont however, the PZC and maximum flocculation values were attained when the CEC of the clay was satisfied. As stated previously, the PZC and maximum flocculation values for addition of FL15 to 3xNa-mont and 3xCs-mont occurred at values corresponding to 80% and 60% of the CEC respectively.

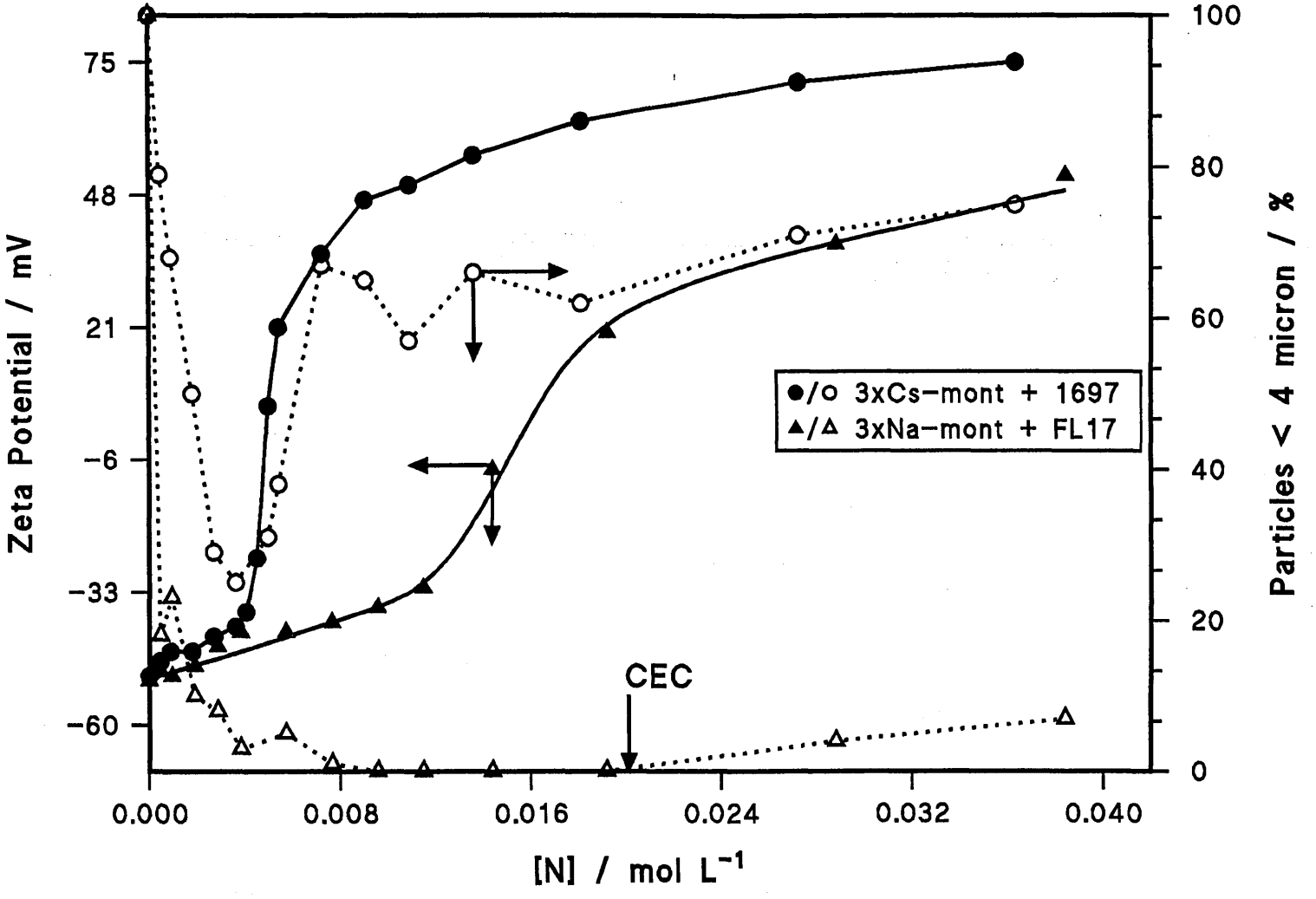

Figure 54. Variations in the zeta potential and particle size upon addition of Magnafloc 1697 and FL17 to 3xZ-mont.

6.2 Discussion Concerning the Interactions Taking Place Between Cationic Species and Westone-L.

The use of WBM containing cationic polymer additives has been forced upon the oil industry by the need to replace the superior, yet environmentally unacceptable OBM, (section 1). Cationic polymer additives in WBM are not the only alternative to OBM however they have been found to possess good shale inhibition properties with performances approaching those of OBM. The major problems with these cationic polymer additives is however their high depletion rates which dramatically escalates drilling costs.[12,14]

When in aqueous suspension, clay particles usually aggregate into tactoids.[134] The degree of aggregation is largely dependant upon the ionic strength of the medium, the particle size of the clay platelets and the exchange cation associated with the clay.[135] In this study the sedimentation and exhaustive washing to remove extraneous ions as described in section 5.1.2, minimises the effects of ionic strength and particle size on aggregation of clay platelets. Consequently, in this study, it is the effect of the exchangeable cation which dominates tactoid formation and therefore the amount of surface area available for interaction with cationic species, including polycations. It has been shown in previous studies that when the exchange sites are occupied by Na^+ or Li^+, the clay platelets are dispersed or peptised.[38,136] When the exchange cation is other than Na^+ or Li^+, the clay platelets tend to aggregate and form tactoids more readily thus reducing the available basal surface of the clay.[38,136,137] Consequently both the 3xK-mont and 3xCs-mont used in this study have a reduced surface area when compared to 3xNa-mont. The cation dependence of the Q_{max} values, shown by the adsorption isotherms (Figure 31 and Figure 32) reflects the level of aggregation of the clay platelets in aqueous

suspension. These figures also show that FL15, FL17 and Magnafloc 1697 all exhibited high affinity adsorption isotherms with all forms of cation exchanged Westone-L. Figure 55 however shows that FL17 has a greater affinity for the clay surface than Magnafloc 1697, shown by the gradient of the initial portion of the curve. The observed differences in affinity of these polycations for the surface of the clay is considered to be predominantly due to two reasons. Firstly, due to its smaller bulk size, FL17 is able to penetrate the interlayers of the clay more readily than Magnafloc 1697. Secondly, the distance between cationic groups upon the polymer and anionic sites upon the surface of the clay is thought to be important when considering polycation affinity. The distance between cationic groups upon FL17 is in fact 5.5 Å whereas the distance between anionic sites upon the clay surface is approximately 11.0 Å.[56] Consequently alternate N groups on the polycation exactly match the distance between anionic sites on the clay surface, resulting in strong affinity for the clay. Conversely Magnafloc 1697 with a distance between cationic groups of about 8.5 Å does not show such a strong affinity for the clay surface due to the mismatch in charge separation. The adsorption isotherm observed for TMA^+, which was used as a model for the cationic portion of the polymers, was of lower affinity. This weaker interaction between TMA^+ and clay resulted in a Q_{max} value of 60 mg g^{-1} in the region studied, but would clearly be higher if this range was extended.

The calculated amount of polycation required to completely satisfy the CEC of Westone-L corresponded to Q_{max} values of 83 mg g^{-1} for FL17 and 102 mg g^{-1} for Magnafloc 1697. On contacting 3xNa-mont with FL17 or Magnafloc 1697, Q_{max} was equal to 171 and 177 mg g^{-1} respectively, this was approximately double the amount required to satisfy the exchange capacity of the clay, (Figure 55).

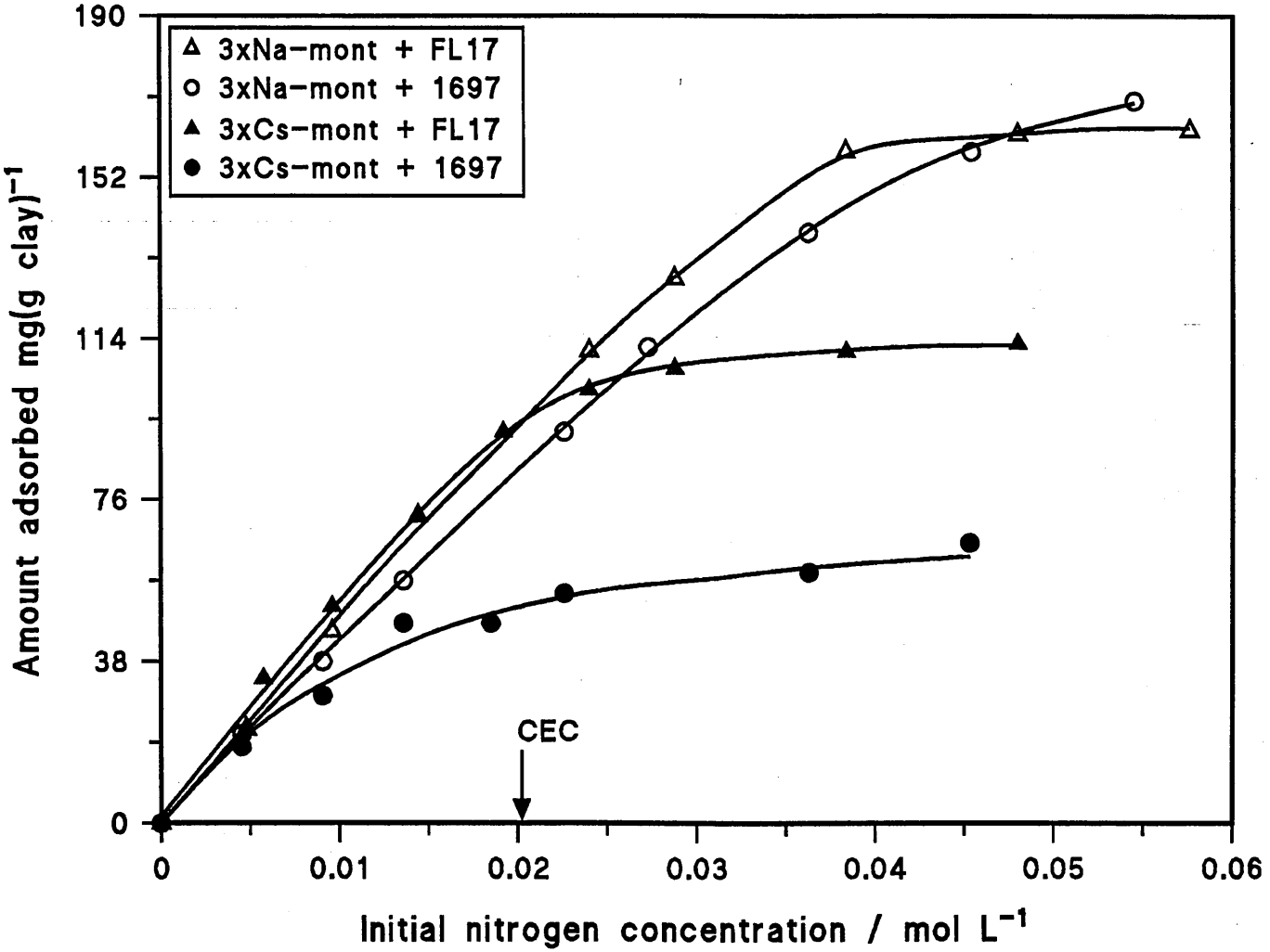

Figure 55. Adsorption isotherms obtained for the addition of FL17 and Magnafloc 1697 to 3xZ-mont.

The fact that FL17 and Magnafloc 1697 were adsorbed onto 3xNa-mont with similar Q_{max} values again suggests that both these polymers with their different structures were able to access both faces of each clay platelet when in aqueous suspension. Conversely, Figure 55 shows that the amount of FL17 and Magnafloc 1697 adsorbed by 3xCs-mont was dependant upon the structure of the polymer, shown by the large variation in the values of Q_{max}. For example, Q_{max} for the addition of FL17 to 3xCs-mont was equal to 113 mg g^{-1} which exceeded the exchange capacity of the clay by 32%. Conversely the bulkier Magnafloc 1697 was limited to a Q_{max} value of 74 mg g^{-1}, a value corresponding to only 73% of the exchange capacity being satisfied by polymer. One plausible explanation for the difference in Q_{max} would be restricted entry for the bulkier Magnafloc 1697 into some interlayer regions. The same type of phenomenon was also observed for high molecular weight cationic polysaccharides which were excluded from the interlayer of illite.[45] The Q_{max} values observed for the addition of FL17 and Magnafloc 1697 to 3xK-mont were between those observed for 3xNa-mont and 3xCs-mont as would be expected when considering that tactoid size increases as $Na^{+}<K^{+}<Cs^{+}$.

The representative XRD traces support the preceding interpretations regarding the location of the different polymers in the different cation exchanged montmorillonite. This was apparent because on contacting 3xNa-mont with low loadings of FL17 or Magnafloc 1697, (4.80×10^{-3} mol L^{-1} N, 20% of the CEC satisfied), a d 001 basal spacing consistent with one layer of either polymer between the sheets was observed at temperatures above 50°C. Above 50°C it also became apparent, due to the presence of two peaks, that both FL17 and Magnafloc 1697 were segregated in different interlayers at these low polymer loadings, (Figure 33, Figure 34). As stated previously, (section 6.1.3) below 50°C, two poorly resolved peaks were observed due to the presence of

polymer in some layers and water in others which resulted in a smaller than expected d 001 spacing. The relevant XRD traces imply that a large proportion of the water associated with the clay is lost upon thermal treatment at 50°C for 25 minutes. On first inspection this appears to be a rather low temperature to cause the loss of most of the water associated with the clay. Other studies are however in agreement with this observation, showing that the basal spacing of Na-montmorillonite collapses to 10.4 Å upon thermal treatment at 40°C while the basal spacing observed for Ca-montmorillonite collapses to 10.3 Å between 55-80°C.[133] Other types of clay such as Mg-vermiculite were also found to dehydrate at low temperatures comparable to that observed for montmorillonite.[138] The diffraction traces observed for the addition of low loadings of FL17 and Magnafloc 1697 to 3xNa-mont also indicate that Magnafloc 1697 is more thermally stable than FL17 on intercalation. This only becomes apparent upon thermal treatment of the 3xNa-mont/FL17 complex, where at temperatures exceeding 150°C, the polymer filled layers collapsed due to breakdown of the polymer and the appropriate peak disappeared, (peak **a**, Figure 33). Conversely, no collapse of the polymer filled layers and therefore no denaturing of the polymer was observed for the 3xNa-mont/Magnafloc 1697 complex even at temperatures up to 250°C, (peak **a**, Figure 34). At high polymer loadings, (3.84×10^{-2} mol L^{-1} N, >100% of the CEC), an increase in the quantity of FL17 or Magnafloc 1697 residing in the interlayer of the 3xNa-mont was implied by an increase in d-spacing from 13.0 Å to 16.0 and 15.1 Å respectively. This suggests that contacting 3xNa-mont with high loadings of either polycation, results in the presence of more than one layer of polymer in some interlayers of the clay. Conversely the diffraction traces obtained from samples of 3xCs-mont containing FL17 or Magnafloc 1697 at 20% of the CEC indicated that no polymer was intercalated between the layers.

This was supported by the 11.5 Å d-spacing observed at temperatures above 50°C which is characteristic of a collapsed Cs-montmorillonite. The corresponding diffraction trace for 3xK-mont with the same quantity of added Magnafloc 1697 showed that this clay/polymer complex behaved in a similar manner in that no spacing suggesting the presence of polymer between the layers was observed. Addition of low loadings of FL17 to 3xK-mont however resulted in basal spacings of 10.7 and 14.5 Å at 50°C, indicating that this polymer was again segregated in different interlayers of the clay at low loadings as was the case with its addition to 3xNa-mont. This is further evidence that the behaviour of 3xK-mont with respect to polymer adsorption is intermediate between that of 3xNa-mont and 3xCs-mont. It also underlines the superior ability of FL17 over Magnafloc 1697 to enter the interlayer of the 3xCs-mont and 3xK-mont as was intimated by the adsorption isotherm results. At high polymer loadings, (3.84×10^{-2} mol L^{-1} N, >100% CEC), all the cation exchanged clays exhibited basal spacings representative of at least one layer of polycation residing in the interlayer of the clay. Even 3xCs-mont showed basal spacings of 14.7 and 12.8 Å at 50°C for the addition of 3.84×10^{-2} mol L^{-1} N from FL17 or Magnafloc 1697 respectively, (Figure 38). This result again indicates that more FL17 rather than Magnafloc 1697 was able to penetrate the interlayer of the clay.

The thermogravimetric results support the preceding interpretations regarding the values of Q_{max} and the thermal stability of the polymer. These analyses show that on contacting 3xNa-mont with either FL17 or Magnafloc 1697 that the maximum amount of polymer desorbed from the clay was similar, (Table 11). This suggests that the same quantity of either polymer was initially adsorbed onto this type of cation exchanged clay. Further, the TGA results suggest that significantly more FL17 than Magnafloc 1697 was

adsorbed on 3xCs-mont, shown by the difference in the maximum percent weight losses from 160 to 520°C. Both these observations are in agreement with the results obtained from the adsorption isotherms in that the Q_{max} values observed for the addition of either polymer to 3xNa-mont were similar. Conversely Q_{max} for the addition of FL17 to 3xCs-mont was significantly larger than that observed for Magnafloc 1697. The TGA traces recorded for 3xCs-mont and 3xNa-mont contacted with increasing volumes of FL17, (Figure 39) show that the maximum polymer weight loss occurs at about 280°C. This polycation however begins to break down upon thermal treatment at about 170°C. Conversely, the maximum weight loss of Magnafloc 1697 from either clay occurs at 450°C, (Figure 40) whereas the temperature at which this polycation begins to break down is about 250°C. This is in agreement with XRD data which also indicates that FL17 is less thermally stable than Magnafloc 1697, shown by the collapse of the basal spacing at lower temperatures, (Figure 33).

The correlation between the adsorption isotherm, XRD and TGA data was not unexpected considering that the samples from which the information was gained underwent similar preparation procedures. Both the adsorption isotherm and TGA samples underwent a centrifugation step during preparation which may be significant in that any unattached cationic groups on the polymers would come into contact with exchange sites on neighbouring clay particles as the water was forced out of the sample. Consequently, the data obtained from these and the XRD samples, which were all dried prior to analysis may therefore represent clay/polymer complexes in which a greater proportion of the exchange cations had been displaced from the clay surface than was the case in aqueous suspension. Had it been possible, the clay/polymer complexes would have been analysed using the previously mentioned techniques in aqueous suspension,

therefore dispelling any concern about whether a dry sample can truly represent the clay polymer reactions which took place in aqueous suspension.

In section 3.1.3 the large amount of investigative work by a group of French workers concerning the interactions taking place between polycations and charged particles, including Na-montmorillonite and silica was reviewed. They observed that the interactions of the cationic polymer, PCMA, with Na-montmorillonite depended largely on both the cationicity, τ, and the molecular weight of the added polycation.[56,61] Durand-Piana *et al.*[61] have shown that the amount of polymer adsorbed onto Na-montmorillonite decreases as τ increases, reaching a minimum Q_{max} value of 320 mg g^{-1} at 100% cationicity. In this thesis the polycations investigated, FL17 and Magnafloc 1697, were 100% cationic and contacting 3xNa-mont with either one, resulted in a Q_{max} value of approximately 180 mg g^{-1}. By taking into account the different weights of the monomer units in PCMA and FL17, it was calculated that Q_{max} for the PCMA becomes 206 mg g^{-1} which was remarkably similar to the 180 mg g^{-1} observed for FL17 and Magnafloc 1697. This similarity in adjusted Q_{max} values becomes even more remarkable when considering the differences in the type and concentration of clay suspension used (0.5 gL^{-1}) and the differences in the polymer structure.

The cationicity of the polycation as stated above has a large bearing upon the value of Q_{max}, it also has a large bearing upon the mechanism by which the polymer adsorbs onto the clay surface.[56,61] Denoyel *et al.*[56] who investigated PCMA with molecular weights as large as 2.1×10^6, noted that at τ values < 15%, the polycation adopts a more extended conformation and is predominantly adsorbed via a particle bridging mechanism. Conversely at τ values > 15%, the dominant adsorption mechanism is charge neutralisation where the polymer is adsorbed in trains across the surface of the

clay. These two mechanisms of polycation adsorption for differing cationicities of the PCMA were corroborated by work carried out by Wang *et al.*[62,66] who investigated addition of the same polymer to silica particles. In both studies, the addition of low cationicity polymer to clay or silica particles, results in a dominant bridging mechanism which causes flocculation of the suspended particles and therefore should result an increase in the observed particle size. With this type of adsorption the amount of exchange cation displaced may be low because it is unlikely that all the cationic groups on the polymer will satisfy an exchange site on the clay. In contrast when charge neutralisation becomes the dominant mechanism and the polycation adsorbs onto the clay in a series of trains, the number of displaced cations should reflect the number of cationic units in contact with the clay surface. Consequently, it was anticipated that the combination of ^{133}Cs and ^{23}Na NMR information together with the particle size and zeta potential data would provide an insight into the mechanism by which the polycation adsorbed onto Westone-L in aqueous suspension and this was indeed the case.

Figure 44 shows the representative spectra obtained for the addition of FL17 to 3xCs-mont. Spectra 1-4 show an increase in intensity and a decrease in linewidth on increasing the amount of FL17 added to the 3xCs-mont, the quantitative data obtained from these and related spectra are shown in Figure 45 and Figure 46. Figure 45 shows that for a sample of 3xCs-mont without added cationic species, the measured linewidth is large with a value of about 1500 Hz. With the addition of polycation to 3xCs-mont, it was expected that a steady decrease in the ^{133}Cs linewidth would be observed until 100% of the clay's CEC was satisfied by polymer. After which it was thought that the linewidth would remain constant or decrease gradually, depending upon whether or not Cs^+ was associated with a second coordination sphere. Figure 45 however shows that

the polycations FL15, FL17 and Magnafloc 1697, when added to 3xCs-mont, caused the linewidth of the ^{133}Cs signal to decrease tenfold from 1500 to 150 Hz when < 20% of the CEC had been satisfied by polymer. Subsequent polycation additions, > 20% CEC, caused the linewidth to decrease only gradually. Charge balance arguments make it unreasonable to suggest that the polycation offered has replaced all the Cs^+ associated with the clay at loadings < 20% of the CEC and therefore something unexpected is happening. One plausible explanation why the linewidth of the ^{133}Cs signal initially decreased 10 fold upon addition of low polycation loadings could be as follows. The 3xCs-mont used in this study was washed free of extraneous Cs^+ ions and consequently all the Cs^+ in the sample was associated with the clay platelets. Without addition of cationic species to 3xCs-mont, it is reasonable to assume that the Cs^+ associated with a particular platelet cannot escape from its surface due to electrostatic attractions. It is highly probable however that the Cs^+ is not rigidly held and can therefore move about upon the surface of a particular platelet. Consequently, the peak for 3xCs-mont is thought to have a large linewidth because it is composed of a number of smaller linewidth peaks with varying chemical shifts due to the Cs^+ on different clay platelets. This variance in chemical shift arises due to the slightly different environments sampled by the Cs^+ cations on the different platelets. It is likely that these different environments sampled by the Cs^+ are due to Fe_2O_3 impurities in the clay. With the addition of increasing amounts of polycation to 3xCs-mont, more and more Cs^+ is displaced into solution which is then free to associate with other clay platelets. Eventually an averaging of the ^{133}Cs signals over all the clay platelets will result, the efficiency of which will depend upon the quantity of Cs^+ in solution and ultimately the ability of the displaced cations to diffuse from one platelet to another. This averaging of the ^{133}Cs signal is consequently thought to be responsible for the large decrease in the linewidth from 1500

to approximately 150 Hz when < 20% of the CEC had been satisfied by polycation. It is also plausible that the 150 Hz linewidth observed after the initial large decrease in peak width is a crude estimate of what might be the linewidth for Cs^+ on an individual clay platelet. If this were true, subsequent additions of polycation to 3xCs-mont should show only a steady decrease in linewidth proportional to the amount of polycation added and therefore the quantity of Cs^+ displaced from the clay platelets into solution. Figure 45 in fact shows that this is indeed the case. For the FL series of polymers, additions of polycation at loadings > 20% of the CEC caused the linewidth to decrease much more gradually from 150 Hz to a minimum of about 12 Hz which was observed when 100% of the CEC had been satisfied. Magnafloc 1697 showed a similar behaviour, this time however the minimum linewidth reached at the CEC of the clay was about 80 Hz, suggesting that a good proportion of the exchangeable Cs^+ was still associated with the clay which is indeed the case, as will be shown later. The efficient reduction in ^{133}Cs linewidth by the polycations was also observed for the addition of small quantities of K^+ to 3xCs-mont. After the initial large reduction in linewidth for the addition of up to 2.40 x 10^{-3} mol L^{-1} K^+, the linewidth reducing effectiveness of the K^+ decreased markedly in comparison to that of the polycations. Indeed after this point, the curve for the addition of K^+ closely resembled that observed for the addition of Na^+ to the 3xCs-mont in that both inorganic cations were ineffective at displacing large quantities of Cs^+ from the clay. This was indicated by the large linewidths observed for addition of the inorganic cations in quantities > 100% of the CEC. K^+ does however seem to possess the ability to selectively replace Cs^+ from a number of sites at the clay surface which initially results in the effective narrowing the ^{133}Cs NMR linewidth. When the K^+ has replaced all the Cs^+ from this small number of sites on the clay, addition of further K^+ results in proportionately less Cs^+ being displaced and consequently the ^{133}Cs NMR linewidth

narrows only slightly. In a related study, ^{133}Cs MAS-NMR spectra of Cs^+ exchanged hectorite in a 0.1 mol L^{-1} CsCl slurry exhibit two resonances at temperatures below -20°C which have been attributed to Cs^+ strongly bound in the Stern layer via interactions with the basal oxygens (δ = -28 ppm) and a more loosely held Cs^+ ion in the Gouy layer (δ = -3 ppm).[127] Both these peaks were distinct from the signal observed for the Cs^+, in the form of CsCl in solution (δ = 1 ppm). Even at temperatures between -20 and +50°C, where the two peaks relating to Cs^+ in the Gouy and Stern layers had become motionally averaged (δ = -17 ppm) the peak due to Cs^+ in solution was still clearly distinguishable. This suggests that exchange between Cs^+ in solution and Cs^+ associated with the clay is a slow process on the NMR time scale or a single averaged peak would have been observed. The Cs^+ in the Gouy layer is less strongly associated with the clay than Cs^+ in the Stern layer, it is therefore possible that the Cs^+ displaced from the clay by K^+ which caused the initial rapid decrease in linewidth is in fact Cs^+ in the Gouy layer. The fact that the same effect was not observed for the addition of Na^+ to 3xCs-mont can be attributed to the place that this cation holds in the replaceability series which is in the order $Cs^+ > K^+ > Na^+$.[16] The addition of TMA^+ to 3xCs-mont causes the ^{133}Cs NMR linewidth to decrease steadily as increasing amounts of Cs^+ are displaced from the clay. This steady decrease is because TMA^+ is not as effective as any of the polycations investigated at displacing Cs^+ from the clay, TMA^+ is however superior to the inorganic cations K^+ and Na^+ at displacing Cs^+. Conversely, the addition of paraquat to 3xCs-mont results in an effective decrease in the linewidth, indicating that this cationic species has a high affinity for the clay surface which results in the efficient displacement of Cs^+.

Figure 46 shows that the quantity of Cs^+ detected by NMR for a sample of 3xCs-mont with no added cationic species is 0.004 mol L^{-1}. This quantity of Cs^+ is equal to

20% of the total Cs^+ associated with the clay. An aligned ^{133}Cs spectrum consists of seven equally spaced lines of relative intensity 7:12:15:16:15:12:7. [131] It is proposed that the ^{133}Cs signal observed for 3xCs-mont arose predominantly from the central +1/2→-1/2 transition which accounts for 19% of the total ^{133}Cs signal. It is thought that the other transitions were not detected because they were very broad and thus lost in the background. The displacement of exchangeable Cs^+ from the clay surface upon addition of cationic species causes a proportion of the ^{133}Cs peak intensity to be due to Cs^+ in the bulk solution for which all seven transitions are degenerate and are observed. Consequently, the resulting peak with a weighted average between Cs^+ associated with the clay and Cs^+ in solution increases in intensity upon addition of cationic species. This is because an increasing amount of Cs^+ is displaced from the clay into the bulk solution, thus allowing an increasing proportion of the previously unobserved transitions to become visible to NMR. Figure 46 shows the quantity of Cs^+ which was detected by ^{133}Cs NMR upon addition of increasing amounts of different cationic species to 3xCs-mont. As indicated earlier, there is a correlation between the quantity of Cs^+ detected and the observed reduction in linewidth. The adsorption isotherms, illustrated in Figure 31, show that Q_{max} values for the addition of FL15 or FL17 to 3xCs-mont were in excess of the CEC. This suggests that all the Cs^+ was displaced from the clay at these polymer loadings. Figure 46 in fact shows this to be true where approximately 2.00×10^{-2} mol L^{-1} Cs^+, which is equal to the total amount associated with the clay, was displaced from 3xCs-mont upon addition of $\geq 1.92 \times 10^{-2}$ mol L^{-1} N^+ from either FL15 or FL17. This also indicates that at the CEC, one N^+ group from the polymer replaces one Cs^+ cation associated with the clay and therefore the configuration of the polymer at the clay surface cannot comprise of loops and tails. Indeed, there initially exists a linear relationship between the amount of N^+ added from either FL15 or FL17 and the concentration of Cs^+

detected by NMR. Figure 46 also shows that the addition of paraquat to 3xCs-mont was similar in that there is a linear relationship between the amount of N^+ added and the amount of Cs^+ displaced. Unfortunately no adsorption isotherm data could be obtained for the addition of paraquat to 3xCs-mont which therefore makes comparison with the results obtained for FL15 and FL17 difficult. It was however noted from Figure 46 that paraquat is not quite as effective at displacing Cs^+ from the clay as FL15 or FL17, shown by the shallower gradient of the upward portion of the curve and subsequent delayed onset of the plateau region. The correlation between the adsorption isotherms and the amount of Cs^+ detected by NMR upon addition of cationic species to 3xCs-mont can be further underlined by considering the isotherms obtained for the addition of Magnafloc 1697 and TMA^+ to 3xCs-mont, (Figure 31 and Figure 32). The addition of either of these cationic species to 3xCs-mont resulted in relatively low Q_{max} values, which were too small to indicate that either species satisfied the CEC of the clay independently. This therefore indicates that some Cs^+ must still have been associated with the clay in the range of added N^+ studied. Further, the fact that Q_{max} for the addition of Magnafloc 1697 was greater than that for TMA^+ indicated that more Cs^+ was displaced from 3xCs-mont by the polymer than by TMA^+. Figure 46 shows that Magnafloc 1697 did in fact displace more Cs^+ than TMA^+ however neither cationic species satisfied the CEC of the clay in the region of added N^+ studied and consequently neither displaced all the Cs^+ associated with 3xCs-mont. The inorganic cations Na^+ and K^+ were not very effective at displacing Cs^+ from the clay surface, indicated by the shallow gradient curves recorded in Figure 46. This was not unexpected since as reported earlier the replaceability series is in the order $Cs^+>K^+>Na^+$.[16] This order of replacement can be attributed in this case to the magnitude of the hydration energy of the exchangeable cation since the type of clay and mixing conditions were both kept constant throughout all experiments. Cs^+ has a low

hydration energy and thus causes interlayer dehydration and layer collapse ensuring that this cation is held strongly in the interlayer sites in the clay.[130] Conversely, the presence of cations with higher hydration energies, such as Na^+, result in water expanded layers and less strongly bound cations. Consequently, it is easier for Cs^+ to replace Na^+ than *vice versa*. This is why K^+, which has a hydration energy intermediate between that of Cs^+ and Na^+, displaces more Cs^+ than Na^+ does. The importance of the hydration energy in the displacement of Cs^+ from the surface of the clay was reinforced by the comparative effectiveness of TMA^+ which has a hydration energy similar to that of Cs^+.

In addition to ^{133}Cs NMR, ^{23}Na NMR was also utilised to investigate the interactions between FL17 and Westone-L in aqueous suspension. Two graphs illustrating the change in ^{23}Na linewidth and concentration were plotted, (Figure 48 and Figure 49). Figure 48 shows that for a sample of 3xNa-mont without added cationic species, the recorded linewidth is large with a value of 154 Hz. This measured linewidth is however relatively small when compared with that observed for 3xCs-mont which was equal to 1500 Hz. As was proposed for ^{133}Cs NMR, this 154 Hz linewidth is thought to be a composite peak consisting of a large number of smaller linewidth peaks of slightly different chemical shift. The variance in chemical shift again arises due to the slightly different environments sampled by the Na^+ cations on the different platelets. It is likely that these different environments sampled by the cation arise due to Fe_2O_3 impurities in the clay. One plausible reason why a smaller linewidth was observed for 3xNa-mont rather than 3xCs-mont is because the ^{133}Cs nuclei experiences larger chemical shifts, leading to a broader composite peak. This was thought to be possible since the hydration sphere surrounding the Na^+ cations will not allow them to sample the clay surface to the same degree as the Cs^+ cation which looses its associated water readily, thus allowing

direct contact with the clay surface. Figure 48 also shows that the addition of increasing amounts of FL17 to 3xNa-mont, caused a progressive decrease in linewidth from 154 to 17 Hz following the addition of 3.84×10^{-2} mol L^{-1} N^{+}. As with the addition of FL17 to 3xCs-mont, this decrease in linewidth was due to the fact that polymer displaces the exchangeable cation from the clay surface into the bulk solution. The initial large decrease in linewidth observed upon addition of a small quantity of FL17 to 3xCs-mont was however not observed for addition of the same polymer to 3xNa-mont. Again, this is considered to be due to the fact that the Na^{+} cation does not sample the clay surface to the same degree as Cs^{+}. Consequently any changes in linewidth are less pronounced.

Figure 49 shows that there is a discrepancy in the concentration of each cation initially detected by NMR in that approximately 20% of the total Cs^{+} was observed for samples of 3xCs-mont whereas with 3xNa-mont, 35% of the total Na^{+} was observed. This can be explained by considering the intensity of the different transitions in a ^{23}Na spectrum. An aligned ^{23}Na spectrum consists of three lines of relative intensities 3:4:3 corresponding to transitions between the spin states $+3/2 \rightarrow +1/2$, $+1/2 \rightarrow -1/2$, $-1/2 \rightarrow -3/2$ respectively.[139] It is proposed that the ^{23}Na signal for 3xNa-mont with no added cationic species arose predominantly from the central $+1/2 \rightarrow -1/2$ transition which accounts for 40% of the total ^{23}Na signal. It is thought that the $+3/2 \rightarrow +1/2$ and $-1/2 \rightarrow -3/2$ transitions were not detected because they were very broad and thus lost in the background signal. The displacement of exchangeable cations from the clay surface upon addition of FL17 causes a proportion of the ^{23}Na peak intensity to be due to Na^{+} in the bulk solution for which all three transitions are degenerate and are observed. The resulting peak with a weighted average between Na^{+} associated with the clay and Na^{+} in solution, increases in intensity upon addition of cationic species because more Na^{+} is displaced from the clay,

allowing an increasing proportion of the +3/2→+1/2 and -1/2→-3/2 transitions to be observed. Figure 49 shows an initial flat portion in the curve where the addition of up to 6.72 x 10^{-3} mol L^{-1} N^+ from FL17 caused little change in the concentration of Na^+ detected by NMR. This is in direct contrast to the results recorded for the addition of FL17 to 3xCs-mont which show that the concentration of Cs^+ detected by NMR increases linearly upon addition of polycation, (Figure 46). The addition of 2.00 x 10^{-2} mol L^{-1} of N^+ from FL17 to either cation exchanged clay however results in the displacement of all the respective exchangeable cation shown by the onset of the plateau region which coincided with the CEC of the clay, (Figure 46 and Figure 49).

Particle size and zeta potential measurements provided complementary information about the state of flocculation and surface charge of the clay platelets in aqueous suspension. It should be noted at this point that Na^+, Cs^+ and K^+ exchanged clay suspensions with no added polymer, all had a similar particle size of about 1.6 microns. As mentioned earlier, the platelets in Na^+ exchanged clay are known to exist predominantly as single entities whereas they stack into tactoids when the clay is Cs^+ or K^+ exchanged. The stacking of platelets into tactoids occurs through FF association which does not lead to a large increase in particle size. Consequently, the Microtrac Particle Size Analyser used in this study does not distinguish between the differences in tactoid size of a Na^+, Cs^+ or K^+ exchanged clay, shown by the similar particle sizes observed for each cation exchanged clay suspension.

The addition of FL15, FL17 or Magnafloc 1697 to 3xNa-mont, 3xCs-mont and 3xK-mont caused flocculation of the platelets. Figure 51 shows the particle size data recorded for the addition of increasing amounts of FL15 to 3xNa-mont. This figure indicates that the peak at 1.6 microns, relating to 3xNa-mont with no added polymer,

decreases progressively in intensity to zero upon addition of 1.44×10^{-2} mol L^{-1} N from FL15. As this small particle size peak decreased in intensity, peaks relating to increased particle size grew in intensity showing that the clay platelets flocculate in the presence of polymer. The floccules formed upon addition of FL15 to 3xNa-mont were large with an average particle size of between 13 to 40 microns. Once flocculated, the 3xNa-mont platelets did not redisperse throughout the range of added FL15.

Figure 50 and Figure 52 illustrate the particle size data recorded for the addition of Magnafloc 1697 and FL15 to 3xCs-mont respectively. These figures show that quite different results were obtained for the addition of cationic polymers to 3xCs-mont than were observed for the addition of the same polymers to 3xNa-mont, (Figure 51). For example, the peak at 1.6 microns, relating to the bare particles, again decreased in intensity upon addition of either Magnafloc 1697 or FL15 to 3xCs-mont. This time however, the addition of larger amounts of either polycation caused the peak to pass through a minimum and then increase in intensity to a value similar to that observed at the outset of the experiment. As the peak at 1.6 microns decreased in intensity, a peak relating to a higher particle size grew in intensity which was the result of flocculation by the polymer. The floccules formed upon addition of either Magnafloc 1697 or FL15 to 3xCs-mont had similar average particle sizes which were equal to about 10 and 8 microns respectively. As mentioned previously, larger additions of either cationic polymer to 3xCs-mont caused the 1.6 micron peak to increase in intensity. This was mirrored by a decrease in intensity of the higher particle size peak. This phenomenon shows that after the initial flocculation by polycation, subsequent additions of Magnafloc 169 / or FL15 to 3xCs-mont caused the floccules to break up, resulting in an increase in intensity of the 1.6 micron peak. Hence the degree of flocculation seems to depend more upon the

exchange cation associated with the clay, rather than the nature of the added polymer in that similar particle size data was recorded for the addition of both Magnafloc 1697 and FL15 to 3xCs-mont, (Figure 50 and Figure 52). Conversely, quite different particle size data was recorded for the addition of FL15 to 3xNa-mont, (Figure 51).

Along with particle size data, investigations into the zeta potential of clay platelets in the presence and absence of added polycation has also been studied in this thesis. Many previous studies have already shown that adsorption of cations onto negatively charged particles may result in charge reversal of the particle if sufficient counterions are adsorbed. [140,141] The adsorption of polycations, onto negatively charged clay platelets are no exception and at high polymer loadings, do in fact cause a charge reversal of the platelets which will be discussed in greater detail later. The point of zero charge or PZC for the adsorption of polycations onto negatively charged clay platelets should be reached when the number of cationic centres matches the number of anionic centres. If the PZC is reached prior to the CEC being satisfied then this indicates that there is a build up of positive charge on the clay/polymer particle.

Figure 53 and Figure 54 illustrate on the same graph the particle size and zeta potential data recorded for the addition of Magnafloc 1697, FL15 and FL17 to 3xCs-mont or 3xNa-mont. Used in conjunction, these two techniques provided much information about how polycations adsorb onto clay. The particle size data illustrated in these figures show that addition of Magnafloc 1697, FL15 and FL17 to 3xCs-mont or 3xNa-mont, resulted in significant flocculation of the platelets. It is extremely unlikely however that this initial increase in flocculation seen for the addition of small quantities of polycation could be caused by bridging flocculation. This was surmised because the polymers investigated in this study did not have very large molecular weights and

therefore have a relatively small chain length, (Table 3). For example FL15 has a molecular weight of 5000 and a chain length of 150 Å while Magnafloc 1697 and FL17 have a molecular weight of 100 000 and approximate chain lengths equal to 3813 Å and 3024 Å respectively. Particle size data suggests that suspensions of 3xCs-mont and 3xNa-mont with no added polymer have a nominal size of 1.6 microns for all cation exchanged clays. Consequently the dimensions of the adsorbed polymer chain are extremely small compared with the size of the clay platelets which would suggest that bridging between platelets is not possible. Bridging seems even more unlikely given that the adsorbed polymer chain has to span the double layer of the platelet that it is attached to and also the double layer of the platelet to which it is trying to bridge.

The flocculation mechanism or mechanisms in operation for the addition of Magnafloc 1697, FL15 and FL17 to 3xCs-mont or 3xNa-mont do not involve particle bridging. Further, a simple charge neutralisation mechanism cannot explain the particle size and zeta potential data illustrated in Figure 53 and Figure 54. This was deduced because if simple charge neutralisation were occurring, zeta potential data would show a change from negative to positive about the CEC of the clay which was not observed for the addition of any polycation to either cation exchanged clay. Also the initial large increase in particle size upon addition of small quantities of polycation cannot be explained by a simple charge neutralisation mechanism. Consequently, the mechanisms by which added Magnafloc 1697, FL15 and FL17 cause flocculation of different cation exchanged clays is considered complex and therefore each case will be discussed separately.

As would be expected, Figure 54 shows that the PZC and maximum flocculation coincided for the adsorption of Magnafloc 1697 on 3xCs-mont albeit at the extremely

low value of 24% of the CEC. The fact that the PZC and maximum flocculation occurred at such a low value suggests that polycation adsorbs predominantly onto the external surfaces of 3xCs-mont, causing the fast build up of positive charge. This is in agreement with the diffraction data where there is little evidence of interlamellar penetration by Magnafloc 1697 on both 3xCs-mont and 3xK-mont at low polymer loadings, (Table 10). It should be remembered at this point that with Cs^+ exchanged clay, the platelets are stacked into tactoids. Consequently, adsorption of Magnafloc 1697 on 3xCs-mont must actually proceed via adsorption onto the external faces of tactoids rather than individual platelets.

Particle size and zeta potential data recorded for addition of Magnafloc 1697 to 3xCs-mont cannot be explained by simple charge neutralisation or particle bridging, it is therefore proposed that some other more complex mechanism of clay/polymer flocculation is occurring. Parazac *et al.*[142] who studied the interactions taking place between montmorillonite and three polycations, two of which were similar to Magnafloc 1697 and FL17, has suggested that a "hydrophobic patch" mechanism may be in operation for their systems. With this type of flocculation, the adsorbed polycation molecules with their charges neutralised by the clay surface, consist of mainly hydrophobic moieties. Parazac *et al.*[142] state that these hydrophobic segments will precipitate onto similar segments adsorbed onto adjacent particles, which they state causes agglomeration. Although Parazac *et al.*[142] investigated similar polymers to Magnafloc 1697 and FL17, the "hydrophobic patch" flocculation mechanism is not considered to be in operation in this study. For flocculation to occur, two hydrophobic areas on colliding particles must come into contact and since the adsorbed polycation is small with respect to the clay platelet, it is extremely unlikely that this flocculation

mechanism would cause the formation of large floccules at low polymer loadings as was observed in this study. The "electrostatic patch" model (section 3.4), invoked by Gregory,[84] is therefore considered responsible for the severe flocculation observed upon addition of low concentrations of polycation. The distance between cationic groups on Magnafloc 1697, a highly charged polymer, is approximately 8.5 Å while the distance between anionic sites on the clay surface is nominally 11.0 Å.[56] Consequently, under conditions of overall neutrality, it would be physically impossible for all the ionic sites on the surface of the clay to be neutralised individually by cationic groups from the polymer. This is reflected in the ^{133}Cs NMR results which show that all the Cs^+ cannot be displaced from 3xCs-mont upon addition of large amounts of Magnafloc 1697, (Figure 46). It should be remembered however that a large proportion of the Cs^+ still in contact with the clay upon addition of large quantities of Magnafloc 1697, results from the inaccessibility of some interlayer regions to this bulky polycation. The mismatch in charge separation between cationic groups on the polymer and anionic sites upon the clay, leads to uneven charge distribution which Gregory states results in an extra attractive contribution to the interaction energy between two such particles. Consequently if a negatively charged patch encounters a positively charged patch on another particle, flocculation will result, leading to the formation of large floccules as were observed in this study. The average particle size of the floccules formed was actually about 10 microns. After sufficient Magnafloc 1697 had been added to 3xCs-mont to reach the PZC, subsequent additions of polycation, caused the flocs to start breaking up, (Figure 54). As expected, the zeta potential moves to increasingly positive values as the particle size decreases, suggesting a build up of positive charge on the surface of the clay. This build up of positive charge, due to polymer adsorption, caused the repulsion between the clay particles which resulted in the decrease in particle size. The fact that the tactoids deflocculate with the

addition of large quantities of Magnafloc 1697 suggests that the floccules formed were weak.

Particle size and zeta potential data recorded for the addition of FL15 to 3xCs-mont were similar to those outlined above for the addition of Magnafloc 1697 to the same cation exchanged clay. This time however, the PZC and maximum particle flocculation coincided at 60% of the CEC, rather than the 24% observed for the addition of Magnafloc 1697 to the same clay, (Figure 53). It is thought that the PZC and maximum particle flocculation were attained at a later stage for the addition of FL15 because this polymer was able to enter the interlayer of 3xCs-mont with greater ease than the bulkier Magnafloc 1697 at low polymer loadings. Consequently the build up of charge upon the external faces of the tactoids was slower. Although the flocculation is not as severe as that observed for the addition of low loadings of Magnafloc 1697 to 3xCs-mont, an electrostatic patch flocculation mechanism is still thought to be in operation for the addition of FL15 to 3xCs-mont. This is because the distance between cationic groups on this highly charged polymer is 5.5 Å which is exactly half the distance between anionic sites upon the surface of the clay. Consequently the addition of FL15 to 3xCs-mont results in alternate cationic groups being satisfied at the clay surface. The cationic groups associated with the polymer which are not satisfied by the surface of the clay, all contribute to create areas of high positive charge density. These areas can then interact with areas of relatively weak negative charge such as the bare clay surface of another tactoid, which in turn causes flocculation at low polymer loadings. The average particle size of the floccules formed was 8 microns which was similar to the 10 microns particle size observed for the addition of Magnafloc 1697 to the same cation exchanged clay. With the adsorption of FL15 onto 3xCs-mont, it is possible that the majority of Cs^+

associated with the clay could be displaced because the distance between alternate N^+ groups on the polymer exactly matched the distance between anionic sites upon the surface of the clay. ^{133}Cs NMR results in fact show that approximately 100% of the Cs^+ associated with 3xCs-mont is displaced by FL15 when added to the clay at a concentration equal to the CEC, (Figure 46). Similarly, Figure 53 shows that the size of the clay/polymer particles return to values similar to those observed at the outset of the experiment as the concentration of FL15 added equalled the CEC of the clay. This deflocculation of the floccules was caused by the build up of polymer and therefore the positive charge upon the tactoids, leading to repulsion between them. A plateau relating to the maximum zeta potential recorded was in fact reached when the concentration of N^+ added from FL15 equalled the CEC of the clay. Consequently the maximum zeta potential value and therefore minimum particle size value, both coincide with the CEC of the clay while ^{133}Cs NMR results show that all the Cs^+ is displaced from the 3xCs-mont as the CEC is reached. Similar particle size data was also recorded for the addition of FL17 to 3xCs-mont, (Table 17). This is further evidence suggesting that a bridging mechanism is not responsible for the severe flocculation observed upon addition of low loadings of polycation to 3xCs-mont. This was concluded since FL17 with a chain length approximately 20 times longer than that of FL15 should cause increased flocculation to occur at similar polymer loadings.

The ^{133}Cs NMR experiments carried out in section 6.1.5.2.3 which involved the addition of fresh 3xCs-mont to an exhaustively washed sample of FL17 saturated 3xCs-mont indicated that 0.003 mol L^{-1} of Cs^+ were displaced from the fresh 3xCs-mont on contacting the two suspensions. The FL17 saturated 3xCs-mont is basically deflocculated at these polymer loadings due to the electrostatic repulsions caused by the

net positive charge on the particles arising from the adsorption of large quantities of polymer, (Table 17). Consequently, addition of the bare clay platelets to the polymer saturated ones resulted in more Cs^+ being displaced from the fresh 3xCs-mont. It is probable that the electrostatic patch model was in operation here where the areas of high positive charge on the polymer saturated platelets were strongly attracted to the areas of relatively weak negative charge on the bare clay particles, resulting in the displacement of Cs^+ from the clay.

The particle size and zeta potential data recorded for the addition of FL15 to 3xNa-mont was totally different to that recorded for the addition of the same polymer to 3xCs-mont. This time the PZC and maximum particle flocculation coincided at 80% of the CEC. It should be remembered at this point that the platelets in Na^+ exchanged clay do not associate into tactoids as readily as those in Cs^+ exchanged clay and are therefore considered to exist predominantly as single entities in suspension. This means that the vast majority of the total surface area is available for interaction with the added polycation. Consequently, larger amounts of FL15 had to be added to 3xNa-mont than were added to 3xCs-mont to reach the PZC and maximum flocculation value, (Figure 53). Flocculation of the clay platelets at low polymer loadings was severe for the addition of FL15 to 3xNa-mont, (Figure 53). Similar particle size and zeta potential data was also recorded for the addition of FL17 to 3xNa-mont, again suggesting that a bridging flocculation mechanism was not preferred in these systems, (Figure 54). The distance between cationic groups on FL15 is 5.5 Å which is exactly half the distance between anionic sites upon the surface of the clay. Consequently the distance between alternate cationic groups on FL15 and indeed FL17 matches exactly the distance between anionic sites on the surface of 3xNa-mont. It was therefore expected that the vast

majority of the exchangeable Na^+ would be displaced by these polycations from the clay surface. ^{23}Na NMR results in fact show this to be true for the addition of FL17 to 3xNa-mont, (Figure 49). The 50% of cationic groups on the polymer which were not satisfied by the anionic sites upon the clay surface can then contribute to create areas of high positive charge density. These areas may then be attracted to areas of relatively weak negative charge such as the bare clay surface of another platelet which causes the observed flocculation at such low polymer loadings, (Figure 53). The floccules formed upon addition of FL15 to 3xNa-mont were much larger than those observed for the addition of FL15 or Magnafloc 1697 to 3xCs-mont and had a wide range of particle sizes ranging from 13 to 40 microns in size. These floccules also appeared to be stronger than those formed upon addition of FL15 or Magnafloc 1697 to 3xCs-mont, shown by the fact that the platelets remained flocculated even after the plateau relating to the maximum positive zeta potential had been reached. The flocculation mechanism in operation upon addition of FL15 to 3xNa-mont is therefore considered to be slightly different than that observed for addition of FL15 or indeed Magnafloc 1697 to 3xCs-mont. It is thought that the exchangeable cation associated with the clay and therefore the degree of clay platelet dispersion is responsible for these differences. Finally, Table 16 shows that for the addition of FL15 to 3xK-mont, the platelets again initially flocculate but then redisperse as the CEC of the clay is satisfied by polymer. Consequently, the strength of the floccules formed upon addition of FL15 to 3xCs-mont, 3xNa-mont and 3xK-mont increased in the order 3xCs-mont<3xK-mont<3xNa-mont. This order of increasing floc stability was also observed for the addition of FL17 and Magnafloc 1697 to the same cation exchanged clays. Interestingly, the number of platelets per tactoid decreases in the order Cs^+ exchanged clay>K^+ exchanged clay>Na^+ exchanged clay. This data therefore seems to suggest that the exchangeable cation associated with the clay and therefore the

degree of platelet aggregation into tactoids, governs the strength of the flocs formed upon addition of polycation to a clay suspension.

In summary the particle size and zeta potential results recorded all indicate that an "electrostatic patch" adsorption mechanism was in operation for the addition of Magnafloc 1697, FL15 and FL17 to 3xZ-mont. This was deduced since severe flocculation of the clay resulted upon addition of low concentrations of any of the highly charged polycations investigated, which could not be explained by a simple charge neutralisation or bridging mechanism. Similar particle size and zeta potential results were recorded for the addition of any polycation investigated in this study to a particular cation exchanged clay. The main reason for these similarities was probably because Magnafloc 1697, FL15 and FL17 were all 100% cationic. Major differences however arose in particle size and zeta potential results upon addition of a particular polycation to differing cation exchanged clays. Differences such as how much polycation was required to reach the PZC of a particular clay or how much polycation was required to cause deflocculation of the floccules, if indeed deflocculation occurred, were observed. Once again the nature of the cation associated with the clay has proved to be central in controlling polycation adsorption via clay platelet dispersion.

The differences in the ability of each cationic species to adsorb onto clay and therefore displace the exchangeable cation will now be discussed in detail. It has been shown by ^{133}Cs NMR that the addition of inorganic cations such as Na^+ and K^+ to 3xCs-mont cause the replacement of only a small proportion of the exchangeable Cs^+ associated with the clay. The quantity of Cs^+ replaced is thought to be related to the hydration energy of the cation, consequently Cs^+ with a hydration energy of -277 kJ mol^{-1} is not very easily replaced by K^+ or Na^+ with more negative hydration energies equal to -

321 and -405 kJ mol^{-1} respectively. The adsorption of TMA^+ on 3xCs-mont occurred as expected through an exchange reaction between the exchangeable Cs^+ on the clay and the TMA^+ ions in solution.[143] Theng *et al.*[143] who studied the adsorption of different alkylammonium cations on montmorillonite stated that as the molecular size of the cation was increased, its affinity for the clay surface increases which is usually the case for adsorption of organic cations by montmorillonite.[144,145] This increased affinity for montmorillonite with increasing molecular size may be attributed to the increased contribution of the Van der Waals forces as the size of the cation is increased.[143] Further, TMA^+ has a hydration energy equal to -134 kJ mol^{-1} which is less negative than that for a Cs^+ cation and consequently TMA^+ can compete with Cs^+ effectively for negative sites on the clay surface. The very high affinity of paraquat for the surface of montmorillonite observed in this study was also noted by others.[146,147] Weed *et al.*[146] state that apart from the obvious coulombic interactions, there are also Van der Waals forces which make a significant contribution to the overall adsorption energy of paraquat on montmorillonite. They also state that the separation of positive charge on the paraquat is similar to the distance between negative charge sites on the surface of the clay and therefore these opposite charges may come into close approach resulting in strong adsorption onto the clay surface. ^{133}Cs NMR and representative adsorption isotherms have shown that polycations have a strong affinity for 3xCs-mont. As stated previously, the net segment-surface interaction energy, ε, is approximately 4 kT per cationic unit.[56] The total energy of adsorption for polycations is therefore large because there are many adsorbed segments per polymer molecule. This large adsorption energy accounts for the high affinity of polycations for the surface of the clay. The affinity of FL17 for 3xCs-mont or 3xNa-mont was however seen to be greater than that of Magnafloc 1697, shown by the gradient of the initial portion of the adsorption isotherm,

(Figure 55). The observed differences in affinity of these polycations for the surface of the clay is considered to be predominantly due to two reasons. Firstly, due to a smaller bulk size, FL17 is able to penetrate the interlayers of the clay more readily than Magnafloc 1697. Secondly, the match between cationic groups on the polycation and anionic sites upon the clay surface is considered to be important. Consequently, FL17 shows a high affinity for the clay because the distance between cationic groups on this polymer is 5.5 Å which is exactly half the distance between anionic sites on the surface of the clay. Therefore alternate cationic groups exactly match the distance between anionic sites upon the clay surface, resulting in a strong affinity for the clay. Magnafloc 1697 on the other hand has a distance between cationic groups of 8.5 Å which is a poor match for the anionic sites on the clay surface and therefore results in a lower affinity for the clay surface. The differences observed in the respective Q_{max} values and ^{133}Cs NMR data recorded for the addition of FL17 and Magnafloc 1697 to 3xCs-mont are however a different matter. As stated previously, Q_{max} was equal to 113 and 74 mg g^{-1} for addition of FL17 and Magnafloc 1697 to 3xCs-mont respectively. ^{133}Cs NMR shows that substantially more Cs^+ was displaced by FL17 than by Magnafloc 1697 upon addition of the same quantity of polymer to 3xCs-mont, this was also reflected in the linewidths of the appropriate ^{133}Cs peaks. Conversely, the addition of both these polymers to 3xNa-mont resulted in similar Q_{max} values, (Figure 55). The differences observed in the value of Q_{max} for the addition of FL17 and Magnafloc 1697 to 3xNa-mont and 3xCs-mont may therefore be attributed predominantly to the different effects that the exchangeable cations have on the aggregation and swelling ability of clay platelets. The addition of either polymer to 3xNa-mont results in similar Q_{max} values because the platelets are essentially deflocculated with fully formed double layers on either side. In this case therefore either polymer has an equal chance of adsorbing onto the clay because all the

surface is available for interaction. XRD data corroborate the adsorption isotherm findings in that both FL17 and Magnafloc 1697 are present in the interlayer of 3xNa-mont at low polymer loadings, equal to 20% of the CEC. Conversely with 3xCs-mont the platelets are more flocculated and therefore some interlayer regions may be difficult to access for bulkier adsorbents. XRD data in fact shows that at low polymer loadings, equivalent to 20% of the CEC, both FL17 and Magnafloc 1697 were excluded from the interlayer of 3xCs-mont whereas at high polymer loadings, equivalent to 100% of the CEC, both polymers were present in the interlayer. At these high polymer loadings, the addition of FL17 to 3xCs-mont results in a large basal spacing of 14.6 Å which indicates that this polymer was present in the interlayer in much larger quantities than Magnafloc 1697 which only showed a basal spacing of 12.6 Å. It is known that FL17 is less bulky than Magnafloc 1697 and consequently it is proposed that size exclusion from a proportion of the interlayer of 3xCs-mont is responsible for the differences observed in the values of Q_{max} and quantity of Cs^+ displaced from the clay. Further evidence in favour of this statement comes from data obtained for the addition of both polymers to 3xK-mont. This type of clay is intermediate between Cs^+ and Na^+ cation exchanged clay in its degree of flocculation and swelling ability which is reflected by the adsorption isotherms and XRD data obtained for the addition of either polymer to the clay. For example Q_{max} for the different cation exchanged clays increases in the order $Cs^+<K^+<Na^+$ upon addition of either polymer to the clay. As stated earlier, the increase in Q_{max} is directly related to the state of aggregation of the clay. More significantly however, XRD data shows that FL17 is present in the interlayer of 3xK-mont at low polymer loadings, 20% of the CEC, whereas Magnafloc 1697 is not. It is probable therefore that a size exclusion mechanism is in operation here which allows FL17 to enter the interlayer of the clay but restricts

Magnafloc 1697 from some areas. This is further evidence that the exchangeable cation associated with the clay determines the quantity of polymer adsorbed.

CHAPTER 7

Investigation into the Interactions Taking Place Between the Neutral Polymer DCP101 and Westone-L.

7. Investigation into the Interactions Taking Place Between the Neutral Polymer DCP101 and Westone-L.

The observed interactions taking place between DCP101 and Westone-L will be recorded and discussed in this chapter.

7.1 Results Obtained Using Several Analysis Techniques to Investigate the Interactions Taking Place Between DCP101 and Westone-L.

Investigation into the interactions taking place between Westone-L and DCP101 required the use of several different analysis techniques including:

The results recorded using each of these analysis techniques are outlined below.

7.1.1 CHN Analysis of Westone-L Contacted With DCP101.

CHN analysis provided carbon values which were used to construct representative adsorption isotherms resulting from the addition of increasing volumes of DCP101 to different exchange forms of Westone-L. The % carbon found in each sample was converted to mg of polyglycol adsorbed per g of clay and recorded in Table 18 below. It is important to remember at this point that all samples which underwent CHN analysis were washed once with deionised water to remove any unadsorbed polymer from the clay.

		Amount of polyglycol adsorbed mg g^{-1}				
% v/v polyglycol offered	polyglycol offered / mg	3xCs-mont	3xCs-mont + 0.025 mol L^{-1} KCl	3xK-mont	3xMn-mont	3xNa-mont
0	0	0	0	0	0	0
0.010	4					7
0.025	10					10
0.10	40	15		35	24	17
0.25	100	17		45	42	37
0.50	200	20	40	64	60	50
1.00	400	22	48	67	69	59
1.50	600	23	49	69	83	66
2.00	800	26	50	77	91	72
2.50	1000	30	52	81	100	79
3.00	1200	40		74	105	83
3.50	1400					92
4.00	1600					84
5.00	2000	42	62	78	115	94
6.00	2400					95
7.00	2800	45	68	84	123	96
10.00	4000	48	70	84	129	103
12.00	4800	47				
15.00	6000	49		85	141	
17.00	6800	51				
20.00	8000	51		97	149	

Table 18. The amount of polyglycol detected on 3xZ-mont for the addition of increasing amounts of DCP101 to clay.

It was noted that clay/DCP101 complexes which were not washed once, did not dry out if the quantity of DCP101 offered exceeded 5% v/v. Consequently the representative adsorption isotherms plotted from CHN data reflect clay/polymer complexes which had all the excess and possibly some weakly bound polymer removed. The adsorption isotherms plotted were for the addition of DCP101 to Cs^+, Na^+, K^+ and Mn^{2+} exchanged montmorillonite, (Figure 56).

The arrow marked 3% polyglycol in Figure 56, represents the quantity of this polymer usually used while drilling for oil in the North Sea. In addition to 3% DCP101, drilling muds usually contain other additives to enhance shale inhibition, the main additive being KCl. The effect of KCl on a selected DCP101 adsorption isotherm was therefore investigated. Figure 56 shows that DCP101 exhibited a low affinity for each form of cation exchanged clay, shown by the difference between the amount adsorbed and the amount in solution. Increasing adsorption occurred on going from $Cs^+<K^+<Na^+<Mn^{2+}$ exchanged montmorillonite. The maximum amount of polymer adsorbed by each cation exchanged clay form in the region of study was 48, 84, 103 and 129 mg g^{-1} respectively. The addition of 0.025 mol L^{-1} KCl to 3xCs-mont increased the maximum adsorption value observed for the addition of DCP101 to this form of cation exchanged clay from 48 to 70 mg g^{-1} clay. This increased adsorption was probably due to the fact that upon addition of KCl to 3xCs-mont, a proportion of the clay exchanged to the K^+ form and consequently resembled more closely the Q_{max} of 84 mg g^{-1} observed for 3xK-mont.

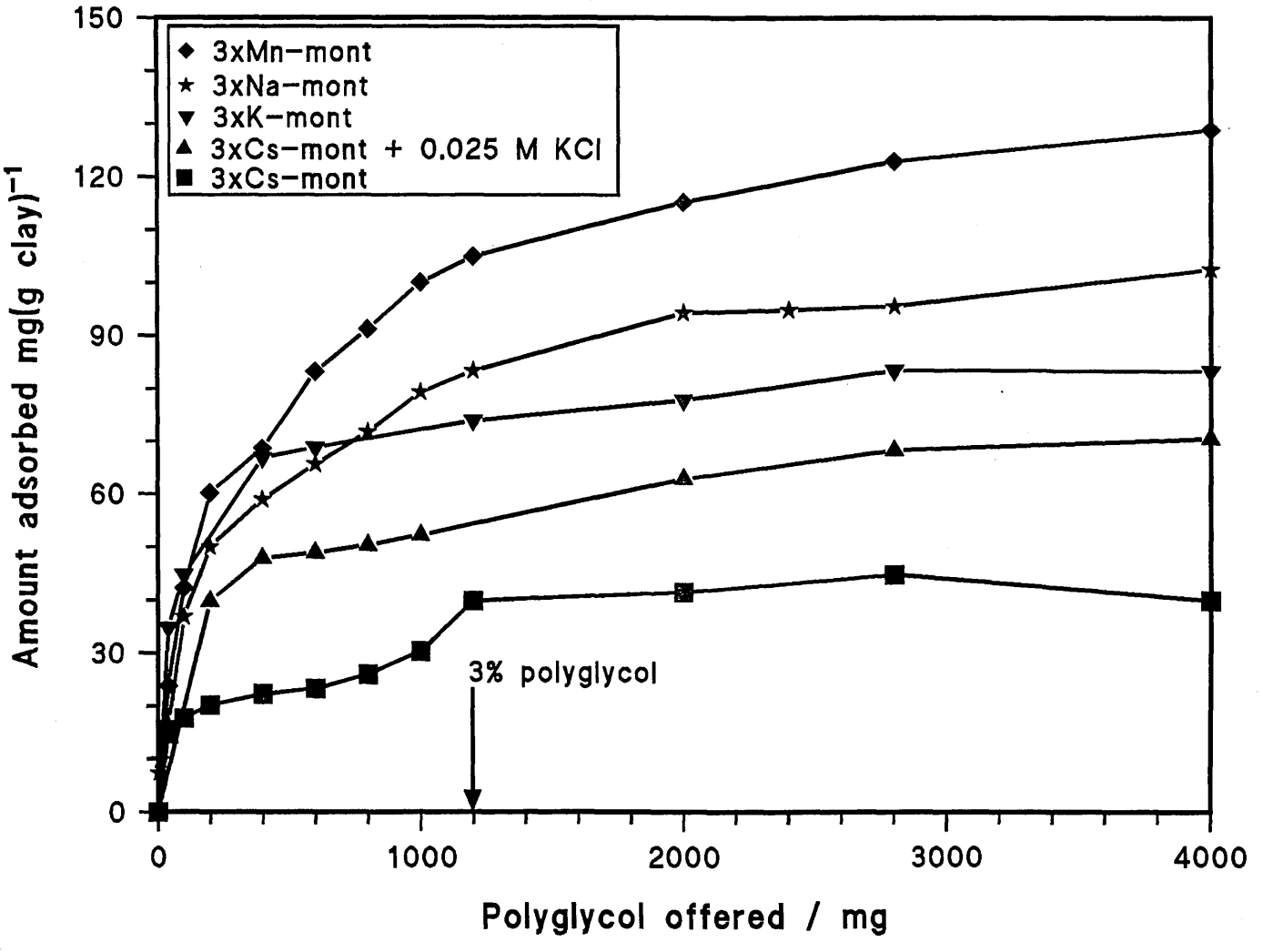

Figure 56. Representative adsorption isotherms for the addition of increasing volumes of DCP101 to different exchange forms of Westone–L.

7.1.2 XRD Analysis of Clay/DCP101 Complexes.

XRD was used to analyse several different cation exchanged clay samples which had been contacted with DCP101 to establish whether or not this neutral polymer was adsorbed exclusively on the surface of the clay or whether some resided between the clay platelets in the interlayer. The presence or absence of polymer in the interlayer may be determined by measuring changes in the d-spacing of the first order basal reflections (d 001 spacing) for each sample, (Table 19). XRD analysis showed that an increase in the first order basal reflection was observed upon addition of 3% DCP101 to all forms of cation exchanged Westone-L. This increase indicated that polyglycol was present between the layers upon drying the clay.

The first order basal spacing observed for 3xNa-mont with no added DCP101 was equal to 13.0 Å at room temperature. Addition of 3% DCP101 to 3xNa-mont resulted in an increase in basal spacing from 13.0 to 18.3 Å at room temperature, (peak **a**, Figure 57). The XRD traces recorded in Figure 57 show five orders of reflection which were maintained up to 150°C, indicating that this system was well ordered. Following thermal treatment at 100°C for 25 minutes, the d-spacing of the 3xNa-mont sample with no added DCP101 collapsed to 10.3 Å due to dehydration whereas the d-spacing observed for the addition of 3% DCP101 to 3xNa-mont remained constant at 18.3 Å. This observed basal spacing is synonymous with the presence of two layers of polyglycol in the interlayer of the clay. Figure 57 shows that the d-spacing of peak **a** remained constant at 18.3 Å until the polyglycol began to denature between 150 to 200°C, this is also illustrated graphically in Figure 59. At 200°C, the collapse in basal spacing to 13.7 Å suggested that approximately one layer of polymer had been lost from the clay, (peak **b**, Figure 57).

	Observed d-spacing for the first order basal reflections Å					
	Ambient	**50°C**	**100°C**	**150°C**	**200°C**	**250°C**
3xCs-mont	12.7	11.8	12.0	10.7	10.3	10.1
+ 0.1% DCP101 (1 wash)	12.9	12.0	11.5	11.5	11.5	11.5
+ 1% DCP101	12.8	12.5	12.3		11.4	
+ 3% DCP101	14.7	14.7	15.3	14.7	11.8	11.6
+ 3% DCP101 (1 wash)	13.4	12.7	12.6	12.5	11.6	11.6
+ 3% DCP101, 0.025 mol L^{-1} KCl	15.8	15.8	15.4	14.5	13.9	11.2
+ 10% DCP101 (1 wash)	13.7	13.3	13.6	13.3		
3xNa-mont	13.0	12.5	10.3	10.3	10.3	10.2
+ 3% DCP101	18.3	18.3	18.3	18.3	13.7	10.1
+ 3% DCP101 (1 wash)	16.3	15.3	18.5 14.3	17.7 14.3	13.5	10.1
+ 3% DCP101, 0.025 mol L^{-1} KCl	18.1	18.1	18.3	14.8	14.2	10.3
3xK-mont	12.1	10.7	10.6	10.5	10.5	10.5
+ 3% DCP101	17.5	17.5	15.1	14.4	13.5	10.5
+ 3% DCP101 (1 wash)	14.6	14.6	14.5	14.2	13.4	10.5
+ 10% DCP101 (1 wash)	14.8	14.7	14.8	14.5	14.2 10.7	10.6
3xMn-mont	15.1	12.8	12.0	10.7	10.3	10.1
+ 1% DCP101	17.7	17.3	17.3	17.5	13.9	13.6
+ 3% DCP101	19.0	18.1	17.9	17.9	13.6	13.5
+ 3% DCP101 (1 wash)	15.1	14.7	17.5 14.3	17.3 14.1	13.7	13.6
+ 3% DCP101, 0.025 mol L^{-1} KCl	18.5	18.5	18.5	15.5	13.9	13.6

Table 19. The first order basal reflections observed for the addition of different amounts of DCP101 to 3xZ-mont.

Thermal treatment at 250°C for 25 minutes resulted in complete collapse of the layers to 10.1 Å, (peak **c**, Figure 57). When 3xNa-mont contacted with 3% DCP101 was washed once to remove excess polymer, the observed basal spacing at room temperature

was 16.3 Å, (peak **a,** Figure 58). The six traces shown in Figure 58 suggested that this washed 3xNa-mont/3% DCP101 system was poorly ordered when compared to the unwashed system with only two weak 001 reflections. The peak associated with this 16.3 Å spacing was broad which indicated a range of spacings. Thermal treatment at 50°C for 25 minutes revealed a poorly resolved shoulder on the low angle side of the peak which was resolved into two clear components upon heating at 100°C, (peak **b**, Figure 58). Peak **b**, the low angle component, had a basal spacing of 18.5 Å which is consistent with two layers of polymer in the interlayer space. The second component of the peak however had a basal spacing of 14.3 Å which is consistent with the presence of only one layer of polymer in the clay interlayer. It is therefore apparent that upon washing the DCP101 treated clay that polymer is displaced from some interlayer regions resulting in the presence of both one and two layers of polymer between the clay platelets. Thermal treatment at 200°C for 25 minutes showed that one broad peak was again observed, indicating a range of spacings. Complete collapse of the d-spacing to 10.1 Å occurred with thermal treatment at 250°C for 25 minutes, (peak **c**, Figure 58).

The d-spacings recorded in Table 19 and illustrated in Figure 59 suggest that a double layer of polymer was also present for the addition of 3% DCP101 to 3xK-mont and 3xMn-mont. The observed d-spacing following addition of 3% DCP101 to 3xK-mont at room temperature decreased from 17.5 to 14.6 Å subsequent to washing the clay/polymer complex once with deionised water. This suggests that polymer was also displaced from the K^+ clay resulting in only one layer of polymer in the interlayer. Only one layer of polymer was detected in the interlayer of the washed clay/polymer complex even when 10% DCP101 was added to 3xK-mont.

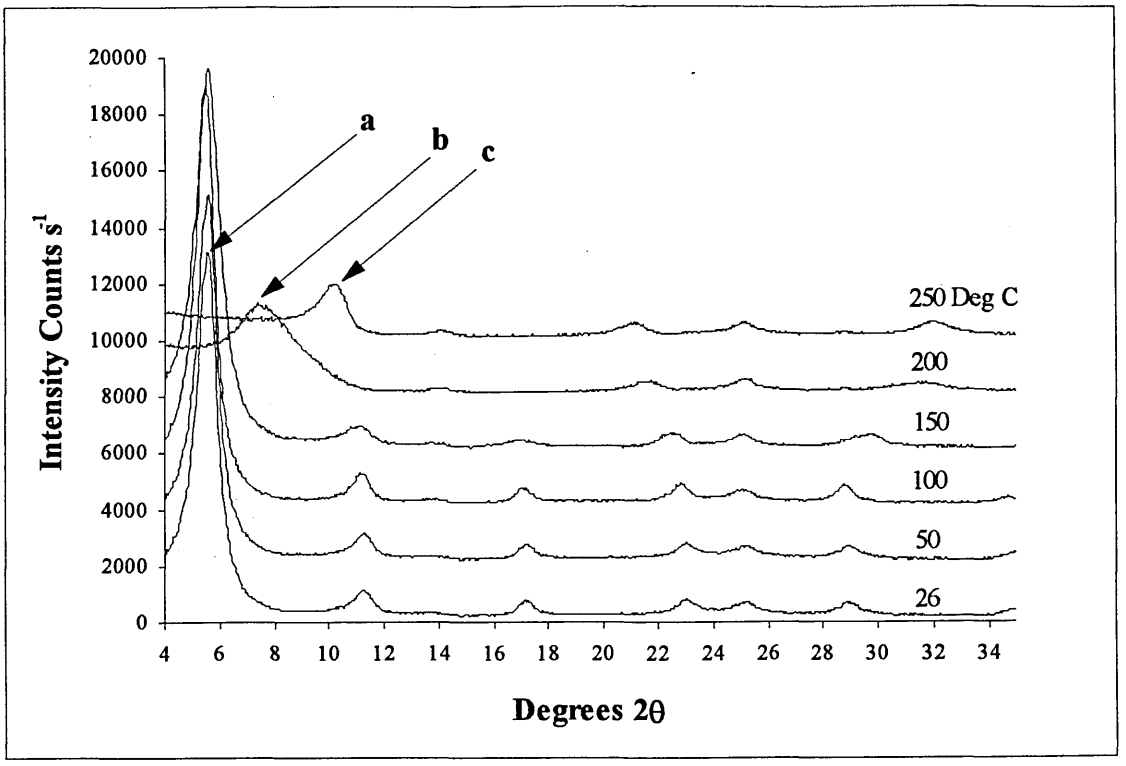

Figure 57. XRD traces showing the change in d 001 spacing with increasing temperature for 3xNa-mont contacted with 3% DCP101. The peaks a, b and c had spacings of 18.3, 13.7 and 10.1 Å respectively.

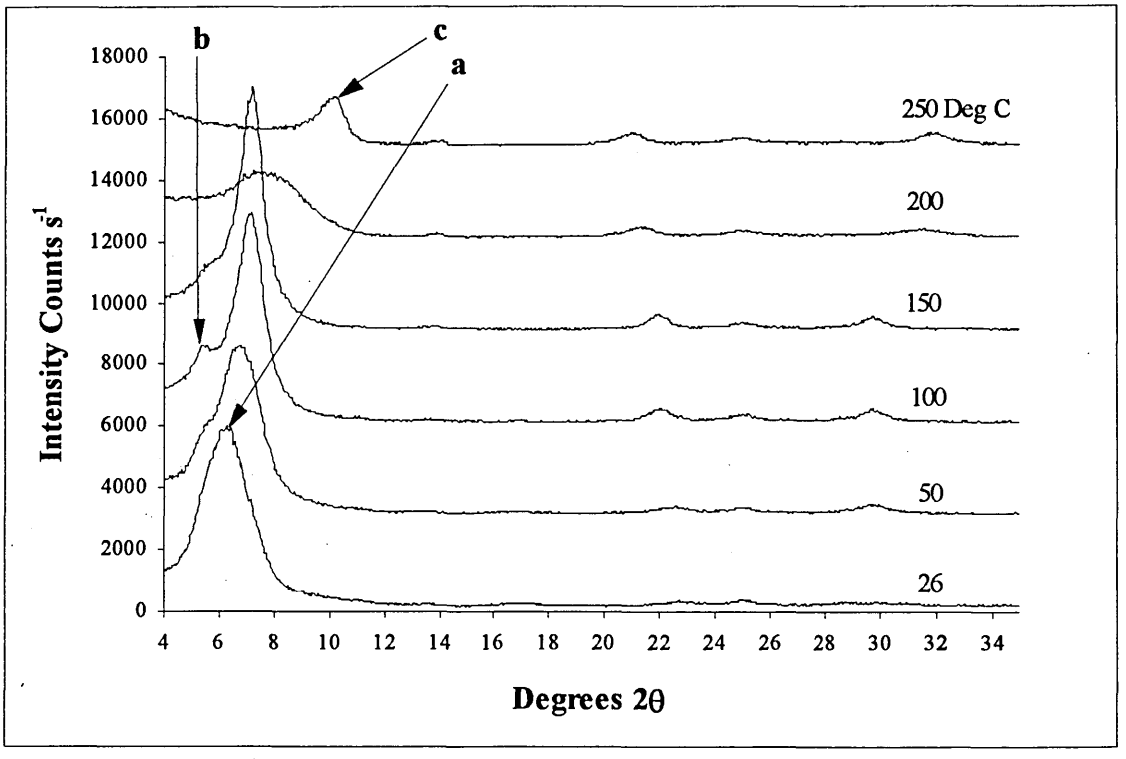

Figure 58. XRD traces showing the change in d-spacing with increasing temperature for 3xNa-mont contacted with 3% DCP101, 1 wash. The peaks a, b and c had spacings of 16.3, 18.5 and 10.1 Å respectively.

The addition of 3% DCP101 to 3xMn-mont caused the observed basal spacing at room temperature to increase to 19.0 Å which is consistent with the presence of a double layer of polymer in the interlayer, (peak **a,** Figure 60). The XRD traces observed for the addition of polyglycol to 3xMn-mont show this system to be the most well ordered of all the DCP101/clay systems studied, indicated by the sharp peaks and smooth lines of the traces. No denaturing of the polymer on 3xMn-mont occurred until the temperature was increased to above 150°C, (Figure 59). In contrast to Na^+ and K^+ exchanged clay, thermal treatment at 250°C for 25 minutes did not cause complete collapse of the clay layers, in fact the minimum basal spacing observed for the addition of either 1 or 3% DCP101 to 3xMn-mont was 13.5 Å, (peak **b**, Figure 60). XRD data for the addition of 3% DCP101 to 3xMn-mont therefore suggests that large quantities of DCP101 adsorb in the interlayer region of 3xMn-mont. Adsorption isotherms for the addition of DCP101 to 3xMn-mont confirm that this exchange form does indeed adsorb larger quantities of DCP101 compared to the other cation exchanged clay forms analysed, (section 7.1.1).

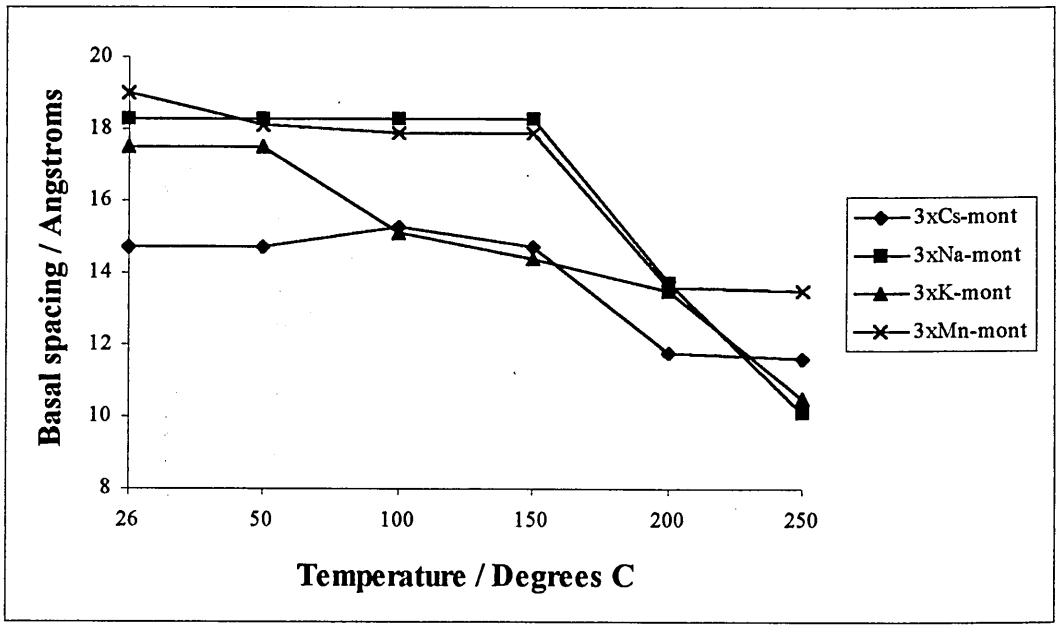

Figure 59. The change in d-spacing with increasing temperature for a series of different cation exchanged clay samples contacted with 3% DCP101, no wash.

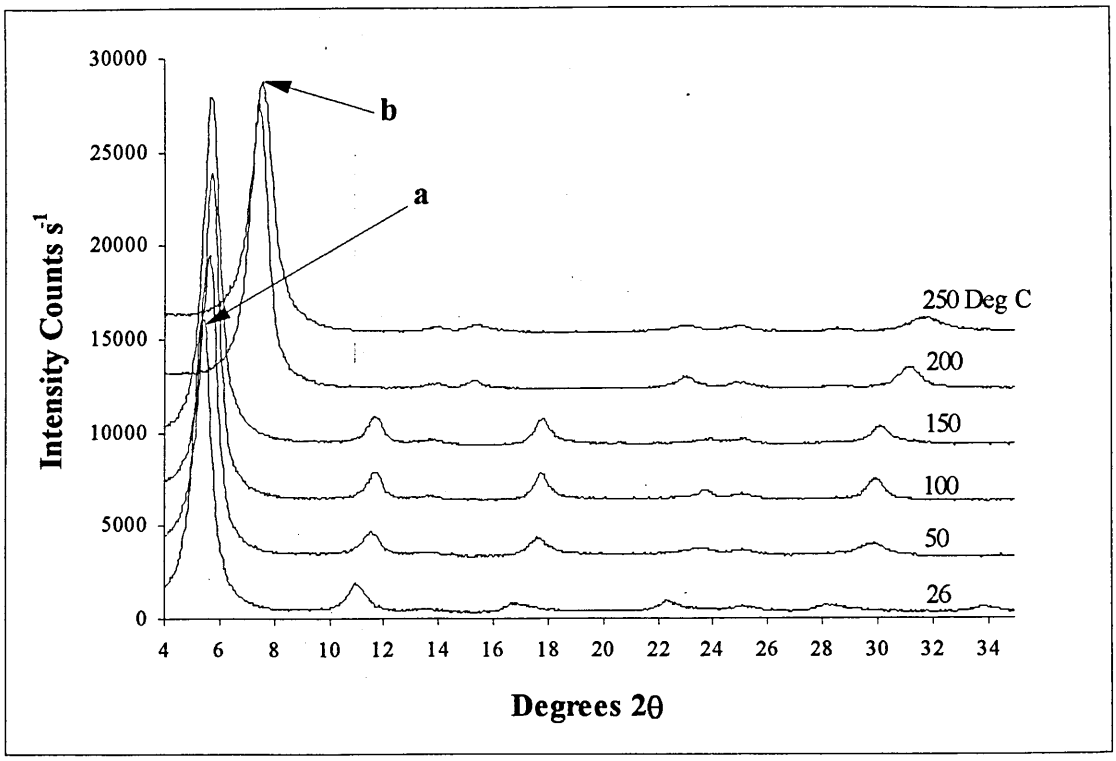

Figure 60. XRD traces showing the change in d 001 spacing with increasing temperature for 3xMn-mont contacted with 3% DCP101. The peaks a and b had spacings of 19.0 and 13.5 Å respectively.

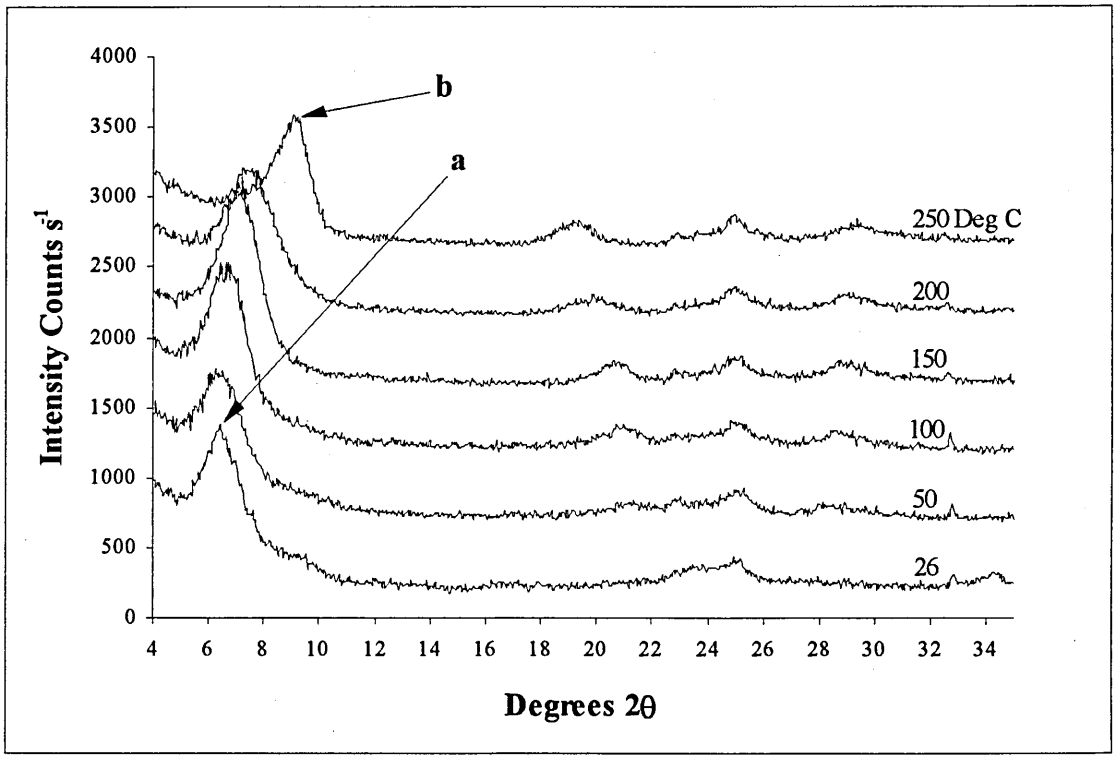

Figure 61. XRD traces showing the change in d 001 spacing with increasing temperature for 3xCs-mont contacted with 3% DCP101 in the presence of 0.025 mol L^{-1} KCl. The peaks a and b had spacings of 15.8 and 11.2 Å respectively.

When 3xMn-mont contacted with 3% DCP101 was washed once to remove excess polymer, the observed basal spacing at room temperature was 15.1 Å. This peak was broad, suggesting a range of basal spacings. Thermal treatment at 100°C revealed a poorly resolved shoulder on the low angle side of the peak with a d-spacing equal to 17.5 Å. This d-spacing is consistent with the presence of two layers of polymer between the platelets. The second component of the peak had a d-spacing equal to 14.3 Å which is consistent with the presence of one layer of polymer between the platelets. Obviously washing the clay removed some of the polymer, resulting in the presence of both one and two layers of polymer between the clay platelets. These results are similar to those recorded for the washed 3xNa-mont/3% DCP101 complex which also showed the presence of both one and two layers of polymer between the clay layers. Thermal treatment of the washed 3xMn-mont/3% DCP101 complex at 200°C for 25 minutes showed that one broad peak was again observed, indicating a range of spacings which were centred around a basal spacing 13.7 Å. Thermal treatment at 250°C for 25 minutes resulted in a basal spacing of 13.6 Å, which was similar to that observed for the unwashed 3xMn-mont/3% DCP101 complex showing that complete collapse of the clay layers did not occur in the range of temperatures investigated in this study.

The XRD trace recorded at room temperature for the addition of 3% DCP101 to 3xCs-mont shows a d-spacing equal to 14.7 Å, (Figure 59). This indicates that only one layer of polymer was present in the interlayer of the clay at these loadings. When 3% DCP101 was added to 3xCs-mont and the resulting clay/polymer complex washed once with deionised water, the observed d-spacing at room temperature decreased to 13.4 Å. The difference in d-spacing between the washed and unwashed samples was further magnified after thermal treatment of both clay/polymer orientated films. Thermal

treatment at 50°C for 25 minutes caused the observed d-spacing of the washed clay/polymer complex to decrease to 12.7 Å. This decreased basal spacing was due to dehydration of the clay and indicated that the 12.7 Å spacing observed after dehydration was due to the presence of only very small quantities of polymer in the interlayer of the washed 3xCs-mont film. The unwashed clay/polymer complex however maintained a d-spacing of around 14.7 Å up to 150°C. Above 150°C, the polymer denatured and the basal spacing collapsed to 11.6 Å, (Figure 59). XRD traces obtained for the addition of 3% DCP101 to 3xCs-mont in the presence of 0.025 mol L^{-1} KCl indicated that this system was extremely disordered, shown by the broad peaks and poor signal to background, (Figure 61). The polyglycol/clay adsorption isotherms recorded in section 7.1.1 show that Q_{max} for the addition of 3% DCP101 to 3xCs-mont increased from 48 to 70 mg g^{-1} upon addition of 0.025 mol L^{-1} KCl to the system. Equally, XRD data showed that the d-spacing observed for the addition of 3% DCP101 to 3xCs-mont increased from 14.7 to 15.8 Å upon addition of 0.025 mol L^{-1} KCl to the system, (peak **a**, Figure 61). This increased basal spacing again suggested that more DCP101 became associated with 3xCs-mont in the presence of added KCl. Thermal treatment at 250°C for 25 minutes caused the d-spacing of this orientated film to collapsed to 11.2 Å, (peak **b**, Figure 61).

7.1.3 TG Analysis of Westone-L Contacted With DCP101.

These analyses were carried out in order to corroborate results obtained by CHN analysis and to establish the stability of the clay/polymer complexes formed which has already been briefly addressed by using variable temperature XRD. Several Cs^{+} exchanged clay samples which had been contacted with increasing amounts of the neutral polymer DCP101 were analysed by TG, some of which had 0.025 mol L^{-1} KCl added to

see what effect addition of this salt had on the results obtained. KCl was added to selected samples because it is used as an additive in drilling muds containing DCP101.

Figure 62 illustrates the TG traces observed for the addition of increasing volumes of DCP101 to 3xCs-mont. The relatively sharp peak centred at a temperature of 90°C was due to interlayer water associated with the clay. All of the interlayer water was lost from the clay at temperatures approaching 150°C. As the amount of DCP101 added to the clay was increased, the intensity of the peak observed at 275°C increased. This peak was therefore due to the polyglycol which obviously desorbed from the clay at the aforementioned temperature. The DCP101 appears to break down more easily in oxygen than nitrogen, shown by the difference in break down temperatures between the TGA and the XRD results. The broad peak observed at 620°C was due to the loss of structural hydroxyl groups from the clay. Figure 63 illustrates the TG traces obtained for the addition of increasing volumes of DCP101 to 3xCs-mont in the presence of 0.025 mol L^{-1} KCl. Here again, the peak centred at 90°C was due to interlayer water. An increase in intensity was observed for the peak at 280°C as the amount of DCP101 added to the clay was increased. This peak was again therefore due to the polyglycol which obviously desorbed from the clay at this temperature. Finally the broad peak observed at about 625°C was again due to the loss of structural hydroxyl groups from the clay.

Table 20 shows the TGA results obtained for the addition of DCP101 to Cs exchanged Westone-L in the presence and absence of 0.025 mol L^{-1} KCl. The sample weights before and after purging with dry N were noted and the weight difference between them recorded in order to gain some idea of the quantity of physisorbed water associated with the clay.

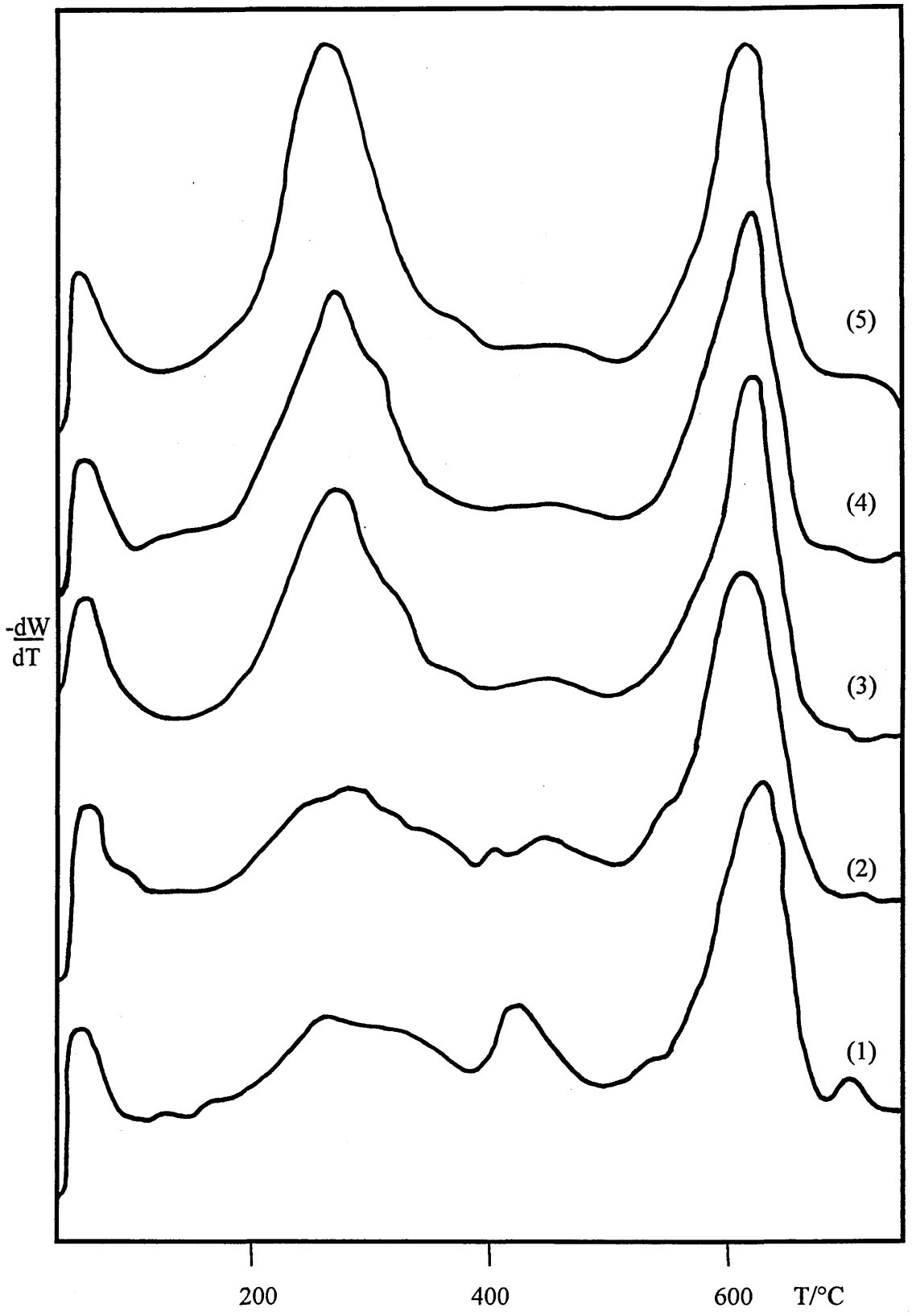

Figure 62. TG traces recorded for the addition of increasing volumes of DCP101 to 3xCs-mont. The numbered traces (1)-(5) relate to the % of polyglycol offered to the clay which was equal to 0.5, 1, 3, 5 and 20% v/v respectively.

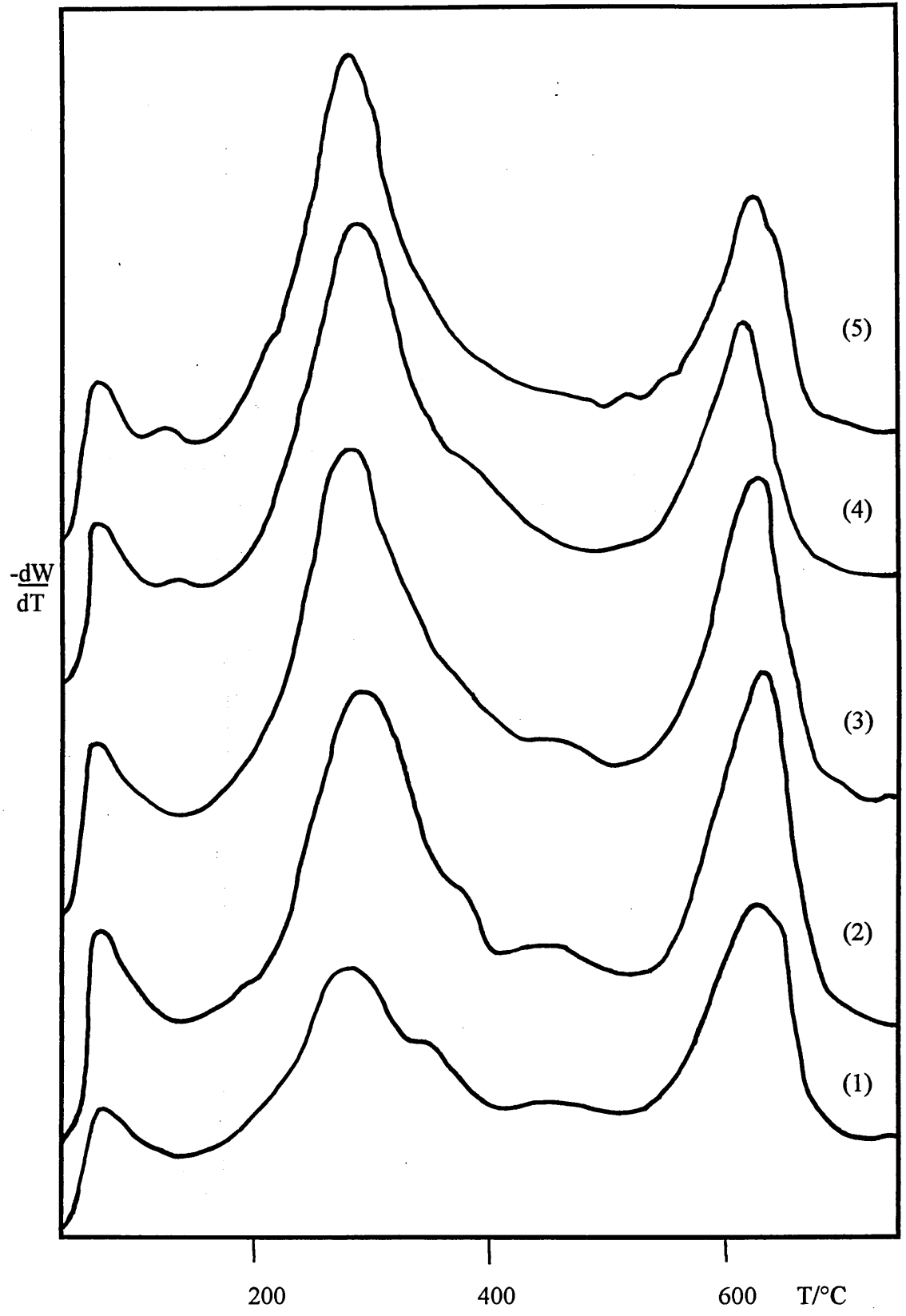

Figure 63. TG traces recorded for the addition of increasing volumes of DCP101 to 3xCs-mont in the presence of 0.025 mol L^{-1} KCl. The numbered traces (1)-(5) relate to the % of polyglycol offered to the clay which was equal 0.5, 1, 2, 5 and 10 % v/v respectively.

Significantly at low polyglycol loadings, < 2.5%, the quantity of physisorbed water associated with the 3xCs-mont /DCP101 complexes was low, shown by the small weight difference, (Table 20). Above a DCP101 loading of 3% on 3xCs-mont, the weight difference increased significantly suggesting that at these higher loadings, a greater proportion of physisorbed water was associated with the clay. The weight differences recorded for the addition of increasing amounts of DCP101 to 3xCs-mont in the presence of 0.025 mol L^{-1} KCl were all small even at high loadings of polyglycol. This again suggests that the quantity of physisorbed water associated with these systems was low or indeed that the water was strongly held in the presence of polyglycol, and therefore did not desorb from the clay in the nitrogen stream. This second scenario is however less likely.

% v/v Polyglycol offered	Wt before purging / g	Wt after purging / g	Difference / g	% Wt loss from 160 - 520°C
0.10	7.946	7.877	0.069	3.26
0.25	9.249	9.175	0.074	3.44
0.50	6.765	6.696	0.069	4.12
1.00	7.324	7.262	0.062	3.75
1.50	7.873	7.799	0.074	4.90
2.50	7.620	7.558	0.062	5.10
3.00	8.915	8.721	0.194	5.14
5.00	8.430	8.269	0.161	5.00
20.0	8.352	8.133	0.219	6.52
0.50 + 0.025 mol L^{-1} KCl	9.890	9.823	0.067	5.39
1.00 + 0.025 mol L^{-1} KCl	9.177	9.092	0.085	5.55
2.00 + 0.025 mol L^{-1} KCl	8.817	8.740	0.077	6.72
5.00 + 0.025 mol L^{-1} KCl	8.120	8.012	0.108	7.86
10.0 + 0.025 mol L^{-1} KCl	8.440	8.378	0.062	8.48

Table 20. TG data recorded for the addition of increasing amounts of DCP101 to 3xCs-mont in the presence and absence of 0.025 mol L^{-1} KCl.

The percentage weight losses recorded in Table 20 for the region 160 - 520°C were entirely due to loss of polyglycol from the clay. As the amount of polyglycol added to 3xCs-mont was increased, the percentage polymer weight loss from the clay also

increased as would be expected. The percentage polyglycol weight loss from samples of 3xCs-mont contacted with DCP101 was small when compared to the weight loss of the corresponding clay/polymer complex in the presence of 0.025 mol L^{-1} KCl. This suggested that more polyglycol was adsorbed onto 3xCs-mont in the presence of KCl which was shown to be true by the adsorption isotherms illustrated in section 7.1.1.

Figure 64 shows the amount of DCP101 adsorbed on 3xCs-mont as determined by CHN analysis versus the % weight loss from 160 - 520°C as determined by TGA. Both the line depicting 3xCs-mont contacted with 3% DCP101 and the line depicting 3xCs-mont contacted with 3% DCP101 in the presence of 0.025 mol L^{-1} KCl are not straight. Consequently, TGA % weight loss results may only be used as a rough indication as to the quantity of DCP101 adsorbed upon clay.

TG data was also recorded for unwashed samples of Cs^+, K^+, Na^+, and Mn^{2+} exchanged montmorillonite contacted with 3% DCP101. These samples were investigated to gain some indication about which type of cation exchanged clay adsorbed the largest amount of DCP101 in the absence of washing. The % weight losses shown in Table 21 indicate that the amount of DCP101 adsorbed onto clay increases in the order $Cs^+ < K^+ < Na^+ < Mn^{2+}$ for unwashed clay samples.

Sample	Wt before purging / g	Wt after purging / g	Difference / g	% Wt loss from 160 - 520°C
3xCs-mont + 3% DCP101 (no wash)	9.830	9.679	0.151	9.26
3xK-mont + 3% DCP101 (no wash)	9.200	9.045	0.155	11.81
3xNa-mont + 3% DCP101 (no wash)	9.168	9.018	0.150	14.77
3xMn-mont + 3% DCP101 (no wash)	9.615	9.366	0.249	18.00

Table 21. TGA % weight losses observed for a series of different cation exchanged clay samples contacted with 3% DCP101, no wash.

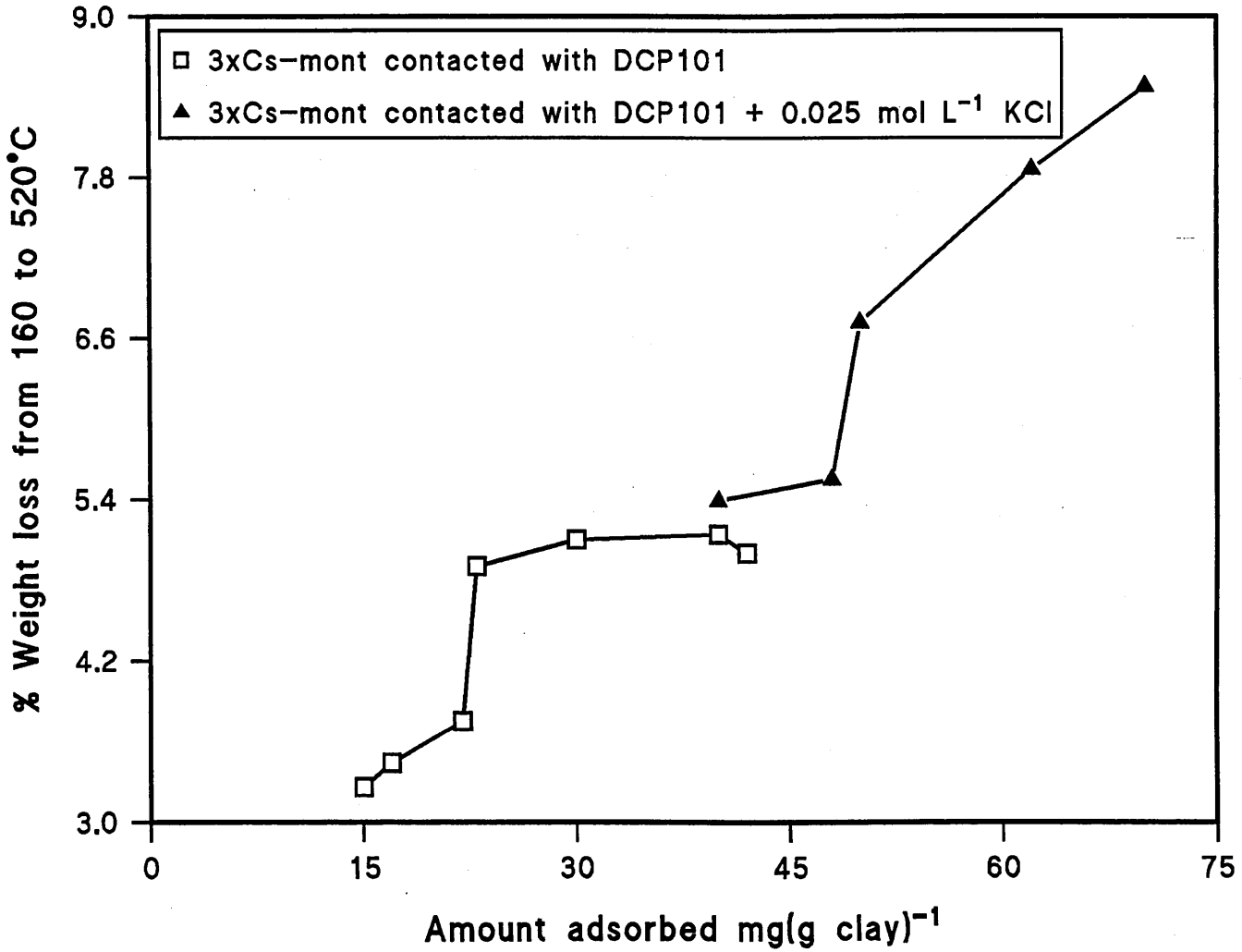

Figure 64. Amount of DCP101 adsorbed versus the % weight loss

Table 21 also shows that the % weight loss between 160 - 520°C for an unwashed 3xCs-mont/3% DCP101 complex was equal to 9.26% which was almost double the 5.14% observed for the same complex which had been washed. This suggests that a quantity of DCP101 is lost from 3xCs-mont upon washing the complex once with deionised water. The differences in weight, before and after purging with N, for Cs^+, K^+ and Na^+ exchanged clay contacted with 3% DCP101 were very similar with a value of about 0.150 g. Conversely, 3xMn-mont had a weight difference of 0.249 g indicating that this clay/polymer complex had more physisorbed water associated with it.

7.1.4 The Use of NMR Spectroscopy to Investigate the Interactions Occurring Between Westone-L and DCP101.

7.1.4.1 ^{133}Cs NMR.

In the North Sea when drilling an oil well through water sensitive strata, such as shale, the drilling mud used nominally contains 3% DCP101 along with other additives such as KCl to enhance shale inhibition. Experiments have therefore been carried out to investigate the interactions taking place between 3xCs-mont and DCP101 in the presence and absence of KCl. The results from three separate series of experiments are shown below.

A. Samples were made up consisting of 3xCs-mont and increasing volumes of DCP101. Each sample was then analysed by ^{133}Cs NMR, the concentration of Cs^+ detected along with the peak linewidth were measured for each sample and recorded in Table 22. Table 22 in fact shows that the addition of increasing aliquots of DCP101 to

3xCs-mont had little effect on the linewidth and concentration of Cs^+ detected. DCP101 alone therefore displaces only a negligible quantity of Cs^+ from 3xCs-mont.

Sample	Linewidth / Hz	Cs^+ / mol L^{-1}
3xCs-mont	1500	4.0×10^{-3}
3xCs-mont + 2.5% v/v DCP101	1203	5.5×10^{-3}
3xCs-mont + 5.0% v/v DCP101	1162	5.2×10^{-3}
3xCs-mont + 7.5% v/v DCP101	1119	5.3×10^{-3}
3xCs-mont + 10.0% v/v DCP101	1265	5.5×10^{-3}

Table 22. ^{133}Cs NMR results showing the change in linewidth and quantity of Cs^+ detected upon addition of increasing volumes of DCP101 to 3xCs-mont.

B. Experiments were then carried out where a range of 3xCs-mont samples containing increasing aliquots of FL15 and a constant 3% v/v quantity of DCP101 were made up and analysed by ^{133}Cs NMR. It has already been shown in section 6.1.5.2.2 that the FL series of polymers have a strong affinity for the surface of clay, shown by the ease with which they displaced the exchangeable cations. Consequently, if there was a strong interaction occurring between Cs^+ and DCP101 at the clay surface, this should be revealed by changes in the usual plots obtained for ^{133}Cs linewidth and concentration of Cs^+ detected upon addition of FL15 to 3xCs-mont, (Figure 45 and Figure 46, section 6.1.5.2.2). Any differences in these plots will therefore indicate that the interaction of FL15 with 3xCs-mont had been modified in some way by the presence of DCP101, (Table 23).

% DCP101 added v/v	N^+ mol L^{-1} added from polymer	Linewidth of ^{133}Cs peak / Hz	Cs^+ / mol L^{-1}
3.0	9.59×10^{-4}	1232	6.1×10^{-3}
3.0	1.44×10^{-3}	762	6.3×10^{-3}
3.0	1.92×10^{-3}	641	6.4×10^{-3}
3.0	2.88×10^{-3}	190	6.8×10^{-3}
3.0	4.80×10^{-3}	120	7.7×10^{-3}
3.0	6.71×10^{-3}	82	9.0×10^{-3}
3.0	9.60×10^{-3}	48	1.2×10^{-2}
3.0	1.44×10^{-2}	27	1.6×10^{-2}
3.0	1.92×10^{-2}	15	1.7×10^{-2}
3.0	2.88×10^{-2}	15	1.8×10^{-2}
3.0	3.84×10^{-2}	15	1.8×10^{-2}

Table 23. ^{133}Cs NMR results showing the change in linewidth and quantity of Cs^+ detected upon addition of increasing amounts of FL15 to 3xCs-mont samples containing 3% DCP101.

Two graphs were then plotted,

1. N / mol L^{-1} versus ^{133}Cs linewidth, (Figure 65)

2. N / mol L^{-1} versus Cs^+ / mol L^{-1}, (Figure 66)

Figure 65 and Figure 66 include the curves obtained for the addition of FL15 alone to 3xCs-mont, recorded in section 6.1.5.2.2.

Figure 65 shows that the same minimum ^{133}Cs linewidth was reached irrespective of whether DCP101 was present in the clay/polymer dispersion medium. This suggested that the same amount of Cs^+ was displaced from the FL15/3xCs-mont complex whether DCP101 was present in the dispersion medium or not. Figure 66 shows that this was not the case because when 3% DCP101 was present in the dispersion medium, only 1.8×10^{-2} mol L^{-1} of Cs^+ were detected by NMR. This is approximately 0.2×10^{-2} mol L^{-1} of Cs^+ less than was seen when only FL15 was added to 3xCs-mont.

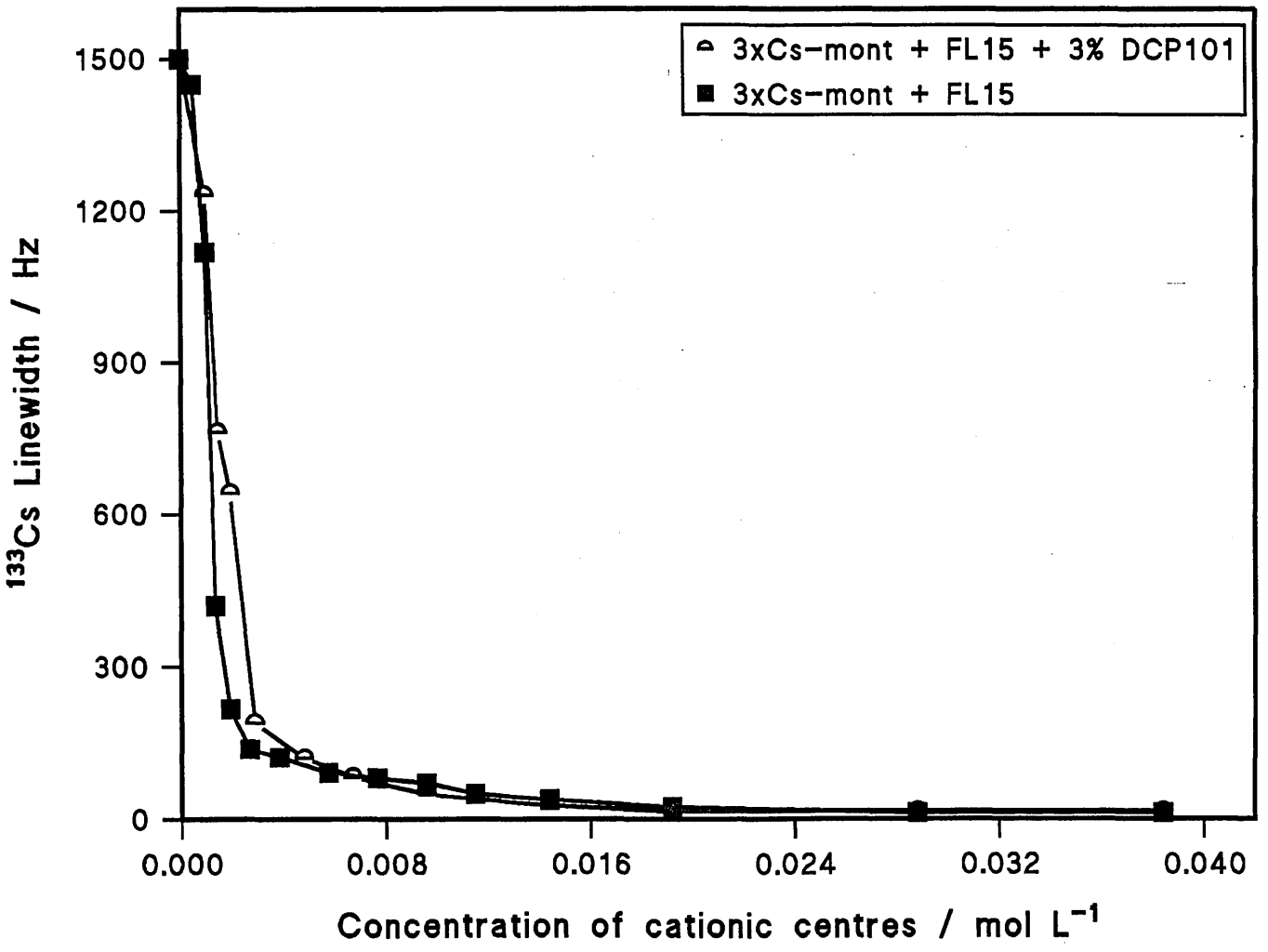

Figure 65. Decrease in ^{133}Cs linewidth upon addition of increasing amounts of FL15 to 3xCs–mont in the presence and absence of 3% DCP101.

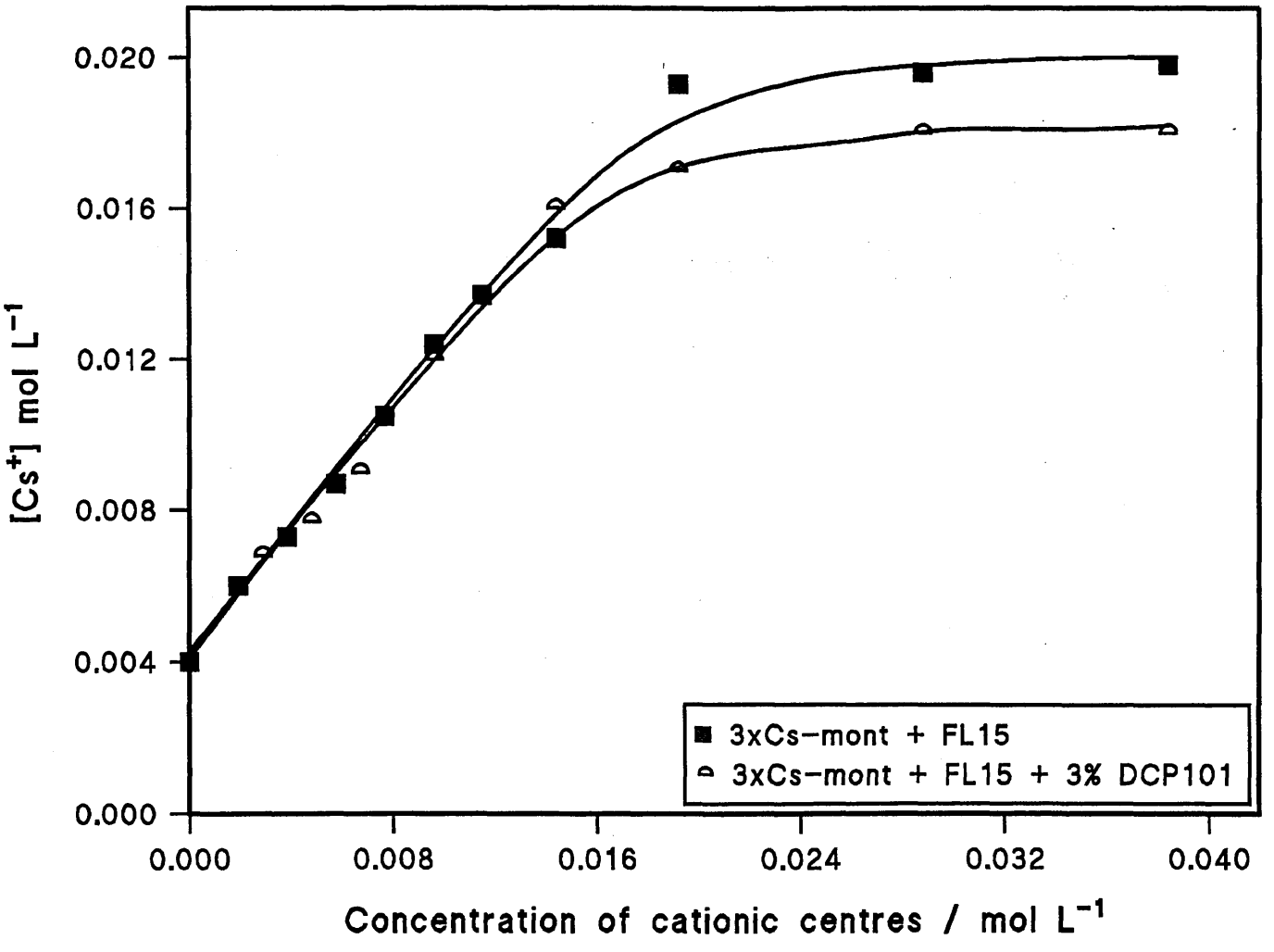

Figure 66. Increase in the observed [Cs^+] upon addition of increasing amounts of FL15 to 3xCs-mont, with and without 3% DCP101 added.

In addition when the same samples were analysed again in the presence of 5% DCP101 in each sample, a plateau was again reached however this time only 1.6×10^{-2} mol L^{-1} of Cs^+ were seen by NMR. Therefore, increasing the quantity of added DCP101 seemed to decrease the ability of FL15 to interact as strongly with the exchangeable cations associated with the clay and as a result, less Cs^+ was displaced.

C. Further experiments were carried out where a range of 3xCs-mont samples containing increasing aliquots of KCl and a fixed quantity of DCP101 were prepared and analysed by ^{133}Cs NMR. For comparison, a further set of baseline samples was also analysed which contained 3xCs-mont plus increasing aliquots of KCl, no DCP101 was however added to these samples. The ^{133}Cs NMR spectra were then recorded for each sample and the quantity of Cs^+ detected by NMR tabulated, (Table 24).

	Cs^+ / mol L^{-1}		
Mol L^{-1} KCl added to 3xCs-mont.	**No DCP101 added.**	**1% DCP101 added.**	**10% DCP101 added.**
8.0×10^{-3}	5.6×10^{-3}	8.1×10^{-3}	7.6×10^{-3}
3.0×10^{-2}	7.0×10^{-3}	8.9×10^{-3}	8.4×10^{-3}
5.0×10^{-2}	7.8×10^{-3}	8.8×10^{-3}	8.9×10^{-3}
7.0×10^{-2}	7.9×10^{-3}	9.8×10^{-3}	9.1×10^{-3}
1.0×10^{-1}	8.6×10^{-3}	1.1×10^{-2}	9.4×10^{-3}
1.5×10^{-1}	8.9×10^{-3}	1.1×10^{-2}	1.0×10^{-2}

Table 24. The quantity of Cs^+ detected by NMR after addition of DCP101 and/or KCl to 3xCs-mont.

Figure 67 shows that upon addition of 0.15 mol L^{-1} of K^+ to 3xCs-mont, 0.009 mol L^{-1} of Cs^+ were detected by NMR. This is double the quantity of Cs^+ detected for a sample of 3xCs-mont with no added KCl, showing that the K^+ displaced a significant

quantity of the exchangeable Cs^+ from the clay. Figure 67 also shows that the maximum amount of KCl added to the clay was far in excess of the CEC and was also far greater than the maximum quantity of KCl added to 3xCs-mont in the polycation study, (section 6.1.5.2.2). Samples analysed containing both K^+ and a fixed aliquot of DCP101 whether 1% or 10% all showed that more Cs^+ was displaced from the clay compared to the addition of K^+ alone. More Cs^+ was however displaced from 3xCs-mont when 1%, rather than 10% DCP101 was added to the clay in the presence of KCl. It is possible that this phenomenon may be due to flocculation of the clay at higher DCP101 loadings which consequently prevents easy displacement of the Cs^+ associated with the clay.

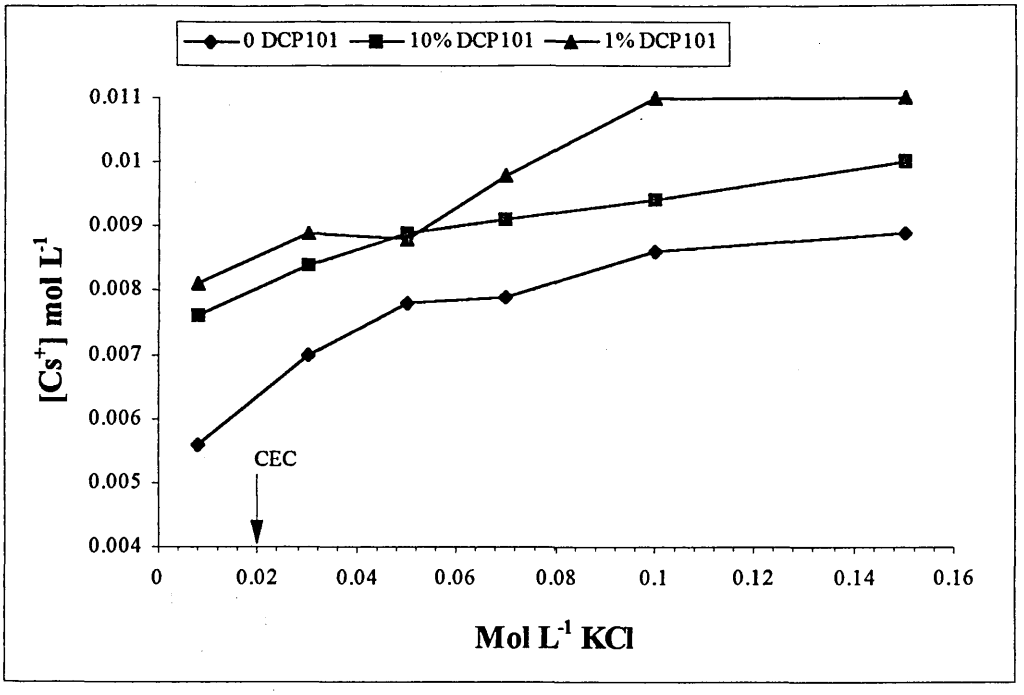

Figure 67. Change in quantity of Cs^+ seen by NMR upon increasing the amount of KCl added to 3xCs-mont in the presence and absence of DCP101.

7.1.4.2 ^{1}H NMR of the Water Peak Associated With 3xMn-mont.

^{1}H NMR spectra were recorded for a series of 3xMn-mont clay samples spanning a concentration range from 0.6 to 23 gL^{-1} and the results recorded below, (Table 25). A graph was then plotted of 3xMn-mont clay concentration versus the ^{1}H linewidth, (Figure 68).

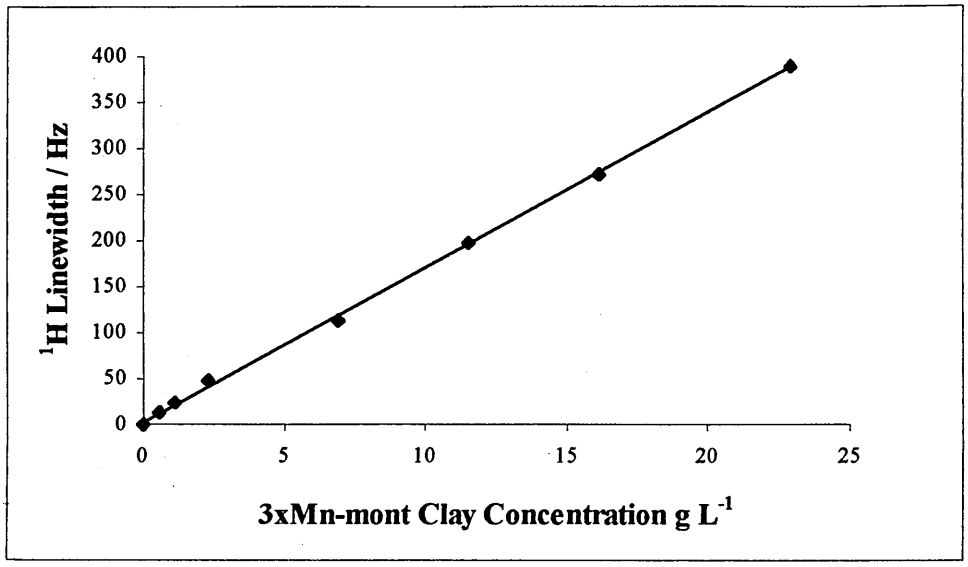

Figure 68. The change in ^{1}H linewidth with increasing 3xMn-mont clay concentration.

The graph shows that the linewidth of the ^{1}H signal from the water protons increases linearly as the concentration of manganese clay in suspension increased. The increased linewidth reflects the proportion of water molecules which are found in the hydration shell surrounding the Mn^{2+} cation. The ^{1}H nuclei in these water molecules relax rapidly due to their proximity to the paramagnetic cation and as a result very broad ^{1}H NMR spectra were observed. Conversely protons associated with water molecules in the bulk solution relax much more slowly and therefore show considerably narrower ^{1}H

spectra. An average of the two water environments will therefore be seen in the ^1H NMR spectra.

A set of 3xMn-mont samples spanning the same clay concentration range outlined above were then made up. To each of these samples however was added 0.001% v/v 1,2-diaminoethane. This molecule was chosen for addition to 3xMn-mont because it was suspected that it would displace water from the Mn^{2+} hydration shell and therefore a decrease in the gradient of the line should be observed if the method was valid. Only a low concentration of this molecule was added to 3xMn-mont because addition of higher concentrations caused severe flocculation. The ^1H NMR spectra were then recorded for each sample and the results shown below, (Table 25).

	Observed ^1H NMR linewidth / Hz	
3xMn-mont clay concentration / gL^{-1}	**3xMn-mont**	**3xMn-mont + 0.001% v/v 1,2-diaminoethane**
0.6	13	11
1.2	24	14
2.3	48	18
4.6	75	32
11.5	198	120
16.1	272	166
23.0	390	287

Table 25. ^1H NMR linewidth observed for increasing concentrations of 3xMn-mont with and without the addition of 1,2-diaminoethane.

A graph was then plotted showing the observed ^1H NMR linewidth versus the 3xMn-mont clay concentration, (Figure 69). Figure 69 shows a decrease in the gradient of the line obtained for the addition of aliquots of 0.001% v/v 1,2 diaminoethane to a range of 3xMn-mont clay samples spanning the same concentration range as described previously. The decrease in the gradient of the line reflects a decrease in the water peak

linewidth which suggests that some water molecules have been displaced from the Mn^{2+} hydration shell into the bulk solution.

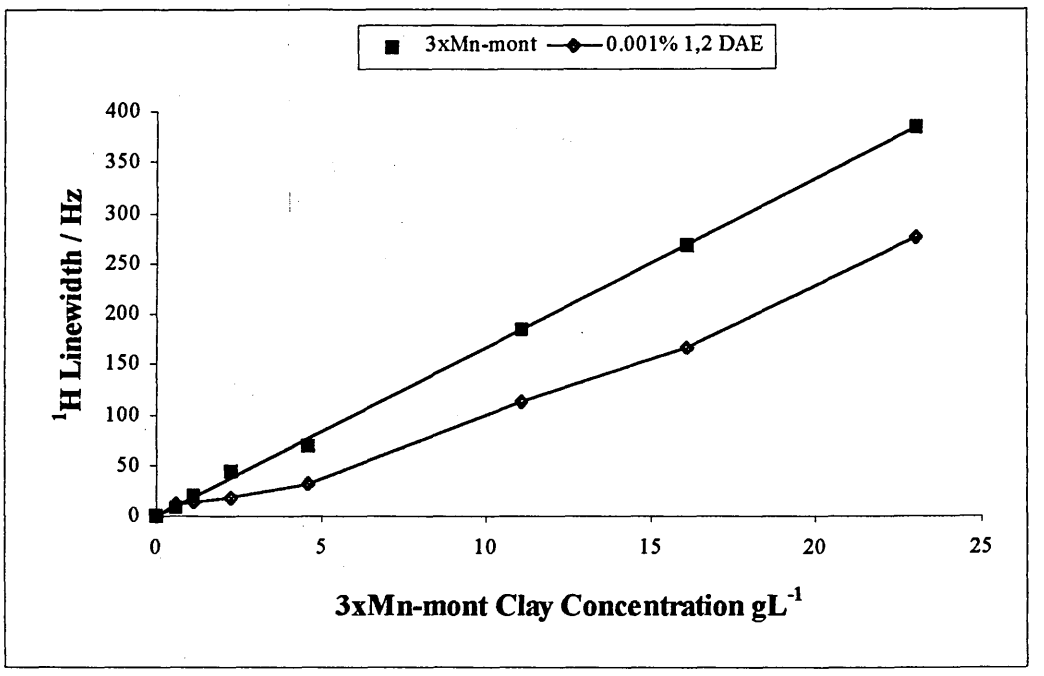

Figure 69. The change in the observed ^{1}H NMR linewidth following the addition of 1,2-diaminoethane (1,2 DAE) to 3xMn-mont, also shown is the linewidth curve for 3xMn-mont without added 1,2 DAE.

Three series of samples were then made up spanning the same 3xMn-mont clay concentration range outlined above. This time however, to each sample in a series was added a fixed quantity of DCP101 with values equal to either 0.1, 2.0 or 10%. ^{1}H NMR spectra were then recorded for each sample and the results tabulated, (Table 26).

3xMn-mont clay concentration / gL^{-1}	Linewidth after addition of 0.1% DCP101 / Hz	Linewidth after addition of 2.0% DCP101 / Hz	Linewidth after addition of 10% DCP101 / Hz
0.6	18	15	15
1.2	21	17	19
2.3	39	38	36
6.9	126	140	140
11.5	185	199	206
16.1	240	262	271
23.0	340	382	412

Table 26. The change in ^{1}H linewidth for the addition of differing amounts of DCP101 to 3xMn-mont.

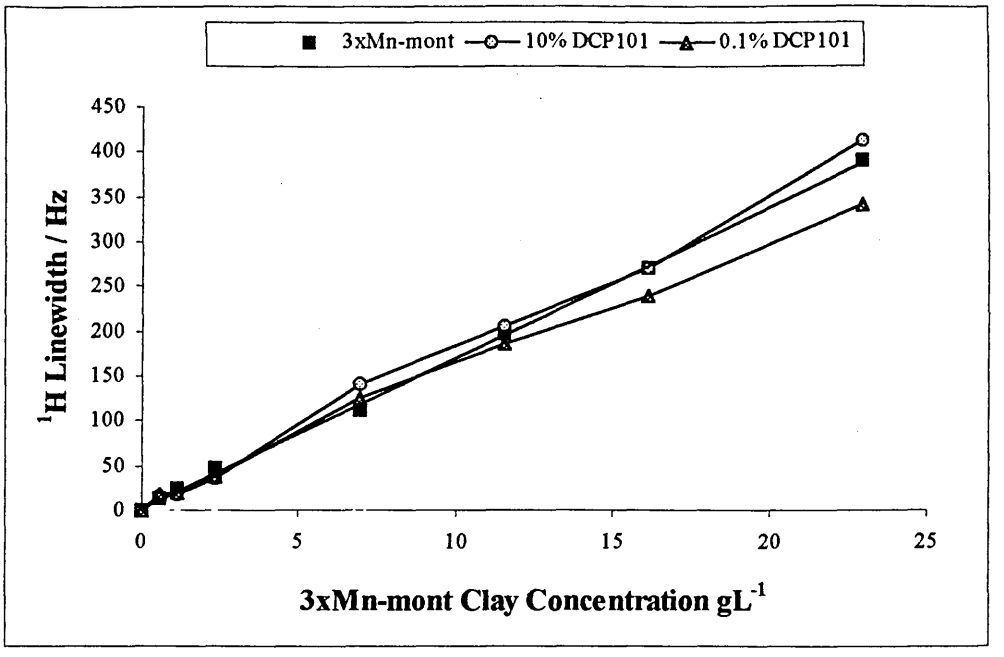

Figure 70. The change in ^{1}H linewidth upon addition of 10 and 0.1% v/v DCP101 to a range of differing concentrations of 3xMn-mont. Also shown is the change in ^{1}H linewidth for increasing concentrations of 3xMn-mont with no added DCP101.

Figure 70 shows that the gradient of the curves obtained for the addition of 0.1 and 10% DCP101 to 3xMn-mont were almost identical to that obtained for differing concentrations of 3xMn-mont alone. This indicated that addition of 0.1 and 10% DCP101 to 3xMn-mont had very little effect on the ^{1}H NMR linewidth and consequently the water molecules in the Mn^{2+} hydration shell must remain largely undisturbed.

Figure 71 shows the affect that addition of a fixed quantity of DCP101 or 1,2 DAE to increasing concentrations of 3xMn-mont had on the observed ^{1}H NMR linewidth. Any deviation of a curve from the x axis, indicated the difference between the ^{1}H NMR linewidths observed for increasing concentrations of 3xMn-mont and the linewidths observed for the same 3xMn-mont concentrations with added DCP101 or 1,2 DAE. The curve relating to the addition of 1,2 DAE to 3xMn-mont showed a steep departure from the x axis to increasingly negative values, indicating that water molecules

were displaced from the Mn^{2+} hydration shell into the bulk solution, as was suggested earlier. Conversely, when 0.1, 2 and 10% DCP101 were offered to 3xMn-mont, none of the resulting curves showed a large deviation from the x axis upon increasing the clay concentration, again suggesting that the water molecules in the Mn^{2+} hydration shell remained largely undisturbed.

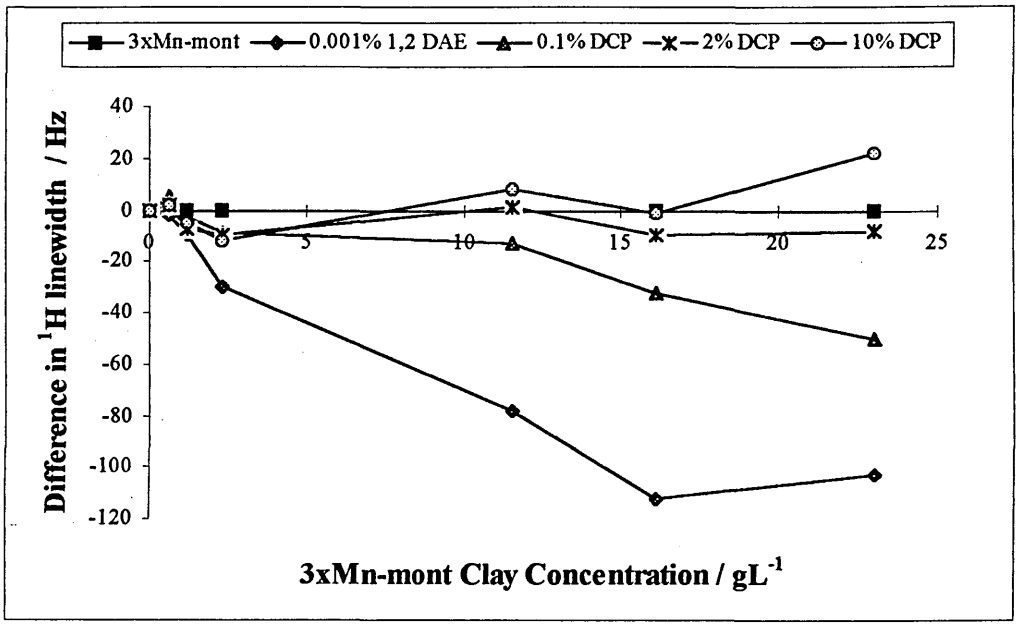

Figure 71. The difference between the ^{1}H NMR linewidths observed for increasing concentrations of 3xMn-mont and the linewidths observed for the same 3xMn-mont clay concentrations in the presence of added DCP101 or 1,2 DAE.

7.2 Discussion Concerning the Interactions Taking Place Between DCP101 and Westone-L.

The use of WBM containing polyglycol additives is a relatively new development in drilling fluid technology brought about by the need to replace the environmentally unacceptable OBM, (Chapter 1). Polyglycols are added to WBM because they have been shown to possess excellent shale inhibitive properties whilst drilling through reactive shale strata.[12] These water soluble compounds are typically used at low concentrations of around 3% by weight however concentrations up to 10% have sometimes been used. The mechanism by which polyglycols effect shale inhibition is as yet not fully understood. Several theories have however been proposed, the more popular of which are outlined below:

1. Some researchers state that the cloud point behaviour of polyglycols is the central feature of their inhibition mechanism.[148] They propose that insoluble polyglycol droplets, which form when the temperature of the mud rises above the cloud point, plug the pores of the newly exposed clay surface thereby preventing ingress of water. This theory may be valid in some cases however it does not explain why polyglycols with no cloud point also posses shale inhibitive properties or why those polyglycols which have cloud points are also effective below the critical temperature.[149]

2. It is well known that water molecules interact with the clay surface by forming hydrogen bonds with the silicate oxygens.[109,150] Water molecules may also interact with the exchangeable cations associated with the clay surface.[109,151] A water structure is therefore built up around the clay platelets or tactoids as each subsequent water layer hydrogen bonds to the water layer ahead of it. A more plausible theory therefore is that polyglycols compete with water molecules for adsorption sites on the clay surface and in

doing so interfere with the hydrogen bonding between the surface of the clay and water.[12,149,152] Once adsorbed the polyglycol molecules could then prevent water molecules from forming the organised structures which eventually lead to swelling and dispersion of the clay. All research carried out in this area has concluded that the presence of added salt, especially KCl, in polyglycol drilling fluids is critical for enhanced shale inhibition.[149,152]

The extensive research carried out in this study into the interactions of polyglycol (DCP101), with Westone-L will now be discussed in detail in an attempt to gain some understanding as to the mechanism of polyglycol shale inhibition. With the addition of increasing amounts of DCP101 to different cation exchanged forms of Westone-L, the amount of polymer adsorbed increased, (Figure 56). It should be remembered at this point that all the clay samples used to produce the adsorption isotherms were washed once to remove excess DCP101 before being analysed by CHN analysis. All clay/DCP101 samples were washed once because at DCP101 loadings > 5%, the resulting clay/polymer complexes would not dry. This point has been made because Parfitt and Greenland,[33] found that more than 80% of PEG with a molecular weight of 300 could be removed from Ca montmorillonite by repeated washing with deionised water. Only 15% was however desorbed by washing the clay once with deionised water. Conversely they also noted that PEG with a molecular weight of 2000 could not be desorbed from the same clay by washing with distilled water. DCP101 however has a molecular weight of 600 and therefore it is not unreasonable to suspect with this intermediate case that some weakly adsorbed polymer may be displaced from the clay upon washing. XRD and TGA data recorded in this study actually indicated that some DCP101 is displaced from the clay upon washing, this will be discussed in more detail later. Figure 56 shows that the cation exchange form of the clay played a significant role

in determining the value of Q_{max}. Increasing adsorption occurred on going from $Cs^+<K^+<Na^+<Mn^{2+}$ exchanged montmorillonites, where Q_{max} equalled 48, 84, 103 and 129 mg g^{-1} respectively. A similar exchangeable cation dependence upon addition of PEG was noted by Parfitt and Greenland,[33] who observed an increase in Q_{max} on changing from a Ca^{2+} exchanged clay to a Na^+ exchanged one.

These changes in the value of Q_{max} upon changing the cation associated with the clay are most likely due to the state of aggregation of the platelets. For example, it is well known that cation type can greatly effect the swelling behaviour of clay minerals in water.[153,154] It stands to reason therefore that the clay with cations associated to it which cause the greatest swelling of the platelets will therefore adsorb the largest amounts of DCP101. Quirk,[155] has in fact shown that the swelling of various cation exchange forms of clay in dilute suspension follows the order:

$$\mathbf{Li^+ \approx Na^+ > Ca^{2+} \approx Mg^{2+} > K^+ > Cs^+}$$

This theory fits the data recorded in this study in that Q_{max} increased in the order $Cs^+<K^+<Na^+<Mn^{2+}$, similar to the increase in swelling order recorded by Quirk.[155] In a related study Levy *et al.*,[156] indicated that increased adsorption of the neutral polymer polyvinylpyrrolidone, was taking place when exchangeable cations known to cause increased swelling of the platelets were exchanged with the clay.

As stated previously, salt is usually added to DCP101 drilling fluids because it is known that they do not generally perform well in the absence of it. KCl and CsCl have proven to be the two best types of salt at promoting shale inhibition properties of DCP101 although KCl is generally used due to the toxicity problems thought to be associated with CsCl.[168] The role of K^+ in the shale inhibition mechanism is not yet fully understood although its effectiveness more than likely has something to do with the low

hydration energy of this cation and indeed the Cs^+ cation with respect to the exchangeable cations usually found in naturally occurring clay. With the addition of 0.025 mol L^{-1} KCl to a 25 gL^{-1} suspension of 3xCs-mont containing DCP101, the value of Q_{max} increased dramatically from 48 to 70 mg g^{-1}, (Figure 56). It is suggested that the low concentration of salt added in this study is not sufficient to cause excessive aggregation and therefore the expected decrease in Q_{max} was not observed. It is quite probable however that the initially Cs^+ exchanged clay may have become a mixture of both Cs^+ and K^+ exchanged upon addition of KCl to the dispersion medium. This would obviously result in an intermediate Q_{max} value between that observed for 3xCs-mont and 3xK-mont, which was in fact the case. These results again indicate that the exchangeable cation associated with the clay plays a large role in determining the value of Q_{max}.

In a recent study, Cliffe *et al.*[149] noted that large quantities of polyglycol were adsorbed from distilled water on to a less than 2 μm fraction of Wyoming bentonite. The bentonite used was in its natural exchange form with Ca^{2+} and Na^+ counterions. With their experiments, Q_{max} was equal to approximately 1200 mg g^{-1} clay, far in excess of the Q_{max} values recorded in this study for any form of cation exchanged clay. This increased polyglycol uptake probably occurred because both the methods they used to determine adsorption data did not require the clay/polyglycol complex to be washed free of excess polymer before adsorption data could be measured. As mentioned earlier, washing the clay to remove any unadsorbed polyglycol, also removes some weakly bound polyglycol which in this study resulted in low Q_{max} values. The two methods Cliffe *et al.*[149] used to record adsorption isotherm data are outlined below. The first made use of air-dried clay films which were immersed in the test polyglycol solution, the amount of adsorbed polyglycol was then measured directly by recording the FTIR spectra of the

clay/polyglycol film. Considering the results obtained in this thesis, it is probable that the clay/polyglycol films included a good quantity of undried polymer, therefore resulting in the high Q_{max} values observed. The second method involved the addition of polyglycol to a 20 gL^{-1} suspension of the clay which was then allowed to equilibrate for several hours. A sample of clear supernatant was then taken after centrifugation and analysed for polyglycol content by gel permeation. It is quite possible that the centrifugation step employed in this method may include a low density centrifugate which traps a quantity of unadsorbed polyglycol, resulting in high adsorption values. Both methods were in agreement as to the value of Q_{max} for addition of polyglycol from distilled water. When 1.0 mol L^{-1} KCl was added however, method 2 indicated that 3 times more polyglycol was adsorbed than was detected by method 1. Both methods however show that less polyglycol was adsorbed when KCl was added to the clay/polyglycol suspension. This decrease in Q_{max} is probably due to platelet aggregation and a decrease in the swelling ability of the clay which obviously occurs when exchanging from a mixed Ca^{2+}/Na^{+} exchanged clay to a predominantly K^{+} exchanged form. This is in agreement with the results obtained in this study in that addition of 0.025 mol L^{-1} KCl to a 3xCs-mont/polyglycol suspension, caused an increase in the value of Q_{max}. As stated earlier, addition of KCl probably caused the Cs^{+} clay to partially exchange to the K^{+} form, thus allowing slightly more swelling of the clay which lead to increased adsorption.

The representative XRD traces support the preceding interpretations regarding the quantity of polymer adsorbed by the different cation exchanged montmorillonites. This was apparent because on contacting the different cation exchanged clays with 3% DCP101, the d-spacing increased in the order $Cs^{+}<K^{+}<Na^{+}\approx Mn^{2+}$ for unwashed samples. The same order of increasing basal spacing, suggesting increasing polymer adsorption,

was also observed for identical samples which like all the isotherm samples had been washed once to remove excess polymer.

A basal spacing of only 14.7 Å was observed for the addition of 3% DCP101 to 3xCs-mont, this corresponds to one layer of polymer in the interlayer of the clay. This was deduced because in related studies involving the addition of ethylene glycol to several cation exchanged clays, a similar d-spacing was observed which was shown to be due to adsorption of a single layer of ethylene glycol.[157,158] Upon washing this sample, the d-spacing decreased to about 12.7 Å, a value which the complex retains even with thermal treatment for 25 minutes at 150°C, (Figure 61). This observed d-spacing at raised temperatures is therefore not simply due to the hydration state of the clay and therefore a small quantity of polyglycol must remain between the clay sheets even after the clay had been washed once.

With the addition of 3% DCP101 to K^+ Na^+ or Mn^{2+} exchanged montmorillonite, the unwashed clay/polymer complexes formed show a d-spacing representative of two layers of polyglycol resident in the interlayer of the clay. This was surmised because several authors observed similar basal spacings for the addition of ethylene glycol, a related molecule, to the same cation exchanged clays. [159,160,161] These authors have stated that the observed basal spacings relate to the adsorption of a bilayer of ethylene glycol. Upon washing these clay/polymer complexes once with deionised water, the d-spacings recorded for all three samples indicated that some polymer had been lost from the interlayer. The basal spacing recorded for the 3xK-mont/3% DCP101 complex in fact collapsed from 17.5 Å to 14.6 Å after washing the clay once. The observed basal spacing of 14.6 Å is again representative of one layer of polyglycol between the clay layers.

The basal spacing recorded for the 3xNa-mont/3% DCP101 complex also showed a decrease in spacing upon washing once with deionised water, (Figure 57 and Figure 58). This time however the spacing decreased from 18.3 Å to 16.3 Å. Thermal treatment at 100°C for 25 minutes however showed that the broad peak at 16.3 Å was in fact a composite peak. Thermal treatment obviously caused weakly bound DCP101 to desorb from the clay revealing two peaks with basal spacings of 14.3 and 18.5 Å. These peaks corresponded to the presence of 1 and 2 layers of polyglycol between the sheets respectively, (peaks **a** and **b**, Figure 58). Cliffe *et al.*[149] also noted the presence of two peaks upon addition of 0.2% polyglycol to Wyoming bentonite in the Ca^{2+} and Na^{+} exchanged form. At these low polyglycol loadings, the major peak observed occurred at 14 Å. This peak however had a shoulder on the higher spacing side, suggesting the presence of material with a higher basal spacing. When they added greater quantities of polyglycol, the 14 Å peak disappeared and was replaced by a peak at approximately 17.5 Å. As in this study, the peak at higher basal spacing remained stable upon further polyglycol additions. Cliffe *et al.*[149] also interpret the 14 Å and 17.5 Å complexes as clay platelets separated by one and two layers of flat lying polyglycol molecules respectively. These results tie in nicely with data outlined above for the washed 3xNa-mont/3% DCP101 complex.

Finally the d-spacing recorded for the 3xMn-mont/3% DCP101 complex again showed a decrease in spacing upon washing once with deionised water. The room temperature d-spacing of the unwashed complex was however the largest of all the clay/DCP101 complexes recorded having a value of 19 Å which decreased to 15.1 Å upon washing. Thermal treatment at 100°C for 25 minutes of the washed 3xMn-mont/3% DCP101 complex caused some weakly bound DCP101 to desorb from the clay

revealing a peak with a basal spacing of 14.3 Å which had a shoulder on its lower angle side with a basal spacing of 17.5 Å. These results are similar to those observed for the washed 3xNa-mont/3% DCP101 complex in that at raised temperatures, two different d-spacings were recorded corresponding to the presence of 1 and 2 layers of polyglycol between the layers respectively. The two peaks were however better resolved in the washed 3xNa-mont/3% DCP101 complex.

Thermal treatment at 200°C for 25 minutes of all the unwashed clay/3% DCP101 complexes resulted in the loss of one layer of polymer from the clay. Thus the Na^+, K^+ and Mn^{2+} exchanged clays with d-spacings around 13.6 Å, all had approximately one layer of polymer remaining at this elevated temperature, (Figure 59). The Cs^+ exchanged clay on the other hand had a basal spacing of 11.8 Å, suggesting that no DCP101 resided in the interlayer of the clay at this temperature. One peculiar result however was the fact that the d spacing of the 3xK-mont/3% DCP101 complex decreased prematurely from 17.5 Å to 15.1 Å upon thermal treatment at 100°C for 25 minutes. Thermal treatment at 250°C for 25 minutes caused the second layer of polymer to be lost from the K^+ and Na^+ exchanged clays. Conversely the Mn^{2+} exchanged clay retained approximately one layer of polymer at this elevated temperature, again suggesting that this clay adsorbed greater quantities of DCP101, (Figure 59). The basal spacings observed for the addition of 3% DCP101 to 3xCs-mont were seen to increase from 14.7 to 15.8 Å in the presence of 0.025 mol L^{-1} KCl, (Table 19). This further supports the evidence from the adsorption isotherm, Figure 56, which showed that the presence of KCl resulted in an increase in Q_{max}. The bilayer of polymer observed for the addition of 3% DCP101 to 3xMn-mont and 3xNa-mont becomes less thermally stable when 0.025 mol L^{-1} KCl was added to each clay/polymer complex. For example thermal treatment at 150°C for 25 minutes of

both these clay/polymer complexes resulted in collapse of the basal spacing to values consistent with one layer of polymer. As stated above, when there was no KCl present in the system, the bilayer of polymer collapsed to a single layer upon thermal treatment at 200°C. Along with the evidence from the 3xK-mont/3% DCP 101 complex, this suggests that the presence of K^+ in clay/DCP101 complexes, destabilises the bilayer of polymer resulting in its premature collapse to a single layer upon thermal treatment. Cliffe *et al.*[149] also noted a similar phenomenon, they state that when K^+ is present in a clay/polyglycol system, the 17.5 Å bilayer complex does not form readily. Several related studies have also indicated that K^+ exchanged smectites behave differently from other cation exchanged clays when contacted with ethylene glycol.[162,163] These studies have indicated that K^+ smectites with a high net layer charge form 14 Å monolayer complexes with ethylene glycol. Obviously the K^+ cation and indeed the Cs^+ cation, have some as yet unknown effect on polyglycol adsorption which leads to the preference of monolayer adsorption. Aston *et al.*[152] have in fact shown that the shale inhibition properties of polyglycols depend heavily upon the type of salt present in the drilling fluid and not upon the amount of polyglycol adsorbed.

Representative TG traces support the preceding data obtained from the adsorption isotherm and x-ray diffraction studies concerning the clay/polyglycol complexes. This was expected since relevant TG samples were prepared in the same way as the isotherm and relevant XRD samples. As stated earlier this involved washing the clay once to remove unadsorbed polyglycol. The TGA results show that a steady increase in the % weight loss of polyglycol occurred between 160 - 520°C for the addition of increasing amounts of polyglycol to 3xCs-mont. This is consistent with the adsorption isotherm data in that an increase in the quantity of polyglycol added to 3xCs-

mont resulted in an increase in the proportion of polyglycol detected. Further, TG evidence shows that addition of 0.025 mol L^{-1} KCl to selected 3xCs-mont/DCP101 samples caused the % weight loss between 160 - 520°C to increase, suggesting that more polymer was adsorbed onto the clay in the presence of KCl. Again this is in agreement with the adsorption isotherm obtained from similar samples. As stated earlier, this increased polyglycol uptake in the presence of KCl is thought to be because the initially Cs^+ exchanged clay partially exchanges to the K^+ form which was found to have an increased capacity for polyglycol adsorption.

The weight difference between when the sample was first introduced into the stream of nitrogen in the TG oven and when the sample weight became constant, was also recorded. The time taken for the weight to become constant, before analysis could begin, usually took about twenty minutes. This weight difference was seen as a rough indication as to the amount of physisorbed water associated with the clay. Interestingly, it appears that the quantity of physisorbed water increases as the amount of polyglycol added to the clay increases, (Table 20). The presence of K^+ ions in the sample seems to reduce the amount of physisorbed water at these higher polyglycol loadings, shown by the reduced weight difference, (Table 20). This could possibly be one reason why the presence of K^+ in drilling fluids has such an effect upon the shale inhibition properties of polyglycol. Obviously from this data it is impossible to determine conclusively whether or not the above is true and as such, no firm conclusions can be drawn.

Four clay/DCP101 complexes were prepared which were not washed free of excess DCP101 before TG analysis. The four samples were Cs^+, K^+, Na^+ and Mn^{2+} exchanged montmorillonite contacted with 3% DCP101. The recorded weight losses between 160 - 520°C for the four samples indicate that the amount of DCP101 adsorbed

onto the clay increased in the following order $Cs^+<K^+<Na^+<Mn^{2+}$. This order of increasing DCP101 adsorption on the different cation exchanged clays is in agreement with adsorption isotherm data recorded for the same clay/DCP101 complexes which had been washed once. The % weight loss between 160 - 520°C for an unwashed 3xCs-mont/3% DCP101 complex was equal to 9.26% which is almost double the 5.14% observed for the same clay/polymer complex which had been washed. Obviously some of the adsorbed DCP101 is lost from the clay by washing with deionised water, which as mentioned previously was also indicated by the XRD results. Apart from the removal of weakly bound DCP101 from the clay upon washing, one probable reason why the % weight loss recorded for the unwashed 3xCs-mont/3% DCP101 sample is so much higher than that recorded for the washed version is because a proportion of unadsorbed DCP101 may become trapped by the clay sample during centrifugation. The large % weight losses shown in Table 21 however suggest that if the clay is not washed, large Q_{max} values may be recorded as Cliffe *et al.*[149] observed. The differences in the weight before and after purging with N for the unwashed Cs^+, K^+, and Na^+ exchanged clay samples contacted with 3% DCP101 were very similar with a value of about 0.150 g. Conversely, 3xMn-mont had a weight difference of 0.249 g indicating that this clay/polymer complex had more physisorbed water associated with it.

As was expected, the isotherm, XRD and TGA data did not provide information concerning the mechanism of adsorption of polyglycols on clay. These analyses did however provide quantitative data and gave some insight as to the location of adsorbed polymer on the clay. It is likely that the information gained by these techniques may not be wholly representative of the situation occurring in aqueous suspensions like drilling fluids. Consequently it was anticipated that the use of ^{133}Cs and ^1H NMR in conjunction

with the previously mentioned techniques would provide an insight in to the mechanism by which polyglycols adsorb onto clay in aqueous suspension.

Initially ^{133}Cs NMR experiments were undertaken which were similar to those carried out for the addition of cationic polymer to 3xCs-mont, (section 6.1.5). These experiments were used to show what effect, if any, the addition of DCP101 to 3xCs-mont had on the exchangeable cations associated with the clay. Table 22 shows that upon addition of increasing amounts of DCP101 to 3xCs-mont, the observed ^{133}Cs NMR linewidth and integral did not change significantly, even upon addition of up to 10% v/v DCP101. Using the previously explained cationic polymer work as a model, (section 6.1.5), it is evident from this data that the addition of polyglycol to clay does not cause a significant quantity of the exchangeable cation to be displaced, at least in the case of Cs^+ exchanged clay. The fact that the Cs^+ exchanged ions remain largely undisturbed upon addition of DCP101 to 3xCs-mont is not unexpected when considering that this polymer is neutral.

Laboratory tests show that Cs^+ cations are comparable to K^+ cations at enhancing the shale inhibition properties of DCP101 drilling fluids.[152] This indicates that the Cs^+ cation will be a good substitute for K^+, which due to its lack of NMR sensitivity cannot be utilised in the following NMR study. Experiments were therefore performed to determine whether or not there was a strong Cs^+/DCP101 interaction at the clay surface. These experiments were carried out by adding increasing amounts of FL15, one of the cationic polymers previously studied, to 3xCs-mont suspensions treated with 3% DCP101. Obviously if there was any form of Cs^+/DCP101 interaction at the clay surface, the ^{133}Cs linewidth and concentration of Cs^+ detected by ^{133}Cs NMR values would be dissimilar to those previously observed for the addition of cationic polymer alone to

3xCs-mont, (section 6.1.5). In fact the observed ^{133}Cs linewidth data were very similar to results obtained when FL15 was added to 3xCs-mont alone. Conversely, Cs^+ concentration data indicated that 0.2 x 10^{-2} mol L^{-1} less Cs^+ were detected at FL15 loadings ≥ the CEC of the clay. Further, when FL15 was added to 3xCs-mont systems containing 5% DCP101, the quantity of Cs^+ detected by NMR was reduced by a further 0.2 x 10^{-2} mol L^{-1} upon addition of FL15 loadings ≥ the CEC of the clay. It is therefore possible that some Cs^+/DCP101 interaction is taking place at the clay surface which prevents the cationic FL15 displacing the Cs^+ with the same ease as was previously observed when there was no added DCP101. It is also not unreasonable to suggest that flocculation of the clay upon polyglycol addition may be causing the reduction in Cs^+ detected.

One further set of experiments were carried out using ^{133}Cs NMR where increasing aliquots of KCl were added to 3xCs-mont samples containing a fixed quantity of DCP101. The ^{133}Cs-NMR integrals observed from each sample were then recorded. These experiments were carried out in an attempt to monitor the effects of extraneous K^+ ions on the exchangeable Cs^+ ions in the presence of a fixed quantity of DCP101. These experiments were considered important because whilst drilling an oil well, large quantities of KCl are added to the drilling fluids to enhance shale stabilisation. Consequently, it is reasonable to expect that the clay exposed at the drill hole wall will exchange to the K^+ form. It is possible that the presence of polyglycol may enhance this exchange process therefore promoting shale inhibition.

Figure 67 shows that upon addition of 0.15 mol L^{-1} KCl to 3xCs-mont, 0.9 x 10^{-2} mol L^{-1} of Cs^+ were detected by ^{133}Cs NMR. Interestingly the addition of DCP101 to the clay suspension caused the amount of Cs^+ that was detected by NMR to increase. In fact

with the addition of 1% DCP101 and 0.015 mol L^{-1} of K^+ to 3xCs-mont, 1.1 x 10^{-2} mol L^{-1} of Cs^+ were detected by ^{133}Cs NMR. Strangely, the amount of Cs^+ detected by NMR decreased to 1.0 x 10^{-2} mol L^{-1} when 10% DCP101 was added to 3xCs-mont along with 0.15 mol L^{-1} KCl. This decrease may be caused by flocculation of the platelets at these higher polyglycol loadings which therefore restricts access to some of the clay's surface. It appears therefore that the presence of DCP101 in the 3xCs-mont suspensions causes the K^+ ion to become more effective at replacing the Cs^+ cation associated with the clay.

In general the adsorption of neutral polymers onto the surface of clay proceeds as a direct result of the entropy gained by the desorption of numerous water molecules.[33,34,35] It is not unreasonable to expect therefore that the neutral polymer DCP101 also adsorbs onto clay by an entropy driven process involving the desorption of numerous water molecules. Cliffe *et al.*[149] have actually shown by infrared measurements that water is displaced from clay films as polyglycol is taken up. Several authors state that it is precisely because of this desorption of water upon polyglycol adsorption that contributes to the excellent shale inhibition properties of this polymer.[149,152] These authors have also stated that DCP101 may compete with the water of hydration around the adsorbed cations associated with the clay. The effect of polyglycol addition on these water molecules have therefore been investigated using ^1H NMR. Mn^{2+} exchanged clay was utilised in these studies since this cation is paramagnetic and as such an NMR investigation of the water molecules in its hydration shell will result in unusually broad ^1H peaks. This consequently provides a handle with which to study the addition of polyglycol to the system. The unusually broad peaks occur because the protons in the water molecules associated with the cation's hydration shell are able to relax rapidly due to their proximity to the Mn^{2+} cation. Figure 68 shows that as the 3xMn-mont clay concentration in aqueous suspension was increased, the ^1H NMR linewidth increased

linearly. This was because an increase in the clay concentration relates to an increase in Mn^{2+} concentration. Consequently a greater proportion of the H_2O molecules in the clay suspension become associated with the cation, thus causing line broadening. The ^1H NMR linewidth for pure water was in fact found to be less than 1 Hz under the experimental conditions utilised in this study whereas the presence of 23 gL^{-1} 3xMn-mont in aqueous suspension caused the linewidth to increase to almost 400 Hz. If therefore a compound is added to each 3xMn-mont clay concentration shown in Figure 68 which is known to preferentially interact with Mn^{2+}, then the ^1H NMR linewidth will decrease as water molecules from the cation's hydration shell are displaced. This is exactly what happened upon addition of 0.001% v/v 1,2 diaminoethane (1,2 DAE) to each 3xMn-mont clay concentration. Although the quantity of 1,2 DAE added was small, it still had a profound effect upon the ^1H linewidth, causing a reduction of over 100 Hz for a 23 gL^{-1} aqueous suspensions of 3xMn-mont containing the 1,2 DAE, (Figure 69). It was therefore anticipated that the addition of DCP101 to the same concentrations of 3xMn-mont would also cause a reduction in linewidth if the displacement of hydration shell water occurred. Figure 71 indicates that this was not the case, shown by the similar line gradients observed for the addition of 0, 0.1, 2 and 10% DCP101 to the different concentrations of 3xMn-mont. This shows conclusively that the addition of DCP101 to 3xMn-mont does not cause a significant quantity of the water in the Mn^{2+} hydration shell to be disturbed. Consequently the suggestion put forward by Cliffe *et al.*[149] and Aston *et al.*[152] that polyglycols may interact with the water molecules associated with exchangeable cation appears unlikely. In agreement with this statement, Parfitt *et al.*[33] also indicate that the exchangeable cations on montmorillonite retain their hydration shells upon adsorption of the related polymer, PEG.

CHAPTER 8

NMR Investigation into the Observed ^2H Residual Quadrupolar Splitting of D_2O Molecules Associated with Clay.

8. NMR Investigation into the Observed ^2H Residual Quadrupolar Splitting of D_2O Molecules Associated with Clay.

It was anticipated that the deuterium residual quadrupolar splitting observed when D_2O molecules become associated with the surface of clay in aqueous suspension may be utilised to see how the presence of polymers affect the interaction of water with clay. The interactions of D_2O molecules with three types of natural clay and one synthetic clay were therefore studied. The natural clays included Westone-L, Mineral Colloid and Texas bentonite, whereas the synthetic clay investigated was Laponite.

8.1 The ^2H NMR Results Observed for D_2O Molecules Associated with the Surface of Several Different Clays in Aqueous Suspension.

All natural clay suspensions were adjusted to exactly 40 gL^{-1} before recording NMR spectra since the concentration of clay in aqueous suspension was found to have a substantial effect on the ^2H splitting for every type of natural clay studied, (Figure 72). For the synthetic clay Laponite, a 20 gL^{-1} suspension was used because at increased clay concentrations the clay suspension was extremely viscous. No ^2H splitting was however observed for this synthetic clay.

Great care was taken to mix all clay suspensions thoroughly before recording the ^2H NMR spectrum. This was to ensure that any time dependence in the alignment of the clay platelets and therefore the time taken to reach maximum splitting was not due to poor mixing. For all three types of natural clay investigated, aqueous suspensions of the clay platelets aligned rapidly in the magnetic field requiring less than 15 seconds to reach maximum splitting.

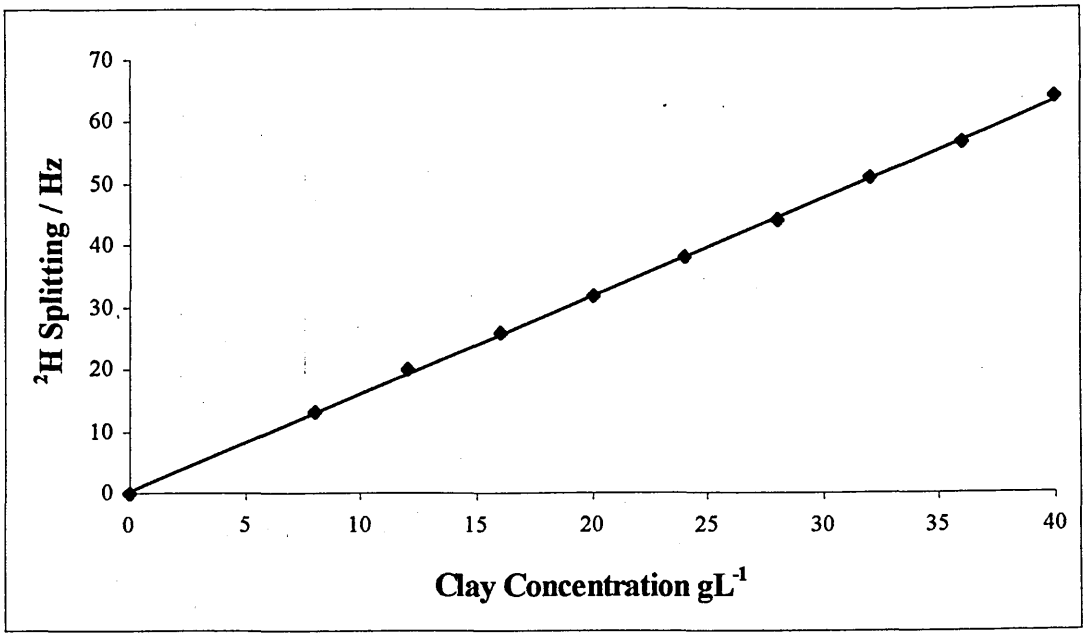

Figure 72. The increase in ^{2}H splitting on increasing the concentration of clay in aqueous suspension. Ca^{2+} exchanged Mineral Colloid was the clay used to record this data.

The data in Table 27 shows that a 40 gL^{-1} suspension of the < 0.3 μm clay fraction gives an increased ^{2}H splitting when compared to a 40 gL^{-1} suspension of the < 2 μm clay fraction from which it was prepared. This suggested that the increased surface area of the < 0.3 μm clay fraction allows more D_2O molecules to become associated with the clay surface and therefore an increase in ^{2}H splitting was observed. Table 27 also shows that increasing the number of times that Westone-L was exchanged with Na^+ or Ca^{2+}, tended to increase the splitting of the ^{2}H doublet. The Na^+ exchanged Westone-L samples however all exhibited a smaller splitting than the 46 Hz found for the initial < 2 μm fraction of the unexchanged, sedimented clay. Moreover the largest Na^+ clay splitting was less than the smallest Ca^{2+} clay splitting even though both Na^+ and Ca^{2+} clays showed a positive splitting defined by the broader component of the doublet occurring at higher frequency.

Clay Type	Sample	Splitting / Hz	T_1 seconds	Nature	Sign
Westone-L	< 0.3 μm fraction	52			+
	< 2 μm fraction	46	0.436		+
	1xNa-mont	19	0.427	Sharp	+
	2xNa-mont	29	0.429	Sharp	+
	3xNa-mont	36	0.432	Sharp	+
	1xCa-mont	61	0.423	Broad	+
	2xCa-mont	72	0.405	Broad	+
	3xCa-mont	72	0.438	Broad	+
	1xTMA-mont	56	0.432	Broad	+
Mineral Colloid	< 2 μm fraction	24		Sharp	-
	1xNa-bent	32		Sharp	-
	3xNa-bent	32		Sharp	-
	3xCa-bent	66		Broad	-
Texas bentonite	40 gL^{-1}	53		Sharp	-
Laponite	20 gL^{-1}	No Splitting			

Table 27. ^2H NMR results for different types of clay. The < 2 μm clay fractions were purified but not exchanged with the desired cation.

The ^2H NMR spectra recorded for 3xNa-mont and 3xCa-mont, illustrated in Figure 73, show that the main difference between the two types of cation exchanged clay was the linewidth of the doublets. The wings of the Na doublets were sharp and well resolved while the calcium doublets were broad and poorly resolved. The doublet observed for the Na^+ exchanged clay became sharper and better resolved with successive Na^+ exchanges. The observed doublet for the < 2 μm fraction of unexchanged, sedimented Mineral Colloid bentonite was well resolved with a splitting of 24 Hz. On exchanging this clay three times with Na^+, the resulting 3xNa-Bent showed an increase in the observed

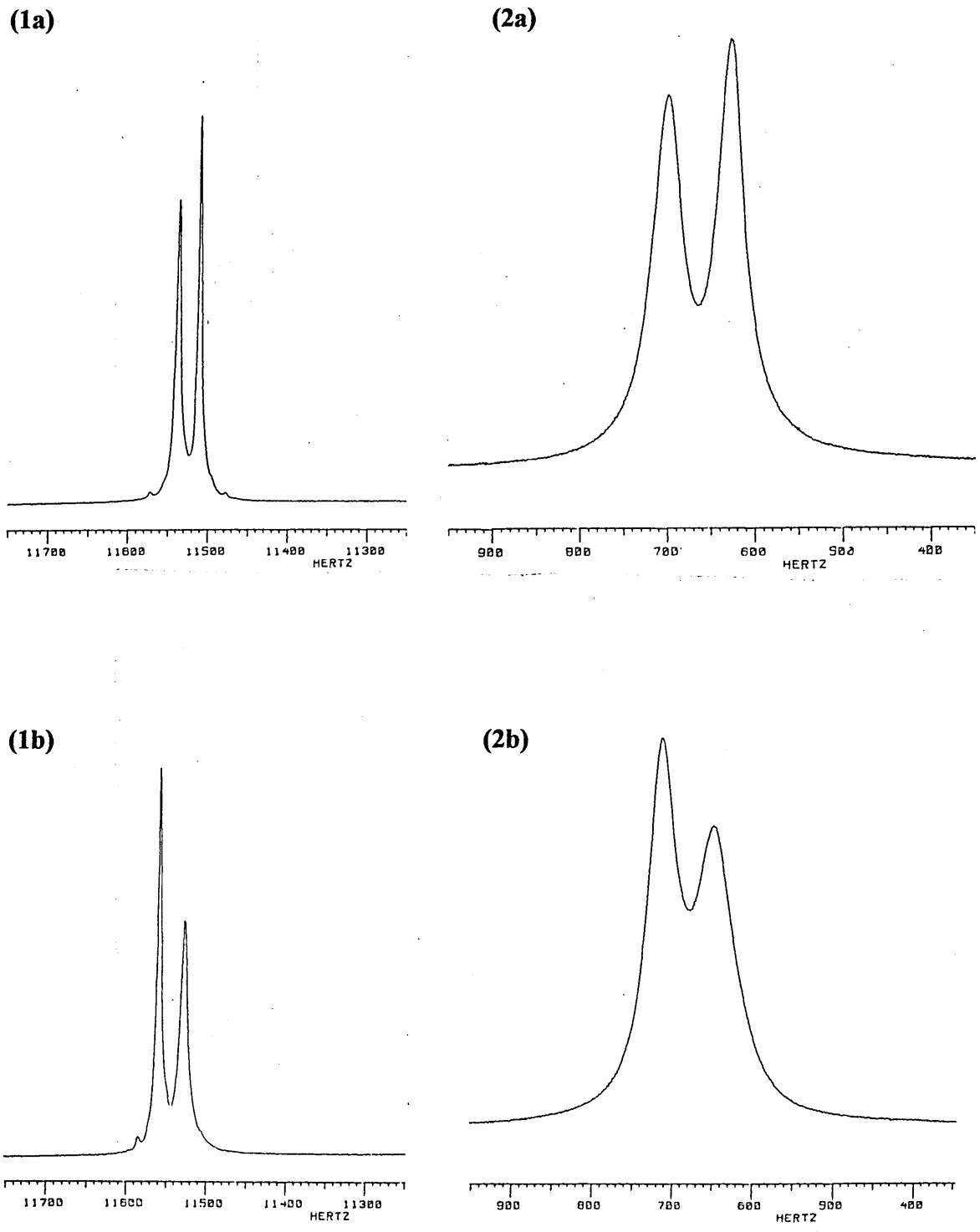

Figure 73. The ^{2}H NMR spectra observed for (1a) 3xNa-mont, (2a) 3xCa-mont, (1b) 3xNa-bent and (2b) 3xCa-bent.

splitting from 24 to 32 Hz and the wings of the doublet became marginally broader, (Figure 73, 1b). On exchanging Mineral Colloid three times with Ca^{2+}, the resulting 3xCa-bent also showed an increase in deuterium splitting from 24 to 66 Hz and the wings of the doublet became broader still, (Figure 73, 2b). As stated above, the opposite was noted with Westone-L where the splitting decreased from 46 to 19 Hz and the wings of the doublet became sharper following exchange of the < 2 μm fraction with Na^+ ions. In contrast to Westone-L, both the Mineral Colloid and Texas bentonite showed a negative splitting, with the broader component at lower frequency. As mentioned previously, the synthetic clay Laponite did not display any splitting of the ^2H doublet, (Table 27).

Table 27 above, shows that exchanging 3xNa-mont with TMA^+ caused an increase in the observed splitting from 36 to 56 Hz. Also T_1 for both the sodium and calcium exchanged montmorillonite showed good agreement with values around 0.43 seconds.

8.1.1 The Effect of Added Salt on the ^2H Splitting.

Figure 74 shows that addition of < 1.0×10^{-2} mol L^{-1} NaCl to a 40 gL^{-1} aqueous suspension of Na-montmorillonite, resulted in a small increase in ^2H splitting from 24 to 28 Hz. Subsequent NaCl additions however resulted in a decrease in the ^2H splitting until a singlet was observed following the addition of 1.88×10^{-2} mol L^{-1} NaCl. Further additions of NaCl also resulted in the observation of a singlet.

The magnitude of the ^2H splitting observed for Ca-montmorillonite was found to be more susceptible to additions of extraneous ions than that observed for Na-montmorillonite. Here, only 8.0×10^{-4} mol L^{-1} of $Ca(NO_3)_2$ were required to cause

complete collapse of the ^2H splitting, (Figure 75). Subsequent additions of $Ca(NO_3)_2$ again resulted in the observation of a singlet.

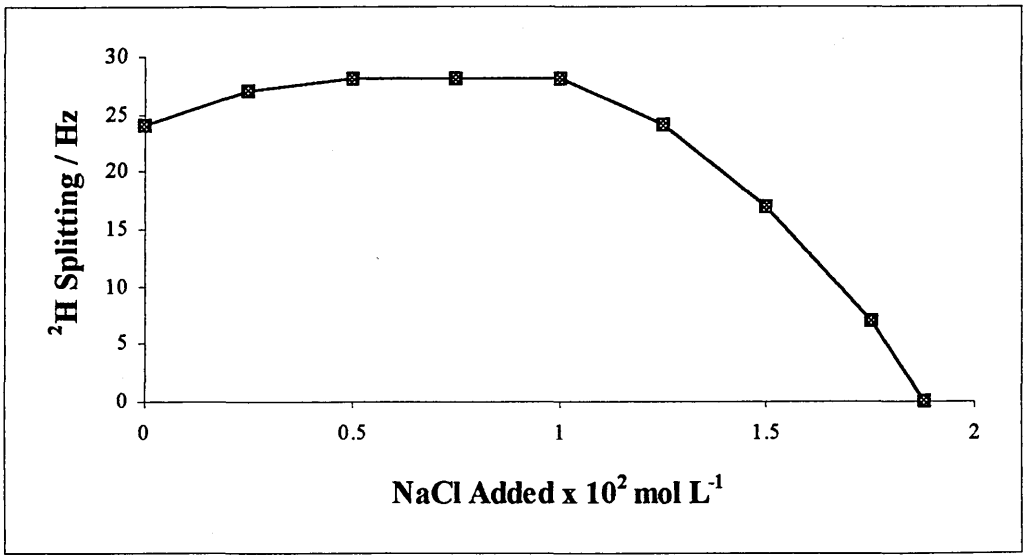

Figure 74. The change in ^2H splitting upon addition of increasing amounts of NaCl to Na-montmorillonite. A singlet was observed for the addition of Na^+ at a concentration equal to 94% of the CEC.

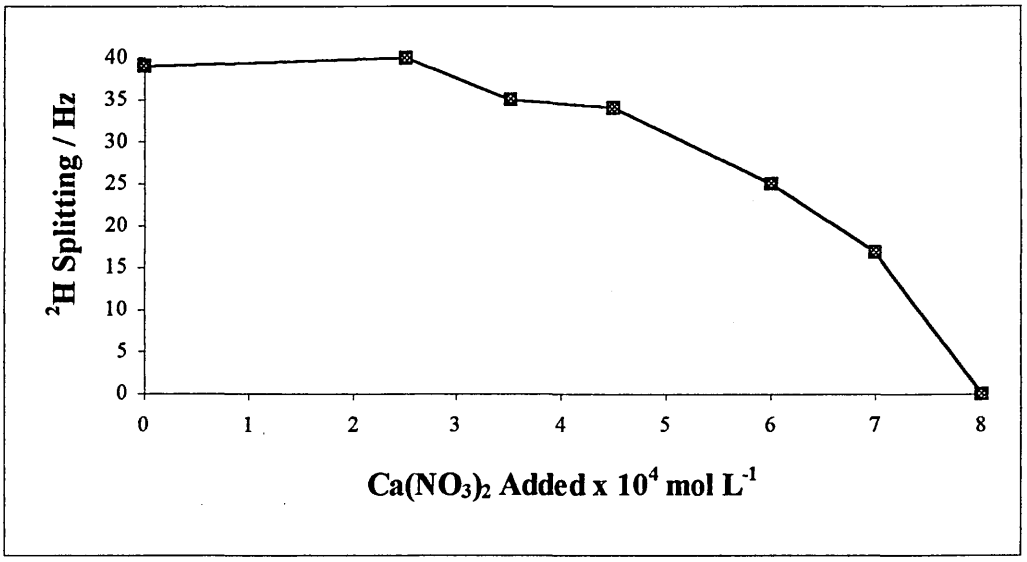

Figure 75. The change in ^2H splitting upon addition of increasing amounts of $Ca(NO_3)_2$ to Ca-montmorillonite. A singlet was observed for the addition of Ca^{2+} at a concentration equal to 25% of the CEC.

With Na-montmorillonite, complete collapse of the ^2H splitting to a singlet occurred for the addition of only 4.06×10^{-3} mol L^{-1} of $Ca(NO_3)_2$. Obviously this salt

was more effective than NaCl at causing collapse of the ^2H splitting observed for aqueous suspensions of Na-montmorillonite. Similarly 6.25 x 10^{-3} mol L^{-1} of NaCl were required to cause complete collapse of the ^2H splitting observed for aqueous suspensions Ca-montmorillonite, which was 8 times more than the 8.0 x 10^{-4} mol L^{-1} of $Ca(NO_3)_2$ which were required. It may therefore be concluded that the presence and type of extraneous ions in an aqueous suspension of clay has a large bearing upon the magnitude of the resulting ^2H splitting.

8.1.2 The Effect of Added Polymer on the ^2H Splitting.

Addition of anionic PHPA to Na-montmorillonite increased the alignment time of the clay platelets in the magnetic field. Maximum splitting was attained after two hours in the field although the increase in splitting after 30 minutes was very slight (< 1.5 Hz). The effect of the polymer on the ^2H splitting was marked, showing a progressive loss in splitting with the addition of increasing volumes of PHPA, (Figure 76).

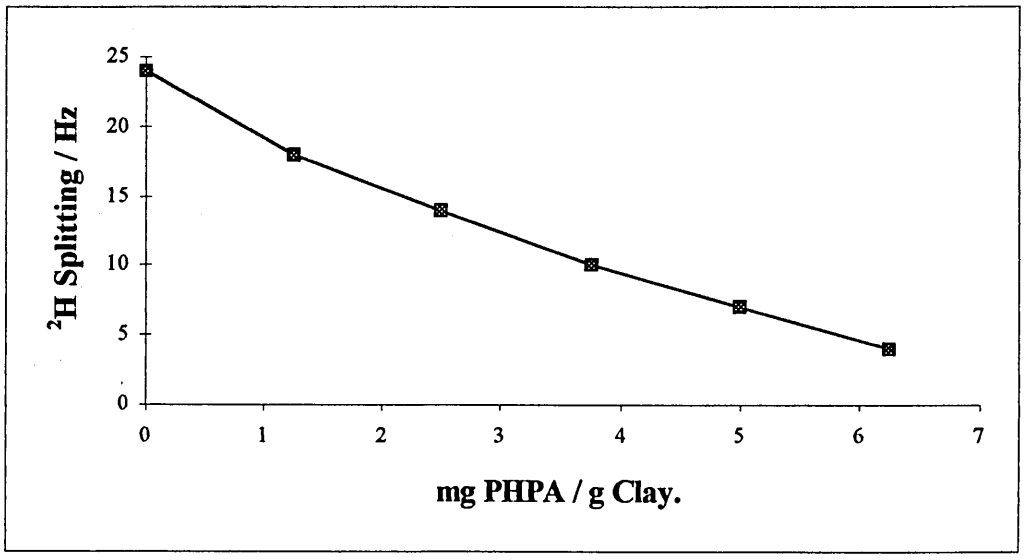

Figure 76. The observed decrease in ^2H splitting upon addition of increasing aliquots of PHPA to 3xNa-mont.

PHPA was also added to a 10% D_2O/H_2O solution to establish whether or not a splitting could be seen in the absence of suspended clay. As would be expected, no splitting was observed.

8.1.3 ^2H NMR Analysis of 3xNa-mont Contacted with the Synthesised, Deuterated HEG Compound.

The deuterated HEG compound was synthesised in the hope that ^2H NMR of clay suspensions containing this compound could provide some insight into how the neutral polymer, DCP101, interacts with clay. It was hoped that this deuterated compound would show a ^2H splitting when added to a clay suspension in the same way as D_2O molecules do. No deuterium splitting was however observed upon addition of increasing aliquots, up to 10% v/v, of the deuterated HEG compound to a suspension of 3xNa-mont. It was therefore decided not to proceed any further with these experiments.

8.2 Discussion Concerning the NMR Investigation into the Observed ^2H Residual Quadrupolar Splitting of D_2O Molecules Associated with Clay.

Grandjean and Laszlo have demonstrated that ^2H NMR spectroscopy can be of great value in investigating the interactions of water molecules with clays.[109,110] It was hoped that by monitoring these clay/D_2O interactions that information about clay/polymer systems in aqueous suspension would be forthcoming. As described in section 4.3, the basis of Grandjean and Laszlo's work involved the suspension of clay platelets in a 10% D_2O/H_2O solution and the subsequent introduction of the sample into the magnet of a normal NMR spectrometer. Grandjean and Laszlo state that it takes a few minutes for the clay platelets to reorient themselves once in the NMR magnet. This alignment of the platelets puts those water molecules that are associated with them in an anisotropic environment which results in the quadrupolar ^2H nuclei having non-degenerate transitions. Since the quadrupolar coupling constant for deuterons in heavy water is very large, in the order of 213 MHz, the ^2H nuclei displays a residual quadrupolar splitting even in the presence of fast exchange between the interfacial water molecules and the bulk solution. According to Halle *et al.*[164] this residual quadrupolar splitting, Δ, is the product of three terms:

1. The quadrupolar coupling constant, χ, which for the nucleus in question is equal to (e^2qQ/h).

2. The dipolar term $(3\cos^2\Theta_{LD} - 1)$ where Θ_{LD} denotes the angle between the laboratory and the director coordinate systems. This is simply the angle made between the static magnetic field, B_0, and the local order director of the orientated platelets, perpendicular to their parallel surfaces.

3. The residual anisotropy A, which is related to the order parameters and has values between -1 and +1. Its actual value depends upon the orientation of water molecules with respect to the surface of the clay, (the local director).

The measured deuterium splitting is therefore the product of the three terms listed above. These three terms may be combined into one equation from which it is theoretically possible to calculate the ^2H residual quadrupolar splitting, (Equation 6).[165]

$$\Delta = \frac{e^2qQ}{4I(2I-1)h}(3\cos^2\Theta_{LD} - 1)A$$

Equation 6. From which it is theoretically possible to calculate the deuterium splitting. I is the spin quantum number which for ^2H = 1.

Great care was taken in the preparation of samples for this study because it was found that some physical properties of the clay suspensions effected the magnitude of the ^2H splitting. For example the total surface area of the clay platelets in suspension was critical in that the greater the proportion of surface area available for interaction with D_2O molecules, the greater the ^2H splitting observed. This was shown by the increase in splitting observed when a < 2 μm montmorillonite fraction with a splitting of 46 Hz was taken and centrifuged to give a less than 0.3 μm clay fraction, (section 5.12). This reduced particle size clay fraction which obviously had a greater total surface area showed an increase in splitting to 52 Hz. Both clay fractions were suspended in solution at a concentration of 40 gL^{-1}. Similarly, control of the clay concentration in aqueous suspension was found to be critical for reproducible ^2H splittings. For all natural clays investigated, a decrease in the clay concentration lead to a decrease in the ^2H splitting, (Figure 72). The decrease in splitting at decreasing clay concentrations occurred because there was less surface area available for interaction with D_2O molecules at reduced clay

concentrations. Consequently fewer D_2O molecules will be ordered at the clay surface and the ^2H splitting will be smaller.

The state of clay platelets in aqueous suspension, when placed into the magnetic field, also had a large effect upon the ^2H splitting. For example, Grandjean and Laszlo noted that for a 25 gL^{-1} sample of Ecca Gum BP bentonite, it took several minutes ($\approx$ 20) to reach the maximum observed splitting.[110] Further, the time taken to reach maximum splitting depended upon the field strength of the magnet, the stronger the magnetic field, the less time taken. In this study, the maximum splitting was attained in less than 1 minute for 40 gL^{-1} suspensions of both the Mineral Colloid and Westone-L at the same magnetic field strength of 9.4 T used by Grandjean and Laszlo. The time taken for the maximum splitting to be reached is actually a function of the degree of platelet alignment in the magnetic field. Obviously, as Grandjean and Laszlo found, an increase in the field strength causes the platelets to align more quickly and as a result the maximum splitting is reached in less time. The difference in alignment time between the Ecca Gum BP bentonite studied by Grandjean and Laszlo and the clays investigated in this study must therefore be due to differences in the preparation of the clay suspensions. Stawinski *et al.*[51] found that the dominant type of clay aggregation in such concentrated clay suspensions is EF which results in 3D floccules. The repeated homogenisation used in this study while washing the clay samples free of extraneous ions may have had the effect of breaking up these 3D floccules. With fewer EF bonds present, the alignment times will be reduced as ordering of the platelets in the magnetic field is made easier. Consequently, the long alignment times observed by Grandjean and Laszlo, who used dialysis to wash their clay rather than repeated homogenisation, may be due to the fact that the dominant EF bonded aggregates in the clay need to be broken before alignment

can proceed. The ^2H NMR spectrum for the synthetic clay Laponite gave a singlet, suggesting that no alignment of the clay platelets had occurred even after 15 minutes in the magnet.

The maximum ^2H splitting observed for a less than 2 μm fraction of unexchanged Westone-L was 46 Hz. Prior to exchanging, this clay was predominantly in the Ca^{2+} exchanged form although a small proportion of Na^+ was also present. On exchanging once with Na^+, the splitting decreased to 19 Hz and the wings of the doublet became narrower. With three successive Na^+ exchanges however, the splitting increased to a maximum of 36 Hz. The initial decrease in the ^2H splitting on exchanging once with Na^+ was obviously due to the replacement of Ca^{2+} ions with Na^+ ions. This was later proved by exchanging the <2 μm clay fraction once with Ca^{2+}. This had the effect of increasing the ^2H splitting from 46 to 61 Hz and the wings of the doublet became broader. Again subsequent exchanges with Ca^{2+} caused an increase in splitting until a maximum of 72 Hz was observed upon exchanging the clay twice with Ca^{2+}.

One interpretation for the increased ^2H splitting and linewidth seen with 3xCa-mont with respect to 3xNa-mont, is the difference in charge between the two counter ions. Obviously the larger 2^+ charge on the Ca ion will effect the ordering of the D_2O molecules at the clay surface to a greater degree than the 1^+ charge on the Na counter ion. Consequently more water layers will be ordered by the Ca^{2+}. In ordering more layers, the Ca^{2+} is essentially causing more water to become associated with the surface of the clay which obviously increases the splitting of the doublet. An interesting point to note is that exchanging the <2 μm fraction of Westone-L once with TMA^+ resulted in an increase in the ^2H splitting from 46 to 56 Hz. The ability of this cation to order water layers at the clay surface and therefore cause an increase in ^2H splitting is surprisingly

good when considering that it possesses a low hydration energy. One similarity between the ^2H doublet observed for Na^+ and Ca^{2+} exchanged montmorillonite was the fact that they both exhibited a positive splitting defined by the broader component of the doublet occurring at higher frequency.[110] It has been shown by Grandjean and Laszlo that the origin of this differential line broadening may be attributed to coupling between two different relaxation mechanisms present in the system.[116] These include a quadrupolar relaxation mechanism and an external dipole-dipole relaxation mechanism. The dipole-dipole mechanism is reliant upon the concentration of paramagnetic centres in the clay which are essentially the origin of the differential line broadening. These paramagnetic centres arise from Fe_2O_3 impurities where the greater the quantity of iron present in the clay, the more pronounced the differential line broadening. For example the Ecca Gum BP bentonite used by Grandjean and Laszlo contained about 4% Fe_2O_3 and showed a marked differential line broadening.[110] Conversely with hectorite, another 2:1 smectite which contained very little iron, 0.05%, no difference in the linewidths of the two components was seen.[110] Further, in this study, the Westone-L investigated contained only 0.7% Fe_2O_3 and as a result the differential line broadening was not very pronounced, (Figure 73, 1 and 2a). On the other hand the Mineral Colloid which contained almost 4% Fe_2O_3 showed a more pronounced differential line broadening similar to that observed by Grandjean and Laszlo for Ecca Gum BP, (Figure 73, 1 and 2b).

Grandjean and Laszlo state that for a 25 gL^{-1} suspension of Ecca Gum BP with an exchangeable cation ratio of $Ca^{2+}/Na^+ = 0.020$ showed a residual quadrupolar splitting of +16.3 Hz. As the ratio of Ca^{2+}/Na^+ was increased however the residual quadrupolar splitting decreased through zero to a minimum of -23 Hz at $Ca^{2+}/Na^+ = 0.575$. Obviously the same phenomenon was not occurring in this study with both the Na^+ and Ca^{2+}

exchanged montmorillonite showing a positive splitting. Consequently it was decided to investigate the interactions of D_2O molecules with Mineral Colloid bentonite because this clay was more representative of the Ecca Gum BP bentonite investigated by Grandjean and Laszlo. On introduction into the magnetic field, the <2 μm suspension of unexchanged Mineral Colloid showed a ^2H residual quadrupolar splitting of 24 Hz. Interestingly the broader component of the doublet was now at lower frequency and consequently the sign of the splitting deemed negative. The peaks of the doublet were also relatively sharp. On exchanging this clay once with Na^+, the wings of the doublet became marginally broader and the ^2H splitting increased to 32 Hz. This was the maximum splitting observed even after exchanging three times with Na^+. Like the < 2μm clay fraction, the splitting of the 3xNa-bent was also negative. On exchanging Mineral Colloid three times with Ca^{2+}, the resulting 3xCa-bent also showed an increase in splitting from 24 to 66 Hz and the wings of the doublet became broader still. 3xCa-bent again showed a negative ^2H splitting. A ^2H splitting of 53 Hz was also observed for a 40 gL^{-1} suspension of unpurified and unexchanged Texas bentonite which like the Mineral Colloid showed a negative ^2H splitting. In summary, Westone-L showed a positive splitting for all exchange forms of clay studied whereas Mineral Colloid exhibited a negative splitting for all exchange forms investigated. No change in the sign of the ^2H doublet was observed on exchanging either of these two clays from the Na^+ form to the Ca^{2+} exchanged form. As stated previously, this is in direct contradiction to the results obtained by Grandjean and Laszlo who saw a change in sign from positive to negative as the amount of exchangeable Ca^{2+} in the predominantly Na^+ exchanged Ecca Gum BP bentonite was increased.

The effect of extraneous Na^+ or Ca^{2+} ions upon the ^2H splitting has also been investigated. This was undertaken because it was initially thought possible that the sign reversal of the ^2H splitting observed by Grandjean and Laszlo for Ecca Gum BP may be somehow dependant on the presence of extraneous ions in solution. This assumption was made because in previous publications by Grandjean and Laszlo, they state that the presence of extraneous ions in solution after exchanging the clay with the desired cation was tested by reaction with $AgNO_3$.[109] In the present study, all clay suspensions were washed until the conductivity of the filtrate recovered after centrifugation of the clay suspension was $\approx$ 30 μS, (section 5.1.3). Using the $AgNO_3$ test, it was found that filtrates which showed no reaction with $AgNO_3$ could have a conductivity of several hundred μS. Consequently all Grandjean and Laszlo's experiments must have been carried out in the presence of extraneous ions. Another reason for investigating the role of extraneous ions in clay suspensions is to gain some idea about what effect the counter ion associated with added polymer will have on the ^2H splitting when the polymer is adsorbed, also all drilling fluids contain a large quantity of added salts, such as KCl.

The addition of small quantities of NaCl, ($< 1.0 \times 10^{-2}$ mol L^{-1}), to a 40 gL^{-1} suspension of Na-montmorillonite initially caused a small 4 Hz increase in the ^2H splitting. This small but significant increase in splitting is most likely due to the fact that more D_2O molecules become associated with the clay. For this to happen, more clay surface area must become available upon addition of small quantities of NaCl. Stawinski *et al.*[51] provide evidence that this may in fact be occurring. They have measured the relationship between the mean aggregation radius, r_m, and the Na^+ or Ca^{2+} concentration in a 5.0 gL^{-1} bentonite suspension. They observed that r_m decreased with an increase of Na^+ and Ca^{2+} concentration, reaching a minimum for both cations at a concentration of

0.3 meq dm^{-3} for Ca^{2+} and 10 meq dm^{-3} for Na^{+}. Stawinski *et al.*[51] have also shown from scanning electron micrographs that for a clay suspension with no extraneous ions, the dominant type of aggregation was EF leading to the formation of 3D floccules. The addition of a low concentration of Na^{+} (<10 meq dm^{-3}) caused the dominant type of aggregation to become EE which obviously means that more surface area is available for interaction and as observed, the ^{2}H splitting will increase. As larger concentrations of Na^{+} were added, Stawinski *et al.*[51] noted from scanning electron micrographs that very compact irregular aggregates were formed having a multilayer structure of the FF type. Obviously this type of aggregation leads to a loss in surface area which will consequently lead to a decrease in ^{2}H splitting. The same effect was observed in this study where addition of > 1.0×10^{-2} mol L^{-1} NaCl, resulted in a rapid decrease in the ^{2}H splitting to zero. The quantity of Na^{+} required to achieve zero splitting was 1.88×10^{-2} mol L^{-1} which was equal to 94% of the CEC. Subsequent additions of NaCl to the clay suspension also resulted in the observation of a singlet. Thus a small increase in salt concentration usually leads to an initial deflocculation of aggregates and then to particle aggregation upon further additions.[135] Similar observations were also made for the addition of $Ca(NO_3)_2$ to a 40 gL^{-1} suspension of Na-montmorillonite. This time however the splitting of the doublet collapsed with the addition of only 4.06×10^{-3} mol L^{-1} $Ca(NO_3)_2$. Subsequent additions of $Ca(NO_3)_2$ to the clay suspension again resulted in the observation of a singlet. The differences in the ability of Ca^{2+} and Na^{+} to cause loss of splitting is marked, with splitting loss occurring for the addition of only small quantities of Ca^{2+} with respect to Na^{+}. These differences probably arise because of differences in the ability of each cation to compress the diffuse double layer associated with the clay.[166] Consequently, Ca^{2+} ions are superior to the Na^{+} ions at causing aggregation of the clay platelets which leads to the loss of splitting. The addition of only 8.0×10^{-4} mol L^{-1} of

$Ca(NO_3)_2$ to a 40 gL^{-1} suspension of Ca-montmorillonite caused the ^2H splitting to collapse, (Figure 75). Conversely when extraneous Na^+ ions were added to the same clay, 6.25 x 10^{-3} mol L^{-1} NaCl were required to cause complete collapse which is significantly more than the quantity of $Ca(NO_3)_2$ required. This again suggested that Ca^{2+} caused more flocculation than Na^+ when added to a clay suspension which resulted in decreasing splitting values. Subsequent additions of either Ca^{2+} or Na^+ to Ca-montmorillonite after the ^2H splitting had collapsed, again resulted in the observation of a singlet. Obviously the presence of extraneous ions in an aqueous suspension of clay causes aggregation of the platelets, leading to a permanent loss of the ^2H splitting. In summary, these experiments have shown that the charge balancing cation associated with anionic polymer can have a profound effect upon the ^2H splitting when it is dissociated from the polymer upon adsorption. They have also shown that the presence of extraneous ions in the clay suspension was not responsible for the sign change observed by Grandjean and Laszlo on increasing the exchangeable Ca^{2+} content of Na^+ exchanged Ecca Gum BP.

Previous work by Grandjean and Laszlo has however attempted to explain the magnitude and sign origin of the ^2H splitting.[105] They have stated that fast exchange of water molecules between the bulk which displays no splitting and two interfacial sites having residual anisotropies, A, of opposite signs was responsible for the sign of the observed ^2H splitting. They state that at the clay surface, water molecules either form H bonds to the negatively charged surface or interact with exchangeable cations. The presence of divalent cations obviously favours the latter cationic site which according to their results observed for Ecca Gum BP, caused the sign reversal from positive to negative as the proportion of exchangeable Ca^{2+} increased. Obviously increasing the

probability of D_2O interaction with the second site, the clay surface, should also have an effect on the ^2H splitting. This was investigated recently by Grandjean and Laszlo who studied the interactions of D_2O molecules with several different clays having isomorphous substitution in different layers.[105] Obviously if isomorphous substitution is found predominantly in the tetrahedral layer of the clay, interactions with D_2O molecules will be strong since the negative charge associated with the clay comes into close approach of the D_2O molecules. Conversely, when isomorphous substitution is exclusively in the octahedral layer, the negative charge cannot interact as strongly with D_2O molecules and association with the exchangeable cation is preferred. Interestingly, Grandjean and Laszlo have shown that when isomorphous substitution occurred exclusively in the octahedral or tetrahedral layers, that the presence of differing ratios of univalent to divalent cation had negligible effect upon the ^2H splitting.[105] They have therefore stated that the intermediate situation of Ecca Gum BP, where isomorphous substitution occurs in both the tetrahedral and octahedral layers, is responsible for the observed cation dependence of the ^2H splitting. This cation dependence occurs because in this intermediate situation, neither interfacial site at the surface of the clay is dominant.[165] In the present study, the Westone-L investigated was shown by ^{27}Al MAS NMR to have isomorphous substitution occurring predominantly in the octahedral layer although some tetrahedral substitution was also present. The fact that no change in the sign of the ^2H splitting occurred on increasing the Ca^{2+} content contradicts the findings by Grandjean and Laszlo.[109,110] These discrepancies may however be because Westone-L had predominantly octahedral substitution and insufficient tetrahedral substitution to cause the sign change.

With the addition of PHPA to Na-montmorillonite, the first interesting point to note is that the splitting of the ^2H doublet is dependant upon residence time in the magnet. Maximum splitting was attained after two hours in the magnet although the increase in splitting after 30 minutes was very slight, <1.5 Hz. The inability of the clay platelets to align rapidly and therefore attain maximum splitting suggests that the polymer ties the platelets up. One mechanism by which this could occur would be if the polymer bridged between platelets therefore slowing alignment and causing the ^2H splitting to be time dependant, (Figure 77).

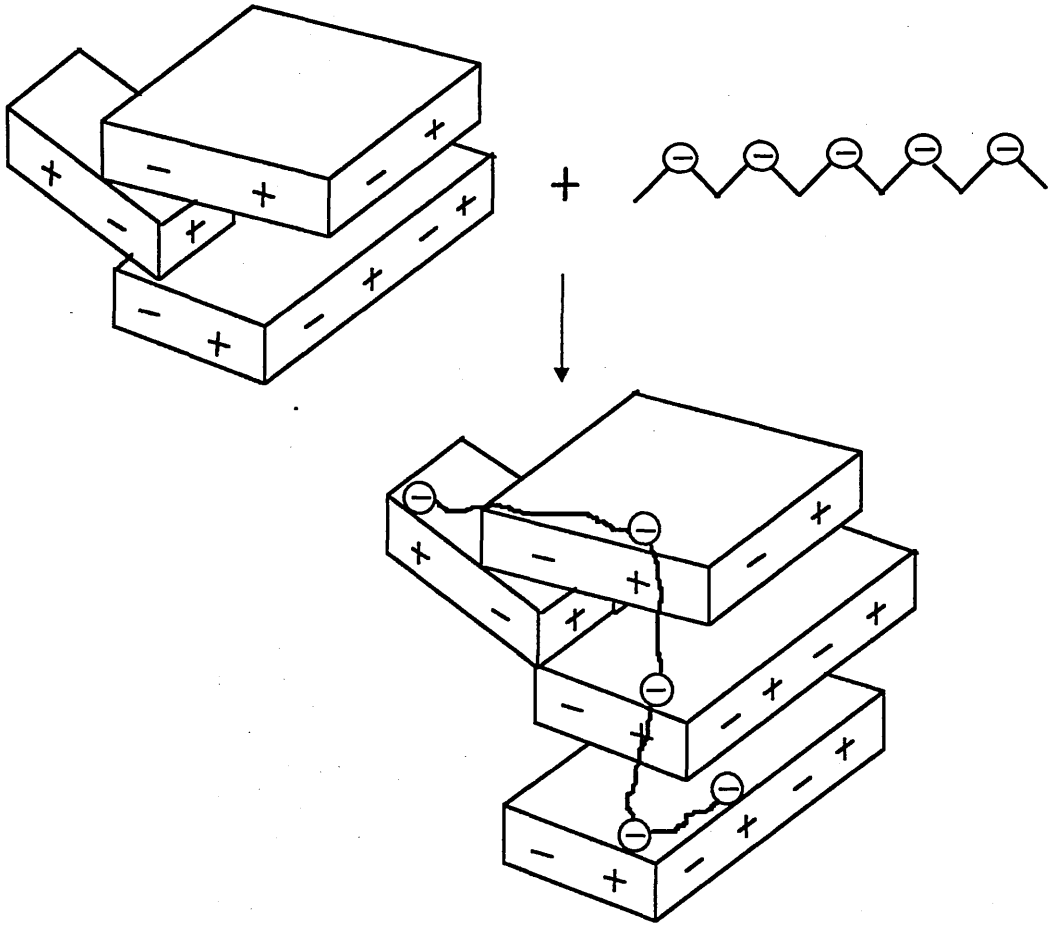

Figure 77. The adsorption of anionic polymer onto clay platelets via a bridging mechanism.

In agreement with this interpretation, the high molecular weight anionic PHPA used in PHPA/KCl drilling muds are thought to adsorb onto clay by a bridging mechanism.[167]

These anionic polymers attach themselves to positive broken bond sites on the edges of adjoining shale particles, holding them together, thus reducing platelet dispersion.[168]

The ^2H NMR results recorded for the addition of PHPA to a 40 gL^{-1} suspension of Na-montmorillonite were very disappointing. This was because a steady decrease in splitting was observed for the addition of only very small amounts of polymer to the clay. With the addition of just over 6 mg PHPA/g clay, the splitting had collapsed to 4 Hz. The large decrease in the ^2H NMR splitting upon addition of only small quantities of polymer may have been due to one or a combination of the factors outlined below.

1. The platelets could not align in the magnetic field because bridging of the adsorbed polymer prevented them from doing so. This is unlikely since selected samples were left in the magnetic field for long periods of time which should have caused some platelet alignment if this were the problem.

2. The counter ion associated with the polymer and indeed the polymer itself may have caused significant flocculation of the clay, resulting in the loss of splitting.

3. Adsorption of the polymer at the clay surface may have caused a reduction in the quantity of D_2O molecules associated with it which consequently reduces the ^2H splitting. It is thought that this last case could not have caused complete loss of the ^2H splitting at such low polymer loadings.

The rapid reduction in ^2H splitting for the addition of such low loadings of polymer is probably due to a combination of all these factors outlined above. It was therefore surmised that the window from which useful information could be gained about clay/polymer interactions was extremely sensitive to added polymer and the counter ions associated with it.

The loss of the ^2H splitting may therefore be traced back to the fact that insufficient D_2O molecules were allowed to associate with the surface of the clay upon addition of polymer. Whether this was because of the flocculation effects due to added polymer and counter ion or because the polymer adsorbs strongly onto the clay surface thereby preventing its interaction with water molecules is not known. If the probe D_2O molecule is substituted for a deuterated form of the polymer of interest, then the problem of D_2O not sampling the surface of the clay upon addition of polymer is irrelevant. Consequently, it was hoped that addition of deuterated polymer to a clay suspension would result in the observation of a ^2H doublet from which it may be possible to gain some information about clay/polymer interactions. Obviously deuterated forms of the polymers used in drilling fluids were not available and therefore a deuterated compound had to be synthesised which was similar to the polymer of interest. It was therefore decided to react two hexaethylene glycol (HEG) compounds together via a bridging compound of deuterated dimethylmaleate. The compound formed was similar in weight and composition to DCP101, the neutral polymer which is presently finding widespread use in drilling fluids. A major advantage of investigating neutral polymers is the fact that upon adsorption on the clay surface, there is no counter ion to displace and therefore cause aggregation. Unfortunately no ^2H splitting was seen with the addition of the deuterated HEG compound to 3xNa-mont, this may be due to a number of reasons.

1. The affinity of the deuterated HEG compound for the clay surface may be very low and consequently the majority of the added compound could be found in the bulk solution, resulting in no ^2H splitting.

2. The addition of the deuterated HEG compound to the clay may have caused significant aggregation, leading to loss of surface area available for interaction and possibly non alignment of the clay platelets in the magnetic field.

The use of the deuterium splitting to investigate how the presence of polymers affected the interaction of water with the surface of clay has not been successful in this study. Significantly, Grandjean and Laszlo have gained much information about the state of deuterated CD_3CN associated with the surface of clay from ^2H splitting results.[112,119] It was therefore concluded that the observed ^2H splitting was too sensitive to the adsorption of polymer onto the clay. This sensitivity of the ^2H splitting upon addition of polymer is thought to be primarily due to loss of surface area, through flocculation of the clay.

CHAPTER 9

Conclusions

9. Conclusions

It has been shown that the nature of the exchangeable cation associated with clay and therefore the degree of platelet dispersion plays a major role in determining the quantity of cationic species adsorbed. When simple inorganic cations such as K^+ or Na^+ are added to a clay suspension, the quantity of exchangeable cation displaced is thought to depend heavily upon the hydration energy of the added cation. ^{133}Cs NMR studies have in fact shown that K^+ cations, with a hydration energy of -321 kJ mol^{-1}, replace a greater proportion of the exchangeable Cs^+ than do Na^+ cations, which have a more negative hydration energy to equal to -405 kJ mol^{-1}. Neither K^+ nor Na^+ however displace large quantities of Cs^+ from 3xCs-mont since the Cs^+ cation has a hydration energy of -277 kJ mol^{-1}. Like inorganic cations, the organic cation TMA^+, adsorbs on to montmorillonite via an ion exchange mechanism. This cation has a hydration energy equal to -134 kJ mol^{-1} and therefore has much more success at displacing Cs^+ from the clay, shown by representative adsorption isotherms and ^{133}Cs NMR data. In addition, Van der Waals forces also play a role in the adsorption mechanism of this cation. ^{133}Cs NMR has also shown that paraquat has a high affinity for clay. When added at loadings greater than the CEC, the paraquat displaces all the exchangeable Cs^+ associated with 3xCs-mont. The strong affinity of this organic molecule for the surface of the clay is due to many reasons. Firstly, there are coulombic interactions between the two N^+ groups on each paraquat molecule and the negatively charged clay surface. Secondly the separation of the positive charges on the paraquat is similar to the distance between negative charge sites on the clay surface and consequently the opposite charges may come in to close approach, resulting in strong adsorption. Finally, due to the large size of paraquat, there are significant Van der Waals forces which make a contribution to its adsorption.

Polycations have been shown to have the strongest affinity for clay of all the cationic species investigated in this study. This was indicated by representative adsorption isotherms and confirmed by ^{133}Cs and ^{23}Na NMR data. Representative adsorption isotherms in fact show that FL17 has a greater affinity for the clay surface than Magnafloc 1697 when offered to any cation exchanged clay investigated in this thesis. It is probable that the observed differences in affinity arose because of two main reasons. (i) FL17 is less bulky than Magnafloc 1697 and is therefore able to penetrate the interlayers of the different cation exchanged clays more readily. (ii) Alternate N groups upon FL17 match exactly the distance between negative sites upon the clay surface whereas a poorer match was observed between the cationic groups on Magnafloc 1697 and the negative sites on the clay surface. The high affinity of all the polycations investigated in this thesis for the clay surface arises because their net segment-surface interaction energy, ε, is equal to approximately 4 kT per cationic unit. Obviously there are many adsorbed segments per polymer molecule, resulting in a large total energy of adsorption. In aqueous suspensions of clay, ^{133}Cs NMR has indicated that all polycations investigated adsorb onto the clay surface via a cation exchange mechanism. This involves the replacement of the exchangeable cation associated with the clay with a cationic unit from the polymer. The differences observed in the value of Q_{max} upon addition of FL17 and Magnafloc 1697 to Cs^+, Na^+ and K^+ exchanged montmorillonite can be explained by considering the effect that the exchangeable cation associated with the clay has on its swelling ability and degree of platelet dispersion. With suspensions of montmorillonite in the Na^+ exchanged form, the clay platelets are predominantly deflocculated and consequently the cationic polymer has access to the total surface area of the clay. This was confirmed by ^{23}Na NMR which shows that all the exchangeable Na^+ is displaced from 3xNa-mont by FL17 at loadings $\geq$ the CEC of the clay. Since the

total surface area of 3xNa-mont is available for interaction with polycation, the addition of FL17 or Magnafloc 1697 to 3xNa-mont results in similar Q_{max} values. XRD data also indicates that both these polymers were present in the interlayer of 3xNa-mont at polymer loadings from 20% to ≥ 100% of the CEC. With suspensions of montmorillonite in the Cs^+ exchanged form, the platelets are aggregated into tactoids and the swelling ability of this cation exchanged clay is minimal in comparison to Na^+ exchanged clay. Consequently, due to the aggregation of platelets, this clay shows reduced Q_{max} values for the addition of both Magnafloc 1697 and FL17. The value of Q_{max} for the addition of FL17 to 3xCs-mont is however significantly larger than that observed for Magnafloc 1697. This increased interaction of FL17 with 3xCs-mont was confirmed by ^{133}Cs NMR which showed that more Cs^+ was displaced from the clay by this polymer than by Magnafloc 1697. This suggests that FL17 is visiting more exchange sites upon the clay, resulting in increased adsorption. Further, XRD data also indicated that more FL17 was adsorbed in the interlayer of 3xCs-mont at polymer loadings greater than the CEC of the clay. At polymer loadings equivalent to 20% of the CEC however, there is no evidence from basal spacing data that either Magnafloc 1697 or FL17 are present in the interlayer of 3xCs-mont. The nature of the exchangeable cation associated with the clay is again responsible for the observed differences in the adsorption of FL17 and Magnafloc 1697. Since the swelling ability of Cs^+ exchanged clay in aqueous suspension is known to be poor in comparison with Na^+ exchanged clays, it is proposed that a size exclusion mechanism is in operation where the bulkier Magnafloc 1697 is unable to visit all the interlayer regions that FL17 may visit. This would result in decreasing Q_{max} values, basal spacings and proportion of Cs^+ detected by NMR which were all recorded in this thesis. When in aqueous suspension, 3xK-mont shows a situation intermediate between 3xNa-mont and 3xCs-mont, regarding degree of aggregation and swelling ability. As such,

Q_{max} values for the addition of FL17 or Magnafloc 1697 to 3xK-mont are intermediate between those observed for 3xNa-mont and 3xCs-mont. Interestingly, XRD shows that no Magnafloc 1697 resides in the interlayer of 3xK-mont at a polymer loading equivalent to 20% of the CEC. At the same polymer loading however, a basal spacing of 14.5 Å was observed for the addition of FL17 to 3xK-mont, showing that this polymer was able to access the clay's interlayer, again suggesting restricted access to the interlayer for Magnafloc 1697.

Particle size and zeta potential data indicate that an "electrostatic patch" flocculation mechanism was in operation upon addition of Magnafloc 1697, FL15 and FL17 to all types of cation exchanged clay investigated in this thesis. This was deduced since severe flocculation of the clay resulted upon addition of low concentrations of any of the highly charged polycations investigated which could not be explained by a simple charge neutralisation or bridging mechanism. Similar particle size and zeta potential data were recorded for the addition of any polycation investigated in this study to a particular cation exchanged clay. The main reason for these similarities is probably because Magnafloc 1697, FL15 and FL17 all have relatively low molecular weights and are all 100% cationic. Major differences however arose in particle size and zeta potential data when a particular polycation was added to two different types of cation exchanged clay. Differences in the strength and size of the floccules formed were observed, suggesting that slightly different flocculation mechanisms were in operation which depended upon the type of cation exchanged clay. The cation associated with the clay and therefore the degree of platelet dispersion is consequently thought to be central in controlling the flocculation of clay by the polycations investigated in this thesis.

In conclusion it has been shown by ^{133}Cs and ^{23}Na NMR that polycations adsorb onto the surface of clay in aqueous suspension via an ion exchange reaction. The polycations investigated in this study, which are typical of the ones used commercially in drilling fluids, all showed an extremely high affinity for the surface of the clay. Their proven shale inhibition properties more than likely arise from their high affinity for the surface of clay. Indeed, ^{133}Cs and ^{23}Na NMR has shown that addition of FL17 to clay results in the displacement of all the exchangeable cations from the clay at polycation loadings $\geq$ the CEC. Thus it is expected that whilst drilling an oil well, this polymer covers the whole clay surface which presumably acts as a barrier between the shale and water, thus preventing interaction. One major problem with cationic polymer WBM which has already been found with their use commercially is the high depletion rate from drilling fluids which is a consequence of their high affinity for the surface of clay and other minerals. This leads to escalated drilling costs as the adsorbed polycation has to be replaced and is one of the main factors why WBM containing cationic polymers have not found widespread use. Future work would concentrate upon ^{23}Na NMR because it is anticipated that much more information could be gained from this nucleus concerning the interactions of cationic species with montmorillonite. For example, due to time constraints, ^{23}Na NMR data was not recorded for the addition of Magnafloc 1697 to 3xNa-mont. In conjunction with particle size and zeta potential data, it is expected that ^{23}Na NMR results for the addition of this polymer to 3xNa-mont would provide complementary information about its adsorption mechanism. Further, it would be interesting to see what effect the addition of TMA^+ to 3xNa-mont has on the exchangeable Na^+ associated with the clay. As 3xNa-mont is largely deflocculated in comparison to 3xCs-mont and because TMA^+ has a much less negative hydration energy than Na^+, it is expected that a graph of the concentration of TMA^+ added versus the

concentration of Na^+ detected will be a straight line, indicating that 1 TMA^+ cation replaces 1 Na^+ cation at the clay surface. It may also be worthwhile investigating another exchangeable cation such as ^{87}Rb to give further complementary information. The investigation of a series of chemically similar polycations with different cationicities, molecular weights and therefore chain lengths to deduce what effect these variables have upon their adsorption could also be carried out using the *in situ* techniques outlined in this thesis. Results obtained from this study could then be compared with those recorded for addition of the same series of polymers to other types of negatively charged particles such as silica. These studies would be advantageous since silica does not swell like montmorillonite and therefore the effects of interlayer swelling and tactoid formation on polycation adsorption may be studied.

WBM containing polyglycols have found widespread use in the drilling fluid industry because of their low toxicity and excellent shale inhibition properties. The mechanism by which polyglycols effect shale inhibition is not yet fully understood and as such, a considerable amount of research by the oil exploration companies has been undertaken. In this study the nature of the exchangeable cation was found to have a major influence on the quantity of polyglycol adsorbed. Q_{max} increased for different cation exchanged montmorillonites in the order $Cs^+<K^+<Na^+<Mn^{2+}$. This dependence of Q_{max} upon the exchangeable cation was due to the state of aggregation and swelling ability imparted to each clay suspension by the associated cation. Polyglycol drilling fluids always contain large quantities of K^+, the precise role of which is not understood although many authors have stated the importance of its presence for shale inhibition. Addition of 0.025 mol L^{-1} KCl to a suspension of 3xCs-mont containing added polyglycol caused the value of Q_{max} to increase. It is thought that this occurred because

the 3xCs-mont partially exchanges to the K^+ exchanged form which results in a Q_{max} value intermediate between that observed for 3xCs-mont and 3xK-mont. XRD also indicates that increasing polyglycol adsorption occurred in the order $Cs^+<K^+<Na^+\approx Mn^{2+}$, shown by the increase in observed basal spacing values. With the addition of 0.025 mol L^{-1} KCl to the clay/DCP101 complexes, XRD showed that the bilayer of polyglycol which was initially adsorbed onto Na^+ and Mn^{2+} exchanged clay prematurely collapsed to a single layer upon thermal treatment. The same phenomenon was also observed when DCP101 was added to 3xK-mont, with no added KCl. This time however, thermal treatment at 100°C was sufficient to initiate the collapse of the bilayer of polyglycol. The presence of K^+ exchangeable cations in a clay/DCP101 complex apparently destabilises the bilayer of polyglycol, causing its premature collapse to a monolayer upon thermal treatment at temperatures between 100 and 150°C. TG analysis of unwashed Cs^+, K^+, Na^+ and Mn^{2+} exchanged montmorillonite contacted with 3% DCP101 indicate that the amount of DCP101 adsorbed onto the clay increased in the following order $Cs^+<K^+<Na^+<Mn^{2+}$. This order of increasing DCP101 adsorption on the different cation exchanged clays is again in agreement with the adsorption isotherm data even though the isotherm samples had been washed once to remove excess polyglycol. TG analysis has also shown that washing the clay/polymer complexes once with deionised water removes some of the DCP101 from the clay.

The interactions of polyglycol with clay in aqueous suspension were studied using ^{133}Cs and ^{1}H NMR. It is evident from ^{133}Cs NMR that addition of DCP101 to 3xCs-mont did not cause a measurable quantity of exchangeable cation to be displaced from the clay at loadings up to 10 % v/v. The fact that Cs^+ ions remain largely undisturbed upon addition of DCP101 to 3xCs-mont is not unexpected since this polymer is neutral

and as such does not adsorb onto clay via an ion exchange mechanism. ^{133}Cs NMR has shown that there may be some interaction taking place between the exchangeable Cs^+ cations and DCP101 at the surface of the clay. This has not been confirmed however because flocculation of the clay upon addition of DCP101 may also contribute to the experimental observations. Finally ^{133}Cs NMR has shown that K^+ displaces Cs^+ from 3xCs-mont more effectively in the presence of DCP101. When KCl/DCP101 drilling fluids are used commercially, it is most likely that the K^+ will replace all the exchangeable cations associated with the shale exposed at the drill hole wall. It has been indicated in many previous studies that it is the interaction between shale, DCP101 and the K^+ cations that promotes shale inhibition. Consequently, the effective displacement of cations associated with the clay by K^+ in the presence of DCP101 may be one contributory factor to the effectiveness of this drilling mud.

There is evidence from other studies which indicates that as DCP101 is adsorbed onto clay, water molecules are desorbed. Whether the desorbed water molecules originate from the basal surface of the clay, the hydration shell of the cation or a combination of both is not fully understood. By investigating aqueous suspensions of 3xMn-mont at different concentrations, it was possible by ^1H NMR to investigate the protons in the water molecules of the cation's hydration shell. ^1H NMR indicated that the Mn^{2+} hydration shell remains predominantly intact upon addition of DCP101 to an aqueous suspension of 3xMn-mont. Conversely, the addition of small quantities of 1,2 DAE to 3xMn-mont, resulted in the displacement of a good proportion of the water molecules in the Mn^{2+} hydration shell. Consequently, it is suggested that DCP101 must preferentially displace water molecules associated with the basal surface of the clay and not the hydration shell of the cation, at least in the case of 3xMn-mont.

In conclusion it has been shown that polyglycols adsorb strongly from aqueous solution onto the surfaces of montmorillonite. The value of Q_{max} depends heavily upon the exchangeable cation associated with the clay which in real drilling conditions is predominantly the K^+ cation. It is thought that the DCP101 adsorption mechanism involves the desorption of numerous water molecules from the basal surface of the clay, since it has already been shown that desorption of water molecules from the cation's hydration shell is unlikely. This adsorption mechanism has yet to be proven although it is thought that future studies involving the use of calorimetry should show a gain in entropy synonymous with the desorption of numerous water molecules from the surface of clay. XRD has shown that when DCP101 is added to 3xK-mont or to other cation exchanged clays in the presence of extraneous K^+ ions, that the bilayer of polymer initially adsorbed becomes less thermally stable, collapsing to a monolayer at elevated temperatures. The reason why the combination of DCP101 and K^+ are so effective at promoting shale inhibition is however still not understood and as such, the synthesis of tailor made polyglycols with improved shale inhibition properties is still some way off.

It was hoped that the ^2H NMR splitting observed when 10% D_2O was added to a clay suspension would provide a method with which to probe the way in which polymers affected the interaction of water with the surface of clay. The magnitude of the ^2H splitting was found to be sensitive to the concentration of clay in suspension. It was also noted in this study that the maximum ^2H splitting was attained in seconds, showing that the platelets align in the magnetic field rapidly. It was thought that the method of preparation of the clay suspensions investigated in this study were responsible for the speed at which the platelets aligned. On exchanging a suspension of a particular cation exchanged clay with another cation, the magnitude of the ^2H splitting was seen to vary.

This variation was considered to be a direct result of the charge associated with the exchangeable cation. For example a 2^+ cation such as Ca orders more water molecules at the clay surface than a 1^+ cation such as Na. Consequently the observed ^2H splitting was larger for calcium exchanged clay suspensions. Both Na^+ and Ca^{2+} exchanged montmorillonite however showed a differential line broadening with the broader component of the ^2H doublet at lower field, giving a positive splitting. Mineral Colloid on the other hand showed a negative splitting and a large differential line broadening for both Ca^{2+} and Na^+ exchanged clays. Related studies have shown that the differential line broadening is a consequence of paramagnetic centres present as Fe_2O_3 in the clay matrix. The larger the quantity of Fe_2O_3 present in the clay, the more pronounced the differential line broadening. These findings were confirmed in this study where Mineral Colloid which contained about 4% Fe_2O_3 showed a larger differential broadening than Westone-L which contains about 0.7% Fe_2O_3. The addition of increasing aliquots of NaCl or $Ca(NO)_3$ to Na^+ or Ca^{2+} exchanged Westone-L caused the observed ^2H splitting to eventually decrease to a singlet. This decrease in magnitude was thought to be due to flocculation of the clay which resulted in a decrease of surface area available for interaction with D_2O molecules. This effect was more pronounced for the addition of extraneous Ca^{2+} cations to the clay suspension rather than Na^+ cations because the Ca^{2+} cations compress the diffuse double layer of the clay platelets more effectively than Na^+ cations, thus resulting in increased flocculation. It is interesting to note however that addition of small quantities of NaCl to 3xNa-mont, actually caused a small increase in ^2H splitting. Without added salt, the predominant type of platelet aggregation in clay suspensions is EF. It is thought that the increase in ^2H splitting upon addition of small quantities of NaCl therefore arises from an increase in the quantity of EE bonded platelets in suspension, leading to an increase in surface area of the clay. Upon addition

of PHPA to 3xNa-mont, it was noted that the splitting of the ^2H doublet was dependant upon resident time in the magnet. In fact up to 2 hours were required to attain maximum splitting for some clay/polymer complexes. Bridging of the clay platelets by the PHPA was thought to be the reason why alignment times were so long. The addition of PHPA to a suspension of 3xNa-mont however caused the collapse of the ^2H splitting to 4 Hz for the addition of very small quantities of polymer. This large decrease in splitting upon addition of such a small quantity of polymer was thought to be primarily due to flocculation of the clay, caused by a combination of the polymers bridging mechanism and its compensating cation. Related studies which involved the addition of a synthesised, deuterated HEG compound similar to DCP101 were unsuccessful in that no ^2H splitting was seen at all upon addition of this compound to clay. It may therefore be concluded that the w: dow from which information may be gained about clay/polymer interactions is extrem:ly sensitive to polymer addition. This sensitivity most probably arises because of platelet flocculation, leading to reduced surface area and therefore D_2O interaction. Consequently the results gained by this technique concerning clay/polymer interactions are not very informative.

9.1 Postgraduate Studies

Courses and Conferences.

Those attended and participated in during the period of this research are listed below:

Date	Course/Conference	Location
5/91	Concerted European Action on Pillared Layered Solids (CEA PLS) Mineral Adsorbed Dyes.	Leuven Belgium
12/92	The Mineralogical Society Conference Mineral Surfaces/Mineralogical Applications of Surface Science.	Manchester University
4/93	The Royal Society of Chemistry NMR school High Resolution NMR Spectroscopy.	Sheffield University
6/93	The Royal Society of Chemistry Conference 11th International Meeting on NMR Spectroscopy.	Swansea University
11/93	The Royal Society of Chemistry Conference presented poster: The Interaction of Drilling Fluids with Clays.	RSC Headquarters London
6/91-9/93	Postgraduate NMR course 20 lectures of 1 hour duration.	Sheffield University

Seminars at Sheffield Hallam University:

attendance at school of science seminars.

Seminars with collaborating establishment:

participation at 3 monthly progress meetings with BP at Sheffield Hallam University, annual 4 week visit to BP at Sunbury on Thames.

9.2 REFERENCES

[1] R. P. Steiger, and P. K. Leung, Quantitative Determination of the Mechanical Properties of Shales, SPEDE **181**, Trans., AIME, 293, 1992.

[2] T. J. Ballard, S. P. Beare and T. A. Lawless, Fundamentals of Shale Stabilisation: Water Transport Through Shales, *Society of Petroleum Engineers* **24974**, 1991.

[3] Baroid Oil Mud Manual, Sources of Mud Problems, 1985.

[4] Baroid Oil Mud Manual, Borehole Instability, 1985.

[5] L. Bailey, M. Keall, A. Audibert, and J. Lecourtier, Effect of Clay/Polymer Interactions on Shale Stabilisation During Drilling, *Langmuir*, **10**, No5, 1994.

[6] Baroid Oil Mud Manual, Fundamental Characteristics of Drilling Fluids, 1985.

[7] Department of Energy, Development of Oil and Gas Resources of the UK, 1988.

[8] T. J. Ballard, S. P. Beare and T. A. Lawless, Shale Inhibition with Water Based Muds: The Influence of Polymers on Water Transport Through Shales, *The Proceedings of the Fifth International Symposium on Chemistry in the Oil Industry*, The Royal Society of Chemistry, 38-55, 1994.

[9] R. Bland, Water Based Glycol Systems Acceptable Substitute For Oil Based Muds, *Oil and Gas Journal*, **90**, No 26, 54-59, 1992.

[10] R. C. Minton, R. Begbie, D. Tyldsley and D. Park, Oily Cuttings Cleaning System Ready For Onshore Testing, *Ocean Industry*, Nov 1991.

[11] R. C. Minton, A Review of Developments in Oilfield Drilling, *The Proceedings of the Fifth International Symposium on Chemistry in the Oil Industry*, The royal Society of Chemistry, 1-12, 1994.

[12] P. I. Reid, G. P. Elliot, R. C. Minton, B. D. Chambers and D. A Burt, Reduced Environmental Impact and Improved Drilling Performance With Water-Based Muds Containing Glycols, *Society of Petroleum Engineers* **25989**, 1993.

[13] J. Dorman and E Banka, Development and Application of Cationic Polymer Drilling Fluids for Shale Stabilisation, *The Proceedings of the Fifth International Symposium on Chemistry in the Oil Industry*, The Royal Society of Chemistry, 56-70, 1994.

[14] T. W. Beihoffer, D. S. Dorrough, C. K. Deem, D. D. Schmidt and R. P. Bray, Cationic Drilling Fluid Can Sometimes Replace Oil-Based Mud, *Oil and Gas Journal*, **90**, 47-52, 1992.

[15] C. A. Sawdon and M. H. Hodder, Pseudo Oil Based Muds - The Outlook, *The Proceedings of the Fifth International Symposium on Chemistry in the Oil Field Industry*, The Royal Society of Chemistry, 28-37, 1994.

[16] R. E. Grim, Clay Mineralogy, 2nd edition, McGraw Hill, London, 1968.

[17] C. K. Wentworth, A Scale of Grade and Class Terms for Clastic Sediments, *J. Geol.*, **30**, 377-392, 1922.

[18] A. A. Damour and D. Salvetat, Et Analyses sur un Hydrosilicate D'alumine Trouve a Montmorillion, *Ann. Chim. Phys.*, ser 3, **21**, 376-383, 1847.

[19] J. T. Way, On the Power of Soil to Adsorb Manure, *J. Roy. Agr. Soc.*, **13**, 123-143, 1952.

[20] U. Hoffmann, K. Endell and D. Wilm, Kristallstruktur und Quellung und Montmorillonite, *Z. Krist.*, **86**, 340-348, 1933.

[21] C. E. Marshall, Layer Lattices and Base Exchange Clays, *Z. Krist.*, **91**, 433-449, 1935.

[22] E. Maegdefrau and U. Hofmann, Die Kristalstruktur des Montmorillonite, *Z. Krist.*, **98**, 299-323, 1937.

[23] S. B. Hendricks, Lattice Structure of Clay Minerals and Some Properties of Clays, *J. Geol.*, **50**, 276-290, 1942.

[24] C. H. Edelman and J. C. L. Favejee, On the Crystal Structure of Montmorillonite and Halloysite, *Z Krist.*, **102**, 417-431, 1940.

[25] W. E. Worrall, Clays and Ceramic Raw Materials, Applied Science Publishers LTD, London, 1975.

[26] K. Norrish, The Swelling of Montmorillonite, *Disc. Farad. Soc.*, **18**, 120-134, 1954.

[27] W. N. Haworth, F. Pinkard and M. Stacey, Function of Bacterial Polysaccharides in Soil, *Nature*, **158**, 836-837, 1946.

[28] M. J. Geoghegan and R. C. Brian, Influence of Bacterial Polysaccharides on Aggregate formation in Soils, *Nature*, **158**, 837, 1946.

[29] M. J. Geoghegan and R.C. Brian, Aggregate Formation in Soil . 2. Influence of various carbohydrates and proteins in aggregation of soil particles, *Biochem. J.*, **43**, 5-13, 1948.

[30] H. H. Morris and L.E. Brooks, Pigmentation of Paper Goods, *Pigment Handbook*, Vol. **2**, 205-213, 1974, Wiley, New York.

[31] International Drilling Fluids Technical Drilling Mud Manual, Company Literature.

[32] S. G. Ash, Polymer Adsorption at the Solid/Liquid Interface, *Colloid Science vol.* **1**, *Specialist Periodical Reports*. The chemical society, London, 103-122, 1973.

[33] R. L. Parfitt and D. J. Greenland, The Adsorption of Poly(ethylene Glycols) on Clay Minerals, *Clay Miner.* **8**, 305-315, 1970a.

[34] S. Burchill, P. L. Hall, R. Harrison, M. H. B. Hayes, J. I. Langford, W. R. Livingstone, R. J. Smedley, D. K. Ross and J. J. Tuck, Smectite-Polymer Interactions in Aqueous Systems, *Clay Miner.* **18**, 373-397, 1983.

[35] B. K. G. Theng, Clay-Polymer Interactions: Summary and Perspectives, Clays and Clay Miner. **30**, 1-10, 1982.

[36] A. Silberberg, The Adsorption of Flexible Macromolecules. Part I. The Isolated Macromolecule at a Plane Interface, *J. Phys Chem*, **66**, 1872-1883, 1962.

[37] D. J. Greenland, Adsorption of Polyvinyl Alcohols by Montmorillonite, *Journal of Colloid Sci.* **18**, 647-664, 1963.

[38] A. Banin and N. Lahav, Particle Size and Optical Properties of Montmorillonite in Suspension, *Israel J. Chem*, **6**, 235-250, 1968.

[39] N. Lahav and A. Banin, Tactoid Rearrangement and the Optical Density of Montmorillonite Suspensions during Na-Ca Exchange Reaction, *J. Coll. Int Sci.*, **26**, 238-240, 1968.

[40] K. Norrish and J. P. Quirk, Crystalline Swelling of Montmorillonite, *Nature*, **173**, 255-256,1954.

[41] K. Norrish, Manner of Swelling of Montmorillonite, *Nature*, **173**, 256-257,1954.

[42] F. Hetzel and H. E. Doner, Some Colloidal Properties of Beidellite: Comparison with Low and High Charge Montmorillonites, *Clays and Clay Miner.* **41**, 453-460, 1993.

[43] S. Burchill and M. H. B. Hayes, Adsorption of Poly(vinyl alcohol) by Clay Minerals: in Agrochemicals in Soils, A. Banin and U. Kafkafi, eds., Pergamon, Oxford, 109-121, 1980.

[44] H. Suquet, C. De la Calle and H. Pezerat, Swelling and Structural Organisation of Saponite, *Clays and Clay Miner.* **23**, 1-9, 1975.

[45] B. Gu and H. E. Doner, The Interaction of Polysaccharides with Silver Hill Illite, *Clays and Clay Miner.*, **40**, 151-156, 1992.

[46] R. L. Parfitt and D. J. Greenland, Adsorption of Polysaccharides by Montmorillonite, *Soil. Sci. Soc. Amer. Proc.*, **34**, 862-866, 1970.

[47] C. Chenu, C. H. Pons and M. Robert, Interaction of Kaolinite and Montmorillonite with Neutral Polysacccharides, *Proceedings of the International Clay Conference, Denver*, 1985, L.G. Shultz, H. Van Olphen and F. A. Mumpton, eds., The Clay Minerals Society, Bloomington, Indiana, 375-381, 1987.

[48] J. Y. Bottero, M. Bruant, J. M. Cases, D. Canet and F. Fiessinger, Adsorption of Nonionic Polyacrylamide on Sodium Montmorillonite: Relation between Adsorption, Zeta Potential, Turbidity, Enthalpy of Adsorption Data and ^{13}C-NMR in Aqueous Solution, *J. Colloid Sci.* **124**, 515-527, 1988.

[49] N. Schamp and J. Huylebroeck, Adsorption of Polymers on Clays, *J. Polymer Sci.* **42**, 553-562, 1973.

[50] X Zhao, K Urano and S. Ogasawara, Adsorption of Polyethylene Glycol from Aqueous Solution on Montmorillonite Clays, *Colloid and Polymer Sci.*, **267**, 899-906, 1989.

[51] J. Stawinski, J. Wierzchos and M. T. Gracia-Gonzalez, Influence of Calcium and Sodium Concentration on the Microstructure of Bentonite and Kaolin, *Clays and Clay Miner.* **38**, 617-622, 1990.

[52] C. E. Clapp and W. W. Emerson, Reactions Between C -Montmorillonite and Polysaccharides, *Soil Sci.*, **114**, 210-216, 1971.

[53] M. M. Mortland, Clay-Organic Complexes and Interactions, *Advan. Agron.*, **22**, 75-117, 1970.

[54] A. P. Black, F. B. Birkner and J. J. Morgan, The Effect of Polymer Adsorption on the Electrokinetic Stability of Dilute Clay Suspensions, *J. Coll. Int Sci.*, **21**, 626-648, 1966.

[55] T. Ueda and S. Harada, Adsorption of Cationic Poly-sulfone on Bentonite, *J. Appl. Polymer Sci.*, **12**, 2395-2401, 1968.

[56] R. Denoyel, G. Durand, F. Lafuma and R. Audebert, Adsorption of Cationic Polyelectrolytes onto Montmorillonite and Silica: Microcalorimetric Study of their Conformation, *J. Coll. Int Sci.*, **139**, 281-290, 1990.

[57] E. Killmann, Conformation and Thermodynamics of Adsorbed Macromolecules at the Liquid/Solid Interface, *Polymer*, **17**, 864-869, 1976.

[58] B. K. G. Theng, Formation and Properties of Clay-Polymer complexes, Elsevier, Amsterdam, 243-273, 1979.

[59] R. L. Parfitt, Adsorption of Charged Sugars by Montmorillonite, *J. Soil Sci.*, **113**, 417-421, 1972.

[60] A. Patzko and I. Dekany, Ion Exchange and Molecular Adsorption of a Cationic Surfactant on Clay Minerals, *Colloids and Surfaces A: Physiochemical and Engineering Aspects*, **71**, 299-307, 1993.

[61] G. Durand-Piana, F. Lafuma and R. Audebert, Flocculation and Adsorption Properties of Cationic Polyelectrolytes towards Na-Montmorillonite Dilute Suspensions, *J. Coll. Int Sci.*, **119**, 474-480, 1986.

[62] T. K. Wang and R. Audebert, Flocculation Mechanisms of Silica Suspensions by some Weakly Cationic Polyelectrolytes, *J. Coll. Int. Sci.*, **119**, 459-465, 1987.

[63] S. Vaslin-Reimann, F. Lafuma and R. Audebert, Reversible Flocculation of Silica Suspensions by Water Soluble Polymers, *Colloid Poll. Sci.*, **268**, 476-483, 1990.

[64] F. Mabire, R. Audebert and C. Quivoron, Flocculation Properties of Some Water Soluble Cationic Copolymers towards Silica Suspensions: A Semiquantitative Intepretation of the Role of Molecular Weight and Cationicity through a "Patchwork" Model, *J. Coll. Int Sci.*, **97**, 1984.

[65] M. Ben-Hur, M. Malik, J. Letey and U. Mingelgrin, Adsorption of polymers on clays as Affected by Clay Charge and Structure, Polymer Properties and Water Quality, *Soil Sci.*, **153**, 349-356, 1992.

[66] T. K. Wang and R. Audebert, Adsorption of Cationic Copolymers of Acrylamide at the Silica-Water Interface: Hydrodynamic Layer Thickness Measurements, *J. Coll. Int. Sci.*, **121**, 32-41, 1988.

[67] M. A. Cohen Stuart, T. Cosgrove and B. Vincent, Experimental Aspects of Polymer Adsorption at Solid/Solution Interfaces, *Adv. Colloid Interface Sci.*, **24**, 143-239, 1986.

[68] F. Th. Hesselink, On the Theory of Polyelectrolyte Adsorption, *J. Coll. Int. Sci.*, **60**, 448-465, 1977.

[69] S. M. Aly and J. Letey, Polymer and Water Quality Effects on Flocculation of Montmorillonite, *Soil Sci. Soc. Am. J.*, **52**, 1453-1458, 1988.

[70] G. R. Saini and A. A. MacLean, Adsorption-Flocculation Reactions of Soil Polysaccharides with Kaolinite, *Soil Sci. Soc. Amer. Proc.*, **30**, 697-699, 1966.

[71] R. A. Ruehrwain and D. W. Ward, Mechanism of Clay Aggregation by Polyelectrolytes, *Soil Sci.* **73**, 485-492, 1952.

[72] A. S. Michaels and S. Morelos, Polyelectrolyte adsorption by Kaolinite, *Ind. Eng. Chem.*, **47**, 1801-1809, 1955.

[73] J. L. Mortensen, Adsorption of Hydrolysed Polyacrylonitrile on Kaolinite, Clays and Clay Miner. Proc. 9th Natl Conf., West Lafayette, Indiana, Ada Swineford, Ed., Pergamon Press, New York, 530-545, 1962.

[74] T. Stutzmann and B Siffert, Contribution to the Adsorption Mechanism of Acetamide and Polyacrylamide onto Clay, *Clays and Clay Miner.*, **25**, 392-406, 1977.

[75] M. Schnitzer and H. Kodama, Montmorillonite: effect of pH on its adsorption of a soil humic compound, *Science*, **153**, 70-71, 1966.

[76] L. T. Lee, R. Rahbari, J. Lecourtier and G. Chauveteau, Adsorption of Polyacrylamides on the Different Faces of Kaolinites, *J. Coll. Int Sci.*, **147**, 351-357, 1991.

[77] P. Espinasse and B. Siffert, Acetamide and Polyacrylamide Adsorption onto Clays: Influence of the Exchangeable Cation and the Salinity of the Medium, *Clays and Clay Miner.*, **27**, 279-284, 1979.

[78] B. K. G. Theng, Interactions between Montmorillonite and Fulvic Acid, *Geoderma*, **15**, 243-251, 1976.

[79] J. L. Mortensen, Adsorption of Hydrolysed Polyacrylonitrile on Kaolinite: II. Effect of Solution Electrolytes, *Soil Sci. Soc. Am Proc.*, **23**, 199-202, 1959.

[80] A. Katchalsky, Solutions of Polyelectrolytes and Mechanochemical Systems, *J. Pol. Sci.*, 7, 393-412, 1951.

[81] M. Page, J. Lecourtier, C. Noik, and A. Foissy, Adsorption of Polyacrylamides and of Polysaccharides on Siliceous Materials and Kaolinite: Influence of Temperature, *J. Coll. Int. Sci.*, **161**, 450-454, 1993.

[82] D. H. Napper, Polymeric Stabilisation of Colloidal Dispersions, Academic Press, London, 1983.

[83] T. Sato and R. Ruch, Stabilisation of Colloidal Dispersions by Polymer Adsorption, Marcel Decker, Inc, New York, 1980.

[84] J. Gregory, Rates of Flocculation of Latex Particles by Cationic Polymers, *J. Coll. Int. Sci.*, **42**, 448-456, 1972.

[85] J. Papenhuijzen, H. A. Van der Schee and G. J. Fleer, Polyelectrolyte Adsorption 1. A New Lattice Theory, *J. Coll. Int. Sci.*, **104**, 540, 1985.

[86] E. Dickinson and L. Eriksson, Particle Flocculation by Adsorbing Polymers, *Adv. Coll. Int. Sci.*, **34**, 1-29, 1991.

[87] S. P. Altaner, R. J. Kirkpatrick and C. A. Weiss, Magic Angle Spinning Nuclear Magnetic Resonance Investigation of Phyllosilicates, Proceedings of the 9th

International Clay Conference, Strasbourg, 1989, V. C. Farmer and Y. Tardy (Eds) Sci. Geol., Mem., **89**, 159-168, 1990.

[88] J. Hougardy, W. E. E. Stone and J. J. Fripiat, NMR Study of Adsorbed Water. Molecular Orientation and Protic Motions in the Two Layer Hydrate of a Na Vermiculite, *J. Chem. Phys.*, **64**, 3840-3851, 1976.

[89] M. Kadi-Hanifi, Proton Nuclear Magnetic Resonance Studies of "One Layer" Hydrates of Orientated Hectorite, *Clays and Clay Min.*, **28**, 65-66, 1980.

[90] M. Lipsicas, C. Straley, P. M. Costanzo and R. F. Giese, Static and Dynamic Structures of Water in Hydrated Kaolinites, *J. Coll. Int. Sci.*, **107**, 221-230, 1985.

[91] W. E. E. Stone, The Use of NMR in the Study of Clay Minerals, in Advanced Techniques for Clay Mineral Analysis, Developments in Sedimentology, **34**, 77-112, 1982.

[92] S. Bank, J. F. Bank and P. D. Ellis, Solid State ^{113}Cd Nuclear Magnetic Resonance Study of Exchanged Montmorillonite, *J. Phys. Chem.*, **93**, 4847-4855,1989.

[93] V. Luca, C. M. Cardile and R. H. Meinhold, High Resolution Multinuclear NMR Study of Cation Migration in Montmorillonite, *Clay Miner.*, **24**, 115-119, 1989.

[94] C. A. Weiss, S. P. Altaner and R. J. Kirkpatrick, High Resolution ^{29}Si Nuclear Magnetic Resonance Spectroscopy of 2:1 Layer Silicates, *American Mineralogist*, **72**, 935-942, 1987.

[95] R. A. Kinsey, R. J. Kirkpatrick, J. Hower, K. A. Smith and E. Oldfield, High Resolution ^{27}Al and ^{29}Si Nuclear Magnetic Resonance Spectroscopic Study of Layer Silicates, Including Clay Minerals, *American Mineralogist*, **70**, 537-548, 1985.

[96] D. E. Woessner, Characterisation of Clay Minerals by ^{27}Al Nuclear Magnetic Resonance Spectroscopy, *American Mineralogist*, **74**, 203-215, 1989.

[97] W. Loewenstein, The Distribution of Aluminum in the Tetrahedra of Silicates and Aluminates, *American Mineralogist*, **39**, 92-96, 1954.

[98] M. Lipsicas, R. H. Raythatha, T. J. Pinnavaia, I. D. Johnson, R. F. Giese, P. M. Costanzo and J. L. Robert, Silicon and Aluminium Site Distributions in 2:1 Layered Silicate Clays, *Nature*, **309**, 604-607, 1984.

[99] P. F. Barron, P. Slade and R. L. Frost, Ordering of Aluminium in Tetrahedral Sites in Mixed Layer 2:1 Phyllosilicates by Solid State High Resolution NMR, *J. Phys. Chem.*, **89**, 3880-3885, 1985.

[100] J. Sanz and J. M. Serratosa, ^{29}Si and ^{27}Al High Resolution MAS NMR Spectra of Phyllosilicates, *J. Amer. Chem. Soc.*, **106,** 4790-4793, 1984a.

[101] C. P. Herrero, J. Sanz and J. M. Serratosa, Tetrahedral Cation Ordering in Layer Sillicates by ^{29}Si NMR Spectroscopy, *Solid State Communications*, **53**, No.2, 151-154, 1985.

[102] J. Sanz and J. M. Serratosa, Distinction of Tetrahedrally and Octahedrally Coordinated Al in Phyllosilicates by NMR Spectroscopy, *Clay Minerals*, **19**, 113-115, 1984.

[103] J. G. Thompson, ^{29}Si and ^{27}Al Nuclear Magnetic Resonance Spectroscopy of 2:1 Clay Minerals, *Clay Minerals*, **19**, 229-236, 1984.

[104] N. C. M. Alma, G. R. Hays, A. V. Samoson and E. T. Lippmaa, Characterisation of Synthetic Dioctahedral Clays by Solid-State 29Si and 27Al Nuclear Magnetic Resonance Spectroscopy, *Anal. Chem*, **56**, 729-733, 1984.

[105] J. Grandjean and P. Laszlo, Deuterium and Oxygen-17 Nuclear Magnetic Resonance of Aqueous Clay Suspensions, *Magnetic Resonance Imaging*, **12**, 375-377, 1994.

[106] P. Laszlo, NMR of Newly Accessible Nuclei, Academic Press, San Diego, 1983.

[107] D. E. Woessner and B. S. Snowden, NMR Doublet Splitting in Aqueous Montmorillonite Gels, *J. Chem. Phys.*, **50**, 1516-1523, 1969.

[108] D. E. Woessner and B. S. Snowden, A Study of The Orientation of Adsorbed Water Molecules on Montmorillonite Clays by Pulsed NMR, *J. Coll. Int. Sci.*, **30,** 54-68, 1969.

[109] J. Grandjean and P. Laszlo, Deuterium Nuclear Magnetic Resonance Studies of Water Molecules Restrained by Their Proximity to a Clay Surface, *Clays and Clay Minerals*, **37**, 403-408, 1989.

[110] A. Delville, J. Grandjean and P. Laszlo, Order Aquisition by Clay Platelets in a Magnetic Field. NMR Study of the Structure and Microdynamics of the Adsorbed Water Layer, *J. Phys. Chem.*, **95**, 1383-1392, 1991.

[111] J. Grandjean, NMR Studies of Interfacial Phenomena, Ann. Rep. NMR Spectr., **24**, 181-217, 1992.

[112] J. Grandjean and P. Laszlo, Structuring at Solid Interfaces in Binary Solvent Mixtures, *Pure and Appl. Chem.*, **65**, No. 12, 2539-2542, 1993.

[113] J. Grandjean and P. Laszlo, Multinuclear and Pulsed Gradient Magnetic Resonance Studies of Sodium Cations and of Water Reorientation at the Interface of a Clay, *J. Mag. Res.*, **83**, 128-137, 1989.

[114] P. Waldstein, S. Rabideau and J. A. Jackson, Nuclear Magnetic Resonance of Single Crystals of D_2O Ice, *J. Chem. Phys.*, **41**, 3407-3411, 1964.

[115] D. T. Edmonds and A. L. Mackay, The Pure Quadrupole Resonance of the Deuteron in Ice, *J. Mag. Res.*, **20**, 515-519, 1975.

[116] D. Petit, J. P. Korb, A. Delville, J. Grandjean and P. Laszlo, Theory of Nuclear Spin Relaxation in Heterogeneous Media and Application to the Cross Correlation Between Quadrupolar and Dipolar Fluctuations of Deuterons in Clay Gels, *J. Mag Res.*, **96**, 252-279, 1992.

[117] G. Sposito and R. Prost, Structure of Water Adsorbed on Smectites, *Chem. Rev.*, **82**, 554-573, 1982.

[118] W. F. Bleam, The Nature of Cation Substitution Sites in Phyllosilicates, *Clays and Clay Miner.*, **38**, 527-536, 1990

[119] J. Grandjean and P. Laszlo, Nuclear Magnetic Resonance Study of Saponite Hydration and of Acetonitrile-Water Competition, *J. Am. Chem. Soc.*, **116**, 3980-3987, 1994.

[120] J. Conard, Structure of Water and Hydrogen-Bonding on Clays Studied by ^{7}Li and ^{1}H Resonance, *J. Mag. Res.* Colloid Interface Sci. **9,** 85-96, 1976.

[121] Po-Jen. Chu, B. C. Gerstein, J. Nunan and K. Klier, A Study of Solid-State NMR of ^{133}Cs and ^{1}H of a Hydrated and Dehydrated Cesium Mordenite, *J. Phys. Chem.*, **91**, 3588-3592, 1987.

[122] T. Tokuhiro, M. Mattingly, L. E. Iton and M. K. Ahn, Variable-Temperature Magic-Angle-Spinning Technique for Studies of Mobile Species in Solid-State NMR, *J. Phys. Chem.*, **93**, 5584-5587, 1989.

[123] V. Laperche, J. F. Lambert, R. Prost and J.J. Fripiat, High Resolution Solid-State NMR of Exchangeable Cations in The Interlayer Surface of a Swelling Mica: ^{23}Na, ^{111}Cd and ^{133}Cs Vermiculites., *J. Phys. Chem.*, **94**, 8821-8831, 1990.

[124] A. Labouriau, C. T. Johnston and W. L. Earl, Cation and Water Interactions in the Interlamellae of a Smectite Clay, *Natl. Meet.- Am. Chem. Soc., Div. Environ. Chem.*, 158-160, **33**, 1993.

[125] D. Tinet, N. P. Faugere and R. Prost, ^{113}Cd-NMR Chemical Shift Tensor Analysis of Cadmiun-Exchanged Clays and Clay Gels, *J. Phys. Chem.*, **95**, 8804-8807, 1991.

[126] J. F. Lambert, R. Prost and M. E Smith, ^{39}K Solid-State NMR Studies of Potassium Tecto and Phyllosilicates: The In Situ Detection of Hydratable K^{+} in Smectites, *Clays and Clay Miner.*, **40**, No. 3. 253-261, 1992.

[127] C. A. Weiss, R. J. Kirkpatrick and S. P. Altaner, The Structural Environments of Cations Adsorbed onto Clays: ^{133}Cs Variable -Temperature MAS NMR Spectroscopic Study of Hectorite, *Geochimica et Cosmochimica Acta.*, **54**, 1655-1669, 1990.

[128] R. K. Harris and B. E. Mann, NMR and the Periodic Table., Academic Press, 1978.

[129] R. K. Harris, Nuclear Magnetic Resonance Spectroscopy, Longman Scientific and Technical, 1986.

[130] B. L. Sawhney, Selective Sorption and Fixation of Cations by Clay Minerals: A Review. *Clays and Clay Miner.*, **20**, 93-100, 1972.

[131] N. Boden, S. A. Corne, P. Halford-Maw, P. Fogarty and K. W. Jolley, Sample Cell or High Precision Temperature Dependence NMR Experiments, *J. Mag. Res.* **98**, 92-108, 1992.

[132] J. W. Akitt, NMR and Chemistry: An Introduction to the Fourier Transform Multinuclear Era, Second Edition, J. W. Arrowsmith Ltd, Bristol, 1983.

[133] D. R. Collins, A. N. Fitch, C. Richard and A. Catlow, Dehydration of Vermiculites and Montmorillonites: A Time Resolved Powder Neutron Diffraction Study, *J. Mater. Chem.*, **2**, 865-873, 1992.

[134] J. Fripiat, J. Cases, M. Francois and M. Letellier, Thermodynamic and Microdynamic Behaviour of Water in Clay Suspensions and Gels, *J. Coll. Int. Sci.*, **89**, 1982.

[135] H. Van Olphen, An Introduction to Clay Colloid Chemistry, Second Edition, Wiley-Interscience, New York, 1977.

[136] D. J. Cebula, R. K. Thomas and J. W. White, Small Angle Neutron Scattering from Dilute Aqueous Dispersions of Clay, *J. Chem. Soc. Faraday Trans. 1*, **76**, 314-321, 1980.

[137] M. Morvan, D. Espinat, R. Szymanski and R. Ober, Characterisation of Montmorillonite Suspensions by Small Angle X-Ray Scattering (SAXS), Light Scattering (LS) and Nuclear Magnetic Resonance (NMR), *Collect. Colloq. Semin. (Inst. Fr. Pet.)*, 273-274, **50**, 1992.

[138] D. R. Collins, A. N. Fitch, C. Richard and A. Catlow, Time-Resolved Powder Neutron Diffraction Study of Thermal Reactions in Clay Minerals, *J. Mater. Chem.*, **1**, 965-970, 1991.

[139] P. Laszlo, Quadrupolar Metallic Nuclei: ^{23}Na NMR Studies of Cation Binding by Natural and Synthetic Ionophores, *Am. Chem. Soc. Symp. Ser.*, 63-95, 1982.

[140] A. Delgado, F. Gonzales-caballero and J. M. Bruque, The Zeta Potential and Surface Charge Density of Montmorillonite in Aqueous Clay Suspensions. *J. Coll. Int. Sci.*, **113**, 203-211, 1986.

[141] S. Lee Swartzen-allen and E. Matijevic, Colloid and Surface Properties of Clay Suspensions, *J. Coll. Int Sci.*, **56**, 159-167, 1976.

[142] D. P. Parazac, C. W. Burkhardt, K. J. McCarthy and M. P. Stehlin, Hydrophobic Flocculation, *J. Coll. Int. Sci.*, **123**, 59-72, 1988.

[143] B. K. G. Theng, D. J. Greenland and J. P. Quirk, Adsorption of Alkylammonium Cations by Montmorillonite, *Clay Miner.*, **7**, 1-17, 1967.

[144] C. T. Cowan and D. White, The Mechanism of Exchange Reactions Occurring Between Sodium Montmorillonite and Various n-Primary Aliphatic Amine Salts, *Trans. Faraday Soc.*, **54**, 691- 697, 1958.

[145] D. J. Greenland and J. P. Quirk, Adsorption of 1-n-Alkyl Pyridinium Bromides by Montmorillonite, *Clays and Clay Miner.*, **9**, 484-499, 1962.

[146] S. B. Weed and J. B. Weber, The Effect of Adsorbent Charge on the Competative Adsorption of Divalent Organic Cations by Layer Silicate Materials, *Amer. Mineral.*, **53**, 478-490, 1968.

[147] J. B. Weber, P. W. Perry and R. P. Upchurch, The Influence of Temperature and Time on the Adsorption of Paraquat, Diaquot, 2,4-D and Prometone by Clays, Charcoal and Anion Exchange Resin, *Soil Sci. Soc. Amer. Proc.*, **29**, 678-688, 1965.

[148] J. D. Downs, E. Van Oort, D. I. Redman, D. Ripley and B. Rothman, A New Concept in Water-Based Drilling Fluids for Shales, *Society of Petroleum Engineers* **26699**, Offshore Europe Conference, Aberdeen, 1993.

[149] S. Cliffe, B. Dolan and P. Reid, Mechanisms of Shale Inhibition by Polyols in Water-Based Drilling Fluids, *Society of Petroleum Engineers* **28960**, International Symposium on Oilfield Chemistry, Texas, 1995.

[150] P. F. Low, The Swelling of Clay: II Montmorillonites, *Soil Sci. Amer. J.*, **44**, 667-676, 1980.

[151] I. Shainberg and W. D. Kemper, Hydration status of Adsorbed Cations, *Soil Sci. Amer. Proc.*, **30**, 707-713, 1966.

[152] M. S. Aston and G. P. Elliot, Water-Based Glycol Drilling Muds: Shale Inhibition Mechanisms, *Society of Petroleum Engineers* **28818**, European Petroleum Conference, London, 1994.

[153] R. W. Mooney, A. G. Keenan and L. A. Wood, Adsorption of Water Vapour by Montmorillonite. II. Effect of Exchangeable Ions and Lattice Swelling as Measured by X-ray Diffraction, *J. Amer. Chem. Soc.*, **74**, 1331-1374, 1952.

[154] R. Keren and I. Shainberg, Water Vapour Isotherms and Heat of Immersion of Na/Ca Montnorillonite Systems-I: Homoionic Clay, *Clays and Clay Miner.*, **23**, 193-200, 1975.

[155] J. P. Quirk, Particle Interaction and Soil Swelling, *Israel J. Chem.*, **6**, 213-234, 1968.

[156] R. Levy and C. W. Francis, Interlayer Adsorption of polyvinylpyrrolidone on montmorillonite, *J. Coll. Int. Sci.*, **50**, 442-450, 1975.

[157] G. W. Brindley, Ethylene Glycol and Glycerol Complexes of Smectites and Vermiculites, *Clay Miner.*, **6**, 237-259, 1966.

[158] D. M. C. MacEwan, Complexes of Clays with Inorganic Compounds-I: Complex Formation between Montmorillonite and Halloysite and Certain Organic Liquids, *Trans. Faraday Soc.*, **44**, 349, 1948.

[159] R. C. Reynolds, An X-ray Study of an Ethylene Glycol Montmorillonite Complex, *Am. Miner.*, **50**, 990-1001, 1965.

[160] H. Suquet, C. De la Calle and H Pezerat, Swelling and Structural Organisation of Saponite, *Clays and Clay Miner.*, **23**, 1-9, 1975.

[161] G. W. Brindley and G. Brown, Crystal Structures of Clay Minerals and their X-ray Identification, Mineralogical Society, Spottiswoode Ballantyne Ltd, London 1980.

[162] T. Sato, T. Watanabe and R. Otsuka, Effects of Layer Charge, Charge Location and Energy Change on Expansion Properties of Dioctahedral Smectites, *Clays and Clay Miner.*, **40**, 103-113, 1992.

[163] H. Suquet, J. T. Iiyama, H. Kodama and H. Pezerat, Synthesis and Swelling Properties of Saponites with Increasing Layer Charge, *Clays and Clay Miner*, **25**, 231-242,1977.

[164] B. Halle and H. Wennerstrom, Interpretation of Magnetic Resonance Data from Water Nuclei in Heterogeneous Systems, *J. Chem. Phys.*, **75**, 1928-1943, 1981.

[165] J. Grandjean and P. Laszlo, Octahedral or Tetrahedral Isomorphous Substitution: How it Affects Water and Acetonitrile Interaction with a Clay, as Seen by NMR, *Clays and Clay Miner.*, **42**, 652-654, 1994.

[166] S. Swartzen-Allen and E. Matyevic, Surface and Colloid Chemistry of Clays, *Chem. Rev.*, **74**, 385-400, 1974.

[167] L. Bailey, P. I. Reid and J. D. Sherwood, Mechanisms and Solutions for Chemical Inhibition of Shale Swelling and Failure, *The Proceedings of the Fifth International Symposium on Chemistry in the Oil Industry*, The Royal Society of Chemistry, 13-27, 1994.

[168] R. P. Steiger, Fundamentals and Use of Potassium/Polymer Drilling Fluids to Minimise Drilling and Completion Problems Associated With Hydratable Clays, *J. Petr. Tech.*, 1661-1670, 1982.